



**NRPDPT Program for Postgraduate Research**

**at the Norwich Research Park**

# *Doctor of Philosophy* Thesis

to validate the

**PhD studentship at the University of East Anglia, for research conducted at the Quadram Institute Bioscience**

---

## *EXPLORING THE POTENTIAL ADJUVANT ROLE OF BACTERIAL EXTRACELLULAR VESICLES DERIVED FROM BIFIDOBACTERIUM PSEUDOCATENULATUM STRAINS*

---

Presented by

**Anne Jordan**

| | |
|---|---|
| Student Number: | 100299121 |
| Primary Supervisor: | Prof Simon Carding |
| Secondary Supervisor: | Prof Lindsay Hall |
| Submission Date: | 31/07/2024 |
| Resubmission Date: | 30/11/2025 |

# ABSTRACT

*Bifidobacterium* is a known microbiota determinant of early-life immune function and overall health. Many studies have reported the multifaceted immune stimulatory and regulatory properties of different *Bifidobacterium* strains. However, little research has investigated the potential for immune modulation by bacterial extracellular vesicles (BEVs) derived from *Bifidobacterium*. In this project, I focused on understanding BEV production and potential immune stimulation of BEVs derived from two strains belonging to a key but understudied early-life microbiota species - *Bifidobacterium pseudocatenulatum*.

I determined bacterial growth conditions for optimal BEV harvesting time points via CFU and OD growth assays. Following optimisation of bifidobacterial BEV purification, I evaluated several biophysiological properties and proteomic load of BEV batches, showing abundance of different potentially immunostimulatory proteins in a BEV preparation-dependent manner. Moreover, I confirmed uptake of BEVs into the epithelial barrier and potential underlying endocytosis pathways in Caco-2 cells using confocal microscopy. *In vitro* studies, using different cell lines, indicated potential modulation of the intestinal barrier via TJ gene induction, stimulation of the NF-κB pathway, production of TNF-α, IL-1β, IL-10, IL-6, IL-8, and TSLP in human monocytes and macrophages. Additionally, I performed e*x vivo* characterisations, including stimulation of murine splenocytes, resulting in production of IL-6, KC, and TNF-α, confirming potential immunostimulation by bifidobacterial BEVs. Further investigations, using additional *in vitro* and *ex vivo* studies, resulted in induced production of TNF-α in human PBMCs, and IgA production in murine Peyer's patch fragments in a strain- and time point-dependent manner. Simulation of an infection, using LPS, showed evidence for protective properties of bifidobacterial BEVs in cultured epithelial cells and macrophages. To date, there are limited studies on bifidobacterial BEVs, and no studies on BEVs derived from *B. pseudocatenulatum* strains have been undertaken. These data may provide insights into the potential immunostimulatory and protective properties of products from health-promoting *B. pseudocatenulatum,* which could facilitate development of novel immune adjuvants.

# ACCESS CONDITIONS & AGREEMENT

Each deposit in the UEA Digital Repository is protected by copyright and other intellectual property rights, and duplication or sale of all or part of any of the Data Collections is not permitted, except that material may be duplicated by you for your research use or educational purposes in electronic or print form. You must obtain permission from the copyright holder, usually the author, for any other use. Exceptions only apply where a deposit may be explicitly provided under a stated licence, such as a Creative Commons Licence or Open Government Licence.

Electronic or print copies may not be offered, whether for sale or otherwise to anyone unless explicitly stated under a Creative Commons or Open Government Licence. The unauthorised reproduction, editing or reformatting for resale purposes is explicitly prohibited (except where approved by the copyright holder themselves) and UEA reserves the right to take immediate 'take down' action on behalf of the copyright holder if this Access Condition of the UEA Digital Repository is breached. Any material in this database has been supplied on the understanding that it is copyright material and that no quotation from the material may be published without proper acknowledgement.

# PREFACE & COVID-IMPACT STATEMENT

This thesis was submitted to the University of East Anglia (Norwich, UK) for the degree of Doctor of Philosophy. The work presented herein was undertaken at the Quadram Institute Bioscience (Norwich, UK) from October 2019 to July 2024 and fully funded for 4 years and 10 months supported by the UKRI Biotechnology and Biological Sciences Research Council and Norwich Research Park Biosciences Doctoral Training Partnership (Grant number BB/ M011216/1).

## COVID-Impact Statement

The pandemic and its aftermath have had, and still have, long-term consequences for me both professionally and personally. Research facilities were closed for several months, and distancing regulations impacted experimental planning and performance opportunities. The lockdown began just as I had finished most of my theoretical training and lab inductions, which meant that no data could be collected and analysed for an extended period. Instead, I focused on preparing my probation and started working on a literature review about the impact of early-life microbiota on vaccination efficacy. However, the publication of this review was delayed due to my mental health and COVID-related financial and housing issues.

Due to the cancellation or delay of critical in-person training, I had to pivot and re-focus my PhD project. Initially, my project was supposed to involve screening a broader selection of *B. pseudocatenulatum* strains from different geographical origins such as Vietnam for potential immunomodulatory properties *in vitro*. These strains would have been used to create a diverse set of BEVs for use in various experiments. Unfortunately, I had to exclude experiments such as confocal imaging of fluorescently labelled epithelial cells treated with different endocytosis antagonists to study the uptake pathways of BEVs, as well as imaging of potential interactions between the BEVs and macrophages and dendritic cells, and translocation dynamics in epithelial organoids, due to lack of lab-based facilities during social distancing periods, and health-associated breaks.

Another significant part of my project that had to be excluded was *in vivo* work. My original plan was to study the effects of selected BEVs on healthy mice, including potential shifts in immune cells, differences in gene expression, biodistribution of BEVs, and optimisation of administration. Additionally, I had planned to assess differences in immunogenicity following vaccination against flu (and potentially other diseases with heterogeneous efficacy) in BEV-treated mice and to establish 'humanised' mouse models to investigate immunological and microbial changes in BEV-treated mice with human infant microbiotas. Although I obtained my animal license shortly before the pandemic, I was unable to receive the practical training necessary to perform animal work due to social distancing restrictions within the animal facility (DMU).

Thus, I had to change the focus of my research from studying the potential vaccine adjuvancy of bifidobacterial BEV in mice to conducting a much more detailed BEV analysis of the two *B. pseudocatenulatum* strains (using cutting-edge assays) and more general *in vitro* immune stimulation characterisation. I also faced delays in receiving reagents and materials, including a shipping period of over 7 months for BEV cross-filters. The pandemic also limited my opportunities for outreach and networking, such as attending conferences, seminars, and public engagement activities between 2020 and 2022, which affected my overall PhD experience. Additionally, travel restrictions made it challenging to visit my loved ones, increasing the stress of isolation, and to easily return to the UK, causing stress due to missing out on lab work.

The pandemic and personal challenges have greatly affected my mental health. I have experienced depression, anxiety, insomnia, loss of motivation, crippling migraines, and heightened stress. As a result, I have been unable to work for several months (which was partly compensated via granted extensions) and these effects may continue for years.

# ACKNOWLEDGEMENTS

I would like to express my gratitude to my supervisory team, including Prof Lindsay Hall, Prof Simon Carding, Dr Regis Stentz, Dr Aimee Parker, and Dr Mark Webber, for their guidance, feedback, patience, and support throughout my project. A special thank you to Dr Regis Stentz for his significant help and support during the often-frustrating optimisation of BEV preparations, as well as his encouragement and assistance with housing issues. Merci beaucoup, Regis!

I'm deeply grateful to Dr Mark Webber for being there for me during a crucial moment. His caring words and support were a lifeline for me. I also want to express my heartfelt thanks to Dr Paul Kroon for understanding my struggles and guiding me towards solutions.

I want to thank all my colleagues and scientific contributors for providing invaluable services, expertise, and assistance which have been essential for the successful completion of my project. I would like to extend my heartfelt thanks to Dr Nancy Teng, Iliana Serghiou, and Dr Magdalena Kujawska for their warm welcome, guidance, and knowledge-sharing at the beginning of my project. Special acknowledgement goes to Dr David Baker and the QIB Sequencing Facility for their invaluable contribution in performing Whole Genome Sequencing of the strains used in my project. I am truly indebted to Dr Magdalena Kujawska and Dr Raymond Kiu for their expert analysis of genomic data and guidance in bioinformatics. A huge thank you to the QIBAM and JIC BioImaging Facility, particularly Dr Catherine Booth, for their support in TEM imaging and confocal microscope training. I am sincerely thankful to Dr Emily Jones for her comprehensive training across various project aspects, including ZetaView usage, SEC performance, proficiency in *in vitro* experiments, and insights into confocal imaging and analysis. Similarly, I want to thank Dr Sree Gowrinadh Javvadi for initial inductions in *in vitro* experiments. Dr Rokas Juodeikis' encouragement and explanation of lipid quantification have been immensely valuable. I wish to express my gratitude to Dr Carlo Martins and Dr Gerhard Saalbach from the JIC Proteomics Facility for their expertise in proteomic analysis of my BEVs, and to Dr Matthew Dalby for his guidance in R and data visualisation. A big thank you to Dr Christopher Price, Dr Sally Dreger, and Dr Alicia Nicklin from the Robinson group for their collaboration,

assistance in animal work, tissue preparation training, and support in flow cytometric analysis. Many thanks to Dr George Savva for the statistics Q&A. Lastly, a heartfelt thank you to Mar Moreno-Gonzales and Dr Olla Al-Jaibaji, who helped me with the final experimental miles to complete this PhD marathon.

Many thanks to past and present members of the Hall and Carding group.

I am extremely grateful to all the lovely people, colleagues, friends and family for your patience during this long and difficult time of me complaining about work, failed experiments, deadlines, inconvenient incubation times, sleepless nights, English food and weather, the traffic, the housing situation, the pandemic, politics, humanity, and so much more. Every little gesture, chat, meme, chocolate bar, cup of tea, and walk made my days less grey. Huge thanks to my mum and dad, Tante Nani, who now crosses her fingers for me from above, and my friends at home Chulia, Resi, Jule, Anja, Shymolie, and Bilge! I missed you all so much! Very special and heartfelt thanks to my friends, Dr Nancy Teng, Dr Hélène Yvanne, Dr Wouter van Bakel, Dr Victor Laplanche, Dr Iliana Serghiou Daley, Peter Smith, Tom Atkinson and Megan Mortimer, who went through the same journey with me and made everything more bearable!

And finally, infinite and whole-hearted gratitude to my partner, Maxime Laird, who was always there for me despite the 1675km that separated us for the most part.

Thank you!

# TABLE OF CONTENTS

# LIST OF FIGURES

# LIST OF TABLES

# I. INTRODUCTION

## 1. Early life colonisation and development of a beneficial gut microbiota-immune relationship

### 1.1. Functions of the gastrointestinal microbiota

The intestinal microbiota contains a complex community of more than 100 trillion microorganisms, including bacteria, archaea, viruses, fungi and protozoa of varying composition along the gastrointestinal tract (GIT) of every individual.[1,2] This microbial ecosystem is crucial for key health-beneficial physiological functions for the host, such as food digestion, synthesis of essential vitamins[3], protection against invading pathogens[3–5], development of the mucosal and systemic immune system[6,7], maintenance of intestinal homeostasis[8], and tolerance to antigens derived from food, the environment, and commensal bacteria.[1,9–11] Perturbances of the GIT microbiota, dysbiosis, are associated with various morbidities and metabolic disorders.[12,13] Also, risk, progression, and potential treatment outcomes of various cancer types, such as breast cancer or melanoma, have been linked to GIT microbiota dysbiosis.[14–16] Central to this thesis, the GIT microbiota is a key factor influencing immunity in early life.[1] Several studies in germ-free (GF) mice and humans have demonstrated increased intestinal barrier permeability and disruption of the inner mucous layer[17], leading to systemic inflammation[18] and compromised immunity.[19] GF mice and rats also exhibit reduced immune cell levels and activity mucosally and systemically, as well as deficiencies in immune tolerance.[20,21] However, these conditions are improved through microbial colonisation, faecal microbiota transplantation (FMT), or probiotic intervention, emphasising the critical role of a healthy GIT microbiota in maintaining overall health.

Development of the GIT microbiota overlaps with the development and maturation of the immune system, with innate and adaptive immune responses and their specialised immune cells depending on microbial cues from the microbiota to promote and sustain immune tolerance and pathogen resistance.[22]

## 1.2. Microbial immune stimulation for efficient protection

### *1.2.1. Innate immune response and antigen-presentation*

Specialised systemic and tissue-resident immune cells, which express different specific pattern recognition receptors (PRRs) on their cell surface, survey the host for the presence of non-self antigens. Recognition of microbe-associated molecular patterns (MAMPs) and/or danger-associated molecular patterns (DAMPs), present in the body through vaccination, infection or injury, induces a signal cascade leading to the maturation of these antigen-presenting cells (APCs).[23] This includes antigen uptake and processing followed by enhanced expression of surface ligands such as cluster of differentiation (CD) 80, CD86 and major histocompatibility complex (MHC) I and MHC II that contribute to antigen presentation. Additionally, activated APCs produce pro- or anti-inflammatory cytokines and specific chemokines for immune cell recruitment and cell-to-cell interaction.[24] Dendritic cells (DCs), and to a lesser degree macrophages, are major APCs directing the subsequent immune response via different complex interactions with other immune cells of the innate and adaptive immune system (see Figure 1). Such innate immune cells include mononuclear myeloid cells, such as monocytes, neutrophils, natural killer (NK) cells and innate lymphoid cells (ILCs). In addition to their immediate immune response towards pathogenic containment and clearance, these cells contribute to trained innate immunity following infection, resulting in increased antimicrobial effector function and enhanced cytokine and reactive oxygen species (ROS) production.[25] Additionally, neutrophils, NK cells, and non-immune cells such as epithelial cells can directly influence DC function.[26]

The expression of co-stimulatory ligands and production of specific cytokine profiles by DCs depends on the activation of distinct PRR families expressed by DCs. These include Toll-like receptors (TLRs) and NOD-like receptors (NLRs), which recognise specific microbial antigens.[27] For instance, surface-associated TLRs recognise membrane-derived microbial structures such as lipopolysaccharide (LPS; TLR4), Flagellin (TLR5), and *Toxoplasma gondii* profilin (TLR12), whereas cytosolic TLRs are stimulated by double-stranded (ds) RNA (TLR3), single-stranded (ss) RNA (TLR7) and unmethylated dsDNA (TLR9).[26–28] Stimulation of TLRs induces activation of the nuclear factor ‘κ-light chain enhancer’ of activated B cells (NF-κB) transcription factor

controlling production of many key immune modulatory cytokines, chemokines and adhesion molecules such as interleukin (IL)-1β, IL-6, IL-8, tumour necrosis factor-alpha (TNF-α), IL-12, monocyte chemoattractant protein 1 (MCP-1), and chemokine c-c motif ligand 5 (CCL5; also known as regulated on activation, normal T cell expressed and secreted [RANTES]).[26]

Upon activation and maturation, DCs migrate to secondary lymphoid organs such as adjacent lymph nodes and the spleen to prime naïve T cells via CD28 ligation by co-stimulatory molecules CD80 and CD86.[26] Primed T cells clonally expand and differentiate into different subtypes dependent on inflammatory signals from DCs and cytokines, and catalyse the adaptive immune response.[29] The polarisation of the adaptive immune response depends on the nature of the antigen, microenvironment stimuli (including cytokines), type of DC and their maturation state, and activated PRRs, as well as the subsequent specific inflammatory signals following this activation (see Figure 1).[30,31]

### *1.2.2. Adaptive immunity and long-term protection*

DCs mediate an important connection between innate and adaptive immunity. There are different subtypes of DCs: conventional DCs (cDCs) type 1 and 2, responsible for inducing cellular and humoral responses[32,33], plasmacytoid DCs (pDCs) mostly supporting antiviral responses via increased production of type I and III interferons (IFNs)[34], and follicular DCs (fDCs) within germinal centres (GCs) presenting antigens to B cells over long periods, leading to T cell-independent responses as well as GC reactions.[32,35]

#### a) CD4⁺ T cell responses

Essential for T cell-dependent humoral responses is the ability of cDC2 to activate $CD4^+$ T cells, inducing polarisation into specific effector subtypes, including T helper (Th) cells type 1, 2, and 17, T follicular helper cells (Tfh), and regulatory T cells (Tregs).

Th1 differentiation is initiated in response to MHCII-processed antigens from intracellular bacteria and/or viral infection and IL-12 and IL-1β signalling. Antiviral responses are driven by enhanced production of IFN-γ, activation of $CD8^+$ cytotoxic T cells (Tct), macrophages and B cell stimulation.[26]

Infection with parasites and subsequent increase in IL-2, IL-4, IL-25, IL-33, and thymic stromal lymphopoietin (TSLP) levels leads to the development of Th2 cells. These cells also activate B cells and produce IL-4, IL-5, IL-9 and IL-13[36], which promote antibody isotype class-switching in B cells and macrophage activation, induce tissue repair[37], and intestinal smooth-muscle contractions to facilitate parasite ejection from the GIT.[26]

Th17 populations are essential in the response to extracellular bacteria, fungi, and viral infection and are induced by IL-6, IL-23, IL-21, IL-1β, and transforming growth factor-beta (TGF-β).[26,36,38] They secrete IL-3, IL-17A, IL-17F, IL-22, TNF-α, and granulocyte-macrophage colony-stimulating factor (GM-CSF) and play a crucial role in mucosal immunity, stimulating production of antimicrobial peptides (AMPs) by intestinal epithelial cells (IECs)[39], inducing tissue inflammation, activating B cells and neutrophils[40], and promoting formation of ectopic lymphoid follicles in tissues.[36,41]

As a major anti-inflammatory driver, Tregs play a critical role in restoring homeostasis after infection via inhibition of pro-inflammatory effector T cells, reduction of infection-related immunopathology and production of IL-10, which inhibits antigen presentation, expression of MHC II, and DC differentiation.[42,43] Natural Tregs are fully mature functional lymphocytes produced in the thymus, whereas naïve $CD4^+$ T cells can also differentiate into Tregs in the periphery after priming by immature DCs in the presence of TGF-β and retinoic acid (RA).[26,44,45] Additionally, Tregs are crucial for prevention of autoimmune reactions as they regulate immune reactions against self-antigens.[26,36]

Tfh cells, similar to fDCs, are found within lymph nodes, GCs, and the spleen, but only fully differentiate after antigen presentation by cDCs in the presence of TGF-β, IL-12, IL-23, and Activin A, followed by direct interaction with antigen-specific B cells.[32,36] B cells and Tfh cells have a close mutualistic relationship, enabling the development of GCs, facilitating the maturation of B cells into plasma and memory cells, and promoting the production of different antibody classes via secretion of specific cytokines.[26,36] These include IFN-γ promoting immune globulin (Ig) G production, IL-4 promoting IgG and IgE production, and IL-10 promoting IgA production.[36,46] Additionally, Tfh cells also secrete IL-21, CD40 ligand (CD40L), TNF-α, and C-X-C motif chemokine ligand 13 (CXCL13) further supporting GC-B cell responses.[36]

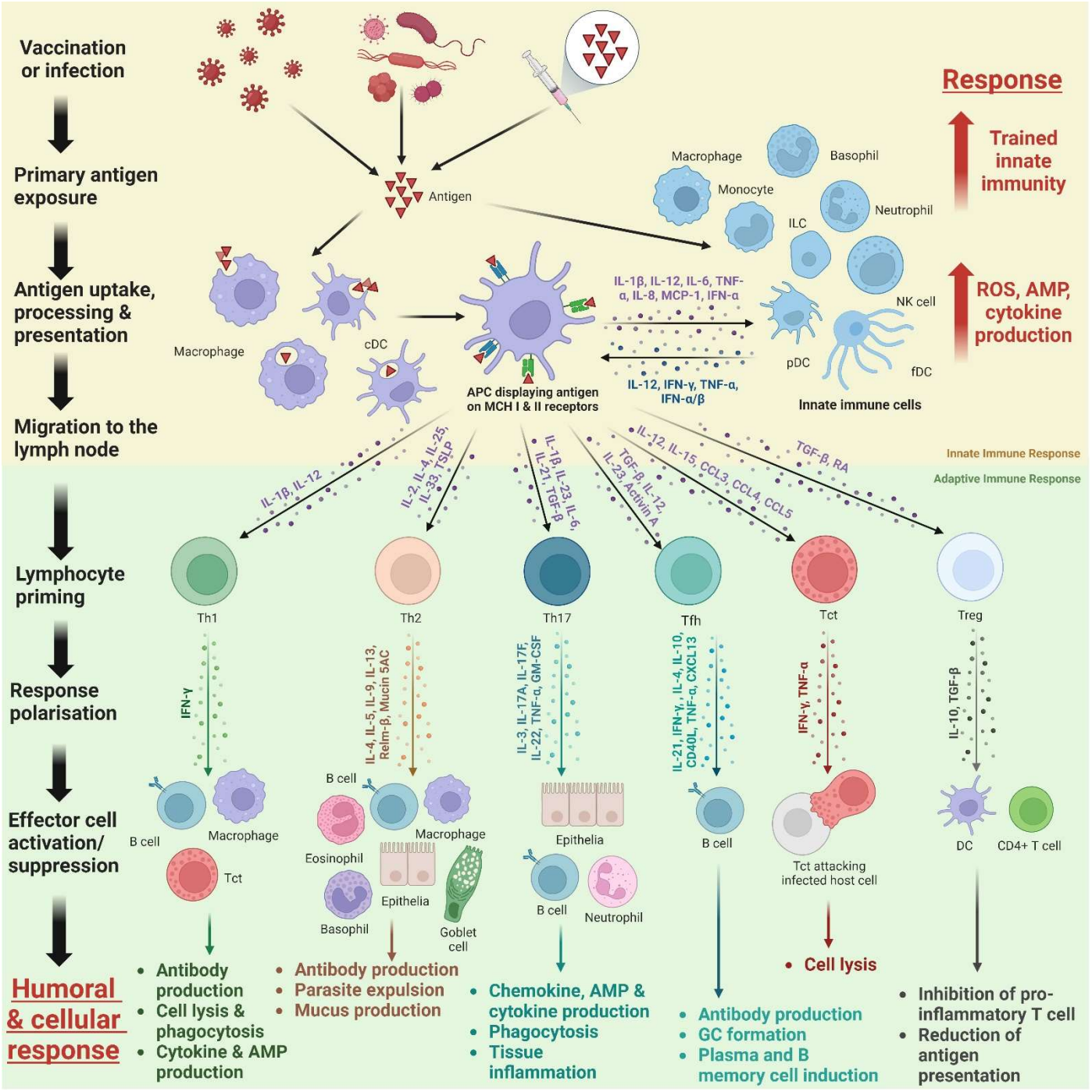


*Figure 1: Overview of innate and adaptive immune responses after vaccination and/or infection. Created with BioRender.com*

### b) B cell responses

B cells contribute to humoral responses and perform two different immune reactions: fast but less efficient extra-follicular responses (T cell-independent) or slow but efficient GC responses (T cell-dependent).

In GC responses, B cells are first activated by APCs and subsequently stimulated by $CD4^+$ effector T cells and their secreted cytokines (as described above), leading to

clonal proliferation, somatic hypermutation, isotype switching and affinity maturation of B cells towards production of high-affinity antibodies against the specific presented antigen. Additionally, effector Th cells provide co-stimulatory signals promoting peripheral tolerance and lowering the risk of autoimmune responses.[47] Stimulated B cells differentiate into long-lasting plasma cells, producing high levels of high-affinity antibodies over prolonged times, building the primary immune response against the introduced antigen.[48,49] Moreover, a portion of stimulated GC-B cells directly differentiates into memory B cells, which stay dormant in lymph nodes until secondary exposure to the same antigen, resulting in the development of memory cells into plasma cells and fast production of high-affinity antibodies as the secondary immune response.[48,49] This humoral response leads to antigen/pathogen clearance via antibody-directed neutralisation, opsonisation or activation of the complement cascade.[26,50]

Alternatively, APC-activated B cells can differentiate into short-lived plasma cells independent of T cell interaction. These plasma cells do not undergo somatic hypermutation or isotype switching and produce IgM antibodies of low to modest affinity within a few days post-infection.[48,51] Due to their reduced lifespan, antibody titers from these plasma cells decline 4-8 weeks after infection.[48,52] Microbial antigens such as LPS and other bacterial capsular polysaccharides induce this type of immune response.[48,53]

### c) CD8$^+$ T cell responses

In addition to humoral responses, the immune system can also mount cellular responses against bacterial or viral intracellular infections, or tumours.[53] Similar to CD4$^+$ T cells, naïve CD8$^+$ T cells are activated via presentation of processed antigens on the MHC I receptor on the surface of DCs and/or infected cells.[48,53] Upon antigen recognition, activated CD8$^+$ T cells differentiate into short-lived effector Tct cells or effector memory CD8$^+$ T (Tct Tem) cells.[48,54] These effector Tct cells mediate cytolysis via secretion of pro-inflammatory cytokines such as TNF-α and IFN-γ, and cytotoxic chemicals allowing poration of the membrane of infected cells and subsequent entry of proteases targeting and degrading pathogenic proteins and inducing cellular apoptosis.[53] Similar to B cell responses, Tct cell responses are mediated by growth factors and cytokines deriving from Th cells[9], and short-lived effector Tct cells enter programmed cell death shortly after primary immune responses.[48] Secondary

responses are driven by Tct Tem cells persisting for long periods and rapidly differentiating and proliferating into effector Tct cells upon repeated exposure to the same antigen.[48] Additionally, $CD8^+$ T cells can differentiate into tissue-resident memory T cells or central memory Tct (Tct Tcm) cells located in non-lymphoid tissues for extended periods, enabling local secondary cellular responses.[48,55]

### d) Immune memory

Exposure to antigens through infection can induce improved and more rapid immune responses via the generation of immune memory cells. Populations of all cell types of the adaptive immune system can differentiate into long-lived memory cells, which stay dormant until re-stimulation. Memory plasma cells migrate to the bone marrow (BM), where they survive for decades and provide systemic low levels of antibodies in the absence of re-exposure to antigens.[47] Conversely, memory B cells are found in the spleen, lymph nodes, and peripheral tissues, also staying quiescent for decades.[47] Upon recognition of cognate antigens, both memory plasma and memory B cells differentiate into effector plasma cells, proliferate and secrete high-affinity antibodies.[47]

Naïve and effector $CD4^+$ and $CD8^+$ T cells require additional stimulation for differentiation into memory cells and long-term maintenance. Both need prolonged stimulation from MHC I- and II-presented antigens, respectively, as well as interaction with IL-7 and IL-15 for homeostatic proliferation and survival.[56,57] Both cytokines elevate expression of anti-apoptotic molecules, such as regulators B cell lymphoma-2 (BCL-2) and myeloid cell leukaemia-1 (MCL-1), in T cells.[57,58] However, $CD4^+$ T cells have a higher activation threshold for differentiation, impacting development of cytokine-producing and non-producing memory cells.[57] Moreover, $CD4^+$ T cells are more dependent on IL-7 versus IL-15 for $CD8^+$ T cells.[56,57,59,60] Interestingly, memory $CD4^+$ T cells deriving from different Th effector subtypes are adaptable and can produce cytokines of alternate Th lineages, which can be used for more efficient long-term protection.[57,61]

Health-promoting microbes can stimulate beneficial immune cell interactions via recognition of MAMPs by PRRs, producing nutrients and immunomodulatory metabolites like bacteriocins and short-chain fatty acids (SCFAs).[62] For instance, in

newborn and young piglets, exposure to commensal microbes upregulated TLRs on DCs and epithelial cells, resulting in increased AMP and IgA levels, enhanced attachment to the mucus layer, and prevention of inflammatory reactions between GIT microbiota and IECs.[63] Sustained exchange between the early-life microbiota and the immune system has a long-lasting impact on well-being far into adulthood.

Intriguingly, factors influencing the GIT microbiota are similar to protective immune responses, highlighting the interconnected relationship between immunity and GIT microbiota.[1] These factors include age[64,65], gender[66,67], environmental and socio-economic conditions[68–70], hygiene[68], chronic infection[71], maternal health[72], mode of delivery[73], preterm birth[71], nutrition[74,75], and early anti- and/or probiotics use.[1,76–79]

## 1.3. Establishment of a microbial profile in early life

### *1.3.1. Mode of delivery, feeding regimen, and postnatal interventions*

Microbial colonisation is initiated at birth, and changes continuously across the life course, with the first 1000 days of life representing a 'window of opportunity', which is also the most vulnerable and unstable period for ecosystem development.[1,4] Birth involves moving from a 'sterile' intrauterine state towards hyperstimulation of the immune system from external antigens and colonising microbes.[80] Priming exposure to early GIT colonisers is dependent on mode of delivery. Vaginally delivered babies are exposed to the maternal vaginal and GIT microbiota, leading to microbial profiles dominated by *Escherichia*, *Lactobacillus*, *Bacteroides*, and *Bifidobacterium* species.[1,81–83] Conversely, newborns born prematurely and/or delivered via caesarean section have primary contact with maternal skin and nosocomial microbes, leading to colonisation by *Streptococcus*, *Staphylococcus* and *Enterococcus* species.[1,73,81]

To prevent intrauterine rejection, foetal and newborn immunity is initially Th2-dominated.[84] Well-balanced microbial stimulation modulates immune responses towards Th1/Th2 equilibrium and Treg activation for effective adaptive immunity.[80]

Another key modulator of microbiota composition is nutrition. Breastfeeding provides newborns with passive protection via maternal antibodies, AMPs, innate immunity factors (e.g. TLR2, TLR4, CD14, and myeloid differentiation protein 2 [MD2]), and delivers crucial dietary components and bacteria that shape the infant's microbiota towards a *Bifidobacterium*-dominant profile (see Figure 2).[1,80,85,86] Human milk oligosaccharides (HMOs) enhance bifidobacterial colonisation and persistence

(accounting for ≤80% of the total microbial community in the early-life GIT microbiota) with initial high abundance of *Bifidobacterium longum* subsp. *infantis, Bifidobacterium breve, Bifidobacterium bifidum, Bifidobacterium catenulatum* and *Bifidobacterium pseudocatenulatum.*[1,87–89] Additionally, metabolism of HMOs leads to increased production of SCFAs, supports health-promoting microbial shifts and immune stimulation, activation of mucosal immunity, enhances expression of tight junctions (TJs), and promotes mucosal barrier homeostasis.[1,80] Indeed, formula-fed infants show lower levels of *Bifidobacterium* (only 5-30%) and higher abundance of pathobionts (i.e., organisms that can cause harm under certain circumstances) such as *Clostridium* species and lack HMO-related health benefits.[90,91]

At the point of weaning, introducing solid dietary sources changes the microbiota and metabolite profiles of the infant GIT. Overall abundance of *Bifidobacterium* species decreases, levels of other early colonisers increase, while other microbial members such as *Ruminococcus*, *Akkermansia* and *Segatella* (formerly *Prevotella*) are introduced.[1,89] Concurrently, the abundance of maternal immune mediators decreases, resulting in increased production of thymus-derived immune cells. Moreover, the immune system actively establishes an immune repertoire in response to food, environmental and microbial antigens, leading to the maturation of the infant's immune system.[92]

Malnutrition can result in GIT microbiota disturbances, rupture of the epithelial barrier, altered metabolism, and immune deficiencies, increasing risk of infection, chronic inflammation and lower seroconversion rates to oral vaccines.[93,94] Equally, antibiotic treatment in early life negatively impacts GIT colonisation, increasing abundance of pathogenic bacteria such as *Klebsiella* and *Enterococcus* species[95], and affects subsequent immune development. Unfortunately, antibiotic administration during childhood is globally widespread. For instance, a child from the US finishes on average up to 3 antibiotic courses by the age of 2 and 10 by the age of 10.[96,97] Perturbation of the GIT microbiota pre- and/or post-weaning can have long-lasting negative consequences for host health including neonatal sepsis[98], necrotising enterocolitis (NEC)[99], chronic inflammatory bowel disease (IBD) and Crohn's disease[100], asthma, and allergies.[101–103]

Thus, colonisation of the 'right' microbes at the 'right' time is crucial to establishing immune defences, effective vaccine responses, cognition, growth, and

homeostasis.[1,80] Once the GIT microbiota reaches a mature, 'adult-like' state, its composition can shift following antibiotic treatment, dietary changes, and GIT infection.[104,105]

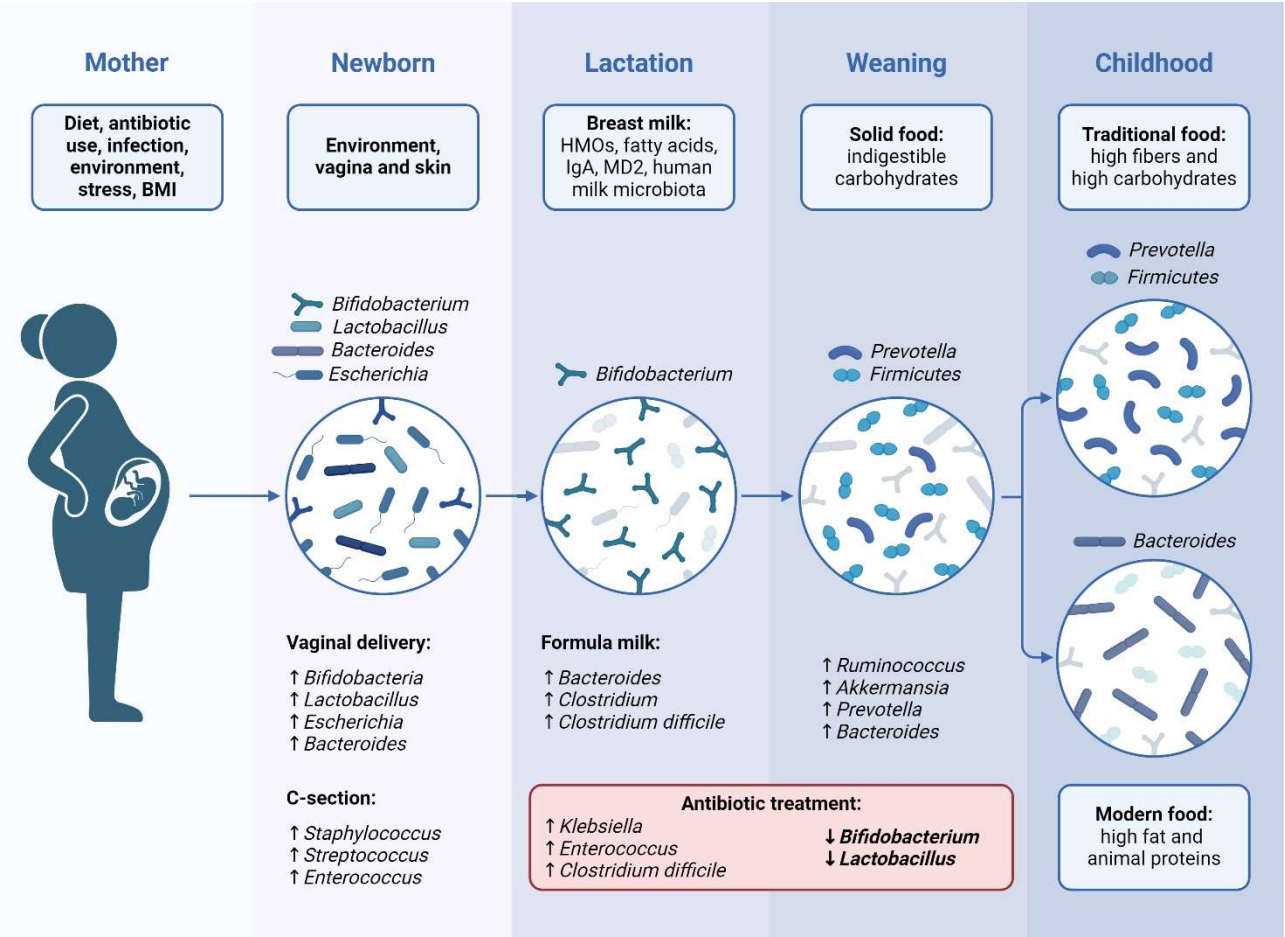


*Figure 2: Gastrointestinal microbiota establishment trajectory in early life.[89] Created with BioRender.com*

### *1.3.2. Geo-socioeconomic factors influencing microbiota composition*

Disturbances in establishing the early-life microbiota can also be attributed to hygiene[68], maternal health status[72], nutrient availability[106,107], housing conditions[108,109], exposure to human immunodeficiency virus (HIV)[110,111], access to sanitation and potable water[112], and pollution.[113]

In addition to these factors directly impacting infant microbiota colonisation, they can also indirectly influence microbial seeding via maternal microbiota and systemic health status. Prenatal maternal microbiota disruptions induced by antibiotics, diet, stress exposure, and infection can impact foetal development, breast milk composition and microbiota transfer to offspring.[114] Indeed, *in vivo* studies and clinical trials revealed

altered infant GIT microbiota establishment trajectories from mothers with perturbed microbiotas.[115–118]

Maternal nutritional stress can lower breast milk IgA levels.[108,119,120] Breast milk can also reflect maternal exposure to pollutants, including microplastics[121], polycarbonated biphenyls (PCBs)[122–124], pesticides[125–127], repellents[128], and other toxins as reported in the breast milk of mothers from Asia, and North and South America.[129–131] Moreover, recent studies indicate a link between air pollution and altered GIT microbiota and HMO composition in breast milk of exposed mothers.[113,132] Maternal diet and body mass index (BMI) can also directly influence microbial transfer from the maternal GIT into breast milk and subsequently into the newborn's gut. For instance, higher BMI in mothers is associated with lower abundance of *Bifidobacterium* species in breast milk.[133]

Equally, prevalence of gastrointestinal infection by intestinal helminths, rotavirus (RV), poliovirus, and norovirus can decrease microbiota diversity and promote pathogenic invasion in both mothers and offspring.[134–138]

## 2. Immune modulatory features of *Bifidobacterium* strains

*Bifidobacterium* is a keystone member of the 'healthy' early-life GIT microbiota (see Figure 2) and, together with *Lactobacillus,* is one of the main pillars of probiotics and postbiotics.[3] They are Gram-positive, anaerobic, non-spore-forming, with a characteristic Y-shaped microscopic appearance, of the Actinomycetota (formerly Actinobacteria) phylum, exerting immunomodulatory properties within the host. The successful adaptation of *Bifidobacterium* to the human GIT from infancy to adulthood may be attributed to the abundance of genes mediating stomach acid tolerance, carbohydrate metabolism, and transport systems.[139] Indeed, *Bifidobacterium* species have a diverse repertoire of carbohydrate-active enzymes (CAZymes), unique metabolic pathways (i.e. bifid shunt), and an arsenal of glycosyl hydrolases (GHs) allowing metabolism of complex polysaccharides, including mucin, HMOs, resistant starch (RS), and other dietary prebiotics, granting adaptability and nutrient competition advantages within their ecological niche.[105,139,140] Since they are vertically transferred from mother to newborn, metabolic diversity and gene expression adjustment are crucial for survival of environmental and substrate-related changes.[140–142] Moreover, bifidobacterial metabolites support cross-feeding of other commensal microbiota

members such as *Bacteroides* and *Lactobacillus* species, while inhibiting colonisation of pathogens such as *Clostridiodes difficile* and *Salmonella*.[143–148]

Many studies reported beneficial effects *in vitro*, *in vivo* and in humans in a species- and strain-dependent manner.[149] For instance, infants with highly abundant *Bifidobacterium* species have elevated counts of memory B cells and express higher levels of IL-5, IL-6, IL-13, TNF-α, and IL-1β, while absence of *Bifidobacterium* leads to dysregulated immunity and lower levels of T cell maturation and decreased circulating plasmablasts, naïve and memory B cells.[18,96,150] In murine obesity models, administration of *B. pseudocatenulatum* CECT7765 or *B. animalis* subsp. *lactis* Ikm512 reduced systemic inflammation, restored a balanced state of Treg and B cells, and lowered IL-17A and TNF-α levels.[151,152] Similarly, DCs, stimulated by different *B. bifidum* and *B. breve* strains mediated Th17 and Treg polarisation of naïve $CD4^+$ T cells *in vitro*.[153] Conversely, *B. bifidum* DSM 20082 lysate stimulated $CD8^+$ Tct cell activity, while not influencing $CD4^+$ T cell activity.[154] Treatment with *B. animalis* subsp. *lactis* IU100 increased serum titres of IgA, IgG, and IgM, and improved cytokine production of IL-1β, IL-2, IL-4, IL-6, TNF-α, and IFN-γ, shifting the Th1/Th2 balance in immunosuppressed mice.[155] Additionally, administration of *Bifidobacterium* species in a murine melanoma model improved tumour-specific immunity, enhanced checkpoint blockade therapy responsiveness and increased overall DC function and $CD8^+$ T cell priming.[156] Co-culture of *B. pseudocatenulatum* SPM1204 with DCs and macrophages increased levels of MHC class I expression and stimulated production of nitric oxide (NO), TNF-α, and IL-1β.[139,157] Conversely, treatment of DCs with *B. bifidum*, *B. longum* subsp. *longum*, and *B. pseudocatenulatum*, but not *B. longum* subsp. *infantis*, activated DCs, increased expression of CD83, and induced Th2 responses and IL-10 production.[158]

## 2.1. *B. pseudocatenulatum* strains

While more prominent *Bifidobacterium* species, such as *B. longum* subsp. *infantis*, *B. longum* subsp. *longum*, *B. bifidum*, *B. breve,* and *B. adolescentis* have traditionally predominated bifidobacterial research; *B. pseudocatenulatum* has recently attracted increasing attention. This interest is largely due to their high intra-species genetic diversity and corresponding metabolic adaptability, enabling them to thrive in the presence of diverse dietary components, such as HMOs and plant-derived

glycans.[159–161] Consequently, *B.pseudocatenulatum* has been detected in the GIT microbiota across the lifespan, from infancy to old age. Notably, centenarians have been reported to have a particularly high abundance of *B. pseudocatenulatum* strains.[162] In a Vietnamese population-based study, *B. pseudocatenulatum* was identified as the most abundant bifidobacterial species in adults and the second most prevalent in children, following *B. longum* subsp*. longum*.[163] Similarly, analyses of European infant cohorts revealed that *B. pseudocatenulatum* strains exhibit metabolic preferences for dietary starch and plant fibres, while showing limited utilisation of HMOs and host-derived glycans. Their persistence in the infant gut appears to rely on cross-feeding networks of HMO-degrading strains.[88] In a study of mother-infant pairs, Kan et al. (2020)[140] demonstrated that *B. pseudocatenulatum* strains are transmitted vertically and display host-diet-dependent metabolic specialisation.

Compared to well-established commercial probiotic strains such as *L. sakei* and *B. longum* subsp. *infantis*, *B. pseudocatenulatum* has shown promising probiotic potential. For example, oral administration of *B. pseudocatenulatum* G7 significantly reduced the severity of colitis in mice, decreased NO production in macrophages *in vitro*, mitigated colitis-associated microbiota changes and positively modulated bile acids and SCFA levels.[164] Another murine colitis study reported similar benefits, including clinical symptom improvement, reduced oxidative stress, restored microbiota perturbations, and enhanced intestinal barrier integrity via increased TJ expression, and modulation of inflammatory responses − lowering TNF-α, IL-1β, and IL-6, while increasing IL-10. These effects were most pronounced in exopolysaccharide (EPS)-producing strains.[165]

Protective effects of *B. pseudocatenulatum* have also been observed in models of liver injury and cirrhosis, where *B. pseudocatenulatum* LI09 ameliorated intestinal injury, ‘corrected’ microbiota dysbiosis, and reduced excessive systemic and hepatic inflammation, while normalising bile acid and SCFA profiles.[166]

In mouse neurological studies, administration of *B. pseudocatenulatum* NCU-08, isolated from a human centenarian, reversed age-related impairments in memory, motor function, and stress response in aged mice. Additionally, the faecal transplant supported tissue repair and homeostasis in the brain and GIT by suppressing apoptosis, reducing inflammation and oxidative stress, mitigating microbiota dysbiosis and maintaining blood-brain and intestinal barrier integrity.[162] Similarly, strain *B.*

*pseudocatenulatum* CECT 7765 modulated the gut-brain axis by increasing neurotransmitter levels in the hypothalamus and small intestine, reshaping gut microbiota composition, and restoring cytokine production towards balance. This intervention reversed brain biochemistry and behaviour changes induced by early-life stress with long-lasting effects into adulthood.[167]

Dietary intervention and probiotic administration studies have linked increased *B. pseudocatenulatum* abundance to improvements in clinical and metabolic parameters, including body mass index, lipid homeostasis, insulin sensitivity, plasma glucose and inflammation marker levels.[168–171] These changes were accompanied by enhanced metabolic and immunological profiles, increased abundance of beneficial bacterial species (e.g. *Akkermansia*), and elevated production of health-beneficial compounds, such as SCFA and EPS (i.e. postbiotics).[90,172–175]

Recently, in pre-clinical models, *B. pseudocatenulatum* 210 (which is identical to strain LH663 used in this thesis) and its EPS were shown to modulate anti-tumour immune responses, improving breast cancer progression and response to standard-of-care therapies in pre-clinical models. This effect was mediated via macrophage and cDC1 activation and maturation, increased TNF-α and IFN-γ production and enhanced polarisation and infiltration of anti-tumour $CD8^+$ T cells.[176]

Due to the strain-dependent ability of *Bifidobacterium,* and particularly *B. pseudocatenulatum,* to induce immune stimulatory or regulatory responses[177], it is crucial to define the immunomodulatory properties of different strains and their products to achieve desired immune responses in any intervention trial. This species is of particular interest in considering its environmental adaptability and metabolic versatility, but also for its capacity to produce SCFAs, EPS and other microbial compounds that may influence host immune responses.

None of the current 10 commercial *Bifidobacterium* probiotic species[164] include *B. pseudocatenulatum* strains, highlighting the need for further research and development in this area, including in-depth characterisation of potential probiotic strains and products of this species.

## 2.2. Modulating the GIT microbiota to enhance immune protection

*In vivo* animal and human studies have investigated the effect of targeted microbiota interventions via stimulation of colonisation of beneficial microbes through pre-, pro-, and postbiotic formulations to increase the abundance of beneficial bacteria, including *Bifidobacterium* and/or use of their products to exert health-promoting effects on the host, including vaccination (see Table 1).

### *2.2.1. Prebiotics*

Prebiotics (defined by Gibson et al. (2017)[178] at the International Scientific Association for Probiotics and Prebiotics as "a substrate that is selectively utilised by host microorganisms conferring a health benefit") are non-digestible fibres that can be metabolised by beneficial microbiota members promoting their prevalence within the host GIT.[1] HMOs can be used as prebiotics to enhance *Bifidobacterium* prevalence (i.e. bifidogenic properties) in early life. Similarly, fructooligosaccharides (FOS), isomaltooligosaccharides (IMO), and galactooligosaccharides (GOS) are highly bifidogenic, while the metabolism of other prebiotics is more strain-dependent.[179] IMO has increased the abundance of *Bifidobacterium*, *Lactobacillus*, and *Bacteroides* species while decreasing *Clostridium* counts in an elderly cohort.[180] Moreover, prebiotics also stimulate the production of SCFAs[181–183], cytokines, and TJ proteins[184], further promoting immune modulation and host health benefits.

Further details on prebiotic metabolism in certain *Bifidobacterium* species are discussed in Results Chapter I.

### *2.2.2. Probiotics*

Defined by the World Health Organisation (WHO) in 2001 as 'live microorganisms, which when administered in adequate amounts confer a health benefit on the host'[185], probiotic use is another strategy to alter GIT microbiota.[1] Some probiotic genera, especially *Bifidobacterium* and *Lactobacillus*, which are generally recognised as safe (GRAS), enhanced humoral responses to RV, typhoid, pneumococcal conjugate vaccine (PCV), and cholera vaccination only after 1-5 weeks of supplement intake (see Table 1).[186] Neonatal piglets given different *Bifidobacterium* strains exhibited distinct immunomodulatory responses. One study showed increased intestinal IL-10 production with *B. longum* subsp. *longum* AH120691[187], while others

found enhanced immune responses and RV vaccine efficacy with *B. animalis* subsp. *lactis* Bb12[8,188], *B. longum* subsp. *infantis* MCC12, and *B. breve* MCC127494.[1,189] This further highlights the strain-specific immune-altering features of *Bifidobacterium*.

Additionally, probiotic treatment is also used to improve IBD severity and antibiotic-induced microbiota disruption and to lower the burden of different infectious diseases.[190–192] Indeed, meta-analysis of 98 studies in low- and middle-income countries (LMICs) revealed probiotic use significantly improved survival of preterm neonates, and lowered overall mortality, NEC and neonatal sepsis incidences.[193] Fermented milk with *L. plantarum* La5 and *B. animalis* subsp. *lactis* BB-12 improved IBD symptoms and increased abundance of beneficial microbiota members.[194]

However, many probiotics used in these interventions do not persist in the GIT (i.e. no long-term colonisation of the used probiotics), and therefore, novel strategies, such as synbiotic formulations (i.e. combinations of specific prebiotics and probiotic strains able to metabolise those prebiotics), may be required to improve long-term microbiota compositional shifts. For instance, *B. pseudocatenulatum* MP80 was only persistent and able to modulate the baseline microbial community and metabolome when administered as a 2'-Fucosyllactose (2'FL)-combined symbiotic, but not as a probiotic alone.[195]

Although colonisation of probiotic strains after intervention seems difficult, promoting colonisation of beneficial strains in vulnerable individuals with dysbiosis could yield overall health gains, including improved vaccine responsiveness.[96]

## 2.3. Postbiotics as alternative immune modulators

Postbiotics are defined by the International Scientific Association for Probiotics and Prebiotics as a 'preparation of inanimate microorganisms and/or their components that confers a health benefit on the host'.[196] This broad term includes microbial metabolites, products, other non-living components and heat-killed bacteria with beneficial immunomodulatory properties.[114] For instance, fermentation products of *B. breve* C50 and *Streptococcus thermophilus* 065 increased delayed-type hypersensitivity responses and galectin release, and promoted Th1- and Th17-type immunity in a murine influenza model.[197] Conversely, faecal water collected from infants undergoing supplementation with *B. longum* subsp. *infantis* supported $CD4^+$ T

cell polarisation from Th2 and Th17 towards Th1 responses via increased galectin-1 production *in vitro*.[18]

They can also provide antimicrobial activities without the risk of anti-microbial resistance (AMR) induction, making them attractive alternatives to antibiotics.[198] Comparing the effect of prebiotic and postbiotic supplementation, neonatal rats showed improved microbial and SCFA profiles following prebiotic treatment, while postbiotics upregulated TLR expression.[199] When challenged with RV infection, both treatments improved severity of symptoms compared to controls.[200]

Generation of the SCFA acetate contributes to the health-promoting abilities of *Bifidobacterium* species. Acetate is a key metabolite directly engaged in essential synthesis pathways of different microbiota members via enzymatic conversion into acetyl-coenzyme A (acetyl-CoA) or butyrate.[1,201] Its absorption in the host provides energy to IECs and lowers intestinal pH levels, preventing pathogenic invasion.[202] Acetate also activates the G-protein coupled receptor 43 (GPR43) found on B cells, different subsets of T cells, neutrophils, macrophages and DCs, as well as IECs. Activation of GPR43 induces proliferation of Treg cells in the lamina propria, maintenance of intestinal barrier integrity and homeostasis, and promotion of intestinal defence mechanisms.[1,139,203–205] Additionally, stimulation of GPR43 by acetate and mediation by RA positively affects intestinal IgA responses.[206,207] GPR43 activity also influences neutrophil chemotaxis and degranulation, regulates macrophages and DCs, and mediates effector T cell polarisation depending on the underlying condition of the intestinal environment.[1,208–211]

Postbiotics offer notable safety advantages compared to probiotics.[212] Their application in critically ill patients, such as premature infants, does not entail risks related to bacterial translocation or induction of bacterial resistance.[213] Furthermore, some studies suggest that using probiotics in patients with diseases leading to severe intestinal inflammation may exacerbate the inflammation. In greatly compromised GIT ecosystems, even benign and supposedly beneficial strains can elicit disadvantageous responses.[213,214]

Many bifidobacterial products, including bacteriocins, lipoteichoic acids (LTA), aromatic lactic acids, pili, acetate, EPSs, and bacterial extracellular vesicles (BEVs), have beneficial effects and immunomodulatory properties.[215–217] The latter two are relevant for this thesis, and they will be discussed in more detail in the following chapter.

*Table 1: List of GIT microbiota modulation vaccine intervention studies performed in human cohorts*[218–221]

| Study subjects | Intervention type | Used agent | Associated vaccine | Immune effect | Location | Ref |
|---|---|---|---|---|---|---|
| Neonates | Probiotic | *B. longum* BB536 | Diphtheria-Tetanus-acellular Pertussis (DTaP), Polio, Hepatitis B | No difference in antigen-specific IgG | China | 151 |
| Neonates | Probiotic | *B. longum* BL999<br>*L. rhamnosus* LPR | Hepatitis B, DTaP | No difference in antigen-specific IgG | Singapore | 222 |
| Neonates | Probiotic | *B. breve* Bbi99<br>*L. rhamnosus* GG<br>*L. rhamnosus* LG705<br>*P. freudenreichii* | DTaP, Haemophilus influenzae type b (Hib) | Increased Hib-specific IgG<br>No difference in DTaP-specific IgG | Finland | 223 |
| Neonates | Probiotic | *B. breve* C50<br>*S. thermophilus* | DTaP, polio, Hib | Increased polio-specific IgA | France | 224 |
| Infants | Probiotic | *B. bifidum*<br>*B. longum* subsp. *infantis*<br>*B. longum* subsp. *longum*<br>*L. acidophilus* | Measles, mumps and rubella (MMR) | Higher overall seroconversion | Israel | 225 |
| Infants | Probiotic | *L. paracasei* F19 | DTaP, Hib, polio | Higher DTaP-specific IgG<br>No difference in anti-Hib and anti-polio IgG | Schweden | 226 |
| Infants | Probiotic | *L. casei* GG | RV | Higher RV-specific IgM and IgA | Finland | 227 |

| Study subjects | Intervention type | Used agent | Associated vaccine | Immune effect | Location | Ref |
|---|---|---|---|---|---|---|
| Infants | Probiotic | *B. animalis* subsp. *lactis* BB-12 | RV, polio | Significant increase in anti-polio IgA<br>Tendency of anti-RV IgA increase | USA | 228 |
| Children | Probiotic | *B. breve* BBG-01 | Cholera | Lower cholera-specific IgA | Bangladesh | 229 |
| Children | Probiotic | *L. acidophilus* CRL730<br>*S. thermophilus* | PCV, DTaP, Hib | No difference in antigen-specific antibody titres | Argentina | 230 |
| Pregnant women | Probiotic | *L. rhamnosus* GG | DTaP, Hib, PCV | Lower PCV- and DTaP-specific IgG<br>No difference in Hib-specific IgG<br>Higher Treg responses | Australia | 231 |
| Adults | Probiotic | *L. coryniformis* CECT 5711 | Hepatitis A | Increase of antigen-specific IgG and IgM | Spain | 232 |
| Adults | Probiotic | *L. coryniformis* CECT 5711 | Severe Acute Respiratory Syndrome Coronavirus-2 (SARS-CoV-2) | No difference in antigen-specific antibody titres | Spain | 233 |
| Adults | Probiotic | *L. paracasei* MCC1849 | Influenza | No difference in antigen-specific antibody titres<br>No difference in NK, neutrophil, phagocytic activity | Japan | 234 |
| Adults | Probiotic | *L. paracasei* 431 | Influenza | No difference in antigen-specific antibody titres | Germany, Denmark | 235 |
| Adults | Probiotic | *L. paracasei* MoLac-1 | Influenza | No difference in antigen-specific antibody titres<br>No difference in NK, neutrophil, phagocytic activity | Japan | 236 |

| Study subjects | Intervention type | Used agent | Associated vaccine | Immune effect | Location | Ref |
|---|---|---|---|---|---|---|
| Adults | Probiotic | *L. casei* Shirota | Influenza | No difference in antigen-specific antibody titres | Belgium | 237 |
| Adults | Probiotic | *L. plantarum* CECT7315/7316 | Influenza | Increase in antigen-specific IgG, IgA and IgM | Spain | 238 |
| Adults | Probiotic | *B. animalis* subsp. *lactis* BB-12<br>*L. paracasei* 431 | Influenza | Higher antigen-specific IgG and IgA<br>No difference in NK, CD4+ T cell, phagocytic activity<br>No difference in INF-γ, IL-2, IL-10 | Italy | 239 |
| Adults | Probiotic | *L rhamnosus* GG | Influenza | No difference in seroconversion rates<br>Increase in hemagglutinin titres | USA | 240 |
| Adults | Probiotic | *B. longum* BB536 | Influenza | Increase in influenza-specific antibody titres<br>No difference in NK and neutrophil activity | Japan | 241 |
| Adults | Probiotic | *L. casei* DN-114 001<br>*L. bulgaricus*<br>*S. thermophilus* | Influenza | Higher influenza-specific IgG | France | 242 |
| Adults | Probiotic | *L. fermentum* CECT5716 | Influenza | Increase in influenza-specific IgA, IgG, and IgM<br>Higher TNF-α levels<br>No difference in B & T, NK cell numbers<br>No difference in IL-10, IL-12, and IFN-γ levels | Spain | 243 |

| Study subjects | Intervention type | Used agent | Associated vaccine | Immune effect | Location | Ref |
|---|---|---|---|---|---|---|
| Adults | Probiotic | *L. acidophilus* CRL431<br>*L. rhamnosus* GG | Oral polio vaccine (OPV) | Increase in polio-specific IgA and IgM<br>No difference in polio-specific IgG | Germany | [244] |
| Adults | Probiotic | *B. animalis* subsp. *lactis* Bi-07<br>*B. animalis* subsp. *lactis* Bi-04<br>*L. acidophilus* La-14<br>*L. acidophilus* NCFM<br>*L. plantarum* Lp-115<br>*L. paracasei* Lpc-37<br>*L. salivarius* Ls-33 | Cholera | Increased cholera-specific IgG, IgA, and IgM | France | [186] |
| Adults | Probiotic | *L. rhamnosus* GG<br>*L. lactis* | Typhoid | No difference in antigen-specific antibody titres<br>Higher CR3 receptor expression on neutrophils | Finland | [245] |
| Adults | Prebiotic & Postbiotic | Enteral formula supplemented with GOS, bifidogenic growth stimulator (BGS) and pasteurised fermented milk products | Influenza | Increase in antigen-specific antibody titres | Japan | [246] |

| Study subjects | Intervention type | Used agent | Associated vaccine | Immune effect | Location | Ref |
|---|---|---|---|---|---|---|
| Adults | Prebiotic & Postbiotic | Enteral formula supplemented with GOS, BGS and pasteurised fermented milk products | Influenza | No difference or decrease in antigen-specific antibody titres | Japan | 247 |
| Adults | Postbiotic | Heat-killed *L. plantarum* L-137 | Influenza | No difference in seroconversion and seroprotection rate or antibody titres | Japan | 248 |
| Adults | Prebiotic | FOS | Influenza | Increase in antigen-specific antibody titres | Chile | 249 |
| Adults | Prebiotic | High oleic safflower oil, soybean oil, FOS, structured triglycerol | Influenza | Increase in antigen-specific antibody titres in serum<br>Higher levels of influenza-activated lymphocytes<br>Lower levels of IL-6 and IL-10 | USA | 250 |
| Adults | Prebiotic | Antioxidants, B vitamins, selenium, zinc, FOS, structured triglycerol | Influenza | Increase in antigen-specific antibody titres in serum<br>Increased lymphocyte proliferation | USA | 251 |
| Adults | Prebiotic | Long-chain inulin and FOS | Influenza | Increase in antigen-specific IgG titres in serum | UK | 252 |
| Adults | Prebiotic & Probiotic | *B. longum* subsp. *infantis* CCUG 52486<br>Glucose-derived oligo-saccharides (Gl-OS) | Influenza | No difference in immune cell numbers, seroconversion and antigen-specific antibody titres | UK | 253 |
| Adults | Prebiotic & Probiotic | *B. longum* subsp. *infantis* CCUG 52486<br>Gl-OS | Influenza | No difference in immune cell numbers, seroconversion and antigen-specific antibody titres | UK | 254 |

# 3. Immune stimulatory properties of selected bifidobacterial products

## 3.1. Exopolysaccharides

EPSs are clusters of mono- or oligosaccharides including glucose, fructose, galactose, fucose and/or rhamnose forming either homo- or heteropolysaccharides.[1,145] These can be secreted into the intestinal environment or associated with the bacterial cell wall.[1,7,143,255] Previous studies have demonstrated that the expression of EPS plays a crucial role in enhancing adhesion to host cells, providing protection from digestion and environmental stress, and facilitating the formation of biofilms, thus contributing to long-term colonisation within the GIT.[1,7,145,255–257] Additionally, bifidobacterial EPS can be metabolised by other microbiota members, promoting beneficial colonisation and altering the GIT metabolite milieu, including levels of SCFAs.[1,255,258–260] Moreover, EPSs can directly stimulate immune cells and IECs via activation of TLR1, 2, 4 and/or TLR6, mediating immune modulatory responses.[1,6,256] Depending on their chemo-physical properties, such as molecular weight and charge[145], EPSs can induce production of distinct cytokine profiles driving naïve $CD4^+$ T cell polarisation in a strain-dependent manner.[1,261] For instance, EPS from *B. longum* subsp. *longum* BCRC14634 and *B. adolescentis* IF1-03 enhance IL-10 secretion by macrophages and subsequent Treg expansion.[6,262] Similarly, *B. longum* subsp. *longum* 35624 producing EPS, but not an isogenic EPS-negative mutant, decreased pro-inflammatory cytokine secretion, suppressing Th17 polarisation.[1,263] EPSs from different *B. breve* strains are linked to 'immune silencing', inhibiting DC maturation and $CD4^+$ T cell activation and lowering pro-inflammatory cytokine levels.[264,265] Conversely, EPS from *B. adolescentis* IF1-11 stimulates macrophage production of high levels of IL-6, IL-17A and TGF-β, and low amounts of IL-10, skewing T cell polarisation towards Th17 responses *in vivo*.[1,6] EPSs from *B. longum* subsp. *longum* XZ01 and *B. breve* H4-2 activate TLR4 on macrophages, inducing expression of IL-1β, IL-6, and TNF-α and increasing phagocytic activity and NO production.[266,267] Interestingly, use of EPS-producing *B. breve* H4-2 in a murine colitis model lowered pro-inflammatory cytokine levels while increasing SCFA, IL-10, mucin, and TJ protein production.[268] Equally, EPSs from *B. longum* subsp. *longum* W11 induced either

immune regulatory or immune stimulatory responses in human peripheral blood mononuclear cells (PBMCs), depending on the underlying inflammatory state.[269] *B. longum* subsp. *infantis* E4 reduced production of NO, IL-1β, IL-6, and TNF-α in macrophages while increasing splenic lymphocyte proliferation and NK cell activity *in vitro*.[270]

These studies emphasise the strain- and condition-dependent immunomodulatory abilities of bifidobacterial EPS, highlighting potential vaccine adjuvant use challenges.[1] Still, Xiu et al. (2018)[271] proposed EPS derived from *L. casei* as a novel adjuvant, opening potential avenues for EPS from probiotics for vaccine optimisation.

More details about potential immune modulation by bifidobacterial EPS are discussed in Results Chapter I.

## 3.2. Extracellular microvesicles

### *3.2.1. Characteristics and function of BEVs*

Vesiculogenesis is an important cellular response mechanism to internal and environmental stressors occurring in all kingdoms of life forms.[272,273]

Although widely studied in Gram-negative bacteria for over 60 years[43,274–276], it was long assumed that Gram-positive bacteria were incapable of producing BEVs due to the presence of a thick peptidoglycan cell wall layer. This assumption persisted until the first report of BEV production by a Gram-positive bacterium emerged in 1990.[277] Given the focus of this thesis, the present chapter concentrates specifically on BEVs derived from Gram-positive bacteria. Comparison with Gram-negative BEVs is included only where relevant, primarily to highlight the significant knowledge gaps between these distinct classes of BEVs.

Studies of BEVs produced by Gram-positive bacteria account for ~16% of all BEV-related studies published between 2015 and 2021, most of which were focused on pathogens.[278]

#### a) Biogenesis of BEV types

BEV biogenesis in Gram-positive bacteria is poorly understood; however, several potential mechanisms for vesiculogenesis have been proposed. These include I) formation of porous regions along the cell wall, releasing BEVs that bud off from protrusions of specific lipid-rich sections with enhanced membrane fluidity of the

cytoplasmic membrane via turgor pressure, II) partial degradation of crosslinking structures of the peptidoglycan layer through different prophage-encoded endolysins, autolysins, proteases, penicillin-binding proteins, and enzymes induced by environmental stress, and III) explosive cell lysis (see Figure 3).[273,275,279–281] None of these mechanisms is unique to Gram-positive bacteria, as they have been previously reported for specific Gram-negative BEV subtypes (blebbing for B-type BEVs and explosive cell lysis for E-type BEVs, respectively).[282,283] Other means of vesiculogenesis documented in Gram-negative bacteria, such as secretion at the division septum, have not been described in Gram-positive bacteria.[273,284] Different internal and external factors regulating BEV release have been studied, including growth stage, nutrient availability, pH, oxidative stress, and exposure to probiotics and antibiotics.[285–287] In certain species, specific genes have been linked to the regulation of vesiculogenesis, such as transcription factor $\sigma^B$ in *Listeria monocytogenes*[288], *psm* in *S. aureus*[289] or *spo0A* and *spf* in Group A Streptococcus.[290] However, conserved genes or general mechanisms applicable to vesiculogenesis in all Gram-positive bacteria have yet to be determined.[291]

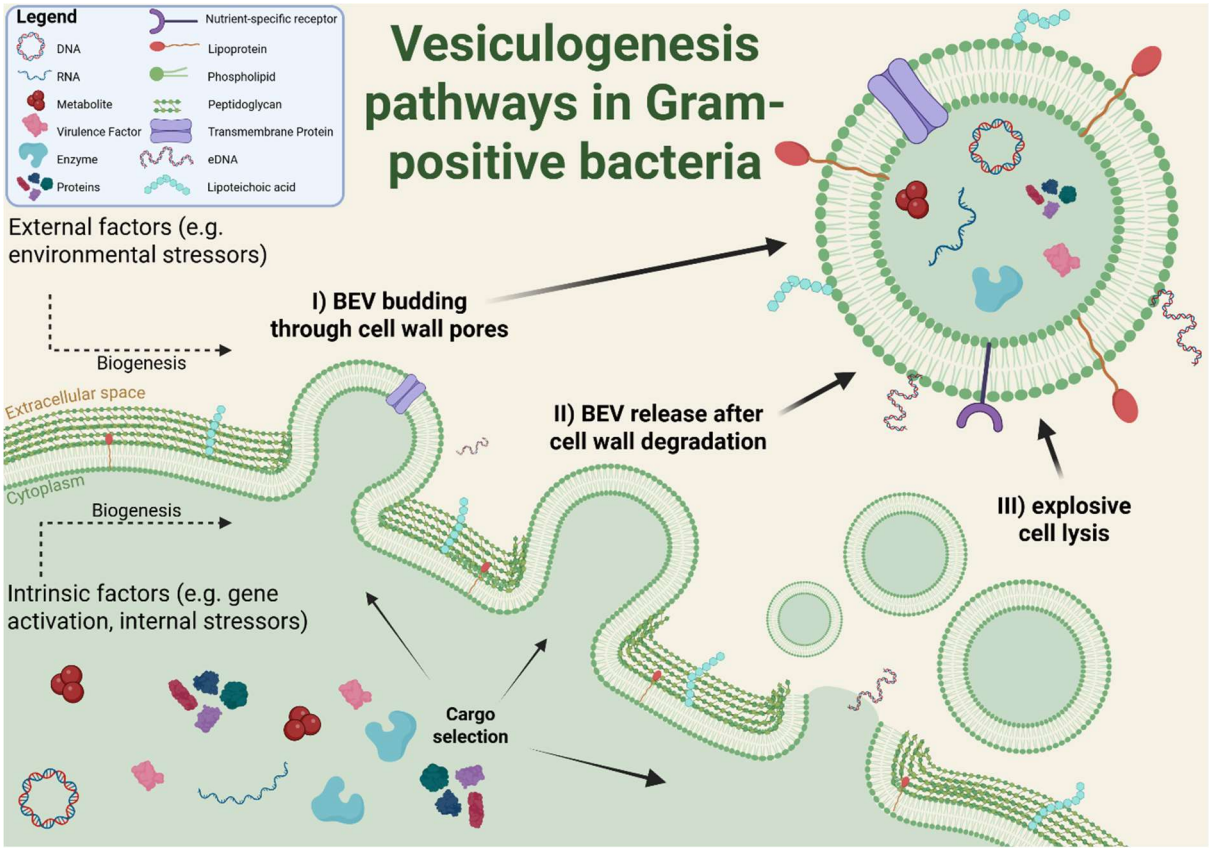


*Figure 3: Scheme of proposed BEV structure and biogenesis mechanisms in Gram-positive bacteria. Created with BioRender.com*

Gram-positive BEVs can be divided into cytoplasmic membrane vesicles (CMVs) or explosive CMVs (ECMVs).[283] However, the nomenclature of BEVs has been inconsistent and current limitations in isolation and separation methodologies, combined with a lack of reliable biomarkers, make it impossible to distinguish BEVs of different biogenetic origin. Consequently, preparations often contain heterogeneous mixtures of multiple BEV subtypes.[283,292] To address this issue, the term BEV has been proposed as an overarching designation for studies involving diverse bacterial vesicles and is therefore used consistently throughout this thesis.[278]

BEV production is a continuous process by metabolically active bacteria, resulting in the release of heterogeneous BEVs varying in biogenesis, size, yield and content, which support various vital cellular functions.[280]

### b) Functions based on content and size

BEVs are nano-sized (20-400nm), spherical, membranous structures, and similar in appearance to Gram-negative BEVs.[278]

Depending on the respective biogenesis pathway and growth cycle, they contain various components of their parental organism, including proteins (both membranal and cytoplasmic)[293,294], peptidoglycan, LTAs, and other elements of the cell membrane[295–297], small genetic molecules such as RNA (including messenger RNA [mRNA], transfer RNA [tRNA], ribosomal RNA [rRNA], and small RNA [sRNA])[295,298–300] and DNA (of chromosomal, plasmid, and prophage origin, as well as extracellular DNA [eDNA])[295,301,302], lipoprotein[303], virulence factors[304], metabolites[305,306] and specific enzymes, that are robustly protected from external degradation.[273] Although cargo selectivity has been documented in different Gram-positive bacteria via differences in multi-omic profiles between bacteria and BEVs[280], active selection and loading pathways in Gram-positive bacteria have yet to be determined.[283,290,303] However, BEVs originating from *S. aureus* have been shown to contain increased numbers of positively charged proteins, suggesting a passive sorting mechanism based on electrostatic interactions between differently charged membrane domains and proteins at the vesicle formation site.[283,307] A further key role that BEVs play for their bacterial host is that they enable the release of molecules that cannot be exported via classical secretion systems.[283]

Factors, such as bacterial growth stage and nutrient availability, influence the biogenesis of BEVs and similarly affect cargo load and size of the released vesicles, in line with specific environmental or internal stress responses. Essential for interspecies and interkingdom communication[308,309], BEVs of both Gram-positive and Gram-negative bacteria can mediate resistance, inactivation and /or degradation of antibiotics[43,310–312], nutrient acquisition and metabolism[313,314], quorum sensing[315], pathogenesis and virulence[291], colonisation, and/or biofilm formation and maintenance.[43,302] The diverse cargo of BEVs enables multifaceted functions, including potential horizontal gene transfer, AMP delivery, and antibiotic and ROS protection to neighbouring bacteria.[105,310,316] They also aid in bacterial survival by removing misfolded proteins.[283]

BEVs derived from pathogens promote adherence to host cells, penetration of the mucosal layer, enhance virulence, and aid in immune evasion.[43,317] Specifically, BEVs can be used as decoys to escape neutrophil extracellular traps (NETs)[318], antimicrobial fatty acids and peptides[319], complement system factors, as well as neutralising phages, and membrane-targeting antibiotics.[283,320,321]

BEVs from commensal bacteria contribute to cooperation and syntrophic interactions among members of complex microbial communities.[1] They also act as mediators of interkingdom communication between members of the GIT microbiota and the host, thus facilitating microbiota homeostasis.[287,322,323] BEVs packaged with degrading enzymes and bacteriocins can be used to exhibit antibacterial and antifungal activity, protecting the host from pathogenic invasion.[273,324] Due to their size and packaged MAMPS, BEVs are ideal for molecular delivery to distant sites within the host. Indeed, BEVs derived from the GIT microbiota have been detected in the bloodstream, from where they can access different tissues, including the brain.[325,326] They can cross the intestinal barrier para- and/or transcellularly and stimulate local and systemic immune responses.[326,327] Interestingly, BEVs from the maternal GIT microbiota can cross the placental barrier and interact with the foetus prenatally, as identical BEV profiles were detected in amniotic fluid and maternal microbiota samples. *In vivo* tests confirmed BEV presence within the amniotic space.[328]

### c) Signalling and cargo delivery

BEVs utilise two distinct mechanisms to exert their effects: I) direct interaction with the target cell membrane and II) delivery of bioactive cargo to target cells.[282] A

direct interaction suggests binding of surface molecules of BEVs to specific receptors on the surface of the respective target cell, which results in downstream signal transduction and activation.[282] This is crucial for many immunomodulatory properties of BEVs and is discussed in more detail below.

Uptake of BEVs by target cells occurs via specific mechanisms, which is dependent on cell type and BEV size and structural surface composition. The majority of cellular uptake of BEV has been associated with pinocytotic and/or endocytotic pathways.[326] Many studies have reported membrane fusion between BEVs of one bacterial strain with other co-cultured bacteria, leading to delivery of bacteriocins, cell-wall-degrading enzymes and other antimicrobial peptides, which in turn inhibit growth of competing, pathogenic strains.[273,324,329] Vesicular inter-bacterial interactions can also support survival of syntrophic microbes through the delivery of specific metabolites, and promoting micronutrient acquisition and cross-feeding.[273,330] Target specificity of BEV-bacterial membrane fusions has been proposed, though the underlying mechanisms still need elucidation.[283] Similarly, BEVs have been shown to fuse with cholesterin-rich domains of host cell membranes to release their content, which can further be facilitated by host cell lipid rafts.[273,283,331] Other modes of delivery to host cells described in Gram-positive BEVs include dynamin-dependent, clathrin-dependent endocytosis and phagocytosis.[280] Interestingly, preferred BEV entry mechanisms for distinct host cell types have been reported, such as clathrin-dependent endocytosis for *Cutibacterium acnes*-derived BEV internalisation in human epidermal keratinocytes, and lipid rafts for *S. aureus* BEV delivery in epithelial cells.[273,332,333] Although currently not documented in Gram-positive BEVs, additional routes of BEV uptake, such as actin-driven micropinocytosis, caveolin-mediated endocytosis, and non-caveolin and non-clathrin-mediated endocytosis, as seen in Gram-negative BEVs, could also potentially exist in Gram-positive BEVs.[280,326] Additionally, BEVs have been shown to translocate transcellularly through epithelial and endothelial cells following similar internalisation routes, as well as via paracellular transport.[283,325]

More details about BEV uptake and translocation are discussed in Results Chapter III.

### *3.2.2. Use of BEVs in immune stimulation and therapeutics*

The immune system responds to the MAMPs and other microbial signals from BEVs by activating specific PRRs and subsequently producing cytokines.[334] For

instance, surface MAMPs of BEVs from *S. aureus* were found to activate TLR2 and TLR4, whereas loaded RNA and DNA of these BEVs were detected by TLR7, 8 and 9, respectively.[43,295] Consequently, BEVs derived from pathogens can induce immune responses against the vesicles themselves and their parental bacterium, while commensally derived BEVs act similarly to other postbiotics.[335]

As a result, BEVs have been gaining importance for applications in drug delivery, immune therapy and vaccination. They remain stable across a wide temperature and pH range. They are resistant to enzymatic degradation, allowing protective delivery of antigens, drugs and/or bacterial compounds directly and needle-free to mucosal sites.[1,274,325,336,337] Indeed, BEVs have been shown to deliver biologically relevant, highly concentrated doses of bioactive molecules, such as β-lactamases, virulence factors, or quorum-sensing molecules, promoting gene expression changes, antibiotic survival or apoptosis in the recipient cell.[283] Additionally, BEVs are non-replicating and inanimate, limiting the risk of potential adverse effects.[1] Still, due to their immunogenic composition and self-adjuvant features, they promote strong innate and adaptive immune responses and protection against infectious diseases.[1,335,338] Compared to live bacteria, BEVs derived from probiotic bacteria have a further enhanced safety profile after administration, thus gaining attention as potential alternatives to probiotics.[339] Due to their proven antimicrobial activity and inhibition of pathogens, including antibiotic-resistant bacteria, probiotic BEVs from *L. paracasei* and *L. plantarum* are proposed as a novel form of antimicrobials.[340–342] Moreover, BEVs have also been found to transfer phage entry receptors to invasive bacteria, further inhibiting pathogenic growth in combination with phage therapy.[280,343]

Postbiotic administration of BEVs derived from probiotic *Escherichia coli* strains to neonatal rats enhanced plasma IgG, IgA and IgM titres, increased splenic Tct and NK cell counts. It promoted gene expression towards maturation, homeostasis and protection of the GIT.[344] Similarly, *Lactobacillus sakei* subsp. *sakei* NBRC15893-derived BEVs promote IgA production in murine PPs via TLR2 activation on DCs and subsequent IL-6, RA and NO production.[345,346]

*In vitro* screening of BEVs derived from different probiotic and commensal *E. coli* strains revealed strong DC stimulation to induce T cell polarisation towards pro- and anti-inflammatory phenotypes via distinct cytokine and exosome profiles in a strain-dependent manner.[347] BEVs from other commensal bacteria, such as *L. plantarum*,

*Clostridium butyricum*, *E. coli* Nissle 1917 and *Bacteroides thetaiotaomicron* also induce anti-inflammatory responses by polarising macrophages towards an M2 phenotype, producing IL-10.[348–353] Additionally, BEVs from *E. coli* Nissle 1917 and *Bacteroides fragilis* also improve the gut barrier by enhancing TJ functionality and production of AMPs and anti-inflammatory cytokines.[354,355] Improvement of gut barrier integrity, enhanced communication with IECs, and reduced permeability – key factors in maintaining immune homeostasis – have been associated with probiotic BEVs in therapeutic *in vivo* studies. These effects are linked to the regulation of TJ proteins, including Zonula Occludens (ZO)-1, occludin, and claudins, and have been demonstrated in models of chronic colon inflammation, irritable bowel syndrome (IBS), ulceritis, and allergies.[286,339,356]

Epithelial cells treated with BEVs from *Faecalibacterium prausnitzii* increased production of TNF-α, IL-4, IL-8 and IL-10 while decreasing IL-1β, IL-2, IL-6, IL-12, IL-17A, and IFN-γ levels.[357] Additionally, BEVs from the GIT microbiota were able to prime neutrophils, inducing production of TNF-α, IL-6, MCP-1, and ROS, and enhancing migration and phagocytosis *in vivo*.[358] They also activate TLR2 and TLR4 in macrophages and IECs, promoting IL-6 and IL-8 secretion, further increasing recruitment of neutrophils.[43] Pathogen-derived BEVs also induce production of NETs, enhancing clearance of the respective pathogen.[359] In macrophages, they have been found to trigger inflammasome activation.[283,303]

The therapeutic potential of BEVs has been demonstrated in different pathological conditions: *L. plantarum* BEVs induced expression of specific microRNAs, which are linked to reduced ischemic neuronal cell death, giving rise to novel ischemic stroke treatments.[360] Oral administration of BEVs from the same species had similar therapeutic effects as hormonal drugs in a chronic skin inflammation mouse model via macrophage polarisation towards anti-inflammatory M2 phenotype.[361] In other studies, BEVs from other *Ligilactobacillus* (formerly *Lactobacillus*) species were able to support wound healing, revascularisation, follicle reconstruction, and scarring reduction through similar anti-inflammatory stimulation.[339,362–364] They have also been found to protect against HIV-1 infection, inhibiting viral attachment and entry into vaginal *ex vivo* tissue[365], as well as osteoporosis, stimulating osteoblast formation and bone density.[366] Similarly, in combination with vitamin D3, they reduce *H. pylori* attachment to gastric cells and lower *H. pylori*-induced inflammation, holding potential for *H. pylori*

therapy.[367] Moreover, BEVs have also been found to improve cancer vaccine and therapy outcomes via induction of long-term anti-tumour responses dependent on IFN-γ without detectable adverse effects.[368] In another study, bioengineered BEVs from *E. coli* were used to carry small interfering RNA (siRNA) to target and kill cancer cells.[369] Recently, *Ligilactobacillus*-derived BEVs were found to induce IL-12 production in DCs via TLR9 activation without promoting IL-10 secretion, mediate T cell polarisation towards Th1 and Tct responses and enhance checkpoint blockade therapy efficacy *in vivo*.[370] In a different study, they were shown to downregulate cancer-specific genes and induce apoptosis, leading to cytotoxic effects on hepatic and colorectal cancer cells and reduced tumour size.[368,371,372]Given that studies focusing on BEVs derived from Gram-positive, commensal and probiotic strains have been scarce, there is potential for novel immunostimulants in vaccine development, immunotherapy and drug delivery, especially when paired with targeted bioengineering.[278] However, to date, no clinical studies on probiotic BEVs in therapeutic settings − against infectious or non-infectious diseases − have been performed.[286]

### *3.2.3. Bifidobacterial BEVs*

Understanding of bifidobacterial BEV properties and potential applications is in its infancy, as only a handful of studies have focused on BEVs derived from *Bifidobacterium* species (see Table 2).

Similar to studies focusing on administration of whole *Bifidobacterium* and/or their metabolites (e.g. EPS, acetate), there are strain-dependent differences in the induced immune modulation by bifidobacterial BEVs. However, due to the limited number of findings and their differing focus and study models, no clear conclusions can be drawn yet. Still, abundance of peptidoglycans and moonlighting proteins that induce immune responses, such as extracellular solute-binding proteins (ESBPs) and chaperone GroEL, appear to be common denominators for immune modulation by bifidobacterial BEVs.

*Table 2: Overview of studies using bifidobacterial BEVs*

| Parental strain | Study model | Immune modulation | Underlying mechanism | Ref |
|---|---|---|---|---|
| *B. bifidum* LMG13195 | DC and naïve T cell co-cultures | Increased production of IL-10<br><br>Enhanced T cell polarisation towards Tregs | Not stated | [373] |

| Parental strain | Study model | Immune modulation | Underlying mechanism | Ref |
|---|---|---|---|---|
| *B. longum* subsp. *longum* KACC91563 | Murine allergy model | Induced apoptosis of mast cells<br><br>No disturbance of T cell responses<br><br>Improved allergy symptoms | ESBPs within BEVs induce immune modulation | 374 |
| *B. longum* subsp. *longum* NCC2705 | *In vitro* mucin<br><br>*In vivo* mice | Increased adhesion and persistence in the GIT | High abundance of mucin-binding proteins | 375 |
| *B. bifidum* BIA-7 | Epithelial cells | Increased expression of TJ proteins | Activation of aryl hydrocarbon receptor (AhR) signalling pathway | 376 |
| *B. longum* subsp. *infantis* JCM1222$^{T}$ | *Ex vivo* murine PP cells<br><br>*In vitro* murine macrophages | Induction of IgA production in PP cells<br><br>Increased IL-6 production in macrophages | ESBPs within BEVs induce immune modulation | 377 |
| *B. longum* subsp. *longum* AO44 | Splenocytes<br><br>DC-CD4$^{+}$ T cell co-cultures | Increased IL-10 production | ESBPs within BEVs induce immune modulation | 308 |
| *B. longum* subsp. *longum* | Mice | Increased TNF-α, CD40 and CD80 levels in splenic macrophages | Increased amounts of peptidoglycan and ODN | 378 |
| *B. longum* subsp. *longum* NSP001 | Colitis mouse model (both pseudo-germfree and non-germfree)<br><br>*In vitro* murine macrophages | Inhibition of M1-type macrophage polarisation and IL-1β, IL-6, IL-17A and TNF-α production<br><br>Restoration of MUC2, ZO-1, and Occludin production<br><br>Reduced macrophage, neutrophil and Th17 cell infiltration; Treg increased<br><br>Increased expression of IL-10 and TGF-β | Inhibition of phosphorylation of STAT3<br><br>Increased SCFA production via microbiota composition shift | 379 |
| Mixture of *B. longum* subsp. *infantis* (Bi26), *B. bifidum* (Bb-02), *B. longum* subsp. *longum* (Bl-05), *B. bifidum* (Bb-06), *B. lactis* (Bl-04), *B. lactis* (Bl-07) and *B. breve* (Bb-03) | Lung cancer mouse model<br><br>*In vitro* human and murine lung cancer cells<br><br>Murine small intestinal tissue and human lung cancer organoids | Increased programmed cell death 1 ligand 1 (PD-L1), IL-2 and IFN-γ expression<br><br>Increased tumour-infiltrating CD8$^{+}$ T cells<br><br>Enhanced therapeutic efficacy of anti-programmed cell death 1 (PD-1)<br><br>Reduced levels of TNF-α | TLR4-NF-κB pathways activation<br><br>Downregulation of Ras-MAPK, TGF-β, and angiogenesis pathways | 380 |

| Parental strain | Study model | Immune modulation | Underlying mechanism | Ref |
|---|---|---|---|---|
| *B. longum* subsp. *infantis* | *In vitro* murine macrophages<br><br>IBD mouse model | Macrophage polarisation driven from M1- to M2-phenotypes<br><br>Reduction of IL-1β, IL-2, IL-6, and TNF-α expression<br><br>Increase of IL-10 and TGF-β levels | Not stated | 381 |
| *B. longum* subsp. *longum 15707* | Hepatocellular carcinoma mouse model | Decreased intracellular ROS levels and apoptosis<br><br>Lowered tumour incidence rate and tumour number<br><br>Increased levels of anti-oxidant proteins | Attenuation TGF-β signalling and Smad3 phosphorylation | 382 |

López et al. (2011)[373] compared immunomodulatory properties of whole *B. bifidum* LMG13195 and their produced BEVs, indicating increased immunosuppression, IL-10 release and Treg cell abundance *in vitro* after exposing DCs to BEV fractions. Equally, BEVs from *B. longum* subsp. *longum* AO44 exerted anti-inflammatory responses, inducing IL-10 production in murine splenocytes and co-cultures of DCs priming naïve $CD4^+$ T cells.[308] Oral administration of *B. longum* subsp. *longum* NSP001- and *B. longum* subsp. *infantis*-derived BEVs resulted in dampening colitis and IBD symptoms, respectively, enhancing intestinal barrier function, reducing pro-inflammatory immune cell differentiation and cytokine production, and promoting anti-inflammatory cytokine secretion, alterations in gut microbiota composition and subsequent SCFA production.[379,381] Similar improvement has also been documented in pseudo-germfree mice (i.e., mice with antibiotic-depleted GIT bacteria), indicating that the anti-inflammatory effects of these BEVs are independent of their microbiota effects.[379]

Tests of *B. longum* subsp. *longum* KACC 91532-derived BEVs revealed beneficial effects in the context of food allergies. Family 5 ESBPs within vesicles directly interacted with resident mast cells in the small intestinal lamina propria to induce targeted apoptosis. The parental *Bifidobacterium* and their BEVs did not induce cell death in T cells, B lymphocytes or eosinophils *in vitro* and *in vivo,* specifically targeting mast cells.[374] Additionally, BEVs derived from *B. longum* subsp. *longum* NCC2705 and *B. bifidum* BIA-7 interact with the epithelial barrier, adhering to mucin, translocating

into IECs and improving the expression of TJ proteins such as occludin and cytochrome P450 family 1 subfamily A member 1 (CYP1A1) through activation of the AhR pathway.[375,376] Interestingly, only treatment with BEVs from *B. bifidum* BIA-7, but not with the whole cell parent, activated AhR signalling.[376]

Immune stimulation was reported for BEVs from *B. longum* subsp. *infantis* JCM1222$^T$ and *B. longum* subsp. *longum,* inducing the production of pro-inflammatory cytokines and co-stimulatory molecules by macrophages.[377,378] Kurata et al. (2022)[377] identified a specific ESBP present within the BEVs to activate TLR2 on macrophages, leading to the release of IL-6 and subsequent promotion of IgA secretion in *ex vivo* PP cell cultures. Comparing the potential immune modulation by BEVs derived from *B. longum* subsp. *longum* and *L. plantarum* WCFS1, Morishita et al. (2023)[378] found that bifidobacterial BEVs have increased potential to promote TNF-α, CD40 and CD80 expression in splenic macrophages compared to *L. plantarum*-derived BEVs. Compositional differences revealed higher levels of cell wall-derived peptidoglycan and ODN in bifidobacterial BEVs. Noteworthy, immune stimulation by both BEV types was only detectable when administered subcutaneously, but not intravenously.[378]

Most recently, oral administration of a cocktail of BEVs from different *Bifidobacterium* strains showed potential synergy with the anti-PD-1 cancer treatment of lung cancer via TLR4 activation, inducing expression of key cytokines and PD-L1, increasing immune cell infiltration into the tumour, and downregulating oncogenic pathways.[380] Taken together, BEVs derived from *Bifidobacterium* strains that possess immunomodulatory properties have great potential to induce similar immune responses as their parent in a cell-free manner. Considering the benefits of *Bifidobacterium* species to overall immunity, bifidobacterial BEVs may be attractive candidates for developing novel therapeutics.

# 4. Bifidobacterial BEVs as potential novel vaccine adjuvants

## 4.1. Influence of the infant GIT microbiota on immunity and vaccination

Given the intimate, bidirectional relationship between the immune system and GIT microbiota, and their concurrent development during the period of major vaccine-induced immunisation, a gut-vaccination axis has emerged. Notably, the abundance

of certain bacterial species positively and/or negatively impacts immune responses to different vaccines.[1] For instance, Huda et al. (2014)[383] reported a positive association between Actinomycetota abundance and systemic immune responses after administration of Bacillus Calmette-Guérin (BCG), tetanus, OPV, and hepatitis B vaccines in Bangladeshi infants. In contrast, predominant Enterobacteria exhibited negative effects on vaccine efficacy.[383] In a follow-up study, Bangladeshi infants with highly abundant *Bifidobacterium* species (i.a. Actinomycetota) showed elevated $CD4^+$ T cell responses and higher levels of antigen-specific IgG and IgA to BCG, tetanus, and polio vaccine at 15 weeks and 2 years of age.[1,90] A comparative study on the microbial profiles of children from Ghana, Pakistan, Bangladesh, and the Netherlands found that responders to RV vaccination shared similar microbiota compositions to healthy age-matched Dutch infants rather than non-responders from the same cohort. This responder microbiota included a higher abundance of *Clostridium* cluster XI and Pseudomonadota and lower amounts of members of the Bacteroidota phylum, highlighting a potential link between distinct microbiota profiles with key bacterial species and subsequent heterologous vaccination outcomes across different populations.[1,4,384,385] However, similar studies conducted in India, Malawi, the UK, Zimbabwe and Nicaragua could not reproduce similar correlations between specific members of the GIT microbiota and RV vaccine efficacy, underlining limitations in comparability and lack of consistency of related studies.[108,386–390] Still, Parker et al. (2021)[108] did find that infants with a more diverse and 'mature' microbiota signature responded less to oral RV vaccination than those with a 'healthy', undisturbed early-life microbiota trajectory (see Figure 2).

Conversely, increased poliovirus-specific IgA responses were attributed to high abundance of *Bifidobacterium* species in Chinese infants following OPV administration.[391] High abundance of *Bifidobacterium* species was also positively associated with higher serum levels of neutralising antibodies in recipients of the CoronaVac SARS-CoV-2 vaccine.[392] In French children receiving the DTaP/Hib vaccine, poliovirus-specific IgA levels were elevated in infants with high abundance of *B. longum* subsp. *infantis*.[224] Similarly, *B. longum* subsp. *infantis* was also found to be a key stimulatory species in BCG high-responders with elevated numbers of $CD4^+$ Tcm and Tem, neutrophils, and lowered levels of pro-inflammatory monocytes, whereas *B. thetaiotaomicron* was predominant in low-responders.[393] However, *B.*

*breve* was inversely correlated to serum IgA titres to polio and cholera vaccination.[90,229]

Taken together, these observations further highlight the intricate interactions between the host's immune system, gut microbiota, and vaccination.[218] The microbiota plays a multi-factorial role in activating and regulating immune responses, affecting vaccination success. Due to this immunomodulatory potential, use of BEVs as possible natural adjuvant and antigen carrier has been investigated to maximise vaccine efficacy.[1,3,81]

## 4.2. BEVs in vaccination studies and formulations

Since immune stimulation by inactivated, subunit or nucleic acid antigens is less effective than seen in live-attenuated vaccines, many established vaccines require adjuvants to boost immunogenicity, contributing to efficacy variations within populations. Adjuvants activate and modulate innate immune responses, enhance the immunogenicity of antigens even at lower doses, and induce T and B cell-directed memory.[81,394,395] Moreover, adjuvants allow fine-tuning specific immune responses (see Table 3).

*Table 3: Overview of different adjuvant types used in vaccine studies[31,395,396]*

| Adjuvant | Type | Immune stimulation | Associated vaccine | Develop-ment Stage | Ref |
|---|---|---|---|---|---|
| Alum | Mineral salt | Controlled antigen release<br><br>Induction of DC and Th2 responses, and inflammasome | Hepatitis A & B, human papillomavirus (HPV), DTaP, Hib, MenA & B, PCV | Licensed for use in humans | 397–400 |
| Alhydroxiquim-II | Alum-absorbed Polyethylene glycol (PEG)–Glucuronid-Linker–Imidazo-[4,5-c]-chinolin | TLR7/8 ligand<br><br>Lymph node antigen delivery and controlled release | SARS-CoV-2 | Licensed for use in humans | 397, 401 |
| Cholera toxin | Toxoid | DC activation<br><br>Increased mucosal antigen uptake<br><br>Mucosal IgA and Th production | Cholera, *Naegleria flowleri*, HIV, Malaria, *Heliobacter pylori* | Licensed for use in humans<br><br>Pre-clinical | 398, 402–408 |

| Adjuvant | Type | Immune stimulation | Associated vaccine | Develop-ment Stage | Ref |
|---|---|---|---|---|---|
| Cytosine-phosphate-guanine oligodeoxy-nucleotides (CpG ODN) | Bacterial oligonucleotide | TLR9 ligand<br><br>Increase of Th1-specific cytokines<br><br>Stimulating $CD8^+$ T cell activity<br><br>Enhanced IgG class switching<br><br>Inducing DC maturation | Hepatitis B, SARS-CoV-2, PCV, HIV | Licensed for use in humans<br><br>Phase I & II | 397, 409–411 |
| Virus-like particle (VLP), Virosomes | Viral proteins | Improved APC antigen uptake<br><br>Promoting T and B cell activation | Hepatitis A & B, HPV, Influenza | Licensed for use in humans | 412–415 |
| MF59, AS03 | Oil-in-water emulsion | APC activation<br><br>Modulation of humoral and cellular immune responses | Influenza | Licensed for use in humans | 416–419 |
| ISA51 | Oil-in-water emulsion | Increased humoral response<br><br>Enhanced T cell activity | Influenza | Phase II | 419–421 |
| Monophos-phoryl lipid A (MPL), AS04 | Non-toxic derivative of LPS | TLR4 ligand<br><br>Induction of APC maturation<br><br>Stimulation of Th1 responses<br><br>Enhanced humoral and cellular immune responses | Hepatitis B, HPV | Licensed for use in humans | 422–424 |
| QS-21 | Purified plant extract containing saponins | Enhanced humoral and cellular immune responses<br><br>Stimulation of Tct responses | Varicella-zoster, Malaria, Respiratory syncytial virus (RSV) | Licensed for use in humans | 425, 426 |
| Matrix-M | Protein nanoparticle | Increased humoral response<br><br>Enhanced T cell activity | SARS-Cov-2 | Phase II | 427, 428 |

| Adjuvant | Type | Immune stimulation | Associated vaccine | Develop-ment Stage | Ref |
|---|---|---|---|---|---|
| VAX2012Q, VAX125 | Bacterial flagellin | TLR5 ligand<br>Increased humoral response<br>Enhanced DC, IEC, T and NK cell activity | Influenza, Plague | Phase II | 429–435 |
| Rintatolimod, PIKA | Poly I:C, dsRNA polymer analogue | TLR3 ligand<br>Increased humoral response<br>Induction of Th1 and Th17 responses | Influenza, Rabies, HIV | Phase I & III | 436–439 |
| GM-CSF | Cytokine | Improved mucosal IgA responses<br>Activation of DCs and T cells | HIV, SARS-CoV-2 | Phase I & II | 440–444 |
| IFN-α | Cytokine | Improved mucosal IgA responses | Influenza | Phase I | 442, 445 |
| CCL3 | Chemokine | Improved mucosal IgA responses | HIV | Pre-clinical | 446 |
| α-GalCer | Glycophingolipid | PRR ligand<br>Induction of Th1 responses<br>Improved mucosal IgA responses | Hepatitis B, Influenza, Malaria, Middle East Respiratory Syndrome (MERS) | Phase II<br>Pre-clinical | 447–450 |
| Chitosan | Polysaccharide | PRR ligand<br>Induction of Th2 responses<br>Improved mucosal IgA responses<br>Activation of complement system | Norovirus<br>*H. pylori* | Phase II | 451–453 |
| **BEVs** | **Bacterial nanoparticles** | **PRR ligand**<br>**Inducing activation and maturation of APCs** | **Meningitis B (MenB)**<br>**Hepatitis B** | **Licensed for use in humans**<br>**Pre-clinical** | 279, 297, 454–456 |

However, many adjuvants have potential safety risks in human use, causing severe adverse effects such as chronic inflammation.[81,457] Due to this, some adjuvants are partly responsible for the increased vaccine hesitancy in recent years.[458]

Additionally, the formulation of optimal vaccines and the discovery of optimal adjuvants remain challenging, especially for mucosal vaccines, as they require different types of adjuvants than those used for parenteral vaccines.[459] Only a few adjuvants are usable in different vaccine types, such as CpG ODN.[396] Ideally, an orally administered adjuvant is resistant to stomach acid and able to induce mucosal immunity without causing adverse GIT symptoms.[31] In a comparative study, BEVs from *Burkholderia pseudomallei* showed superior vaccine adjuvant properties with more robust cellular and humoral responses than traditional adjuvants, including alum, heat-killed bacteria, and CpG ODN.[460] In pre-clinical vaccination trials, *M. tuberculosis* BEV formulations, without additional adjuvants, had similar efficacy as the BCG vaccine, and acted as strong adjuvants when administered in combination with BCG, improving both humoral and cellular immune responses.[280,461] BEVs from non-pathogenic *S. aureus* and *S. pneumoniae* are being used as vaccination platforms in mice, providing cross-protection against pathogenic strains and lowering lethality of sepsis and pneumonia, respectively.[289,462]

To date, three vaccine formulations using *Neisseria meningitidis* BEVs have been commercially used, generating high cross-protection rates in both adults and children.[455,463,464]

Still, BEVs are extremely heterogeneous, varying in size and cargo even when deriving from the same bacterial strain, requiring thorough screening and characterisation of potentially immunomodulatory candidates.[287,465–467] Bioengineering of suitable non-pathogenic and/or probiotic BEVs to carry specific antigens from pathogens and/or altered amounts of eDNA, CpG ODNs, and other immunostimulants could further increase immune activation and vaccine efficacy.[273,286] Consequently, potential probiotic adjuvants such as bifidobacterial BEVs gain increased attention as they robustly deliver MAMPs for immunomodulation with reduced risk of adversity and are suitable for use in vulnerable populations such as infants and the elderly.[81,468]

## 5. Conclusions and perspectives

*Bifidobacterium* plays a major role in immune maturation, intestinal homeostasis, vaccine responsiveness and overall health in early life. Their great immunomodulatory properties have been attributed to several bacterial compounds,

including peptidoglycan, specific surface and cytoplasmic proteins, and DNA, as well as key metabolites such as acetate and EPS. Complex postbiotics such as bifidobacterial BEVs seem to contain a variety of these immune stimulators and promote similar immune responses as their parental strain. Additionally, due to their biophysiological properties, they have advantages over live probiotics regarding robustness and biodistribution. Thus, bifidobacterial BEVs show great potential for distinct immune therapies against allergies, cancer or low immunogenicity, making them attractive novel adjuvant candidates in future vaccination trials. Bacterial compounds and products are becoming increasingly accepted and used within commercial vaccine formulations. However, most of these adjuvants derive from bacterial virulence factors such as LPS and cholera toxin, potentially triggering overstimulation, uncontrolled inflammation and increased intestinal barrier permeability.[395] Thus, potent immunostimulants from probiotic bacteria such as *Bifidobacterium* require more investigation to uncover BEVs that modulate the cytokine network and activate immune cells in a consistent and vaccine-promoting manner. Still, our understanding of optimised bifidobacterial vesiculogenesis, key immunomodulatory BEV components and potential next-step application is still in its infancy.

## 6. Thesis aims and objectives

*B. pseudocatenulatum* has probiotic potential and exhibits numerous beneficial properties, including the ability to induce favourable shifts in metabolic and microbiota profiles, and to mitigate inflammatory responses associated with chronic inflammation, obesity, diabetes, cancer, and other morbidities. Postbiotics derived from immunodulatory *B. pseudocatenulatum* strains also hold promise for novel applications in immune therapy and vaccination.

This thesis aims to test the hypothesis that BEVs from distinct *B. pseudocatenulatum* strains can elicit beneficial immune responses with host cells. The strains used in this thesis were selected due to their previously documented immunomodulatory properties, such as priming DCs, inducing cytokine production, and exerting anti-cancer responses in both healthy and diseased preclinical models. These strains were originally isolated from a healthy, full-term, breastfed British infant prior to weaning[88,469], providing a clinically-relevant context for investigating the mechanistic

basis of the immune-stimulatory properties of their BEVs. The specific aims, therefore, are to classify and quantify the vesicular content of different BEV preparations and to investigate their interactions with various immune cell types *in vitro,* with the ultimate goal of identifying mechanisms that could enhance immunogenicity.

Results Chapter I examines the optimal growth conditions for potential heterological vesiculogenesis in the *B. pseudocatenulatum* strains when utilising simple and complex carbohydrates within a growth medium optimised for next-step BEV purification and human trials. Therefore, I created and optimised a human and animal product-free growth medium using different established medium recipes for ideal bacterial and BEV yield and compared growth dynamics of the *B. pseudocatenulatum* isolates. Finally, I have standardised growth and BEV isolation conditions.

Results Chapter II addresses BEV isolation and purification strategies for *Bifidobacterium* strains to attain reproducibility, composition consistency and purity. Hence, I optimised the bifidobacterial BEV preparation and produced stocks of selected BEVs. Since BEV cargo is multifaceted, biophysiological properties of the BEVs, including morphology using transmission electron microscopy (TEM), concentration and size range using nanoparticle tracking analysis (NTA), and cargo composition using fluorometric quantification, were characterised. Moreover, protein content was identified by proteomic analysis. Proteomic profiles of the BEVs are investigated for protein abundance differences and presence of potential immunomodulatory proteins.

Results Chapter III examines interactions between the BEVs and epithelial and selected immune cells per the detected immunomodulatory proteins. Thus, I determined cytokine profiles of BEV-treated human IECs, monocytes, macrophages and PBMCs, and murine bone-marrow-derived DCs (BMDCs) and splenocytes. I also investigated BEV-IEC interactions in more detail regarding potential uptake and TJ modulation mechanisms. Finally, I investigated the potential release of IgA from BEV-treated *ex vivo* PP cell fragments and initiated quantification of enhanced immune responses in macrophages and IECs following bifidobacterial BEV administration under ‘infection-like’ conditions (i.e., exposure to LPS) *in vitro*.

# II. MATERIALS AND METHODS

## 1. List of Equipment

*Table 4: Overview of all used equipment throughout the project*

| Used Apparatus | Model and Supplier | Notes |
|---|---|---|
| Anaerobic cabinet | Ruskinn Concept Plus (Serial No: 1213NCP02; ~230 Vac-50HZ-200W; Ruskinn Technology Ltd, Pencoed Technology Centre, Pencoed, UK) | Used in initial growth assays but changed later |
| | MiniMACS Anaerobic Workstation (Don Whitley Scientific Ltd, Shipley, UK; Serial No: MM11148WG) | Used in initial growth assays but changed later |
| | Baker Ruskinn Concept 1000 (Serial No: DP0505; Ruskinn Technology Ltd, Pencoed Technology Centre, Pencoed, UK) | Standard for *Bifidobacterium* growth |
| BEV isolation system | Easy-load® Masterflex L/S Economy Drive (Cole Parmer®, Model 7518-00, USA) | Standard for BEV preparation |
| Bottle-top filter unit | Millipore Millivac® Maxi Vacuum pump (Model SD1P014M04; Merck, Darmstadt, Germany) | Standard for BEV preparation |
| Centrifuge | Eppendorf Centrifuge 5810 R (Eppendorf SE, Hamburg, Germany) | Standard for 25-50mL volumes |
| | Eppendorf Centrifuge 5415 D (Eppendorf SE, Hamburg, Germany) | Standard for ≤ 2mL volumes |
| | Beckman J2-HS Centrifuge with JLA 10.500 rotor (Beckman Coulter™, USA) | Standard for ≥ 50mL volumes |
| EVOM² Epithelial voltmeter with chopstick electrode | EVOM² (World Precision Instruments, Sarasota, USA) | Standard for Transepithelial Electrical Resistance (TEER) measurement |
| Flow Cytometer | BD LSRFortessa™ Cell Analyser (Becton, Dickinson and Company, USA) | Used for pilot in vivo characterisation |
| Fluorometer | Qubit®2.0 instrument (Thermo Fisher Scientific [Invitrogen], Hemel Hempstead, UK) | Standard for DNA, RNA, and protein quantification |
| | Qubit 3.0 instrument (Thermo Fisher Scientific [Invitrogen], Hemel Hempstead, UK) | Standard for QIB Sequencing Facility |
| Incubator | Sanyo CO2 incubator (incu safe copper alloy stainless; IR sensor; safe cell UV; Code MCO-20AIC; Serial No: 7010547) | Standard for human cell culture |
| | HERAcell™ 150i CO2 incubator (Thermo Fisher Scientific, Hemel Hempstead, UK) | Standard for murine cell culture |
| Mass spectrometer | Orbitrap Eclipse™ Tribrid™ mass spectrometer (Thermo Fisher Scientific, Hemel Hempstead, UK) | Standard for proteomics at JIC |
| | UltiMate® 3000 RSLCnano LC system (Thermo Fisher Scientific, Hemel Hempstead, UK) | Standard for proteomics at JIC |

| Used Apparatus | Model and Supplier | Notes |
|---|---|---|
| Microplate reader | FLUOstar OPTIMA 95025 photometer (BMG Labtech Ltd, Aylesbury, UK; Programme version 2.22R3) | Standard for Sequencing, QuantiBlue™, enzyme-linked immunosorbent assays (ELISA) |
| | Infinite® F50 Robotic Absorbance Microplate Reader (Tecan Trading AG, Switzerland) | Used in initial growth assays |
| | Stratus Microplate Reader (Cerillo, Charlottesville, USA) | Standard for growth assays |
| | MESO QuickPlex SQ 120 instrument (MSD Inc., Rockville, USA) | Standard for Meso Scale Discovery (MSD) assays |
| Microscope | Zeiss LSM 880 with Airyscan Upright Microscope (Carl Zeiss Microscopy Deutschland GmbH, Germany) | Standard for confocal microscopy at QIB - Advanced Microscopy Facility (QIBAM) |
| | FEI Talos200 TEM (Thermo Fisher Scientific, Hemel Hempstead, UK) | Standard for TEM at JIC |
| MicroBead UltraPure system | MiniMACS separator (Miltenyi Biotec B.V. & Co. KG, Germany) | Used for BMDCs enrichment |
| NTA system | ZetaView® (Particle Metrix, Analytik Ltd, Cambridge, UK) | Standard for BEV preparation |
| | NanoSight LM10 Nanoparticle Analysis System (Malvern Panalytical, Salford Scientific Supplies Ltd, UK) | Used initially for BEV preparation |
| Photo spectrometer | WPA biowave CO8000 Cell Density Meter (Biochrom Ltd, 22 Cambridge Science Park, Milton Road, Cambridge, UK) | Standard for colony forming unit (CFU) assays |
| | NanoDrop ® ND-1000 Spectrophotometer (Thermo Fisher Scientific, Hemel Hempstead, UK) | Standard for RNA and cDNA measurement for Quantitative Reverse Transcriptase Polymerase Chain Reaction (qRT-PCR) |
| Safety cabinet | Walker Safety Cabinet Class II MSC (Walker Safety Ltd; Unit 20 Glossop Brook Road, Glossop, UK; SK13 8GG; Serial No: WSC1443) | Standard for aseptic work |
| Sequencing system | Ilumina® HiSeq X (Ilumina Inc., San Diego, USA) | As stated in whole genome sequencing (WGS) from the Sanger Institute[470] |
| | Illumina® Nextseq500 instrument (Ilumina Inc., San Diego, USA) | Standard for QIB Sequencing Facility |
| Thermal Cycler | AB Applied Biosystems® Veriti™ 96 Well Thermal Cycler (Thermo Fisher Scientific, Hemel Hempstead, UK) | Standard for RT-PCR |
| | AB Applied Biosystems® ViiA™ 7 Real-Time PCR System by life technologies (Thermo Fisher Scientific, Hemel Hempstead, UK) | Standard for qPCR |
| Ultrasonicator | Covaris LE220-plus Focused-Ultrasonicator (Covaris Ltd, Brighton, UK) | As stated in WGS from the Sanger Institute[470] |

| Used Apparatus | Model and Supplier | Notes |
|---|---|---|
| Water bath | Grant JB Aqua 18 Plus (Grant Instruments Ltd, Cambridge, UK) | Standard for human cell culture |

# 2. Growth Optimisation of selected *Bifidobacterium* strains for downstream BEV preparations

## 2.1. Culture and growth of *Bifidobacterium* strains

### *2.1.1. Preparation of stock bank*

*Bifidobacterium* strains LH660 and LH663 used in this project were isolated as part of the Baby-Associated MicroBiota of the Intestine (BAMBI) large longitudinal clinical study.[469] The strains originate from faeces collected from a healthy, full-term, breast-fed British control infant before the introduction of solid food, and were previously described by Lawson et al. (2020).[88] Prior to collection, all infants in the study were not treated with any antibiotics or probiotics. Both strains were isolated from the same donor: a female, vaginally delivered infant from Norfolk, with 3,500g at birth, exclusively breast-fed, and 159d of age at the time of sampling.[88,469]

These pre-selected strains were grown in reinforced clostridial medium broth (RCM; Oxoid, Hampshire, UK) for 48h in an anaerobic cabinet at 37°C. After centrifugation (15min/4000×g/4°C), supernatant was discarded, and the remaining pellet was resuspended in 30% Glycerol-RCM broth. Five samples of each strain were assigned as master stocks and ten samples as working stocks (WS), respectively. All stocks were stored at -80°C. Preparation and handling were performed according to the respective standard operating procedures (SOPs).

### *2.1.2. Decontamination of LH660 strain*

Contaminated working and master stocks of *B. pseudocatenulatum* strain LH660 were streaked out on 1.5% agar (Formedium LTD, Swaffham, King's Lynn, UK) RCM plates and incubated for 48h at 37°C in an anaerobic cabinet. Four single colonies per plate were picked, both re-streaked on new RCM agar plates and inoculated in fresh RCM broth medium and incubated for 48h, respectively. This process was repeated several times until both liquid and plate cultures stopped

displaying signs of contamination or abnormal growth patterns. All liquid cultures were processed for stocks. Stocks were kept at -80°C.

One sample from the decontaminated LH660 cultures was selected based on its genomic distance from *B. pseudocatenulatum* strain LH663 and assigned to be the "new" LH660 strain. Master and working stocks were prepared and stored as described above.

### *2.1.3. Assessment of initial growth media*

Cultures of LH660 and LH663 were prepared from WS in RCM broth, incubated for 48h at 37°C in anaerobic conditions and subsequently subcultured 1:10 in fresh RCM broth for 24h at 37°C in an anaerobic cabinet. A 96-well plate was prepared with 200µL of different established growth media: brain heart infusion (BHI) broth, De Man, Rogosa and Sharpe medium (MRS), RCM and minimal MRS (see Table 5 and Table 6) supplemented with 2% of the HMOs 2'FL and lacto-N-neotetraose (LNnT). Each condition was tested in triplicate with either 1% of the bifidobacterial subculture or with the respective medium only as negative control. Initially, optical density (OD) at 600nm was measured every 15min for 48h at 37°C in anaerobic conditions using an Absorbance Microplate Reader (Tecan, Reading, UK) to estimate bacterial growth. This experiment was repeated after introduction of a new plate reader, Stratus Microplate Reader, to ensure consistency and reproducibility of the growth results (as per SOP).

*Table 5: Composition of minimal MRS growth medium*

| Component | Concentration [g/L] | Source |
|---|---|---|
| Tripticase peptone | 10.0 | Sigma-Aldrich Co LTD (Merck), Gillingham, UK |
| Yeast extract | 2.5 | Thermo Fisher Scientific Diagnostics (Oxoid), Hampshire, UK |
| Tryptose | 3.0 | Sigma-Aldrich Co LTD (Merck), Gillingham, UK |
| $K_2HPO_4$ | 3.0 | Sigma-Aldrich Co LTD (Merck), Gillingham, UK |
| Tri-ammonium citrate | 2.0 | Sigma-Aldrich Co LTD (Merck), Gillingham, UK |

*Table 6: List of needed supplements for minimal MRS growth medium, excluding carbohydrates*

| Component | Concentration [mL/L] | Source |
|---|---|---|
| Pyruvic acid | 0.2 | Thermo Fisher Scientific Diagnostics (Oxoid), Hampshire, UK |
| Cysteine HCl | 1.0 | Sigma-Aldrich Co LTD (Merck), Gillingham, UK |
| Tween 80 | 1.0 | Sigma-Aldrich Co LTD (Merck), Gillingham, UK |
| $MgSO_4 \cdot 7H_2O$ | 2.0 | Sigma-Aldrich Co LTD (Merck), Gillingham, UK |
| $MnSO_4 \cdot 4H_2O$ | 1.0 | Sigma-Aldrich Co LTD (Merck), Gillingham, UK |
| $FeSO_4 \cdot 7H_2O$ | 1.0 | Sigma-Aldrich Co LTD (Merck), Gillingham, UK |

## 2.2. Establishment of optimal animal and human product-free growth medium

For potential next-stage human studies, reagents free from human and animal materials need to be used. Thus, based on initial growth results of the selected *Bifidobacterium* strains in different media as described above, RCM (further called RCMveg) without compounds originating from animal or human sources was formulated. In order to optimise the growth of both strains, another series of growth experiments with the supplementation of different vitamins and 2% 2'FL and LNnT, as well as using 10% 2'FL as alternative primary carbohydrate source, were performed. Additionally, tests with minimised ingredients of RCMveg were performed to keep growth optimised while eliminating potential confounding factors in downstream experiments. The recipe for full RCMveg and a list of all supplemented vitamins are provided below:

*Table 7: Composition of RCMveg growth medium for vaccine-friendly Bifidobacterium culturing based on Oxoid's RCM recipe*

| Component | Concentration [g/L] | Source |
|---|---|---|
| Yeast extract | 13.0 | Thermo Fisher Scientific Diagnostics (Oxoid), Hampshire, UK |
| Soymeal-based peptone | 10.0 | Sigma-Aldrich Co LTD (Merck), Gillingham, UK |
| Soluble starch from potato | 1.0 | Sigma-Aldrich Co LTD (Merck), Gillingham, UK |
| α-D-Glucose | 5.0 | Sigma-Aldrich Co LTD (Merck), Gillingham, UK |
| Cysteine hydrochloride from non-animal source | 0.5 | Sigma-Aldrich Co LTD (Merck), Gillingham, UK |
| Sodium chloride | 5.0 | Sigma-Aldrich Co LTD (Merck), Gillingham, UK |
| Sodium acetate | 3.0 | Sigma-Aldrich Co LTD (Merck), Gillingham, UK |
| Agar* | 0.5 | Formedium LTD, Swaffham, King's Lynn, UK |

*Following optimisation assays, agar was discarded from the final RCMveg formulation

*Table 8: Composition of tested vitamin mix for bifidobacterial growth optimisation[471]*

| Component | Concentration [mg/L] | Source |
|---|---|---|
| Pantothenate | 10.0 | Sigma-Aldrich Co LTD (Merck), Gillingham, UK |
| Nicotinamide | 5.0 | Sigma-Aldrich Co LTD (Merck), Gillingham, UK |
| Thiamine | 4.0 | Sigma-Aldrich Co LTD (Merck), Gillingham, UK |
| Biotin | 2.0 | Sigma-Aldrich Co LTD (Merck), Gillingham, UK |
| Vitamin B12 | 0.5 | Sigma-Aldrich Co LTD (Merck), Gillingham, UK |
| Menadione | 1.0 | Sigma-Aldrich Co LTD (Merck), Gillingham, UK |
| 4-aminobenzoic acid Reagent 99% | 5.0 | Sigma-Aldrich Co LTD (Merck), Gillingham, UK |

## 2.3. Determination of CFU in RCMveg

For next stage *in vitro* and *in vivo* studies, as well as to establish optimal BEV harvesting time points, an accurate determination of bacterial material within a culture is needed. Therefore, a CFU assay was performed for both working strains, LH660

and LH663, in RCMveg with 2% glucose (Glc) supplementation. Strains were subcultured from WS in RCM broth, and 1% of each primary culture was inoculated in 40mL RCMveg medium in triplicate and incubated at 37°C in anaerobic conditions. Samples were collected every 2h, and OD at 600nm was measured immediately. Samples were centrifuged (5min/14000×g/24°C), supernatant discarded, and the pellets resuspended in 100µL phosphate-buffered saline (PBS). A dilution series up to $10^{-8}$ was prepared for each sample (see Figure 4), 100µL of the dilutions $10^{-5}$ to $10^{-8}$ were plated on 1.5% RCM agar plates and incubated for 48h at 37°C in anaerobic conditions. Bacterial colony growth was measured and CFU calculated, respectively, using the formula below:

$$CFU/mL = c \times V \times d$$

c – sum of measured colonies

V – inoculated volume on plate

d – dilution of the corresponding plate

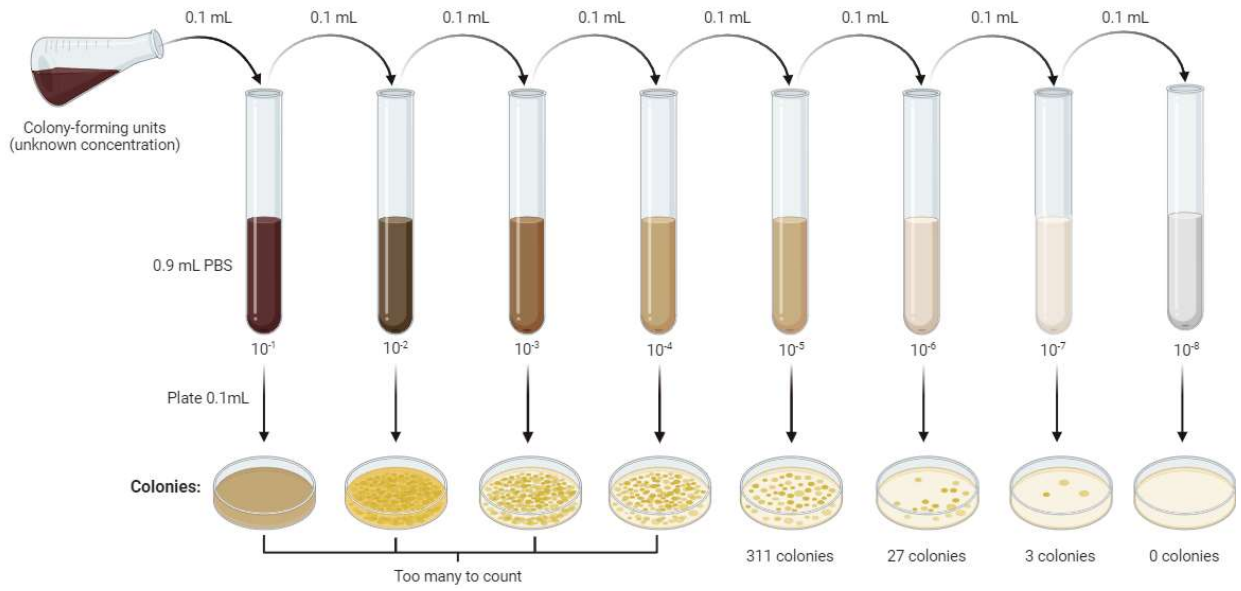


*Figure 4: Experimental set-up for CFU determination. Figure created in BioRender.com*

## 2.4. Visualisation

Explanatory and experimental set-up figures were created in BioRender.com. Growth OD data had been analysed and visualised using Microsoft Excel (version Microsoft Office 2019), displaying growth means as curves ± standard error of the mean (SEM) as error bars. CFU data was analysed and visualised with Microsoft Excel (version Microsoft Office 2019), displaying growth means as bars/curves ± SEM as error bars.

# 3. Characterisation of BEVs derived from selected *B. pseudocatenulatum* strains

## 3.1. Bifidobacterial BEV isolation and purification optimisation

### *3.1.1. Initial isolation following lab SOP*

A first attempt to isolate BEVs from the selected strains was performed using the QIB SOP GMH-SC-024 “Isolation and Concentration of Bacteroides/Prevotella Extracellular Membrane Vesicles” established by the Carding lab group for membrane vesicles from Bacteroides species.[472] Briefly, 1L of RCMveg medium with and without added 2% 2’FL were prepared, reduced overnight, and inoculated with 1% LH663 primary culture (primary growth from stocks as described above; at this point, LH660 was still being decontaminated and thus excluded). Cultures were left to grow for 16h (corresponding to early stationary phase from initial growth experiments as described above; these initial assays were performed prior to the CFU experiments and establishment of BEV harvesting time points), under stirring and anaerobic conditions (16h/37°C/5% $CO_2$). Both cultures were centrifuged (1h/14000×g/4°C), pellets were discarded, and the supernatants sterile filtered using a bottle-top filter unit (Sartolab BT500 PES, 0.2µm, 500mL, PKI12, Epsom, UK). The resulting filtrates were transferred to the reservoir of the membrane vesicle isolation station (see Figure 5), filtered through the cassette system (Sartorius Vivaflow 50R 100,000 MWCO HY, Epsom, UK) and washed with PBS for several hours. 0.5-1 mL of BEV solution retentate from each culture was collected, sterile filtered (Sartorius Filter Minisart Syringe 0.2µm Sterile HF, Epsom, UK), and stored until further use at 4°C. Introduction to, help with, and supervision of this procedure was performed by Dr Regis Stentz.

### *3.1.2. Modification of the filtration protocol*

**a) Serial filter disk system set-up**

The initial BEV preparation process revealed the need for additional purification steps since the established SOP set-up for *Bacteroides* BEVs resulted in a very time-consuming and rather impure first isolation outcome for BEVs derived from the *Bifidobacterium* strains. Since the initial filter disk set-up seemed to get clogged and thus did not perform optimally, we decided to use an additional filtration disk (Sartorius

Vivaflow 200; 0.2µm, Epsom, UK; PES membrane) with a broader cut-off (2000kD), which was installed in series before the initial one (100kD cut-off) to allow primary purification of the filtrate from bigger supernatant contents. Similar to the initial isolation, the filtrate was washed with PBS for several hours, and finally, 500µL of BEV solution retentate was collected, sterile filtered, and stored until further use at 4°C. We performed size exclusion chromatography (SEC, see below) to obtain pure fractions of the BEV solution for further purification. The serial filtration disk set-up was omitted after sufficient results following the filtration of the growth medium prior to inoculation (see below).

**b) Preparational filtration of growth medium prior to inoculation**

Despite the additional filtration disk step and subsequent SEC (see below), the preparation was still time-consuming and did not result in optimally purified isolates with a sufficient BEV yield. Other potential bacterial products and debris of LH663 still seemed to clog the filter system.

Since RCMveg is not a minimal medium and does contain starch, yeast extract and peptone (see Table 7), we wanted to minimise the possibility of potential confounding vesicles deriving from the production of these ingredients. Thus, we decided to filter the growth medium prior to inoculation using the initial filter disk set-up as described previously, only keeping the filtrate instead of the retentate. This filtered growth medium was sterile filtered and reduced prior to inoculation, and cultures were incubated for 20h following the CFU-determined peak of bacterial yield. Following the collection of the retentate, the BEV solutions were concentrated and further purified via filter centrifugation (Satorius Vivaspin 20, 100k MWCO PES, Epsom, UK) and subsequent SEC.

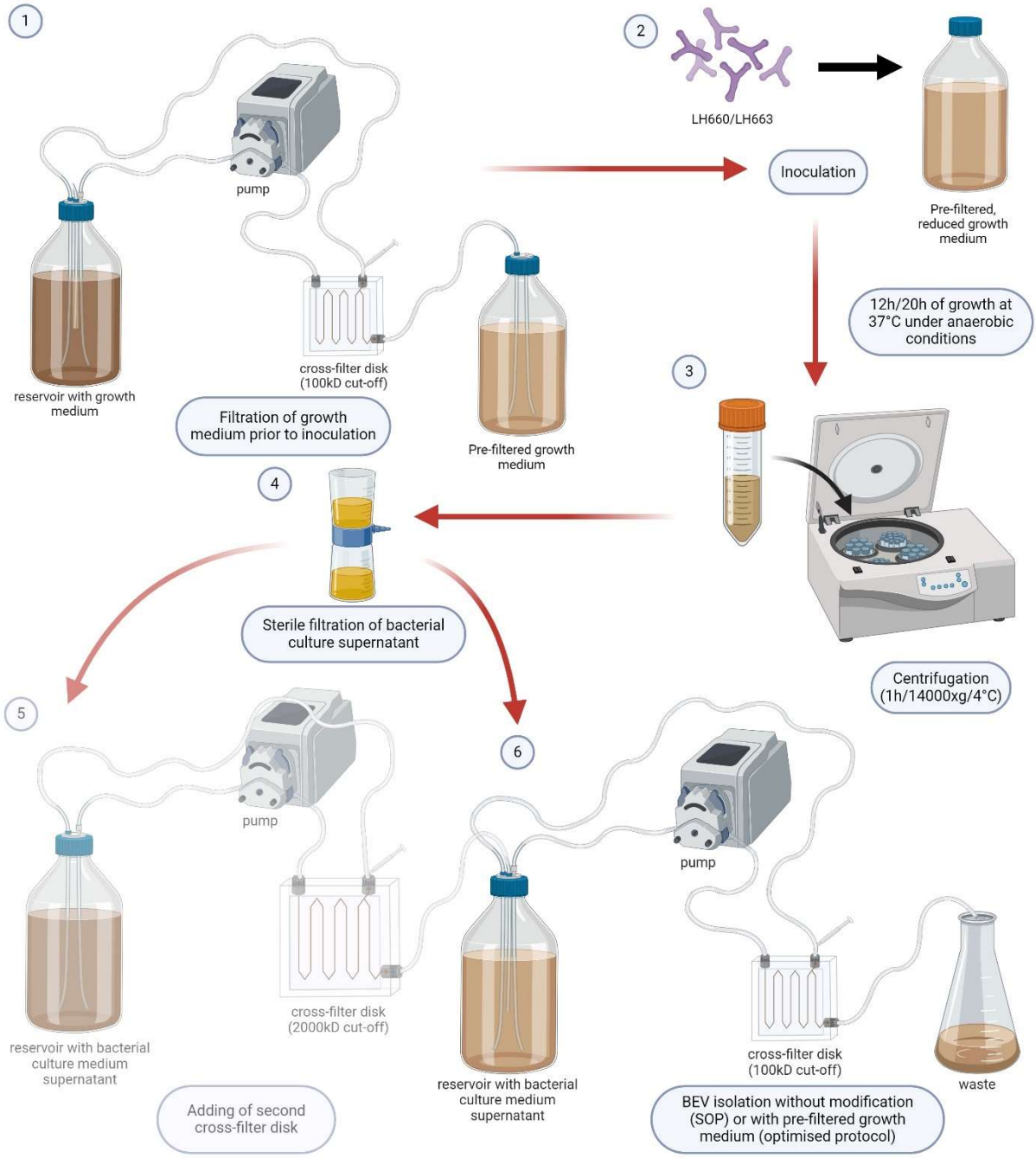


*Figure 5: Overview of BEV isolation process, including different modifications. 1) Filtration of growth medium prior to inoculation as part of optimised bifidobacterial BEV preparation, 2) Inoculation of LH660 or LH663 and subsequent growth conditions, 3) Centrifugation, 4) Filtration of bacterial culture supernatant, 5) first cross-filtration using a second filter disk with broader cut-off (modification of BEV preparation later omitted after optimisation), 6) BEV isolation. Figure created in BioRender.com*

### *3.1.3. SEC for further purification*

To purify the BEV solution, an SEC on the initial modified isolates was performed using a protocol and 15cm-column (qEV original, 35nm Gen 2 column, Izon Science, Lyon, France) provided by Dr Emily Jones, resulting in 24 fractions that were subsequently analysed for potential BEV size and concentration, as well as protein

levels. Briefly, the column was washed twice with 20mL PBS before adding the BEV solution and subsequent filling with PBS. Fractions à 500 µL were collected after discarding 3mL of void column volume, and analysed using NTA and Bradford assay. In the final optimised BEV isolation protocol, only 4-6 fractions were collected and pooled into batches.

**a) Protein concentration testing of SEC fractions**

Following the initial SEC, the resulting 24 sample fractions were tested for protein concentrations using a Bradford kit (Thermo Fisher Scientific, Hampshire, UK) according to the manufacturer's instructions. Later collected fractions (>10) were excluded from subsequent SECs due to the confirmed high protein levels known by the Carding group using their SOP. This procedure was performed by Dr Regis Stentz.

**b) Nanoparticle tracking analysis (NTA)**

To identify suitable, pure fractions of high particle concentration that could be pooled into BEV batches, all SEC fractions were included in NTA using the ZetaView® (version 8.05.12SP1; Particle Metrix, Analytik Ltd., Cambridge, UK). This would give information about size distributions of detectable nanoparticles and their amount per fraction using the 10nm size range, 488nm wavelength SOP with 2 cycle 11 position high frame rate analysis at 25°C including fixed camera control and post-acquisition settings (sensitivity: 80, Frame Rate: 30, Shutter: 100, Brightness: 20min, Max Area: 2000, Min Area: 5, Tracelength: 30, 5nm/Class, 64 Classes/Decade). For this, all fractions were diluted with particle-free dd$H_2O$ to obtain 1/5000, 1/10000, and 1/20000 dilutions, allowing potential BEV solution to attain optimal detection levels of the ZetaView instrument. Induction, help, and supervision of initial use of the ZetaView was performed by Dr Emily Jones.

### *3.1.4. Establishment of BEV batch bank*

Once the optimised and reproducible protocol for BEV isolation and purification derived from *B. pseudocatenulatum* was established, including optimal growth conditions, harvesting time points and suitable filtration, centrifugation, and purification steps, several BEV batches were prepared for subsequent analysis and characterisation. Therefore, suitable fractions of high BEV yield and low protein concentration following SEC and NTA were pooled to obtain several final BEV

preparations of both strains and both selected time points. These were initially stored at 4°C but later kept at -80°C until further use.

## 3.2. Characterisation of BEV preparations

### *3.2.1. Size distribution and particle concentration*

Initial bifidobacterial BEV preparations prior to any isolation modifications were tested for concentration and size distribution by Dr Emily Jones using the NanoSight LM10 Nanoparticle Analysis System. The threshold was set to 10nm. Measurements were performed in quadruplicate. After purchase of the ZetaView system (Particle Metrix, Analytik Ltd., Cambridge, UK), all subsequent NTAs were performed with the ZetaView in triplicate as described above. Mean size distribution and concentration were calculated for each preparation. Replicates of preparations of identical strain of origin and time point were taken individually and merged for better understanding of reproducibility and preparation-dependent differences. These were done in quadruplicate.

### *3.2.2. Quantification of nucleic acid, protein, and lipid amounts present in BEV preparations*

To obtain an estimate of the potential content of the BEV preparations and to compare them in terms of similarity between batches produced under the same conditions and differences between BEV batches from different strains and/or time points, I performed a series of Qubit® assays destined for proteins, RNA and dsDNA, as well as a lipid quantification experiment.

Qubit assays were performed following manufacturer's instructions, related QIB SOP (GMH-LH-003) and provided kits (Qubit® dsDNA High Sensitivity [HS] Assay Kit, Qubit® Protein and Protein Broad Range [BR] Assay Kit, Qubit® RNA HS Assay Kit, Thermo Fisher Scientific, Hampshire, UK) in quadruplet.

Lipid amounts within BEV preparations were quantified as published recently using an established protocol[287] with help of Dr Rokas Juodeikis. Briefly, linoleic acid (Thermo Fisher Scientific, Hampshire, UK) standard solutions were prepared, and 180µL of standards incubated alongside 180µL BEV solutions ($1 \cdot 10^{10}$ particles/mL) with 20µL FM4-64 dye (30µg/mL; Thermo Fisher Scientific, Hampshire, UK) for 10min at 37°C.

Endpoint emission at 720-20nm was measured using excitation at 515-15nm of the BMG FLUOstar Omega Microplate Reader.

### *3.2.3. Transmission Electron Microscopy (TEM)*

As part of the validation of the bifidobacterial BEV isolation protocol, TEM was performed initially and after each major modification of the SOP. Therefore, 20µL of undiluted BEV batch solution was given to the QIBAM in cooperation with the JIC BioImaging Facility and processed as previously described.[310] Samples were prepared with negative staining to carbon-coated 400 Copper grids (Agar Scientific, Rotherham, UK), which had been glow discharged prior to negative staining (20s/10mA). Briefly, 10µL of BEV sample was transferred onto each grid and left for 1min, followed by 10µL of 2% uranyl acetate (UA; Avantor VWR BDH Chemicals, Lutterworth, UK) for 1min. Grids were imaged at JIC using FEI Talos200 TEM. TEM sample preparation was performed by Dr Catherine Booth and Kathryn Gotts, respectively. Initial TEM imaging was performed by Dr Jake Richardson (JIC), and subsequent TEM imaging was performed by Dr Catherine Booth or Kathryn Gotts, respectively. Images stored on OMERO. TEM preparations were done in duplicate, and BEV batches were provided in triplicate or higher replicates per strain.

## 3.3. Proteomic analysis

200µL of undiluted BEV batch samples were given to the JIC Proteomics Facility and processed according to standard procedure as previously reported.[330] BEVs were lysed using 2% sodium dodecyl sulphate (SDS; Sigma-Aldrich Co LTD, Gillingham, UK) followed by boiling and vortexing. Proteins were precipitated with acetone (Sigma-Aldrich Co LTD, Gillingham, UK) and subsequent pellets were resuspended in 2.5% sodium deoxycholate (SDC) with 0.2M EPPS (Sigma-Aldrich Co LTD (Merck), Gillingham, UK) buffer pH8. The protein solution was reduced, alkylated with dithiothreitol and iodoacetamide (Promega, Southampton, UK), and digested with sequencing-grade trypsin (Promega, Southampton, UK) according to standard procedures.[473] The SDC was precipitated by adjusting to 0.5% formic acid, and the peptide lysates were purified from the supernatant using C18 OMIX tips (Agilent, Didcot, UK).

Aliquots of the peptide lysates were analysed by nanoLC-MS/MS on an Orbitrap Eclipse™ Tribrid™ mass spectrometer equipped with a FAIMS Pro Duo device source

and coupled to an UltiMate® 3000 RSLCnano LC system (Thermo Fisher Scientific, Hemel Hempstead, UK). The samples were loaded onto a pre-column (Acclaim™ PepMap™ NEO C18, 5µm, 0.3x5mm, Thermo Fisher Scientific, Hemel Hempstead, UK) with 0.1% Trifluoroacetic acid (TFA; Thermo Fisher Scientific, Hemel Hempstead, UK) at 15µl/min for 3min. The trap column was then switched in-line with the analytical column (nanoEase M/Z column, HSS C18 T3, 100Å, 1.8µm; Waters, Wilmslow, UK) for separation using the following gradient of solvents A (water, 0.1% formic acid; Thermo Fisher Scientific, Hemel Hempstead, UK) and B (80% acetonitrile, 0.1% formic acid; Thermo Fisher Scientific, Hemel Hempstead, UK) at a flow rate of 0.2µl/min: 0-3 min at 3% B (parallel to trapping); 3-10 min increase B to 7%, curve 4; 10-90 min increase B to 50%; followed by a ramp to 99% B and re-equilibration to 3% B. Data were acquired with the following mass spectrometer settings in positive ion mode: MS1/OT: resolution 120K, profile mode, mass range m/z 300-1800, normalised AGC 100%, fill time 50ms; MS2/IT: data dependent analysis was performed using HCD fragmentation and FAIMS cycling between -40V and -60V with the following parameters: 0.7s cycle time in IT turbo mode, centroid mode, isolation window 1Da, charge states 2-5, threshold 1e4, CE=33, AGC target 1e4, max. inject time 35ms, dynamic exclusion 1 count, 15s exclusion, exclusion mass window±10ppm.

The acquired raw data were processed and quantified in Proteome Discoverer 3.0 (Thermo Fisher Scientific, Hemel Hempstead, UK) using the incorporated search engine CHIMERYS (MSAID, Munich, Germany). The processing workflow for both engines included recalibration of MS1 spectra (RC), MS1 quantification by Minora Feature Detector and search on the *B. longum* subsp. *longum* (2399 entries, from NCBI GenBank[474], 14/Nov/2022) database and a common contaminants database, with Percolator validation of the identification results. For CHIMERYS, the Top N Peak Filter was used with 10 peaks per 100Da, fragment tolerance of 0.5Da, trypsin as the endoprotease with 2 missed cleavages allowed, variable modification oxidation (M), fixed modification carbamidomethyl (C).

For the consensus workflow, only unique peptides in the protein group were included in the quantification based on Top 3 precursor abundance, normalised by total peptide amount, scaled by average, protein abundance-based ratio calculation, missing values imputation by low abundance resampling, hypothesis testing by *t*-test (background based), adjusted *p*-value calculation by BH-method.

Proteomics analysis on BEV batches was repeated twice: Initially for reproducibility investigation of BEV batch preparations in triplicate for each strain, and subsequently in triplicate per time point per strain for comparison. Proteomic preparation and data processing were performed by Dr Carlo Martins (JIC) and Dr Gerhard Saalbach (JIC). Gene ontology (GO) and Kyoto Encyclopedia of Genes and Genomes (KEGG) annotations were performed using the UniprotKB[475] and KEGG database.[476]

## 3.4. Visualisation

Explanatory and experimental set-up figures were created in BioRender.com. Help with proteomic data analysis and visualisation was performed by Dr Matthew Dalby using R (Version 4.3.2, packages: tidyverse, vegan). Quantification and NTA concentration data are displayed with mean ± SEM as error bars. NTA size distribution with means of percentiles X10, X90, and mean of detected particle diameters. TEM images were processed using FIJI/imageJ (Version: 1.54f)[477].

# 4. Bifidobacterial BEV-host interaction

## 4.1. Uptake assays

### *4.1.1. Cell culture*

Human colonic epithelial Caco-2 cells (Public Health England, ECACC86020202) were cultured in Dulbecco's Modified Eagle Medium (DMEM; Gibco, Fisher Scientific Limited, Hemel Hempstead, UK) with low Glc (1g/L) and sodium pyruvate (1mM) supplemented with 20% heat-inactivated foetal bovine serum (FBS; Gibco™, Life Technologies Ltd Invitrogen Div, Hemel Hempstead, UK) and 1% penicillin/streptomycin mix (Pen/Strep; 100U/mL, 100µg/mL; Sigma-Aldrich Co LTD, Gillingham, UK).

Co-cultures were seeded at $5 \cdot 10^5$ cells per well in 96-well plates, grown until a monolayer of undifferentiated cells formed (~7d), and then treated with bifidobacterial BEV batch samples ($1 \cdot 10^{11}$ particles/mL) of both strains and time points, PBS (Dulbecco's, Merck Life Science UK Ltd, Gillingham, UK) as negative control, or LPS (Invitrogen™ eBioscience™, Fisher Scientific Ltd, Hemel Hempstead, UK; 200ng/mL) as positive control were added in triplicates at 10%, respectively. Culture condition groups were performed in triplicate and incubated for 24h. Supernatants of each co-culture were collected and stored at -80°C until further use.

### *4.1.2. Transepithelial Electrical Resistance (TEER)*

For TEER measurements, confluent Caco-2 cultures were split as described by the supplier and seeded onto the apical compartment of 0.4µm transparent polyethylene terephthalate (PET) membrane 24-transwell inserts (Thincert, Greiner Bio-One Ltd, Stonehouse, UK) at $5 \cdot 10^5$ cells per well and grown until fully differentiated and confluent (~21d). Basal compartment of 24-well plate (Greiner Bio-One Ltd, Stonehouse, UK) was filled with 1mL growth medium (see above). Bifidobacterial BEV batch samples ($1 \cdot 10^{11}$ particles/mL) of both strains and time points, PBS as negative control, or LPS as positive control, were added in triplicate at 10% to the apical compartment and at least one transwell was kept blank for normalisation. TEER measurements were recorded using an EVOM$^2$ epithelial voltmeter with a chopstick electrode (World Precision Instruments Inc., Hitchin, UK). Protocol[326] and initial help

were provided by Dr Emily Jones. Resistance was calculated following the formula below:

$$Resistance = \left(TEER_{Sample} - TEER_{Blank}\right) \cdot \frac{\pi d^2_{membrane\ area}}{4}$$

Following the initial TEER experiment, a series of similar assays was performed to see potential epithelial protection of the epithelial layer after challenge with LPS. Therefore, one 24-well plate with Caco-2 transwells was first exposed to bifidobacterial BEV batches as described above for 24h and subsequently cultured with 10% LPS for 12h, 24h, and 48h. TEER measurements of all wells were taken throughout the duration of these experiments.

### *4.1.3. Determination of TJ gene expression changes*

#### a) RNA extraction

Fully differentiated Caco-2 cell monolayers (~21d) were collected from transwells, growth medium removed, cells washed in PBS, treated with 250µL tri-reagent (Qiagen, Manchester, UK), and either processed immediately or kept at -20°C. Cells were defrosted where necessary, scraped from transwell inserts, and transferred into RNAse-free 1.5mL tubes (Eppendorf, Stevenage, UK). 100µL chloroform (Sigma-Aldrich Co LTD, Gillingham, UK) were added to the samples and vortexed until sample solution turned cloudy. Samples were centrifuged (13000rpm/ 10min/ 4°C) and the aqueous RNA-containing phase was transferred into new RNAse-free tubes. 250µL iso-propanol (Sigma-Aldrich Co LTD, Gillingham, UK) were added to each sample and vortexed thoroughly. After centrifugation (13000rpm/ 10min/ 4°C), iso-propanol is discarded and the RNA pellet washed twice with 70% ethanol. Ethanol supernatant was discarded, and pellets were left to dry for 10min. After resuspension in RNase-free water, RNA concentrations were analysed using Nanodrop (Thermo Fisher Scientific, Hemel Hempstead, UK).

#### b) qRT-PCR

1µg of extracted RNA in 4.55µL water was kept on ice. 4.45µL of RT-PCR mix (2µL/sample Buffer 5X [Invitrogen, Paisley, UK], 0.5µL/sample dithiothreitol [DTT] 0.1M [Invitrogen, Paisley, UK], 0.6µL/sample 1:10 Random primers [Invitrogen, Paisley, UK], 1µL/sample 1:10 deoxynucleotide triphosphates (dNTPs) [Invitrogen,

Paisley, UK], 0.35µL/sample murine leukaemia virus [MLV] reverse transcriptase enzyme [Invitrogen, Paisley, UK]) were added to each sample, mixed and run in a thermocycler (Thermo Fisher Scientific, Hemel Hempstead, UK; 90min/ 37°C followed by 10min/ 75°C) and kept at 4°C. Finally, 190µL SIGMA water (Sigma-Aldrich Co LTD, Gillingham, UK) was added, and each sample was transferred into new 0.6µL tubes (Eppendorf, Stevenage, UK). Samples were subsequently stored at -20°C.

1.5µL of extracted RNA sample were combined with 4.9µL qPCR mix (3µL/sample SYBR green [Sigma-Aldrich Co LTD, Gillingham, UK], 0.5µL/sample 1:20 primers [Sigma-Aldrich Co LTD, Gillingham, UK], 6.5µL/sample water [Sigma-Aldrich Co LTD, Gillingham, UK]) in a 384-well qPCR plate (FrameStar, Surrey, UK). The sample was centrifuged briefly and run in a Viia7 IFR E228 qPCR cycler (hold stage: 3min/95°C, PCR stage: 40 cycles [15s/95°C followed by 1min/60°C], melt curve stage: continuous [15s/95°C; 1min/60°C; 15s/95°C]). Used primers are listed in Table 9 below.

*Table 9: List of used primers testing human genes encoding for TJ proteins*

| Gene | Primer Type | Sequence |
|---|---|---|
| Human Occludin | Forward | CCAATGTCGAGGAGTGGG |
| | Reverse | CGCTGCTGTAACGAGGCT |
| Human Claudin-1 | Forward | AAGTGCTTGGAAGACGATGA |
| | Reverse | CTTGGTGTTGGGTAAGAGGT |
| Human ZO-1 | Forward | ATCCCTCAAGGAGCCATTC |
| | Reverse | CACTTGTTTTGCCAGGTTTTA |
| Human glyceraldehyde-3-phosphate dehydrogenase (GAPDH; housekeeping) | Forward | AATGAAGGGGTCATTGATG |
| | Reverse | AAGGTGAAGGTCGGAGTCA |

### *4.1.4. Confocal Fluorescence Microscopy*

Confluent Caco-2 cells were split, seeded at $5 \cdot 10^5$ cells per well to collagen-coated (Thistle Scientific, Glasgow, UK) 12-well chamber (Thistle Scientific, Glasgow, UK), and grown until a thin monolayer of undifferentiated cells had formed (~2-3d). Used cell growth medium was removed from each well and replaced with 10% DiO-labelled BEV batch conditioned or PBS control cell media. Cultures were incubated for 24h, rinsed with PBS, and extracellular DiO fluorescence quenched using 0.025% trypan blue (Sigma-Aldrich Co LTD, Gillingham, UK). Afterwards, they were fixed with 4% paraformaldehyde (PFA; Thermo Fisher Scientific, Hemel Hempstead, UK) at room temperature (RT) for 15min and cell nuclei stained using DAPI dye (Sigma-

Aldrich Co LTD, Gillingham, UK). Cells were rinsed carefully with PBS and mounted using Fluoromount G (Thermo Fisher Scientific, Hemel Hempstead, UK).

Potential BEV uptake and translocation were quantified by confocal microscopy using the QIBAM Zeiss LSM 880 with Airyscan Upright Microscope equipped with a Plan-Apochromat 20x/0.8 and a Plan-Apochromat 40x/1.3 objective, and connected to an Axiocam 503 Monochrome camera and ZEN Blue software (Version 3.9; ZEISS, Birmingham, UK). Fluorescence was recorded at 405nm (blue, nuclei; Diode Laser) and 488nm (Dio-green, BEVs; MultiLine Argon Laser). Z-stacks at 0.4µm per slice were acquired using ZEN Black software (Version 2.3; ZEISS, Birmingham, UK) and images stored in OMERO. Image analysis was performed using Fiji (see below). Protocol[326] and help provided by Dr Emily Jones, induction to the confocal microscope by Dr Catherine Booth.

### *4.1.5. Endocytosis assay*

Similar to the preparation described above, as previously published, half of the Caco-2 monolayer cultures were pre-treated with the dynamin-mediated endocytosis inhibitor Dynasore (80µM; Sigma-Aldrich Co LTD, Gillingham, UK) for 1h.[326]

Potential internalisation of DiO-labelled BEVs was quantified in Fiji using sum fluorescent pixel intensity of the field of view (see below). Sample fluorescence units were normalised to PBS controls, and means of each sample group were calculated as average fluorescence intensity units (AU).

## 4.2. BEV activation of immune cells *in vitro*

### *4.2.1. Cell culture and cell differentiation*

Human monocytes THP-1 (ATCC, TIB-202) and reporter cell line THP1-Blue™ NF-κB (Invivogen, Toulouse, France) were cultured under standard conditions (37°C/5% $CO_2$) in Roswell Park Memorial Institute 1640 (RPMI; Gibco™, Life Technologies Ltd Invitrogen Div, Hemel Hempstead, UK) medium containing L-Glutamine (2mM) and 4-(2-hydroxyethyl)-1-piperazine-ethanesulfonic acid (HEPES; 25mM) supplemented with 20% heat-inactivated FBS (Gibco™, Life Technologies Ltd Invitrogen Div, Hemel Hempstead, UK) for initial growth. Subsequent cultures were grown in RPMI supplemented with 10% FBS, 1% Pen/Strep (100U/mL-100µg/mL),

Normacin™ (100µg/mL; Invivogen, Toulouse, France) and alternating addition of Blasticin (10µg/mL; Invivogen, Toulouse, France).

THP-1 monocytes were differentiated into macrophages by culturing in growth medium containing additionally 10ng/mL phorbol 12-myristate 13-acetate (PMA; Sigma-Aldrich Co LTD, Gillingham, UK) for 24h. THP-1 macrophages and THP1-Blue™ cells were seeded at $1 \cdot 10^5$ cells per well into 96-well plates, respectively, and treated with 10% BEV samples ($1 \cdot 10^{11}$ particles/mL), 10% PBS as negative control and 10% LPS as positive control for 24h. Culture condition groups were performed in triplicates. Supernatants of each co-culture were collected and stored at -80°C until further use.

Protocol[478], induction and initial help with cell culture handling provided by Dr Sree Gowrinadh Javvadi.

### *4.2.2. Detection of TLR stimulation using QUANTI-Blue™ assay*

Prior to storage at -80°C, 20µL aliquots of THP1-Blue™ and BEV co-culture supernatants were used in the QUANTI-Blue™ assay to determine activation of TLRs and subsequent NF-κB production of the human monocytes by the bifidobacterial BEVs. The assay was performed as per manufacturer's instructions (Invivogen, Toulouse, France). Briefly, a 96-well plate was prepared with 180µL of QUANTI-Blue™ Solution (Invivogen, Toulouse, France) per well and 20µL BEV or control co-culture supernatant aliquots added, respectively. The plate was incubated at 37°C for a maximum of 6h (or until sufficient colour change was visible), and OD at 650nm was measured using a microplate reader (Fluostar OPTIMA 95025).

### *4.2.3. Cytokine and chemokine production determination*

#### a) qRT-PCR

To further determine potential cytokine induction, RNA from differentiated THP-1 cells treated with bifidobacterial BEVs, PBS or LPS (see 4.2.1) was extracted and used for subsequent qRT-PCR as described above (see 4.1.3). Used primers are listed below (Table 10).

*Table 10: List of used primers testing human genes encoding key cytokines*

| Gene | Primer Type | Sequence |
|---|---|---|
| Human TNF-α | Forward | TCTGTACCTGTCCTGCGTGT |
| | Reverse | GAGAAGGTGGTTGTCTGGGA |
| Human IL-1β | Forward | CGCCAGTGAAATGATGGCTTAT |
| | Reverse | CTGGAAGGAGCACTTCATCTGT |
| Human IL-6 | Forward | GGGGTGTGAGAAGAGAGATGG |
| | Reverse | GTGTGCCAGACACCCTATCTT |
| Human IL-10 | Forward | CTGTGAGGCAAGGCATTTGG |
| | Reverse | CTTCCATGCTTTGGGGTTGG |
| Human GAPDH (housekeeping) | Forward | AATGAAGGGGTCATTGATG |
| | Reverse | AAGGTGAAGGTCGGAGTCA |

**b) ELISA and MSD**

Supernatant from BEV co-cultures with human differentiated epithelial Caco-2 cells, THP-1 differentiated macrophages, and THP1-Blue™ monocytes were used to investigate potential cytokine and chemokine production of these cells after bifidobacterial BEV stimulation. Human IL-6, IL-8, IL-15, and TSLP concentrations were determined using a personalised U-plex MSD platform (MSD Inc., Rockville, USA). The experiment was performed as per manufacturer's instructions, and the prepared plate was read using a MESO QuickPlex SQ 120 instrument. Using the provided MSD kit calibrators allowed calculation of cytokine concentration based on the standard curve within the MSD Discovery Workbench 4.0 software. Further, potential human TNF-α, IL-1β, IL-6, IL-8, IL-10 and IL-12p70 concentrations were tested using respective ELISAs (DuoSet®, DuoSet Ancillary Reagent, and Quantikine® ELISA Development Systems, R&D Systems, USA). Reagents, standards, and plate preparations were performed following the manufacturer's instructions. Absorbance of plates was measured using a microplate reader (Fluostar OPTIMA 95025) at an OD of 450nm.

## 4.3. Visualisation

TEER, ELISA and MSD graphs were analysed and visualised with Microsoft Excel (version Microsoft Office 2019). All experiments were performed in triplicate and are shown as means ± SEM as error bars. Confocal images were processed using FIJI/imageJ (Version: 1.54f)[477].

# 5. Interaction of bifidobacterial BEVs in complex environments

## 5.1. *Ex vivo* immunomodulation in different murine primary cells

### *5.1.1. Isolation of mononuclear cells from bone marrow*

10 wild-type (wt) C57/Blk6 healthy mice of 8-12 weeks of age were euthanised using Schedule 1 methods; $CO_2$ followed by cervical dislocation for confirmation of death, and disinfected with 70% ethanol prior to the isolation process. Tibias and femurs were removed and cleaned of any tissue under sterile conditions. Bone ends were cut off with scissors and placed in prepared 0.5mL Eppendorf tubes poked open at the bottom with a 1mL syringe needle. The bone-containing tubes were then transferred into 2mL Eppendorf tubes for BM collection and centrifuged (300×g/10-30min/RT). Collected BM was resuspended in 10mL PBS and spun down again (300×g/10min/RT). Washed BM pellets were resuspended in 10mL red blood cell (RBC) lysis buffer (containing 82.6g/L $NH_4Cl$ [Sigma-Aldrich Co LTD, Gillingham, UK], 12g/L $NaHCO_3$ [Sigma-Aldrich Co LTD, Gillingham, UK], and 0.5M ethylenediaminetetraacetic acid [EDTA; pH8; Fisher Scientific Limited]) and incubated for 10min at RT. White/colourless cell suspensions are centrifuged (300×g/10min/RT), washed twice in PBS, and strained through a 70µm cell strainer using a 5mL syringe plunger.

Animal handling, induction, help and supervision of BM harvest were performed by Dr Sally Dreger.

### *5.1.2. Cell culture of bone marrow-derived dendritic cells (BMDCs)*

Isolated BM cells were grown in Mercedes growth medium consisting of RPMI-1640 medium, 10% heat-inactivated FBS, 55µM mercaptoethanol (Fisher Scientific Limited, Hemel Hempstead, UK), 1% Pen/Strep, 1mM sodium pyruvate (Gibco™, Fisher Scientific Limited, Hemel Hempstead, UK), and 80ng/mL GM-CSF (Fisher Scientific Limited, Hemel Hempstead, UK) for 6-7d at 37°C and 5% $CO_2$. Living adherent and unattached cells were collected separately and processed for enrichment of CD11c-positive BMDCs. BMDC culture protocol was provided by Dr Victor Laplanche.

### *5.1.3. Enrichment of CD11c-positive BMDCs*

To ensure a high amount of CD11c-positive BMDCs for subsequent co-culture with the BEV batches, cultured BMDCs were enriched using the CD11c MicroBead UltraPure system for mouse samples (Miltenyi Biotec B.V. & Co. KG, Germany). Samples were processed as per manufacturer's instructions. Briefly, the collected cells were centrifuged (300×g/10min/4°C), supernatant discarded, and the cell pellet resuspended in 400µL kit buffer prior to magnetic labelling for 10min. Washed and resuspended cells were magnetically separated using an MS MACS column and MiniMACS separator. Flow-through was collected and labelled as CD11c-negative BMDCs. Retained cells were eluted and collected as CD11c-positive BMDCs.

Both cell sets were seeded at $1 \cdot 10^6$ cells per well in separate 96-well plates in Mercedes growth medium and 10% BEV samples ($1 \cdot 10^{11}$ particles/mL), LPS as positive control, and PBS as negative control, in triplicate, respectively. CD11c-negative BMDC cultures were used as controls as well. Plates were incubated for 24h, and supernatants were collected and stored for further use at -80°C.

### *5.1.4. Co-culture with isolated murine splenocytes*

Spleens from 5 wt healthy C57/Blk6 mice were isolated following euthanising and disinfection. Splenocytes were mechanically dissociated from the spleens and strained through a 70µm cell strainer. Cell solutions were washed in PBS, merged, and finally put in Mercedes growth medium and stored at 37°C and 5%$CO_2$. Resulting splenocytes were centrifuged (300×g/10min/RT) and seeded at $1 \cdot 10^6$ cells per well in 2 separate 96-well plates in Mercedes medium. Triplicates of 10% BEV samples, LPS as positive control, and PBS as negative control were added to both plates and one plate was incubated for 24h, the other for 48h. Supernatants were collected and stored until further use at -80°C.

Animal handling, spleen harvesting, and splenocyte separation were performed by Dr Chris Price.

### *5.1.5. Isolation of Peyer's Patch (PP) and Gut-associated lymphoid tissue (GALT) fragment cells from small intestine tissue*

The same mice used for BMDC preparation were also used to isolate PP and GALT fragments (see above). Abdominal skin and muscular wall were opened and

retracted with scissors and tweezers. Small intestine was isolated, cut between the stomach and caecum, excessive tissue removed, and placed in 10cm Petri dishes thinly covered with cold PBS and 2% Pen/Strep. Faeces were removed, and detected PPs were cut from the intestinal wall (~5 per mouse). PP/GALT fragments were kept in cold RPMI-1640 medium with 2% Pen/Strep, followed by straining through a 70µm cell strainer and washing with the cold RPMI-Pen/Strep solution. When fragments were completely dissociated, cell solutions were centrifuged (400×g/10min/4°C), washed thrice with the cold RPMI-Pen/Strep solution, and finally transferred into culture dishes.

Protocol provided by Pastori and Lopalco (2014; Bio-protocol.com)[479], animal handling was performed by Dr Sally Dreger, supervision and help with PP/GALT fragment isolation was also provided by Dr Sally Dreger.

### *5.1.6. In vitro activation of PP/GALT cells*

PP/GALT fragment cells were seeded in RPMI-1640 growth medium supplemented with 10% heat-inactivated FBS, 1% Pen/Strep, PMA (10ng/mL), Inomycin (500ng/mL; Thermo Scientific Chemicals, Hemel Hempstead, UK) and 100µg/mL Gentamycin (Gibco™, Fisher Scientific Limited, Hemel Hempstead, UK) at $2\times10^6$ cells in a 24-well plate. Triplicates of 10% BEV samples, LPS as positive control, and PBS as negative control were added, and the co-culture was incubated at 37°C and 5% $CO_2$ for 4d.[377] Supernatants were collected and stored at -80°C.

### *5.1.7. Cytokine, chemokine, and IgA secretion quantification*

Supernatant from BEV co-cultures with murine CD11c-positive BMDCs, splenocytes, and PP/GALT fragment cells were used in subsequent ELISA and MSD assays. Similar to chapter 4.2.3, key immunomodulatory cytokines were chosen, and assays were performed according to their provided manufacturer's instructions. Mouse IFN-γ, IL-4, IL-6, IL-1β, IL-12p70, IL-10, IL-22, IL-17A, TNF-α and keratinocyte-derived cytokine (KC) concentrations were determined using a U-plex MSD system as described above. Further, potential mouse IL-10 and IFN-γ concentrations were also tested in separate ELISAs (DuoSet®, DuoSet Ancillary Reagent ELISA Development Systems, R&D Systems, USA). IgA levels were quantified using Invitrogen IgA Mouse Uncoated ELISA Kit (Life Technologies Ltd Invitrogen Div, Thermo Fisher Scientific, Hemel Hempstead, UK) according to manufacturer's instructions.

## 5.2. BEV-human PBMCs co-culture

Human PBMCs (ATCC via LGC Standards) were handled as per supplier's instructions and seeded at $1 \cdot 10^5$ cells per well in RPMI-1640 medium containing 10% heat-inactivated FBS and 1% Pen/Strep in a 48-well plate. Similar to other co-cultures described above, triplicates of 10% BEV samples, LPS as positive control, and PBS as negative control were added, and the co-culture was incubated at 37°C, 5% $CO_2$, for 24h. Supernatants were collected, stored at -80°C, and finally used in the ELISAs mentioned above.

## 5.3. *In vitro* adjuvancy testing of bifidobacterial BEVs

Human macrophages (differentiated THP-1 cells) and differentiated epithelial cells (Caco-2 cells) were cultured and treated with bifidobacterial BEVs, PBS or LPS, respectively, as described above (see 4.1.1 and 4.2.1). Growth medium was changed after 24h, and treated cells were then challenged with LPS for 12-48h to simulate an infection. TEER was measured in epithelial cultures, as described above (see 4.1.2). Supernatant was collected for ELISA, and RNA was extracted from the respective cells for qRT-PCR testing as described above. Used primers are listed in Table 9 and Table 10.

## 5.4. Visualisation

ELISA, MSD and qRT-PCR graphs were analysed and visualised with Microsoft Excel (version Microsoft Office 2019).

# 6. Statistical analysis

Statistics used for proteomic data processing workflow described above. All data are depicted as mean ± SEM with specified replication number. Other statistical analyses were performed using RStudio version 4.3.2 with packages readr, dplyr, tidyr, readxl, rstatix, openxlsx, ggplot2, reshape2, FSA, emmeans, patchwork, and performance.

Data were subjected to model-fitting transformation, where appropriate, and analysed using two-tailed Student's *t*-test (CFU), two-sample Student's *t*-test (endocytosis assay), one-way analysis of variance (ANOVA), followed by Tukey's multiple comparison *post hoc* test (NTA, BEV content quantification) or Dunnett's *post hoc* test (QuantiBlue, ELISA, MSD, qRT-PCR), and two-way ANOVA followed by Dunnett's *post hoc* test (growth curves, TEER assay). Significance was defined as $P \leq 0.05$.

# III. Results Chapter I – Growth Optimisation of Selected *Bifidobacterium* Strains for BEV Production

## 1. Summary

Variation in vaccine efficacy has been linked with individual microbiota composition differences; in particular, high abundances of *Bifidobacterium* species appear to be a key factor for improved immune responses.[1] However, corresponding mechanisms and immune-modulating strains and their products are still poorly understood, which is required to provide novel vaccine interventions. With focus on the understudied species *B. pseudocatenulatum*, which is one of the few *Bifidobacterium* species prevalent in the microbiota of individuals of all ages[89,162], we compared two potentially immunomodulatory strains of *B. pseudocatenulatum* isolated from the same healthy infant host.[88,469] I optimised the growth of the selected strains in animal- and human-product-free medium to allow ideal growth conditions for BEV harvesting, while complying with any subsequent vaccine trial regulations. I identified a diauxic shift in the strains in the optimised growth medium, suggesting production of distinct BEVs with different properties. Appropriate time points were chosen for the BEV isolation protocol, and respective comparison of potential differences in immune modulation properties in BEV preparations were at the core of the project.

## 2. Contributions

Overall supervision and help with the writing of this chapter, as well as experimental suggestions, were provided by Prof Lindsay Hall and Prof Simon Carding. Lab inductions, growth and DNA extraction SOPs were provided by Dr Iliana Serghiou Daley and Dr Nancy Teng. WGS was performed by Dr David Baker and genetic analysis was done by Dr Magdalene Kujawska. Everything else was done by me.

# 3. Background

## 3.1. Discrepancy in global vaccination outcomes

Introduction of vaccines revolutionised public health by reducing mortality and morbidity of infectious diseases globally, and vaccination still prevents approximately 2-3 million deaths per year.[480] However, efficacy of numerous vaccines varies between different populations and even individuals, especially in infants versus adults, and those individuals living in LMICs compared to those in high-income countries. Particularly, orally administered vaccines such as oral rotavirus vaccine (ORV), OPV, and vaccines against cholera and typhoid display discrepancies in immunogenicity in LMICs, with vaccine efficacies of ORV at 44% and 70% for OPV in infants from LMICs compared to 94% and 100% in high-income country infants, respectively.[468,481–483] Even long-established vaccines such as the BCG vaccine showed a 100% immune response against tuberculosis in infants in the UK compared to only 53% of infants from Malawi.[468,484]

A plethora of factors can impact vaccine efficacy, including vaccination-related factors (e.g. type and dose of antigen, use of adjuvants, route and timing of delivery, co-administration of other vaccines)[485], host-intrinsic factors (e.g. age, genetic dispositions[92,486,487], sex[488], comorbidities), perinatal factors (e.g. preterm birth, malnutrition, mode of delivery, form of infant feeding, maternal health), and environmental factors (e.g. exposure to antibiotics and pathogens, chronic infection[489], hygiene, transmission of maternal antibodies[108], microbiota compositions).[1,96,490]

## 3.2. Abundance of *Bifidobacterium* species as a key factor in vaccine efficacy

### *3.2.1. Impact of the early-life GIT microbiome*

Many studies have demonstrated that the GIT microbiota plays a vital role in promoting effective humoral and cellular immune responses to vaccines through various mechanisms, especially in early life.[1,51,491] Indeed, comparison of the microbiota of infants from different geographical and socio-economic settings revealed a correlation between the abundance of specific bacterial genera and species within the GIT and the immune response after vaccination. The microbial profile of ORV-

responders from Ghana and Pakistan was more comparable to the microbiota of age-matched Dutch infants than to the microbial profiles of vaccine non-responders from the same country of origin.[384,385]

Colonisation within the first 1000 days of life has a crucial impact on overall GIT microbiota composition, development of the immune system and health throughout life, which also affects early-life vaccine responses.[96,492,493] Disruption of the 'healthy' trajectory of microbial colonisation during this time window in the infant GIT, driven by similar factors influencing vaccine efficacy, can have a detrimental influence on immune maturation. Many studies have shown the adverse effects of antibiotics on vaccine responses in infants. Chapman et al. (2022)[494] found a negative association between antibody titres to DTaP and pneumococcal conjugate vaccine in children with antibiotic regimes compared to non-antibiotic-exposed children. Similar results had been shown in mice receiving the BCG vaccine after antibiotic treatment, which could not mount a sufficient T cell immune response.[459,495] Moreover, the development of key immune cells such as B cells, NK cells, and DCs was influenced by interactions with the microbiota and was impeded by bacterial dysbiosis early in life.[96,496]

Favourable factors for a 'healthy' microbiota establishment, such as breastfeeding and vaginal delivery, are associated with improved vaccination outcomes, providing the newborn with health-promoting bacterial species, such as *Bifidobacterium*, and their specific nutrients (i.e. HMOs).

### *3.2.2. Focus on Bifidobacterium species*

The 'healthy' GIT microbiota colonisation trajectory is dominated by *Bifidobacterium* species, starting with *B. longum* subsp. *infantis*, *B. breve*, and *B. bifidum* within the first days of life.[87] *B. catenulatum* and *B. pseudocatenulatum* start establishing in the intestine of breast-fed infants at pre-weaning and are still found up to adulthood.[89] *B. longum* subsp. *longum* and *B. adolescentis* are enriched within the adult microbiota.[497,498] High abundances of *Bifidobacterium* within the GIT microbiota have been linked with many health benefits, such as reduction of pathogen colonisation, regulation of intestinal homeostasis, immunomodulation, anticarcinogenic activity and improved vaccine responsiveness.[90,216,499–502]

Indeed, Huda et al. ( 2019)[90] showed that high abundance of *Bifidobacterium* species was positively associated with enhanced antigen-specific T cell responses, IgG

responses and thymic size following OPV, BCG and tetanus toxoid vaccination when compared to infants with intestinal microbial dysbiosis. A similar result has been seen in a cohort of Chinese infants with enhanced OPV-specific vaccine responses and IgA titres in infants with high abundances of *Bifidobacterium* in their GIT microbiota.[391] Moreover, individuals with a *Bifidobacterium*-dominant microbiota were also found to have higher levels of IgA-secreting plasma cells[503], memory B cells[504], and salivary IgA.[90]

### *3.2.3. Emerging importance of B. pseudocatenulatum species*

*B. pseudocatenulatum* strains are gaining increasing interest due to their omnipresence within the non-disrupted GIT microbiota across the human lifespan. Many *B. pseudocatenulatum* strains have been found to metabolise specific carbohydrates from different sources, such as HMOs and plant polysaccharides, depending on the respective intestinal environment. In dietary intervention and probiotic administration studies, increases in *B. pseudocatenulatum* abundance during and post-intervention were associated with improved bioclinical parameters of hosts (i.e., weight loss, improved plasma Glc and lipid homeostasis, decreased inflammation marker levels, microbiota shifts towards 'healthy' communities)[168], as well as improved metabolic and immunologic obesity-associated health changes, and production of health-beneficial compounds, such as SCFAs and EPS (i.e. postbiotics).[172–174] Therefore, this species is of particular interest considering their environmental adaptability and metabolic potential/profiles, and production of SCFAs, EPS and other microbial compounds which may influence immune responses. One aspect of *B. pseudocatenulatum* biology which is of significance in the vaccine field is the ability of its BEVs to act as immunomodulatory agents, which may represent attractive natural adjuvants in vaccine formulations. Therefore, in this project, I focused on the isolation, purification and characterisation of BEVs produced by selected *B. pseudocatenulatum* strains in the context of improving immune modulation and vaccine responses.

# 4. Results

## 4.1. Selection of potential immunomodulatory *Bifidobacterium* isolates

Previous work in the Hall lab (by Shannah Lympany) has screened different bifidobacterial isolates derived from healthy, full-term, breast-fed British babies[88,469], to determine their potential abilities to improve immune responses after vaccination. More details on the origin of the selected strains can be found in the Materials and Methods chapter (under 2.1 Culture and growth of *Bifidobacterium* strains) and in the Introduction chapter (under 6 Thesis aims and objectives). Preliminary (unpublished) data indicated certain isolates were able to induce DC maturation *in vitro*, stimulate cytokine production associated with enhanced vaccine responses (e.g., IL-12), and also boost murine immune response to *Bifidobacterium* supplementation. Based on these data, several *Bifidobacterium* isolates were selected that display immunomodulatory properties, including *B. breve* UCC2003, *B. breve* LH24, *B. longum* subsp. *infantis* LH277, *B. pseudocatenulatum* LH660 and *B. pseudocatenulatum* LH663. Given that *B. breve* and *B. longum* subsp. *infantis* have already been explored for their immune-modulatory properties in detail; here, I focused on *B. pseudocatenulatum*, and in particular isolates LH660 and LH663 originating from the same infant donor.[88,469,505]

### *4.1.1. Establishment of a bank stocks of LH660 and LH663*

As a first step, I created a bank of five master and ten working stocks based on the isolates used by S. Lympany, following the respective SOPs (see Methods chapter 2.1). DNA was isolated from all stocks for WGS.

After pre-processing of the sequencing reads, the data of both *Bifidobacterium* strains LH660 and LH663 were checked for potential contamination by comparison with the MiniKraken database by Dr Magdalena Kujawska. The analysis confirmed that LH663 was free of contaminating sequences derived from other bacteria. However, the WGS data of isolate LH660 showed that the tested master and working stocks were contaminated with at least one other strain, potentially *B. choerinum* based on the Kraken reports (see Appendix, page 202, Supplementary Figure 1 and Supplementary Figure 2). LH660 was omitted from further testing until pure stocks could be obtained.

## 4.2. Growth in optimised medium reveals two key time points for BEV harvesting

### *4.2.1. Efficient growth of selected strains in vegan medium*

**a) <u>Comparison of established media reported for bifidobacterial growth as template for vegan medium option</u>**

Due to regulations within modern vaccinology not accepting vaccines made with or containing animal products, as well as potential interferences in downstream BEV purification and *in vitro* and *in vivo* studies, it is desirable to create reagents and experimental conditions that exclude animal and human-derived compounds. Most *Bifidobacterium* strains are slow-growing (in comparison to e.g., *E. coli*) and difficult to culture without rich media containing animal products. Therefore, I performed a series of growth tests using established media for growth of certain *Bifidobacterium* strains (i.e., RCM, MRS, and BHI), to determine optimal growth conditions of the pre-selected *B. pseudocatenulatum* strains. Both LH660 (Figure 6A) and LH663 (Figure 6B) were sub-cultured from WS and then inoculated in different growth media.

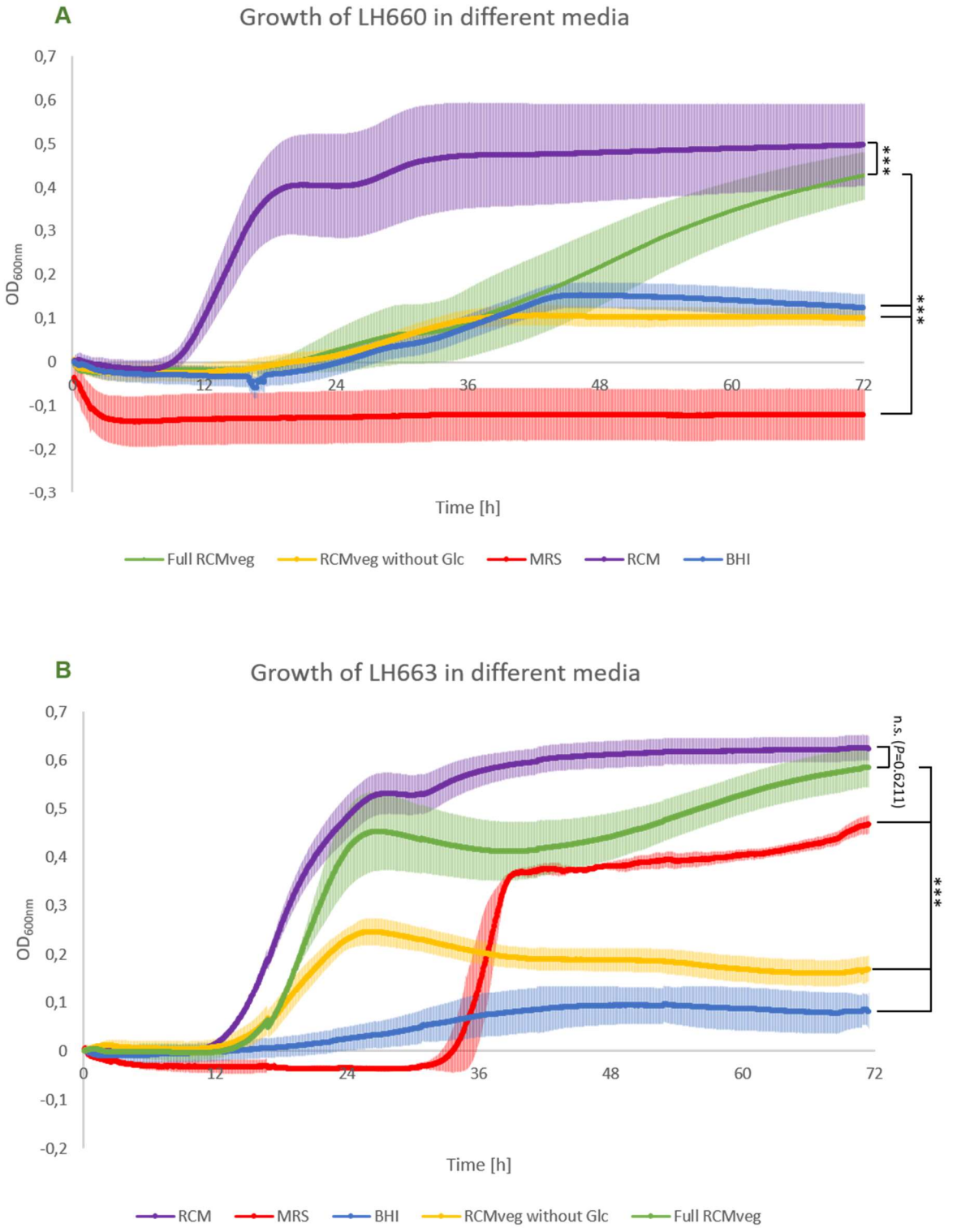


*Figure 6: Growth of Bifidobacterium strains LH660 (A) and LH663 (B) in different established growth media, including RCM, MRS, and BHI, as well as RCMveg growth medium without primary sugar supplement and with Glc supplementation. Mean growth is displayed in bold lines, error bars in respective fainter-coloured lines above and below mean growth at each time point. *** P value ≤ 0.001 (two-way ANOVA, followed by Dunnett's* post hoc *test); N = 3*

Both strains grew best in RCM broth with a short lag phase, entering exponential growth after 12h. Interestingly, LH660 did not grow in MRS, which was unexpected

given the typical use of this medium for growing *Bifidobacterium* strains. LH663, on the other hand, took over 30h to adjust to growth conditions in MRS but displayed a distinct exponential growth leading to relatively high $OD_{600}$ values of 0.37 when reaching stationary growth. Both strains grew poorly in both BHI and RCMveg growth medium without supplemented Glc as the primary carbon source, with RCMveg allowing better growth than BHI for LH663. Since RCMveg without Glc still contains starch as a complex sugar (see Methods Table 7), both strains can metabolise starch, which is consistent with other published data on *B. pseudocatenulatum* metabolism reporting the presence of starch degradation gene clusters.[88,505,506]

**b) Refinement of selected vaccine-friendly growth medium recipe**

To simplify the medium formula, I performed another growth series with both LH660 and LH663 in different modifications of RCMveg. Two components, namely starch and agar, were identified as potential confounding factors for mediocre purification outcomes during initial BEV preparation, as they might hinder the filter system. Moreover, residues of agar could confound or interfere with the outcome of downstream *in vitro* and *in vivo* experiments.

Therefore, I prepared different alternatives of RCMveg containing either all ingredients, no agar, no starch, or neither starch nor agar. The list of the final ingredients of RCMveg can be found in the Methods (see Table 7). The resulting growth curves for LH660 (Figure 7A) and LH663 (Figure 7B) are shown below.

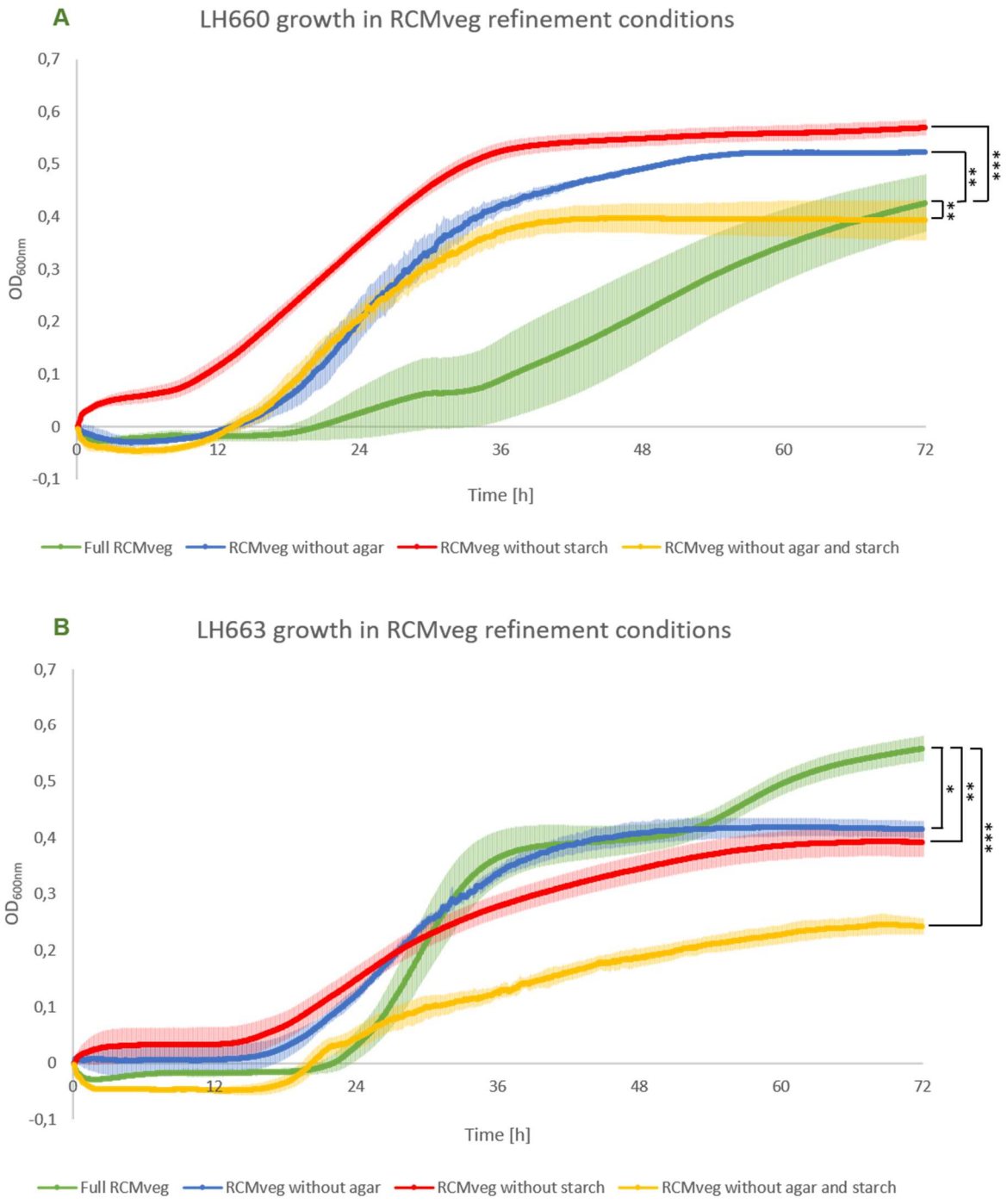


*Figure 7: Growth of the strains LH660 (A) and LH663 (B) in full and minimised RCMveg growth medium. $OD_{600}$ was taken every 4min for over 72h. Mean growth displayed in bold lines, error bars in respective fainter-coloured lines above and below mean growth at each time point. * P value ≤ 0.05, ** P value ≤ 0.01, *** P value ≤ 0.001 (two-way ANOVA, followed by Dunnett's* post hoc *test); N= 3*

As expected, strain LH663 exhibited optimal growth in full RCMveg medium, entering exponential phase after 20h, reaching the first plateau of the stationary phase after 32h and attaining its maximum $OD_{600}$ of 0.53 after 70h of growth. In the absence of agar, LH663 exhibited a shortened lag phase, entering exponential growth after 17-18h. However, growth was significantly reduced (*P*=0.0197), with exponential growth

being less pronounced than in complete media, reaching stationary phase after 37h and a maximum $OD_{600}$ of 0.39. LH663 cultures grown in RCMveg without starch demonstrated similar initial growth as in media without agar. However, the exponential phase in these cultures was shorter, reaching stationary growth at around 27h. Removal of both starch and agar from the growth media significantly ($P$=0.00016) impacted the growth of LH663, decreasing growth due to a short exponential phase between 18h to 20h, hardly reaching an $OD_{600}$ above 0.15.

Surprisingly, LH660 favoured simplified growth conditions as both RCMveg without agar and RCMveg without starch led to significantly ($P$≤0.01) enhanced growth patterns when compared to richer medium. The highest growth was achieved in the absence of starch, with a short lag phase entering exponential growth after 8h and reaching stationary phase after 33-34h with a maximum $OD_{600}$ of over 0.53. The cultures without agar grew with a longer lag phase than the cultures without starch, but with a similar pronounced exponential growth resulting in a maximum $OD_{600}$ of 0.49 after 48h. In rich media, LH660 needed a longer time to adjust with a lag phase of over 24h. Growth without both ingredients was less than with one component removed, but still significantly ($P$≤0.01) higher than growth in rich RCMveg for LH660.

Since removing both ingredients impacted growth in both strains to a higher degree, I removed agar only from the list of components of RCMveg for the rest of this project.

### c) Assessment of medium optimisation through supplementation

To maximise BEV yield, I tried different supplements to enhance bacterial growth, such as a vitamin mix containing seven different vitamins (pantothenate, nicotinamide, thiamine, biotin, vitamin B12, menadione and 4-aminobenzoic acid) that were reported to be beneficial for the growth of different *Bifidobacterium* species.[471]

However, the vitamin cocktail impaired growth of the strains (see initial growth curves in the Appendix, Supplementary Figure 5). Additionally, growth dynamics can be strain-specific and might be toxic for the strains used here. So, growth tests were repeated with strain LH663 in RCMveg medium supplemented with a dilution series of the vitamin cocktail, as well as non-diluted vitamins and no vitamins (Figure 8).

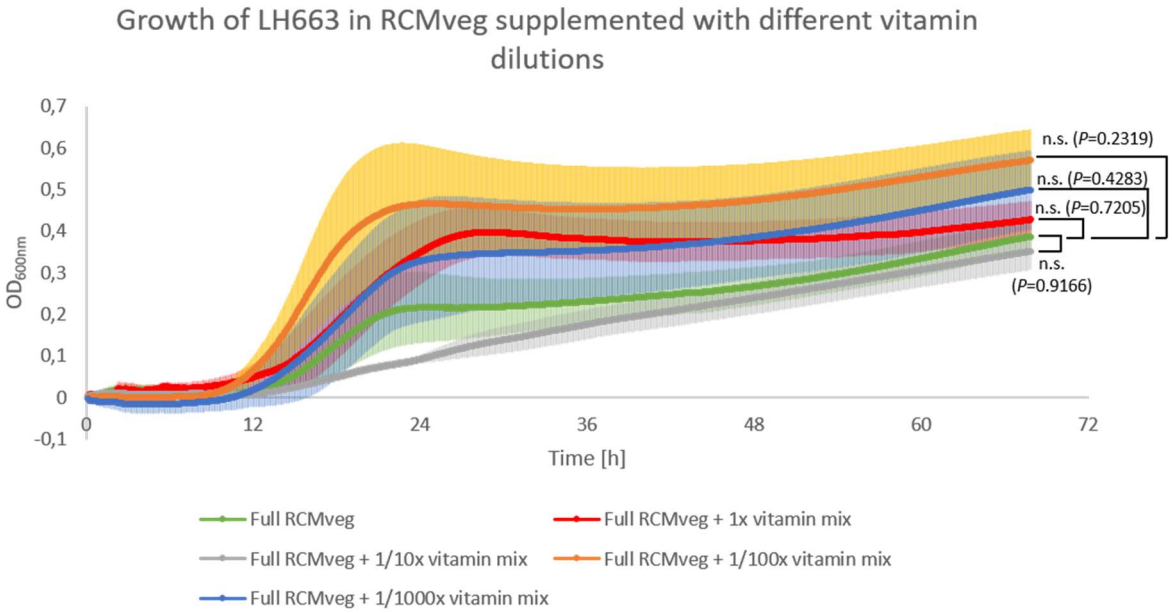


*Figure 8: Growth of the strain LH663 in non-supplemented RCMveg, and growth medium supplemented with an undiluted vitamin mix and a dilution series of the vitamin mix. OD600 was taken every 4min for over 72h. Mean growth displayed in bold lines, error bars in respective fainter-coloured lines above and below mean growth at each time point. (two-way ANOVA, followed by Dunnett's* post hoc *test); N = 3*

Unlike initial findings, almost all dilutions of the vitamin mix resulted in enhanced, but not significantly different ($P \geq 0.05$), growth compared to the non-supplemented RCMveg medium. An exception was the irregular growth of cultures grown in RCMveg medium with a 1:10 dilution of the vitamin cocktail. All other supplemented preparations displayed a shorter lag phase, longer and more pronounced exponential growth and higher $OD_{600}$ values when entering stationary growth and reaching maximum scores compared to the non-supplemented RCMveg medium. The highest growth was in cultures grown in RCMveg with a 1:100 dilution of the vitamin cocktail, entering exponential growth at 10h and stationary growth at 20h with a maximal $OD_{600}$ value of 0.55. In comparison, growth in RCMveg media with no supplementation needed over 14h to enter exponential growth and reached stationary phase at 20h at an $OD_{600}$ of 0.2 with a maximum value of 0.3 after 70h of growth.

These results confirm the bifidobacterial growth-promoting abilities of the published vitamin cocktail, the effect of which was greater after optimising the concentration, but remained non-significant. Moreover, media preparation using this vitamin mix was more laborious and time-intensive, and following optimisation of the BEV preparation protocol, BEV yields were sufficient with the final RCMveg formula. To maintain a refined and standardised growth medium and minimise downstream confounding

factors during BEV purification, I decided to omit the vitamin supplementation for the remainder of this project.

Additionally, I tested bifidobacterial growth dynamics in the presence of different HMOs (i.e. 2'FL and LNnT); as these strains were isolated from faecal samples of a breastfed baby, they would be expected to metabolise HMO. Thus, in another test series, I repeated the growth assays using supplementation of RCMveg growth medium with 2'FL and LNnT, to test if they were metabolised by LH663. As initial tests indicated growth of LH663 only in combination with Glc (see Appendix, Supplementary Figure 3), I re-ran both combinations of the HMOs with Glc, as well as each sugar as the sole simple carbon source (Figure 9). As a negative control, I added the RCMveg growth medium without any supplemented simple sugar. All cultures grown in RCMveg growth media supplemented with HMOs, both solely or in combination with glucose, performed less well when compared to media supplemented with glucose only. All combinations of HMOs with glucose resulted in non-significantly reduced growth ($P \geq 0.05$), with a longer lag phase and a shorter exponential phase than the Glc-only supplements. Similarly, the cultures grown in 2'FL- or LNnT-supplemented RCMveg medium displayed equal growth to those in non-supplemented RCMveg medium, all significantly lower than full RCMveg with Glc ($P \leq 0.05$), implicating that LH663 does not metabolise either HMO but rather Glc and starch present in the medium.

Initial work confirmed that both strains lacked genomic and phenotypic capacity for HMO metabolism. This had also been shown in previously published work.[88] Thus, these growth assays with LH660 in RCMveg and HMO supplementation were not repeated, as no HMO metabolism (see Supplementary Figure 4) was expected and confirmed both in the initial work here and by Lawson et al. (2020).[88]

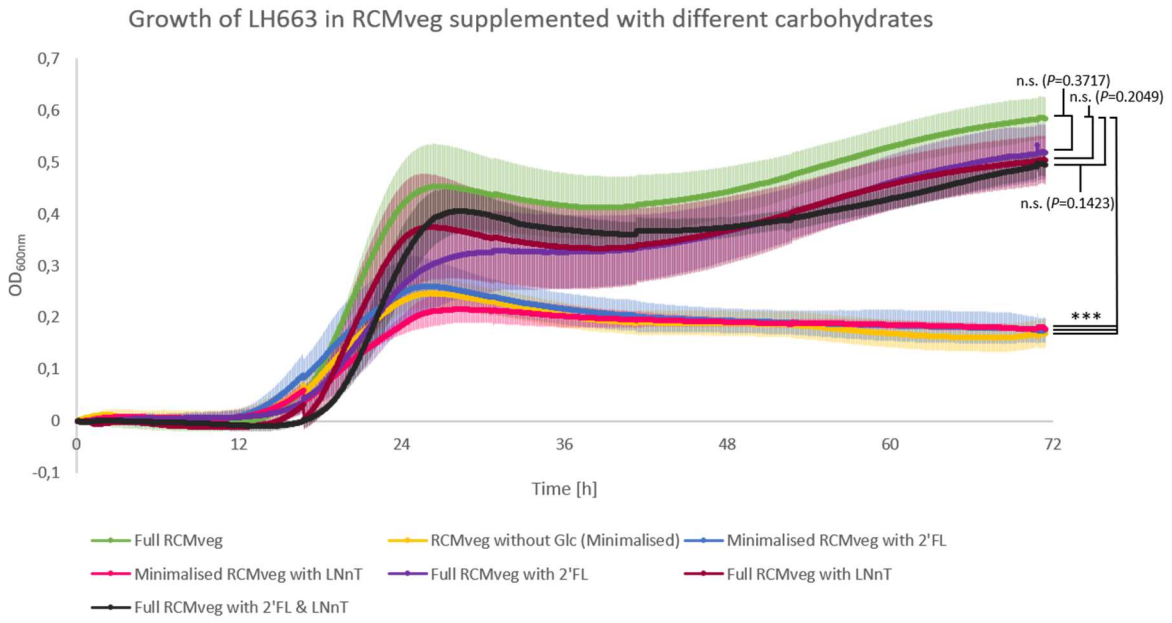


*Figure 9: Growth of LH663 in RCMveg growth medium supplemented with Glc, 2'FL, LNnT and combinations of all three sugars. Non-supplemented RCMveg growth medium served as the negative control. Mean growth is displayed in bold lines, error bars in respective fainter-coloured lines above and below mean growth at each time point. *** P value ≤ 0.001 (two-way ANOVA, followed by Dunnett's post hoc test); N = 3*

### *4.2.2. CFU determinations show a diauxic shift in both LH660 and LH663*

Determination of bacterial yield at a given time of growth is essential for downstream experiments and for evaluating their reproducibility.

As shown in Figure 10, both LH660 and LH663 follow similar growth patterns up to 34h (*P*=0.8976), with LH660 displaying a shorter lag phase (~4h) and more pronounced exponential growth compared to LH663. The OD values showed that both strains entered stationary growth after 16h. Interestingly, the CFU data showed different growth profiles, with several time points displaying a significant difference in bacterial yield between strains (*P*≤0.05). Both LH660 and LH663 followed the growth as seen in the OD data, entering the exponential phase at approximately 6h. However, the CFU data indicated they both reached a peak at 12h (LH660 with $1.31e^{10}$ CFU/mL and LH663 with $8.81e^{9}$ CFU/mL), followed by an abrupt decline in CFU (at 14h, only $1.55e^{9}$ CFU/mL for LH660 and $4.98e^{9}$ CFU/mL for LH663; Figure 10A). Only LH663 showed a slight, non-significant decline in OD at 14h (*P*=0.8976). Similar to a second lag and exponential phase after 12h, both strains reach maximal CFU at 20h ($1.86e^{10}$ CFU/mL for LH660 and $1.4e^{10}$ CFU/mL for LH663) before a decrease in bacterial yield. Thus, CFU data showed that both strains enter the stationary phase after 20h (Figure 10A), which is 4h later than seen using OD measurements.

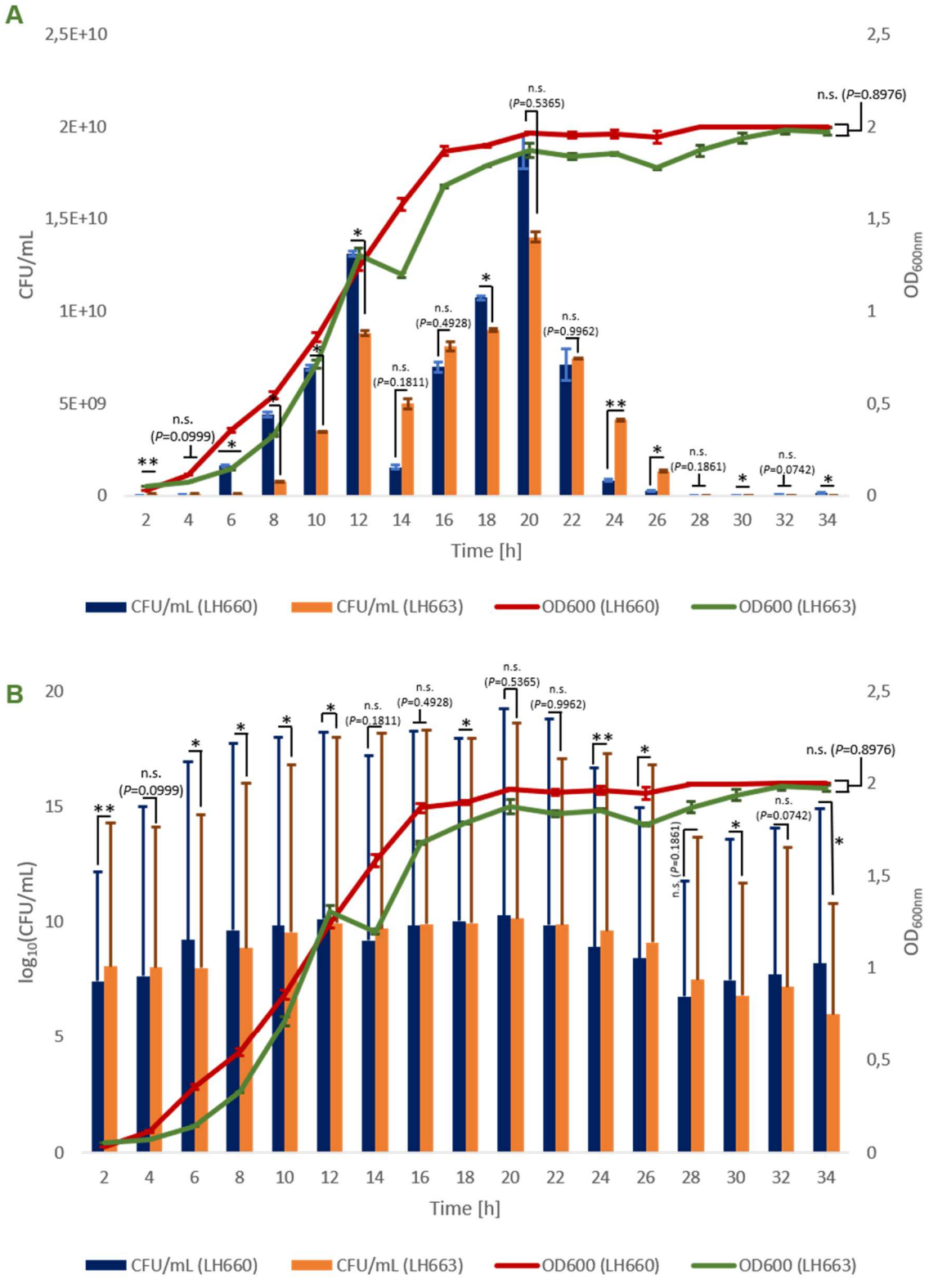


*Figure 10: Bacterial yield of strains LH660 and LH663 over 34h, displaying a diauxic shift after 12h. CFU and OD measurements were taken every 2h. Means displayed as columns (CFU) and lines (OD) with SEM as error bars. A: non-logarithmic CFU/mL data for better visualisation of peaks at 12h and 20h, B: logarithmic CFU/mL data for completeness, showing maximum values at 12h and 20h. * P value ≤ 0.05, ** P value ≤ 0.01 (two-tailed Student's* t-test *for CFU data, two-way ANOVA followed by Dunnett's* post hoc *test for OD data); N = 3*

This growth profile, with two exponential phases and two peaks at 12h and 20h of growth, may be due to a metabolic switch by the strains after consumption of Glc as the primary carbon source, followed by starch metabolism. Since BEV cargo changes in response to different environmental conditions[466], the peaks or maximum $log_{10}$(CFU/mL) (Figure 10B) at 12h and 20h may reflect distinct BEV populations, either driven by metabolic switches or different cell types within the bacterial cultures. Therefore, I chose 12h and 20h as time points for subsequent BEV harvesting.

# 5. Discussion and perspectives

## 5.1. Inclusion of *B. pseudocatenulatum* for vaccine adjuvancy

Studies have shown that the GIT microbiota contributes to host immune response to pathogens and vaccines.[459] Identifying key probiotic strains and their products may be beneficial for effective vaccine formulations. For instance, oral vaccines against HPV using genetically modified lactic acid bacteria as antigen carriers result in stronger systemic and mucosal-specific immune responses against HPV, leading to lower infection and incidence of cervical cancer, underlining the potential adjuvant properties of certain commensal bacteria.[459,507] Modifying the GIT microbiota to improve vaccine immunogenicity is challenging due to individually unique microbiota composition. Several therapeutic strategies have been proposed, including targeted antibiotic regimens, synbiotic supplementation, and FMT. However, due to rising threat of AMR and limited feasibility of FMTs on a global scale (especially in LMIC populations), tailored use of synbiotics and postbiotics can be advantageous for improving vaccine efficacy. [468]

Several target *Bifidobacterium* strains have been identified within our lab for potential immune modulation. This project focused on *B. pseudocatenulatum* strains, which are understudied compared to other probiotic *Bifidobacterium* species. *B. pseudocatenulatum* species are closely related to *B. adolescentis* and *B. catenulatum* species, with the latter two being dominant in the GIT microbiota of adults.[174] Indeed, being constituents of the human GIT microbiota from infancy to old age, *B. pseudocatenulatum* might possess specific properties enabling ‘universality’/high adaptability in changing intestinal environments, which could improve the compromised immunity in individuals at the extremes of life. Therefore, I investigated

if BEVs derived from *B. pseudocatenulatum* display similar immunomodulatory properties, which can be of potential use in novel vaccine interventions while being cost-effective, scalable, and stable, all of which are important for their use in LMICs.

## 5.2. Selected strains of same origin display phenotypic heterogeneity

### *5.2.1. Strains isolated from a breast-fed infant utilise starch instead of tested HMOs, pointing towards potential cross-feeding networks*

Given the fact that both strains originated from a non-weaned, breast-fed infant, HMO metabolism should not be surprising. Consistent with Lawson et al. (2020)[88] who isolated both strains and described LH663 among other *B. pseudocatenulatum* strains, no HMO-related gene clusters were fully or partially present, which they confirmed by growth assays using 2'FL and LNnT. Nevertheless, I repeated their growth assays on potential 2'FL and LNnT metabolism using modified MRS and HMOs (see Appendix, Supplementary Figure 3 and Supplementary Figure 4), as well as RCMveg and HMOs (see Figure 9) and confirmed that LH660 and LH663 are unable to utilise either of the tested HMOs.

However, only the most abundant HMOs, namely 2'FL and LNnT, were tested, leaving room for potential degradation of other HMOs by one or both strains, as this metabolic activity is highly strain- and HMO-type-dependent.[88] Indeed, Bajic et al. (2023)[498] found a preference for utilisation of 3′-Sialyllactose/6'-Sialyllactose (3'SL/6'SL) in their tested *B. pseudocatenulatum* strains. Yet, several studies found that different infant-derived *B. pseudocatenulatum* strains lack the ability to metabolise HMOs.[88,175,508] Consistent with this, no HMO metabolism-related gene clusters were identified.[88] Given that more than 200 distinct HMO structures have been reported to date[161,509], and that optimal growth for subsequent BEV isolation was achieved in RCMveg supplemented with Glc and starch, further testing of potential utilisation of additional HMOs was not pursued.

Interestingly, some bifidobacterial species, such as *B. bifidum*, can initiate HMO degradation extracellularly via extracellular GHs, resulting in mono- and disaccharide availability and potential cross-feeding with other HMO-non-degraders.[88,161,510] Lawson et al. (2020)[88] also demonstrated cross-feeding between bifidobacterial HMO-

degraders and non-degraders originating from the same host, highlighting the altruistic nature of *Bifidobacterium* strains to preserve diversity and dominance within the infant GIT environment. Indeed, other studies report heterogeneous carbohydrate metabolism of many infant-derived *B. pseudocatenulatum* strains as non-degraders of HMOs but starch-degraders at a pre-weaning state, underlining the transitional ability and adaptability of this *Bifidobacterium* species prior, during, and after GIT maturation and nutrient shifts.[88,140,168,175,505,506] Similar metabolic diversity and agility in *Bifidobacterium* have been reported for *B. castoris* strains isolated from wild mice[511] and human-derived *B. longum* strains.[512] Here, I also showed that LH660 and LH663 were able to utilise starch, but neither of the two tested HMOs, which might be important in considering prebiotic-based GIT microbiota interventions.

### *5.2.2. Diauxic growth and bacterial cell yield in medium containing Glc and starch*

The optimised and refined 'vegan' growth medium containing starch supported the growth of both strains in the absence of Glc as a primary carbon source confirming their ability to degrade starch though at a slower rate than other starch-degraders.[505,506] Lawson et al. (2020)[88] and Millar (2023)[505] performed an in-depth study on RS utilisation in different *Bifidobacterium* strains (including LH663 and LH660) and found a high number of CAZymes related to starch metabolism (i.e. GH13, Carbohydrate-Binding Module Family [CBM] 48, CBM25, and CBM74) and to arabinoxylan metabolism (i.e. GH43) indicating adaptation towards solid food substrates rather than breast-milk prior to its introduction. They showed that the number of detected CAZymes varied slightly between otherwise 'clonal' strains of the same host. The most common type of GH in the tested *B. pseudocatenulatum* strains (including LH663 and LH660) was GH13, which represents enzymes for hydrolysing alpha-glucosidic linkages in plant di-, oligo-, and polysaccharides.[88,505,513]

A similar microdiversity between *B. pseudocatenulatum* strains from the same host was also reported in a dietary intervention study, where the analysed strains showed a variation in CAZy genes for plant polysaccharides and strain-specific positive association with beneficial changes in bioclinical parameters (i.e., plasma Glc and lipid homeostasis, weight loss, inflammation marker levels) within the host.[168] Conversely, Kan et al. (2020)[140] found that genetically similar *B. pseudocatenulatum* strains shared between mother-infant pairs showed environment-specific metabolic profiles with maternal strains utilising a greater range of glycans than the infant isolates, underlining

that the genetic microdiversity and gene expression of the strains are also regulated by the given intestinal ecosystem.[142]

Interestingly, a screening study of metabolic gene clusters among *B. pseudocatenulatum* strains revealed that 43.3% of all genomes contained genes associated with starch degradation, with several also linked to EPS production, suggesting a potential connection between these two mechanisms.[160] Both LH660 and LH663 possess EPS gene clusters (data not shown), and EPS production has been confirmed in LH663.[176] This may have implications for BEV production and the possible attachment of EPS to BEVs generated during starch metabolism, a hypothesis explored in Results Chapter II.

The CFU data and, to a lesser degree, the OD data presented here show a distinct diauxic shift towards starch utilisation of both strains in RCMveg media after depletion of Glc, underlining the importance of more precise methods of bacterial quantification in addition to OD measurements. Indeed, several growth curves using OD data alone do not indicate diauxic growth, leading to other time points for exponential and stationary growth.

This metabolic adaptation of diauxie has been seen in numerous studies using media with multiple sugars of varying complexity.[514] Cell division is slowed after starvation stress, induced by the lack of the primary carbohydrate and enzymatic adaptation to the metabolism of the secondary sugar. Interestingly, Solopova et al. (2014)[514] found that in *Lactococcus lactis,* in contrast to the established concept of metabolic shifts, the diauxic lag phase was not due to the time bacteria needed for switching metabolisms from one sugar to the other, but rather that two distinct cell types of the bacterium co-existed in the same culture. These cell types displayed discrete metabolic profiles resulting in discontinued growth of one cell type upon complete exhaustion of the preferred carbon source.

It is unclear if the *B. pseudocatenulatum* strains tested here follow a similar trajectory as seen in *L. lactis*. Both strains display a diauxic lag phase at 13-14h of growth, where bacterial cell numbers decreased more than 8-fold (from $1.31e^{10}$ CFU/mL at 12h to $1.55e^{9}$ CFU/mL at 14h) for LH660 and LH663 CFU is nearly halved (from $8.81e^{9}$ CFU/mL at 12h to $4.98e^{9}$ CFU/mL). This may suggest that LH660 may be less adaptable to environmental changes and nutrient availability, hinting towards the microdiversity of *B. pseudocatenulatum* strains from the same source.

However, further research is needed to uncover strain- and nutrient-specific properties (i.e. HMO utilisation, cross-feeding, growth in presence/absence of certain vitamins and other micronutrients) of potential probiotic strains, their products and metabolites and possible use for immune modulation, especially within vaccine interventions.

## 5.3. Limitations and future work

Based upon the analysis of the two strains, LH660 and LH663, the findings presented here provide insights into the potential phenotypic microdiversity of *B. pseudocatenulatum* strains. Additional *Bifidobacterium* strains from other hosts of different demographic origins and ages would give a more complete understanding of intra-microbial and microbiota-host interactions, leading to the identification of immunomodulatory strains with potential for vaccine adjuvancy.

More testing of different nutrients and supplements is warranted to optimise immune modulation by *B. pseudocatenulatum* (or other beneficial species and genera) and their microbial products. Since specific underlying mechanisms for the many reported health benefits and vaccine response improvements of *Bifidobacterium* are unclear, optimisation and rigorous characterisation are needed to ensure best outcomes, especially in complex systems such as the human body.

Here, I concentrated on two conditions of growth for both strains, pre- and post-diauxic shift, and did not include any further HMOs, other complex glycans, or supplements other than the vitamin cocktail prior to undertaking next series of experiments. However, the use of a refined, animal- and human-product-free growth medium as the standard in this project was intended to minimise the risk of contamination from animal-derived vesicles and other confounding factors introduced by complex ingredients or supplements.[287,339]

Vitamin supplementation yielded inconsistent growth outcomes, with initial tests indicating growth inhibition, whereas subsequent assays revealed enhanced growth rates, particularly in concentration-adjusted samples. This discrepancy may be attributable to differences in the preparation and freshness of the vitamin mix. In the initial tests, a master stock cocktail was prepared in advance and used for media preparation and inoculation. In contrast, repeated experiments used freshly prepared stocks of individual vitamins, which were only combined at the point of media preparation. Potential degradation or interactions among vitamins in the pre-mixed

cocktail could explain the variation observed between initial and repeated assays, and need to be considered for future experiments.

However, given the changing nature of BEVs in response to different environmental conditions, different populations and types of BEVs will be produced using more diverse media.

Despite these limitations, this work provides the basis for investigating BEVs produced by a 'universal' but neglected member of the *Bifidobacterium* genus and the human GIT microbiota and its potential for immune modulation.

## 5.4. Conclusion for further study

Effective characterisation of BEVs requires high-yield numbers under controlled, preferably standardised and simplified growth conditions. The *B. pseudocatenulatum* strains LH660 and LH663 selected for this study showed shorter lag-phases and more pronounced exponential growth in the revised RCM-based medium. To minimise confounding factors during downstream BEV purification, unnecessary ingredients and supplements were omitted, and components of human or animal origin were replaced with vegan alternatives. Glc and starch were selected as the primary and secondary carbohydrate sources based on optimal growth performance and confirmed lack of HMO utilisation among the tested HMOs. This final formulation, designated RCMveg (see Table 7), served as the optimised standard growth medium for subsequent BEV preparation and characterisation throughout the study.

Additionally, CFU data identified distinct time points, 12h and 20h, corresponding to maximal bacterial yield. These time points were adopted as standardised harvesting intervals to enable investigation of potential differences in BEV preparations associated with growth phase and culture conditions.

# IV. Results Chapter II – Characterisation of *B. pseudocatenulatum* BEVs

## 1. Summary

BEVs are key mediators of interkingdom communication, interaction with host cells, and immune modulation. Although BEVs from Gram-negative bacteria have been widely studied, understanding the biological impact and production of BEVs from Gram-positive bacteria is still scarce. This is particularly true for BEVs from commensal bacteria, such as *Bifidobacterium*, which are extremely understudied. Therefore, I optimised the isolation and purification of BEVs produced by the selected *B. pseudocatenulatum* strains and performed initial characterisation of their biophysiological properties. This included determining morphology and size, and quantifying vesicular concentration, content, and proteome. The results demonstrate distinct BEV differences in a strain- and growth-condition-dependent manner. Additionally, several proteins with potential immunomodulatory features were identified. Taken together with the host cell interaction studies I performed (see next Results Chapter), this gives insights into the underlying mechanisms of potential immune stimulation by specific BEV proteins.

## 2. Contributions

Overall supervision and help with this chapter's writing and experimental suggestions were provided by Prof Lindsay Hall and Prof Simon Carding. Lab induction, BEV preparation SOP, and support during optimisation and initial proteomic analysis were provided by Dr Regis Stentz. Dr Emily Jones provided induction and help with NTA and SEC. Lipid quantification was performed under supervision of Dr Rokas Juodeikis. Dr Catherine Booth and Kathryn Gotts performed TEM imaging. Proteomics was performed by Dr Carlo Martins and Dr Gerhard Saalbach. Help with proteomic analysis and visualisation was provided by Dr Matthew Dalby. Everything else was performed by me. For more details, please refer to the Methods chapter 3, page 49.

# 3. Background

## 3.1. BEVs as important immunomodulatory microbial products

### *3.1.1. Characteristics and function of BEVs*

Vesiculogenesis is an important cellular response mechanism in all cells, including members of the GIT microbiota.[272] Essential for interspecies and interkingdom communication[308,309], BEVs contain various components of their parental organism, including proteins[293,294], peptidoglycan[295–297], small genetic molecules such as RNA[295,298–300] and DNA[295,301,302], lipoprotein[303], virulence factors[304], metabolites[305,306] and specific enzymes mediating antibiotic resistance[43,310–312], nutrient acquisition[313,314], quorum sensing[315], and/or biofilm formation and maintenance.[43,302] The diverse cargo of BEVs enables their multifaceted functions. However, underlying mechanisms and factors regulating their production and heterogenicity are still not well understood.[287]

Due to their size (20-400nm), BEVs are ideal for molecule delivery to distant sites within the host.[325,326] The immune system responds to these MAMP-expressing BEVs through recognition via specific PRRs, including TLRs, activation of the NF-κB pathway and production of pro- and anti-inflammatory cytokines.[334]

As a result, BEVs have been gaining more and more importance for applications in drug delivery, immune therapy and vaccination.

### *3.1.2. Implications for the use of BEVs in vaccination*

The combination of high levels of immunostimulatory ligands, innate robustness protecting the cargo from degradation by nucleases and proteases, as well as cost-effective production, their bioengineering capability, and non-replicability, makes them an attractive platform for vaccine delivery.[43] To date, BEV vaccines have been licensed for *V. cholerae* and serogroup B *N. meningitidis*[464,515], with the latter showing potential cross-species protection against *N. gonorrhoeae*.[516] Other experimental BEV vaccines have been reported to induce protective immunity when administered orally or intranasally to mucosal sites, showing increased levels of mucosal vaccine-specific IgA and systemic IgG antibodies.[517–520] However, there are still restrictions for using BEVs from non-commensal and pathogenic bacteria in vaccines, such as undesirable

toxicity due to toxins and DAMPs. Other potential disadvantages include low yield and low expression levels of target antigens, impurities, poor immunogenicity and strain-restricted protection requiring the addition of adjuvants.[43,325,337,517] Thus, licensing of BEV-based vaccines for use in humans requires more research.[335] To overcome these undesirable effects of pathogenic BEVs, bioengineered modifications have been implemented to increase safety. For instance, the second generation of MenB BEV vaccines contains penta-acylated LpxL1 LPS instead of capsular polysaccharides, lowering its endotoxicity.[463,521] Another strategy is genetically engineered heterologous expression of antigens or immunogens from target microbes into BEV carriers of a safer bacterium. Based on this approach, Omp22 antigens from *A. baumannii* and OprI from *P. aeruginosa* were fused into BEVs derived from *E. coli*.[522,523] Similarly, *E. coli* and *S. enterica* have been genetically modified to produce BEVs containing LPS from *S. aureus* species[524] and capsular proteins from *S. pneumoniae*[525,526], inducing antigen-specific antibodies and immune protection against infection in mice. BEVs can also be 'surface-decorated' with various antigens, such as coupling Spike receptor binding domains from SARS-CoV-2 with BEVs derived from *S. enterica* serovar Typhimurium.[527] However, only a few studies have tried a similar approach using BEVs from commensal bacteria. Carvalho and colleagues[322,337] engineered BEVs from *B. thetaiotaomicron* to deliver antigens from Influenza A virus and *Yersinia pestis*, resulting in protective mucosal and systemic immune responses in mice and primates, respectively.

Given the safety issues of BEVs of pathogenic origin, the use of BEVs from commensal bacteria, which are non-toxic with in-built adjuvancy, could lead to novel vaccination strategies.

## 3.2. Immune stimulation potential of bifidobacterial BEVs

Given their many reported health benefits and their probiotic and immune-modulatory properties discussed before, BEVs originating from *Bifidobacterium* strains are promising candidates for vaccine formulations. However, very few studies have investigated BEVs of bifidobacterial origin. López et al. (2012)[373] compared the immunomodulatory properties of whole *B. bifidum* LMG13195 and their BEVs, indicating increased immunosuppression by BEVs; IL-10 release and Treg cell abundance *in vitro* after exposing DCs to BEV fractions. Studies of *B. longum* KACC

91532-derived BEVs revealed beneficial effects in the context of food allergy via their expression of a family of 5 ESBPs that interacted with resident mast cells in the small intestinal lamina propria to induce targeted apoptosis. Both the parental bacteria and their BEVs did not kill T cells, B lymphocytes or eosinophils *in vitro* and *in vivo*; rather, mast cells were specifically targeted.[374] Nishiyama et al. (2020)[375] found that BEVs from *B. longum* NCC2705 contained a high number of mucin-binding proteins that promoted bacterial adhesion and possible GIT establishment. More recently, BEVs from *B. longum* AO44 were found to induce anti-inflammatory responses, including IL-10 and IL-17 production, in splenocytes and DC-CD4$^+$ T cell co-cultures. Subsequent proteomic analysis revealed high abundances of ABC transporters, quorum-sensing proteins, and ESBPs.[308] Kurata et al. (2022)[377] also found an association between ESBP-loaded BEVs from *B. longum* subsp. *infantis* and induction of IL-6 secretion and subsequent IgA production by PP lymphocytes.

Taken together, BEVs from *Bifidobacterium* possess similar immunomodulatory abilities to those of their parental organisms, albeit in a strain-dependent manner, with several proteins, such as ESBPs, being positively associated with immune stimulation.

# 4. Results

## 4.1. Optimisation of BEV isolation and purification

### *4.1.1. Initial preparations produced impure BEV samples*

Based on the growth optimisation results described in Results Chapter I, BEVs were prepared by harvesting cultures of LH660 and LH663 at the CFU peaks corresponding to maximum bacterial yield, at 12h and 20h of growth, in RCMveg medium containing Glc and starch as carbohydrate sources. This approach was used as the standard procedure for downstream BEV preparation throughout the project. With the focus of the Carding lab on *Bacteroides* species, they established an SOP for optimal BEV isolation for *Bacteroides* strains. Following the results of the initial growth assessment and optimisation, I prepared the initial BEV mixture according to this SOP. However, the resulting bifidobacterial BEV solution showed visible impurities as residues of the culture medium caused colouration. An attempt to visualise BEVs using TEM was unsuccessful due to debris and other contaminants within the BEV mixture interfering with the TEM preparation process. Thus, several different modifications of the *Bacteroides* BEV

SOP were tested to optimise bifidobacterial BEV isolation and purification (see Methods, page 49).

### *4.1.2. Combination of additional filtration and purification steps leads to optimised bifidobacterial BEV isolation*

As a first adjustment, I added another cross-filter disk with a lower cut-off and performed an SEC on the resulting BEV suspension. In a single experiment, 24 fractions of these initial preparations were tested for protein concentration using the Bradford assay (see Figure 11) and analysed for concentration and size of potential BEVs (see Figure 12) using NTA (ZetaView) to verify that modified BEV isolation mirrors the trajectory of *Bacteroides* BEV preparations. Fractions with very low to no NTA signal were discarded.

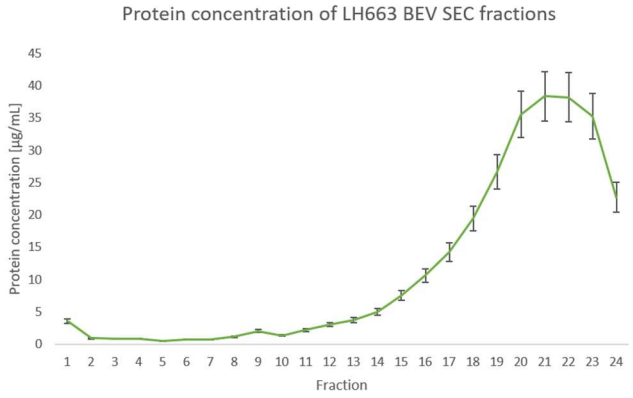


*Figure 11: Detected protein levels in the LH663 BEV solutions after initial preparation modification, SEC purification, and fractioning. Single experiment to verify BEV isolation trajectory similarities to Bacteroides BEV preparations to exclude SEC fractions of low nanoparticle and high protein concentration in future preparations.*

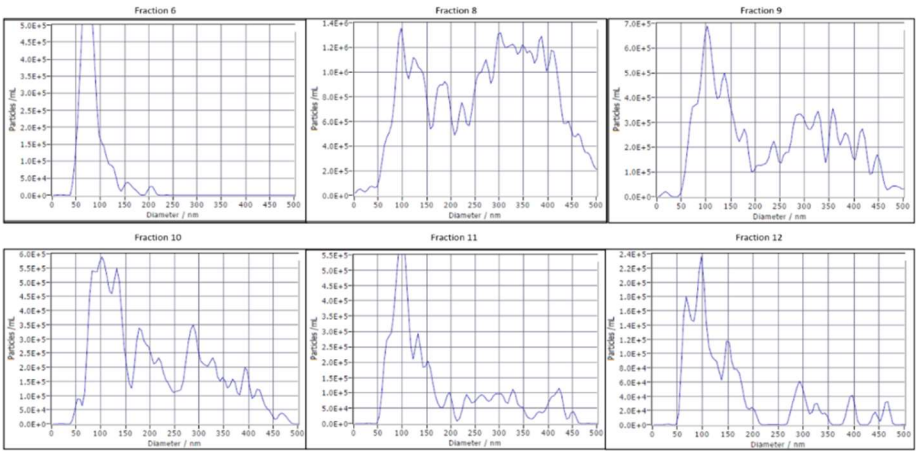


*Figure 12: NTA concentration and size diagrams of SEC fractions containing BEVs as produced by ZetaView analysis programme*

Fractions 13 to 24 showed increasing levels of proteins. Additionally, ZetaView analysis indicated that none of these later eluted fractions contained any

nanoparticles, which was consistent with observations of BEV preparations of *Bacteroides*. Based on this, these fractions were discarded from further use and later eluted SEC fractions of subsequent BEV preparations were excluded as part of the standard procedure. As visible in the NTA diagrams (Figure 12), only fractions 6 and 8 to 12 contained nanoparticles and were subsequently concentrated for TEM imaging (see Figure 13) to confirm improved purity.

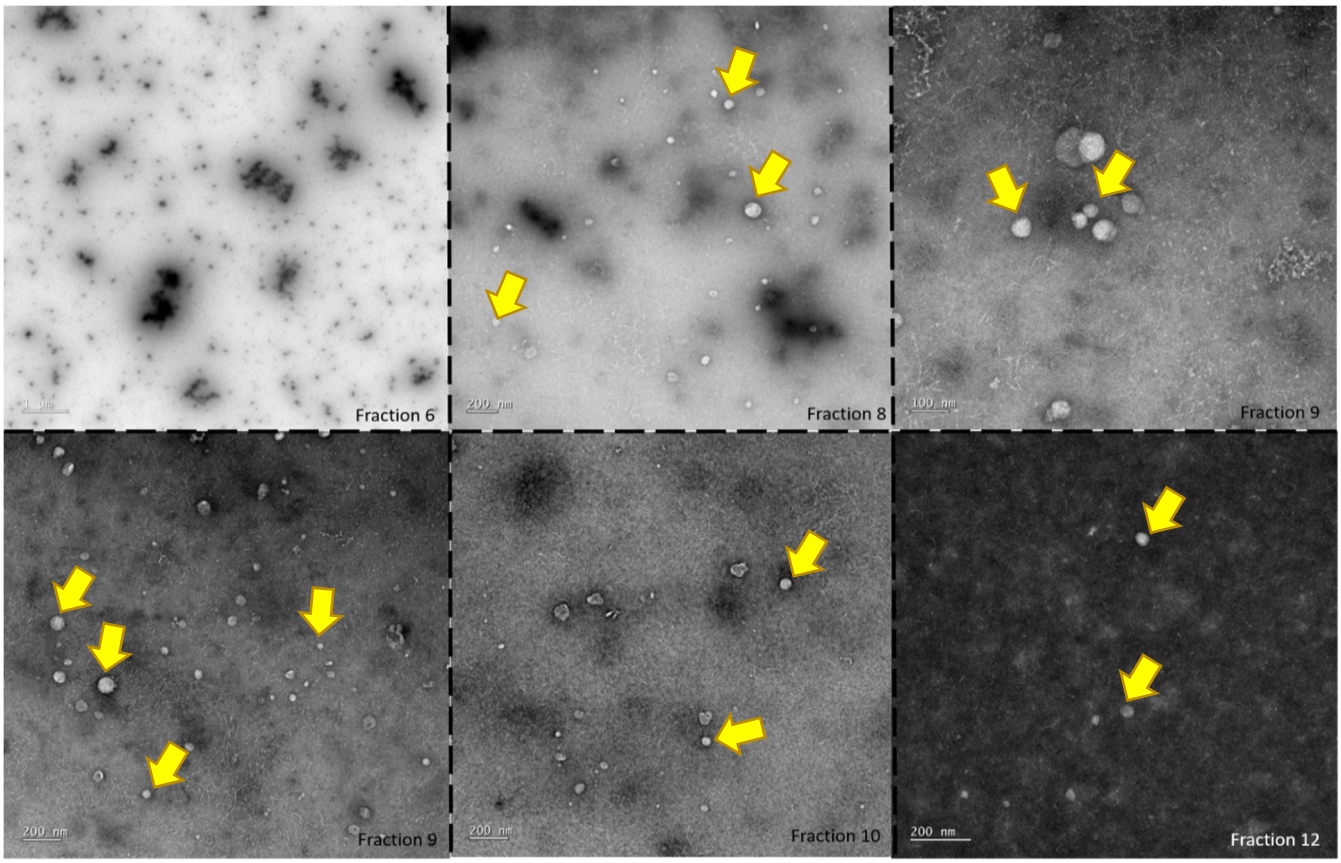


*Figure 13: Selection of TEM images of chosen SEC fractions after modified BEV preparation. Respective scales are depicted in the lower left corner of each image, fraction number in the lower right corner. Arrows identify BEVs*

Although the added cross-filter disk and SEC resulted in bifidobacterial BEV isolation of increased purity compared to the initial preparation, both the NTA and TEM imaging (background and debris) revealed contaminants and low BEV concentrations ($1 \cdot 10^6$ particles/mL compared to expected $1 \cdot 10^{10}$ particles/mL; see Figure 12). Interestingly, fraction 6, which displayed a resolved peak in the NTA particle profile, did not contain any detectable BEVs in TEM, but debris and other 'background signals' from the culture medium, showing that the ZetaView does not discriminate BEVs from other nano-sized particles and debris.

To further optimise BEV preparations, the RCMveg medium was filtered prior to inoculation using the cross-filter system with a cut-off of 100kDA to remove nano-sized particles from the growth medium. This modification improved the isolation process, decreasing the preparation time, matching that from *Bacteroides* BEV preparations and increasing the overall BEV concentration and purity without the use of the secondary ('broader') cross-filter disk. After repeated success of the modified BEV preparation protocol (higher concentrations in NTA, see Figure 14A, and clearer TEM images, see Figure 15), the use of the secondary filter disk was omitted, and over 40 BEV batches were prepared for further characterisation. All batches analysed via ZetaView analysis (see Figure 14A and B) and the first 5 batches with TEM (see Figure 15) showed conformity between batches in terms of concentration, sizes, and morphology (see below). The optimised BEV isolation protocol for *Bifidobacterium* species can, therefore, produce replicable BEV preparations.

## 4.2. BEV particle size range and concentration range are similar between batches

SEC fractions and pooled BEV batches were analysed for concentration and nanoparticle size. Interestingly, the size of BEV populations between different batches from LH660 at both harvest (i.e. growth) time points was constant (*P* values close to 1), ranging between 80nm to 215nm in diameter (see Figure 14B). Some BEVs from LH663 were larger, with sizes reaching up to 225nm in diameter for BEVs harvested at 12h and up to 240nm for LH663 BEVs harvested at 20h. However, the mean size of BEVs of both LH660 and LH663 at both harvest time points was 130nm (see Figure 14B), consistent with initial isolations (see Figure 12) and reported BEV size ranges from other bacteria.[287,308,377]

Conversely, BEV concentration varied between batches, though not significantly ($P \geq 0.05$; see Figure 14A). Although the concentrations were increased 100,000-fold compared to initial preparation trials and were consistently over $1 \cdot 10^{10}$ particles/mL, concentrations varied, with the highest variation seen in BEV batches from LH660 harvested at 20h, with over 12-fold difference between batches ($7.6 \cdot 10^{10}$ particles/mL vs. $9.76 \cdot 10^{11}$ particles/mL), with a mean concentration of $3.91 \cdot 10^{11}$ particles/mL. The concentration of LH663 BEV batches harvested at 20h was 3.89-fold higher with a mean concentration of $3.54 \cdot 10^{11}$ particles/mL.

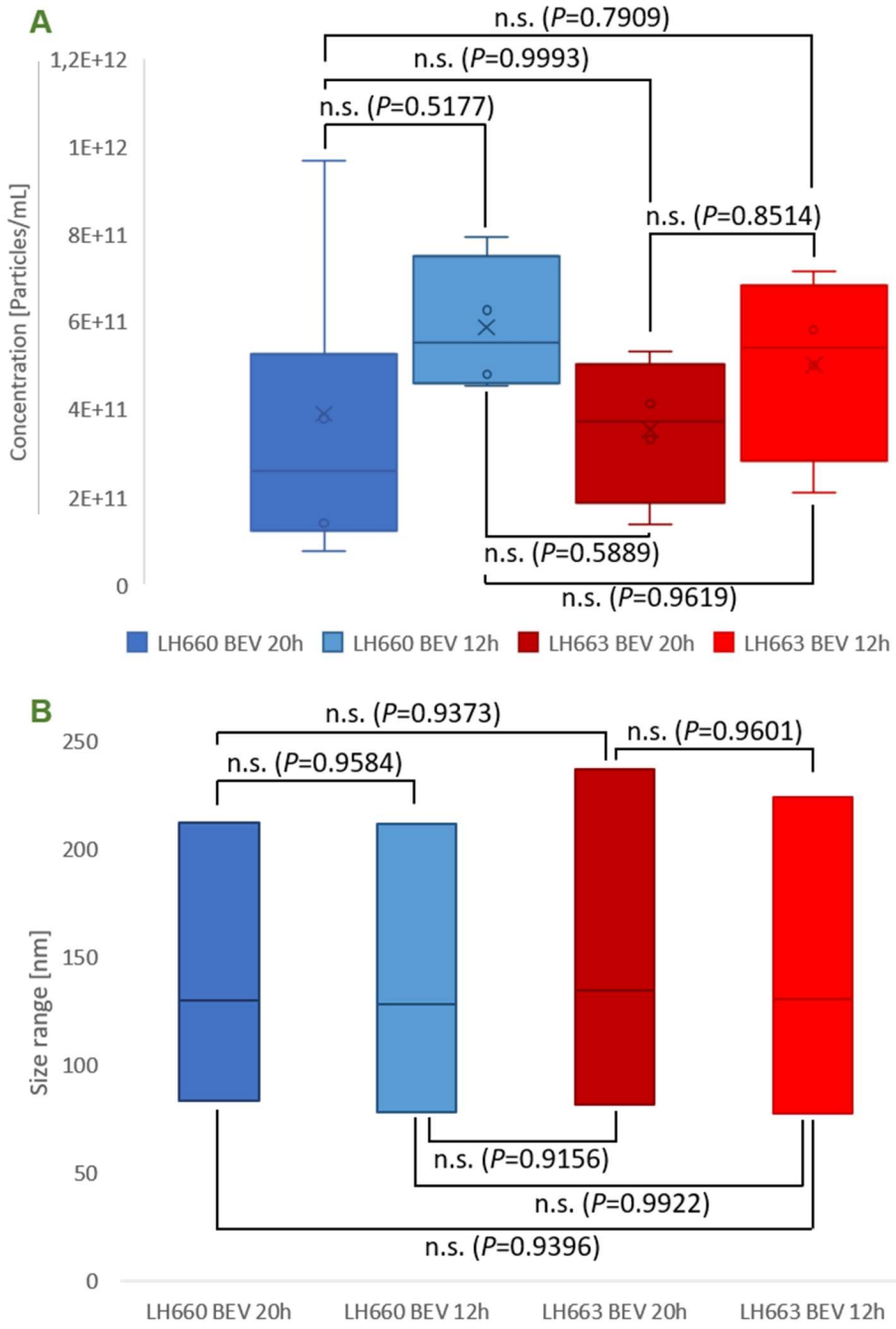


*Figure 14: NTA using ZetaView of LH660 and LH663 BEV batches harvested at 12h and 20h, respectively, showing concentration range (A) and size range (B). Statistical testing with one-way ANOVA followed by Tukey's multiple comparison* post hoc *test, N = 5*

## 4.3. TEM of BEVs confirms absence of surface-associated EPS

TEM imaging was used for visualisation and purity assessment of bifidobacterial BEVs. In contrast to earlier BEV isolations (Figure 13), a selection of TEM images from three different batches of LH660 and LH663 BEVs harvested at 20h (Figure 15) confirmed improved purification and reproducibility.

BEV shape and size were variable between LH660 and LH663. However, overall BEVs of ≤100nm in size were more abundant. In addition, BEVs derived from LH660 and LH663 appeared consistent with previously reported TEM images of BEVs from other *Bifidobacterium* species.[308,374,375,377] However, TEM imaging revealed no detectable EPSs on the surface of LH660 and LH663 BEVs, as the 'additional outer layer' typical for EPS in TEM images[7,255,264] was not detectable.

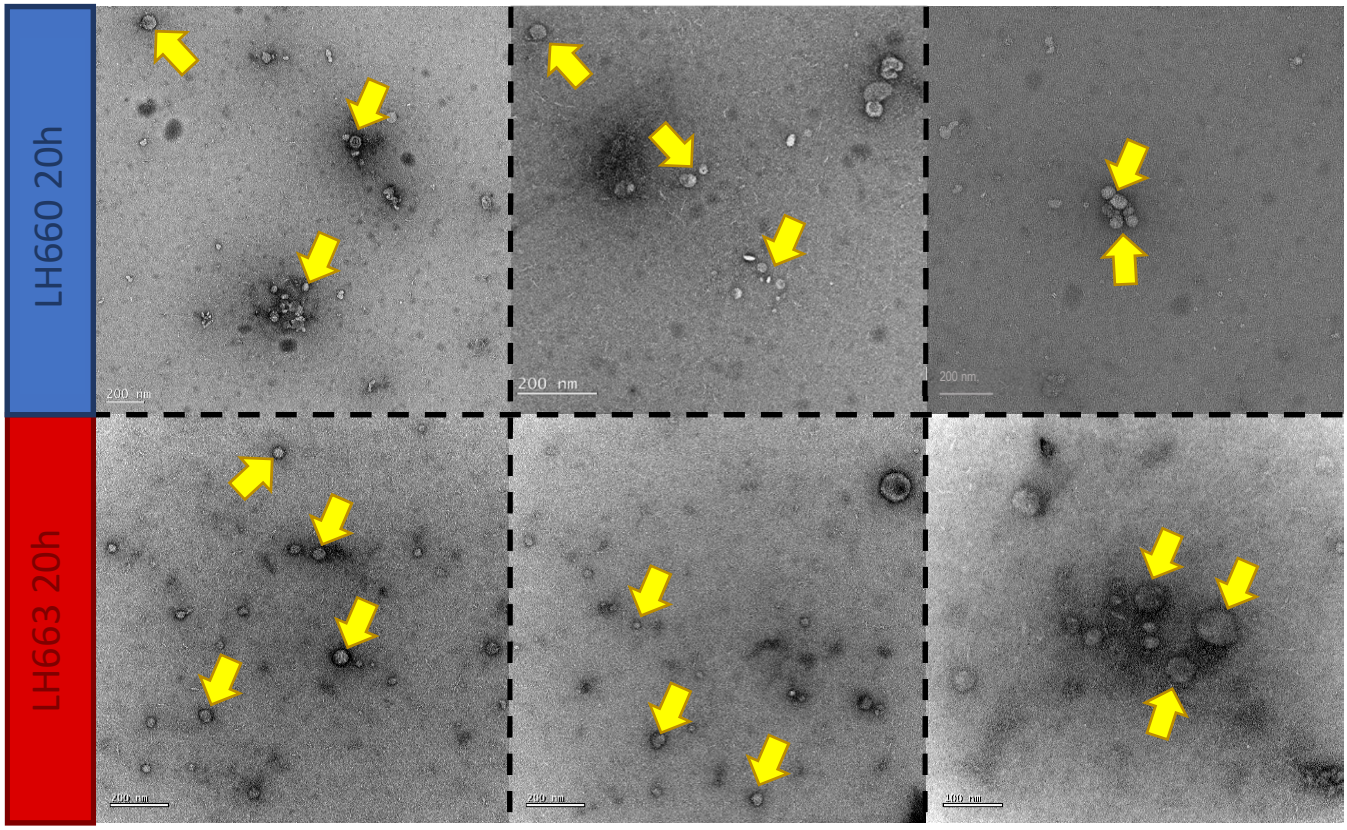


*Figure 15: Selection of TEM images of analysed BEV batches from LH660 (upper panel) and LH663 (lower panel) harvested after 20h. Respective scales are depicted in the lower left corner of each image. Arrows point out BEVs of different sizes*

## 4.4. Quantification of vesicular surface-associated content shows batch-dependent variations

BEV surface-associated RNA, dsDNA, protein, and lipid were next determined. Except for one outlier in LH660 20h BEV batches, lipid concentrations were similar between all BEV batches (*P* values close to 1; Figure 16).

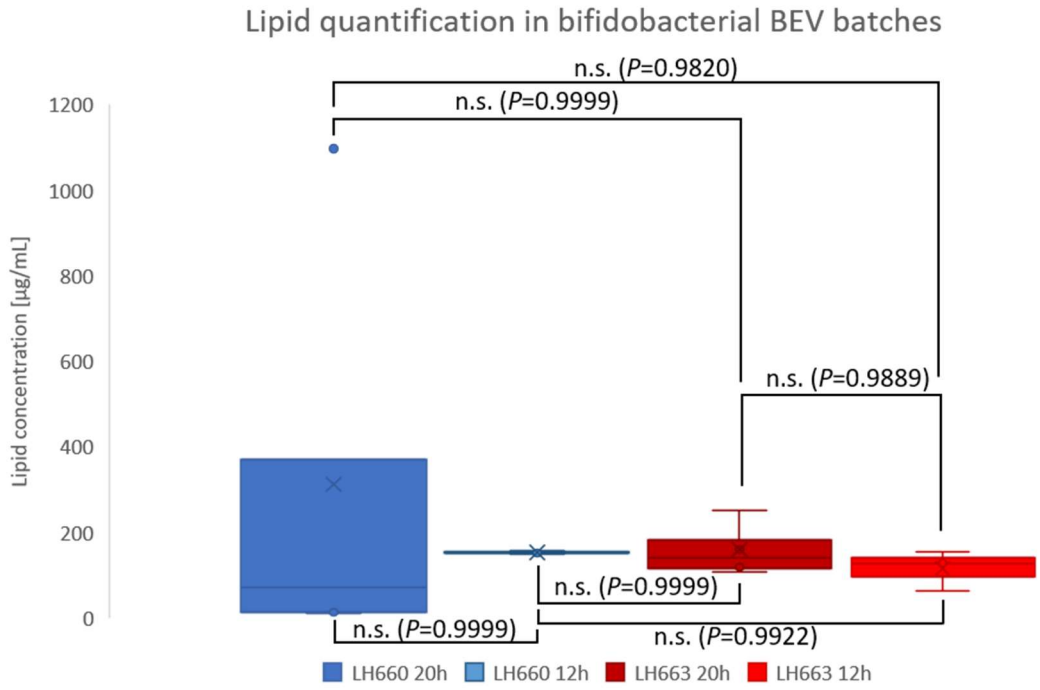


*Figure 16: Calculated lipid levels in bifidobacterial BEV batches. Statistical testing with one-way ANOVA followed by Tukey's multiple comparison* post hoc *test, N = 5*

Similar to the measured particle concentrations, BEV batches from both LH660 and LH663 harvested at 12h showed higher amounts of the tested contents than the respective 20h BEV batches (Figure 17), except for lipid levels, where 20h BEV batches showed higher, though not significantly different, concentrations (Figure 16). The lowest dsDNA and RNA levels were seen in LH660 BEV batches harvested at 20h, whereas the highest nucleic acid levels varied between BEV preparations, with the highest RNA concentrations measured in LH663 BEVs at 12h and highest dsDNA seen in LH660 BEVs at 12h. Protein levels between BEV batches of the same origin and condition were less variable than dsDNA and RNA levels, with less than 2-fold differences ($P \geq 0.3$). BEVs from LH660 had higher amounts of protein compared to LH663 BEVs. All differences in lipid, protein, RNA, and dsDNA concentration between BEV preparations were non-significant ($P \geq 0.05$).

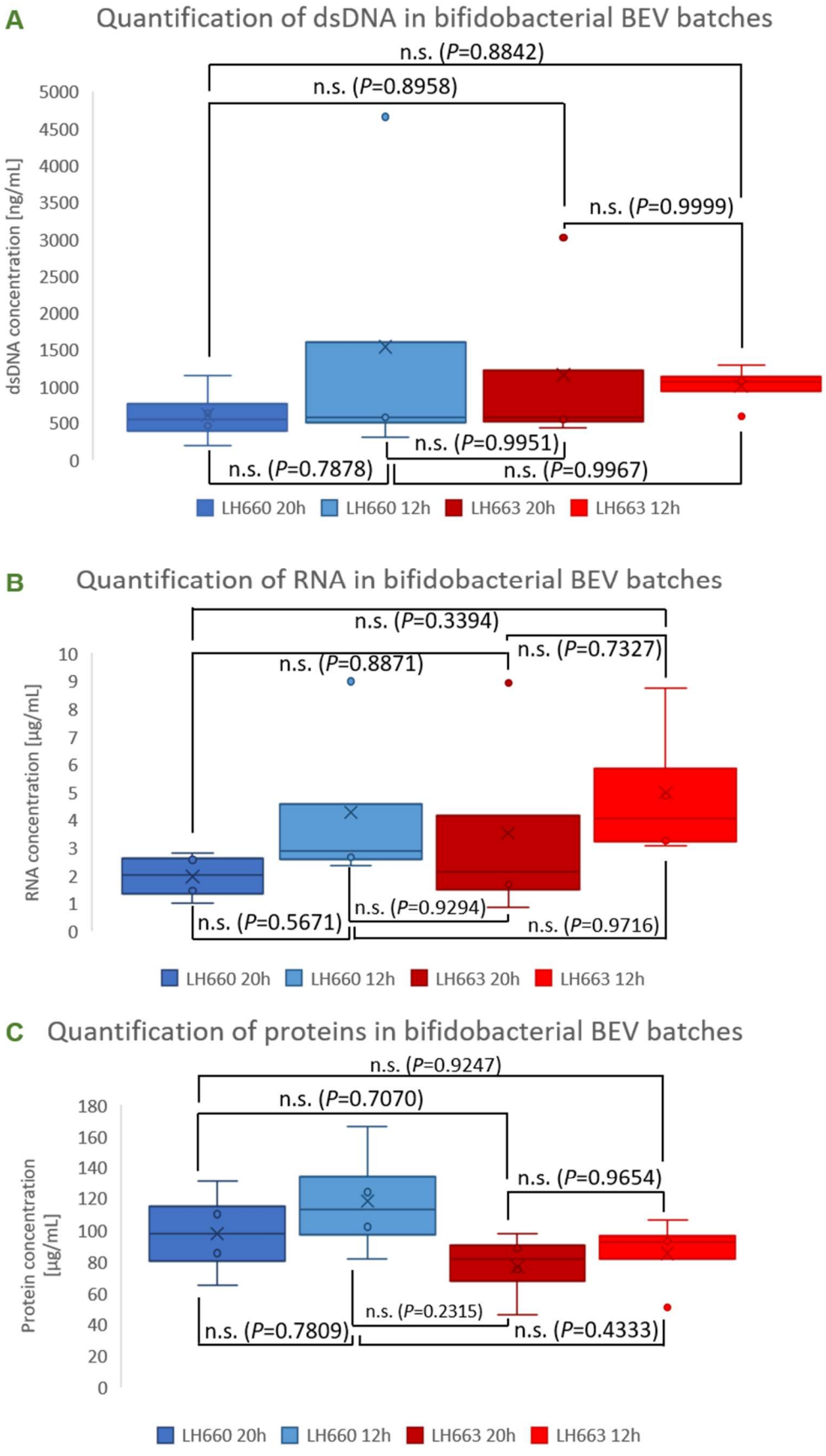


*Figure 17: Measured levels of dsDNA (A), RNA (B), and protein (C) in bifidobacterial BEV batches. Statistical testing with one-way ANOVA followed by Tukey's multiple comparison* post hoc *test, N = 5*

## 4.5. Proteomic analysis shows distinct BEV protein clusters between strains and time points

### *4.5.1. Initial proteomic analysis reveals batch differences dependent on sample age*

Three BEV preparations from LH660 and LH663 harvested at 20h were used for proteomic analysis (see Methods, under 3.3 Proteomic analysis, page 54). Briefly, BEVs were lysed through SDS treatment followed by boiling and vortexing. Proteins were precipitated, pelleted and trypsin-digested, followed by purification. The resulting aliquots were analysed by nanoLC-MS/MS, and unique peptides were quantified and identified using *Bifidobacterium*-specific databases.[474] A total of 1289 proteins were detected, of which 581 were unique peptides with ≥ 10 present in at least one BEV sample from the same strain. Surprisingly, proteomes varied between BEV batches from the same strain and condition, depending on the 'age' of the respective sample (Figure 18). Sample 1 from each strain was isolated one month prior to proteomic analysis, sample 2 one week and sample 3 one day. The distance between the oldest and the freshest samples was increased compared to those prepared a week apart, indicative of sample degradation. Due to this, I stored isolated BEV batches at -80°C instead of 4°C prior to use and prepared new samples for repetition of the proteomic analysis.

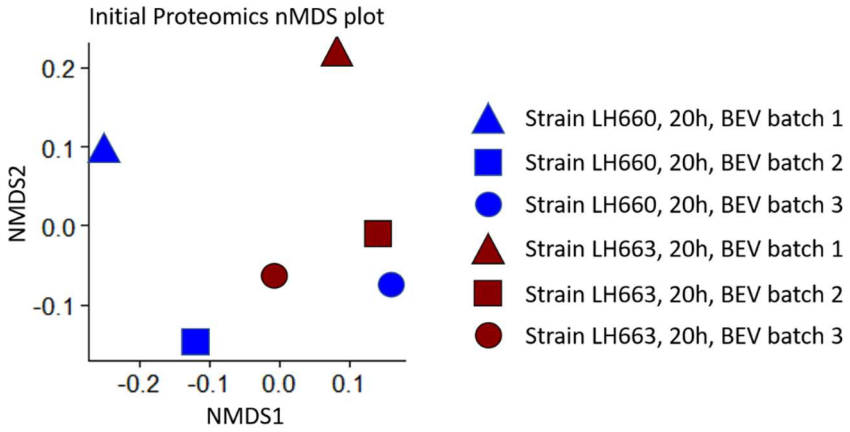


*Figure 18: NMDS plot of LH660 and LH663 BEV batches harvested at 20h showing proteomic differences between respective samples in an age-dependent manner. Isolation of respective batch was performed for batch 1=1 month, batch 2=1 week, batch 3=1 day prior to proteomics analysis*

### *4.5.2. Cellular location and biological function of bifidobacterial BEV proteins*

Repeated proteomic analysis of 'fresh' BEV batches from LH660 and LH663 harvested at 12h and at 20h showed improved proteomic sample similarity, although

samples from the LH660 12h BEVs indicated one outlier (see Figure 18 and Figure 19).

Additionally, more proteins were detected in this repeated proteomic analysis than in the initial run. A total of 1433 proteins were detected, with 862 proteins meeting the threshold criteria mentioned above. GO annotation for cellular location (Figure 20) and biological function (Figure 21) of these 862 proteins revealed that the majority (41%) were cytoplasmic proteins, followed by membranous proteins (30%) and a small portion found in the nucleus (5%), ribosome (5%), and mitochondria (3%). The smallest amount of detected proteins (2%) was identified to be extracellular or associated with the cell surface. However, the cellular location of 14% remained unknown. A similar proteomic distribution was found by Kurata et al. (2022), who analysed BEVs deriving from *B. longum* subsp. *infantis*.[377]

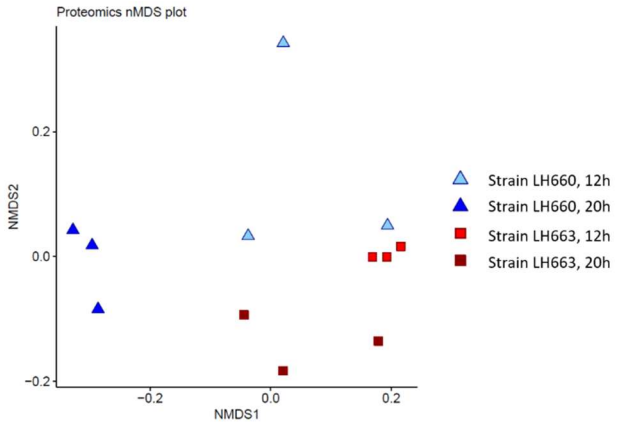


*Figure 19: NMDS plot of LH660 and LH663 BEV batches harvested at 12h and 20h, showing proteomic similarity between respective samples*

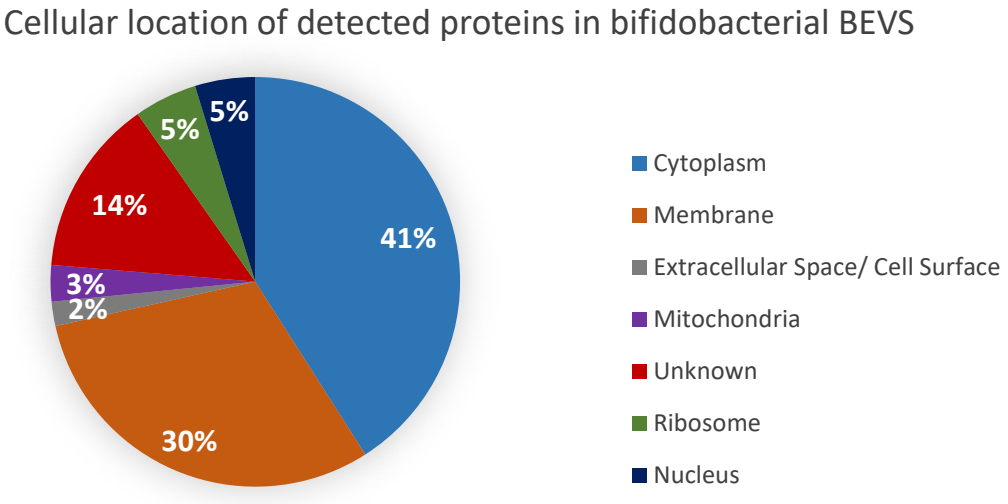


*Figure 20: Overview of GO-annotated cellular location of detected proteins within the bifidobacterial BEV samples from LH660 and LH663*

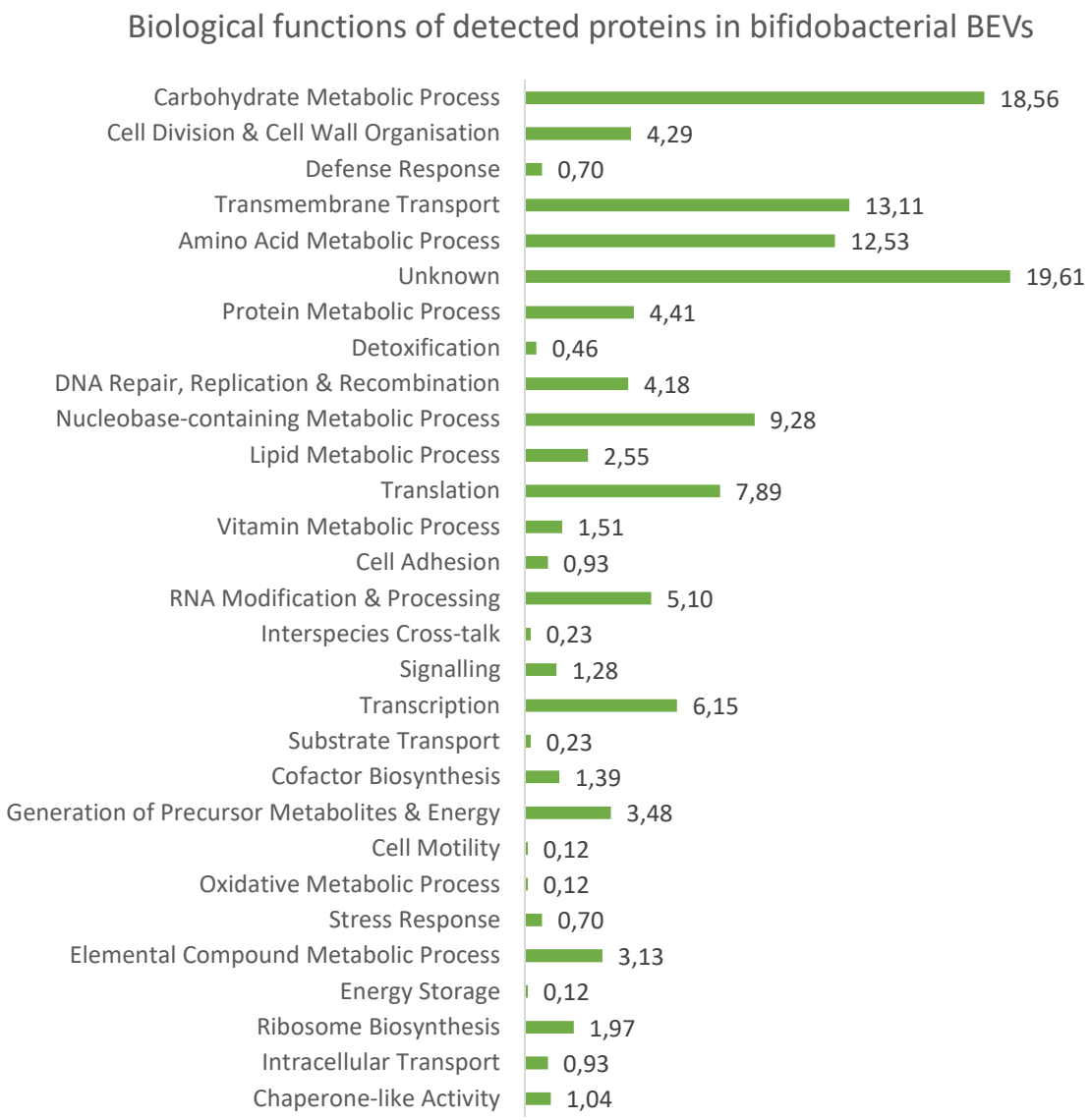


*Figure 21: Percentage of GO-annotated biological functions of detected protein within the bifidobacterial BEVs of LH660 and LH663*

Conversely, comparing BEVs from *B. longum* subsp. *infantis*[377] and the *B. pseudocatenulatum* strains used here (Figure 21) indicated varied functional properties. Proteins linked to carbohydrate metabolic processes and transmembrane transport were approximately 10% of the total, while those related to signalling were over four times lower in the BEV samples here. Proteins linked to translation, vitamin metabolic processes, cofactor biosynthesis, and lipid metabolic processes were twice as much in the BEV samples compared to *B. longum* subsp. *infantis*.[377]

### *4.5.3. Protein abundance varies between both strains and selected conditions*

An in-depth comparison of the BEV batches from LH660 and LH663 at both time points revealed strain-specific differences at the proteome level. Overall abundances of all detected proteins were elevated in LH663 BEVs at both time points compared to LH660 BEVs (Figure 22), although surface-associated protein levels were lower in LH663 BEVs (see Figure 17C). Similarly, BEVs harvested at 12h had higher protein levels, and those proteins present were more abundant than in those harvested at 20h in both strains, meaning fewer proteins were loaded in corresponding BEVs after the diauxic shift in both strains (see Figure 22 and Figure 17C).

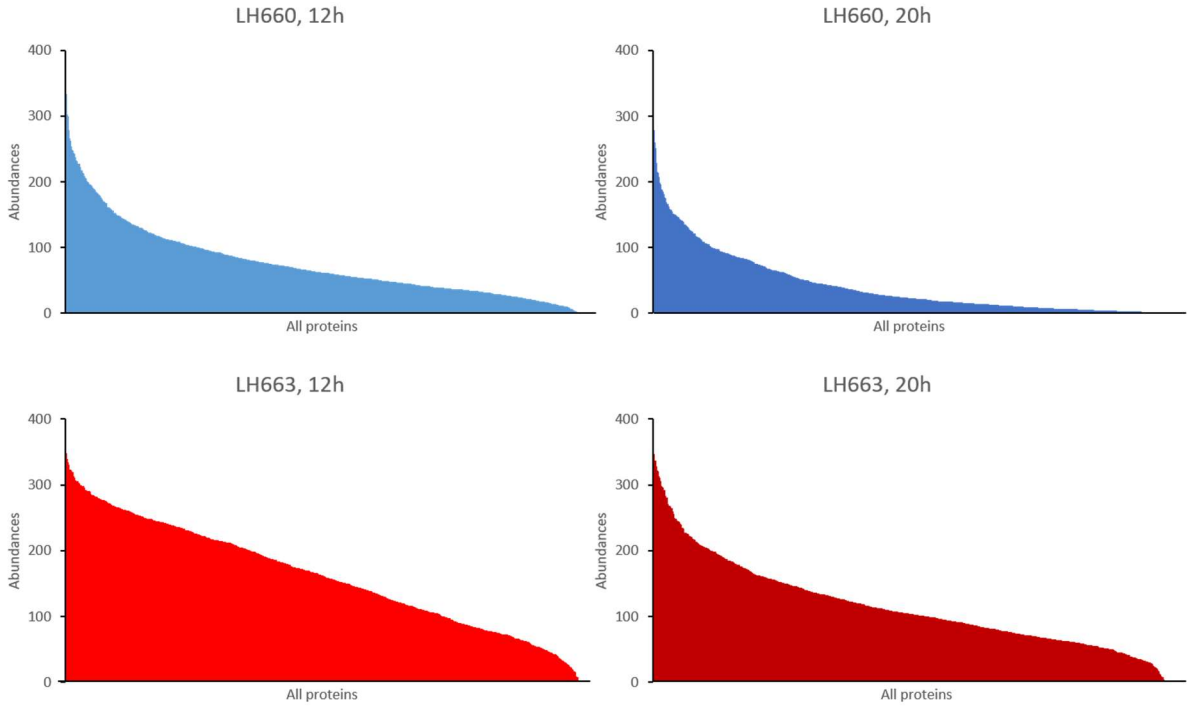


*Figure 22: Abundances of all 1433 proteins detected in the BEV batches of LH660 and LH663 harvested at 12h and 20h*

In LH660 BEVs, differences were seen for NTP pyrophosphohydrolase and fructose-2,6-biphosphatase (Figure 23A). KEGG pathway analysis showed that NTP pyrophosphohydrolase is part of the riboflavin and nicotinate metabolic pathway (KO: K03426/ K01515), whereas fructose-2,6-biphosphatase (KO: K14634) is a key enzyme in the fructose/mannose metabolic pathway.

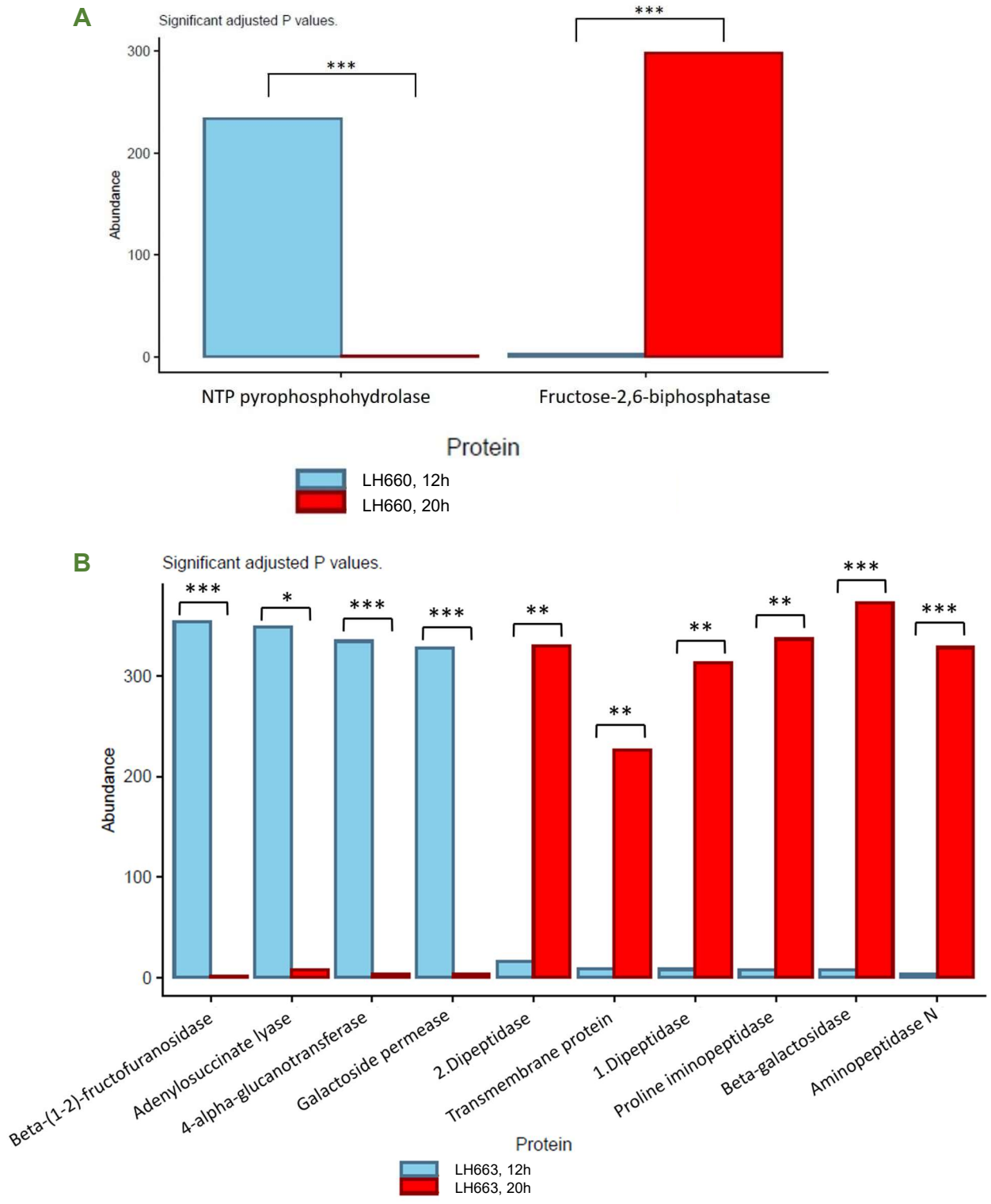


*Figure 23: Proteomic abundance differences between LH660 (A) and LH663 (B) BEVs harvested at 12h (blue) and 20h (red). P values calculated by t-test and adjusted by BH method, *P ≤ 0.05, **P ≤ 0.01, ***P ≤ 0.001*

In LH663 BEVs, 20h preparations contained significantly ($P \leq 0.01$) more proteins linked to glutathione, proline and galactose metabolism, respectively. LH663 12h BEVs, on the other hand, showed a higher abundance of enzymes associated with

galactose metabolism, purine metabolism, glycogen metabolism, and ABC transport of galacto-oligosides.

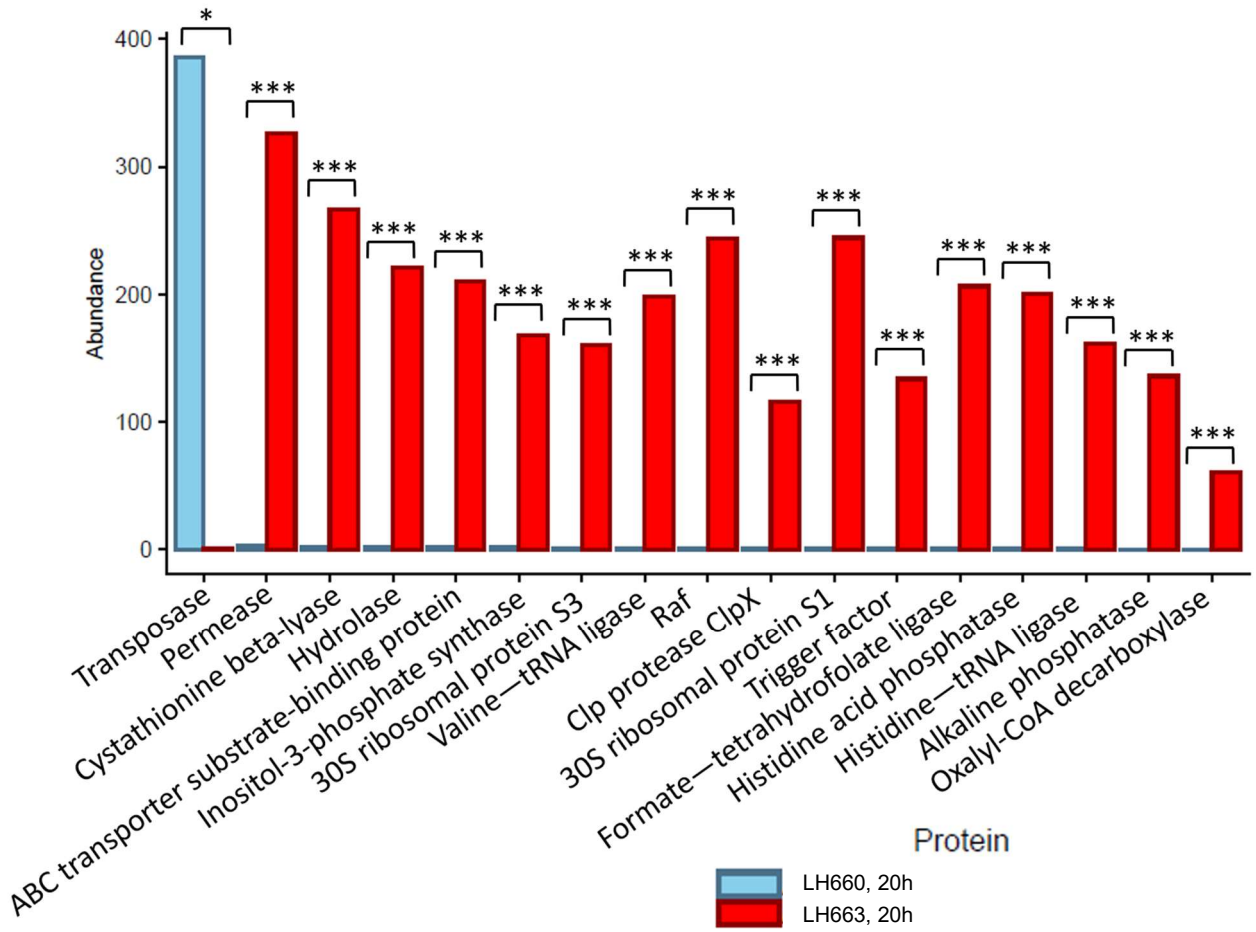


*Figure 24: Proteomic abundance differences between LH660 (blue) and LH663 (red) BEVs harvested at 20h. P values calculated by t-test and adjusted by BH method, *P ≤ 0.05, **P ≤ 0.01, ***P ≤ 0.001*

Finally, a more detailed comparison of protein abundances between LH660 and LH663 BEVs harvested at 20h confirmed significant differences between protein levels between the BEVs of the two strains (Figure 24). LH660 20h BEVs contained significantly ($P$=0.0149) more transposase, which was linked to genetic replication and repair. LH663 20h BEVs had significantly ($P$≤0.001) higher levels of proteins associated with ABC transport, translation and aminoacyl-tRNA biosynthesis, signal transduction, protein processing, one-carbon fixation and several metabolic processes.

### *4.5.4. BEVs from both strains contain potential immunomodulatory proteins*

Further screening, using literature searches, revealed 20 proteins present in LH660 and LH663 BEVs that might facilitate BEV-host cell interactions and induce

immune responses (Table 11 and Figure 25). The abundances of these 20 proteins varied between BEVs of different strains and different time points. However, only one out of these 20 proteins, namely alkaline phosphatase, was significantly ($P$=6.1667e$^{-16}$) different between strains, with no abundance in LH660 BEVs and significant enrichment in LH663 BEVs (Figure 24 and Figure 25).

Although abundance differences were not statistically significant for the other 19 proteins ($P$≥0.05), load variation could still result in distinct immunomodulatory phenotypes. ESBP was more abundant in BEVs harvested at 20h and in LH660 BEVs, while detected levels (abundance values ≥70) were comparable in all BEV preparations. Additionally, ABC transporter substrate-binding protein was also detected in all BEV batch groups, though abundance in LH660 12h BEVs was 2-3-fold less than in the other BEV samples. Equally, both lactate dehydrogenase and diguanylate cyclase were also present in all BEV samples, yet LH663 BEVs contained 3-4-fold more of these proteins than the respective LH660 BEVs. Surprisingly, 11 out of the 20 potentially immunomodulatory proteins had very low to no abundance in LH660 20h BEVs, with 10 being highly abundant in LH660 12h BEVs.

*Table 11: Overview of potential immunomodulatory proteins reported in other species and genera detected in LH660 and LH663 BEV (12h and 20h) proteomic analysis*

| Name | Biological function | Cellular location | Reported potential immunomodulation |
|---|---|---|---|
| ABC transporter substrate-binding protein | Transmembrane transport | Membrane | Adhesion promotion[528] |
| Adhesin | Cell adhesion | Membrane | Adhesion promotion[529] |
| Lactate dehydrogenase | Carbohydrate metabolic process | Cytoplasm, Mitochondria | Induction of epithelial cell differentiation[530] |
| Extracellular solute-binding protein | Substrate transport | Membrane | Induction of IL-6 and IgA production[377] |
| Diguanylate cyclase | Substrate transport | Cell surface | Regulation of biofilm formation[531] |
| Elongation factor Tu | Translation | Cytoplasm | Adhesion promotion[375,529] |
| Phosphoglycerate kinase | Carbohydrate metabolic process, Generation of precursor metabolites and energy, cell adhesion | Cytoplasm | Adhesion promotion[375] Immunoreactivity[532] |
| Alkaline phosphatase | Transcription, Signalling | Cytoplasm, Membrane | Reduction of LPS-mediated inflammation[533,534] |
| Nicotinate phosphoribosyltransferase | Nucleobase-containing metabolic process | Cytoplasm, Nucleus | Activation of inflammatory responses[535] |
| Glyceraldehyde-3-phosphate dehydrogenase | Carbohydrate metabolic process, Cell adhesion | Cytoplasm | Immunoreactivity[532] Adhesion promotion[536–538] |
| Glutamate synthase | Amino acid (AA) metabolic process | Cytoplasm | Positive association with increased intestinal IgA[539] |
| Protein translocase subunit SecA | Transmembrane transport | Cytoplasm, membrane | Induction of Th17 response in PBMCs[540] |
| Enolase | Carbohydrate metabolic process, Generation of precursor metabolites and energy, Cell adhesion | Cell surface | Immunoreactivity[532] Adhesion promotion[541] |
| Aspartokinase | AA metabolic process | Cytoplasm | Immunoreactivity[532] |
| Sortase | Cell adhesion | Membrane | Adhesion promotion[542,543] Bacterium-host cell interaction[542,543] |
| Transaldolase | Carbohydrate metabolic process, Generation of precursor metabolites and energy | Cytoplasm, Membrane | Immunoreactivity[375,532] |

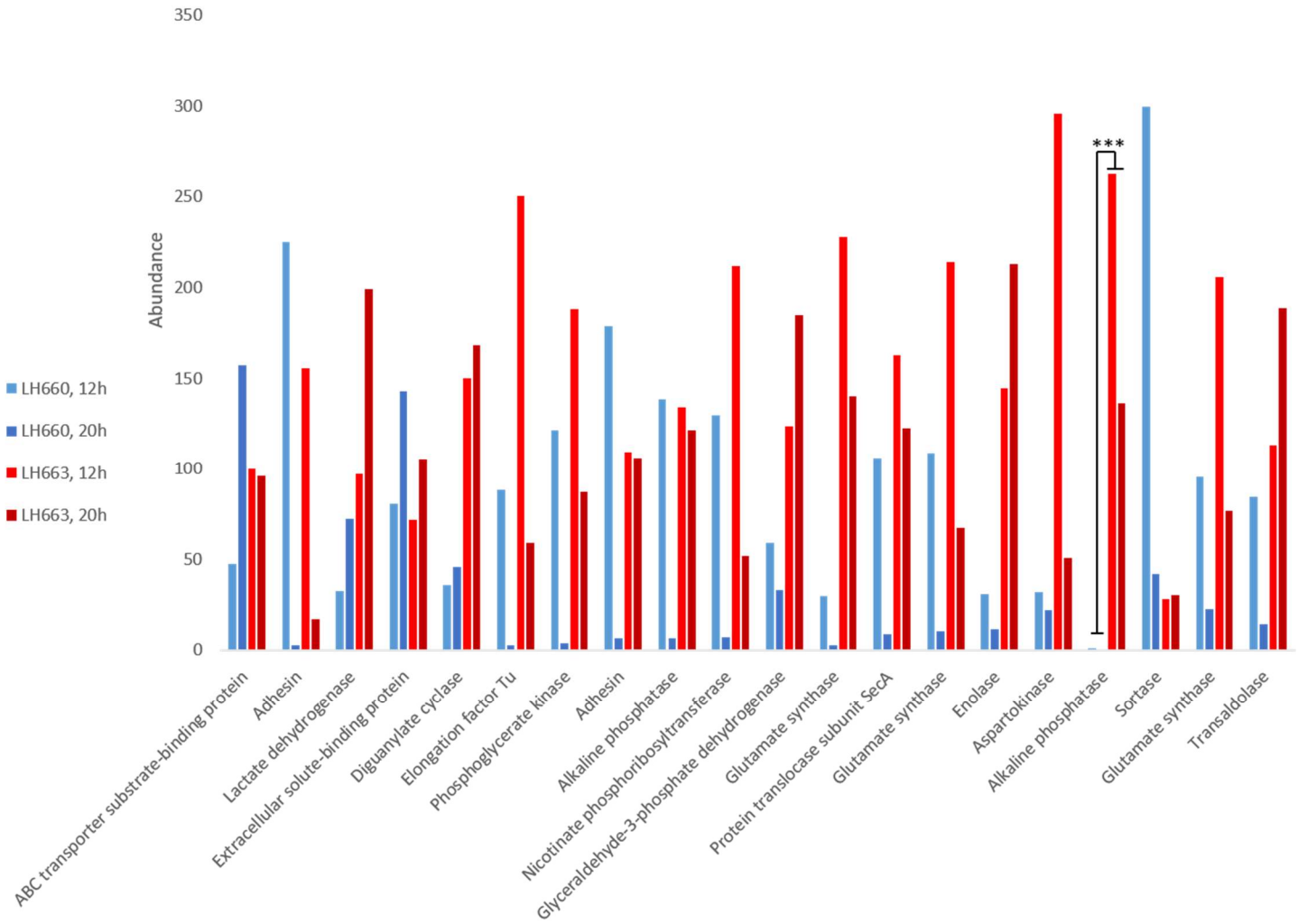


*Figure 25: Abundances of identified proteins with potential immunomodulatory properties in LH660 and LH663 BEVs (12h and 20h) as reported in other bacterial species and genera. P values calculated by t-test and adjusted by BH method, ***P ≤ 0.001, other abundance ratios were non-significant*

# 5. Discussion and perspectives

## 5.1. *B. pseudocatenulatum* strains produce heterogeneous BEVs

### 5.1.1. BEV isolation and characterisation need further standardisation

I have optimised a BEV preparation protocol for the selected *B. pseudocatenulatum* strains based on adapting an SOP for *B. thetaiotaomicron* BEV isolation. By including additional filter steps, I produced LH660 and LH663 BEV batches for characterisation by morphology, size, cargo proteome and presence of immunomodulatory proteins. Being only the 12th study of bifidobacterial BEVs and the first of BEVs derived from *B. pseudocatenulatum* strains, I was able to demonstrate that both LH660 and LH663 released BEVs with a size range of 80-240nm and a similar morphology in line with previously reported bifidobacterial BEVs.[308,374,375,377,544] Concentration of 12h BEV batches from both strains tended to have higher particle numbers compared to the respective 20h BEVs, while protein levels did not follow a similar pattern. Recently, Juodeikis et al. (2024)[287] proposed BEV quantification via a combination of NTA and lipid quantification (detected nano-particles per µg of quantified lipid per mL) as a more accurate method of BEV quantification. Lipid quantification of the BEV batches was overall more consistent, except for one outlier in LH660 20h BEVs. However, differences in lipid packaging and limitations to lipid quantification, like protein assays, can be expected. This highlights the need for further optimisation and standardisation of BEV preparation to allow more comprehensive analysis and less batch-to-batch variation, one of the biggest limitations of upscaled use of BEVs in therapies.[292,545,546]

### 5.1.2. Nucleic acid cargo more elevated in LH663 BEVs than LH660 BEVs

The presence of bifidobacterial RNA and/or DNA is a strong indication of the potential immunomodulatory activity of BEVs due to the genomic composition with high G+C proportions and non-methylated CpG motifs of *Bifidobacterium* species.[540,547] These have been shown to interact with TLR9 of immune cells, promoting Th1 cell responses.[540,547] Levels of both RNA and dsDNA were overall more elevated (although not significantly) in all BEV samples originating from LH663 compared to matching samples from LH660. Conversely, Bitto et al. (2017)[301] found that nucleic acids were

more abundant in BEVs of smaller size (~20nm). Given the fact that BEVs from LH663 were generally larger than LH660 BEVs (although not significantly), bifidobacterial BEVs may follow different loading trajectories than those reported for Gram-negative species. Additionally, several studies in both Gram-negative and Gram-positive bacteria have shown that BEVs harvested at earlier time points carried more nucleic acids.[301,302] This was apparent for RNA only in the majority of the BEV samples, with 12h samples containing twice as much RNA as the 20h batches from both strains. Interestingly, BEVs from *B. longum* subsp. *infantis* rarely contained detectable levels of DNA and RNA, whereas BEVs from *B. longum* NCC2705 showed high DNA levels, although prepared at the same growth stage.[375,377]

It has been proposed for Gram-negative bacteria that genomic DNA (gDNA) is loaded into BEVs during exponential growth and cell division.[301] Since both BEV preparation time points correspond to diauxic stationary growth, this might explain lower DNA cargo in all of the BEV preparations (excluding batch outliers). Since BEVs largely remained intact prior to quantification, the measured nucleic acids were solely present on the surface of the BEVs, and potential internal DNA and RNA were not considered. As significantly more genetic material in BEVs is present externally than internally[287,301,548–550], I decided to omit internal DNA and RNA quantification.

Nevertheless, more in-depth characterisation of external and internal genetic material is required to confirm BEV-loading trajectories for nucleic acids in bifidobacteria. Of note, internal DNA from BEVs of the pathogen *P. aeruginosa* was found to contribute to horizontal gene transfer, whereas external DNA was associated with biofilm formation and protection.[301]

### *5.1.3. BEVs from B. pseudocatenulatum follow reported protein cargo distribution from other bifidobacterial BEVs in their cellular location but not biological function*

Most identified proteins were predicted to localise to the cytoplasm, followed by a large portion of membrane proteins and a smaller number of ribosomal, nuclear, mitochondrial and extracellular proteins. Similar findings were reported for BEVs derived from *B. longum* subsp. *infantis* and *B. longum* NCC2705, showing that bifidobacterial BEVs contain predominantly cytoplasmic proteins.[375,377] However, given the small number of proteomic studies on bifidobacterial BEVs, this observation needs further studies to be confirmed. Additionally, it remains unclear which portion of

proteins might provide immunomodulatory activity. Other findings on whole bacteria attribute the immunomodulatory role of *Bifidobacterium* to specific protein molecules localised in the cell wall or membrane.[532] They also play key roles in the establishment and maintenance of interaction between the bacteria, their environment and the host.[551] Given that 30% of identified proteins were localised in this compartment, the presence of proteins with potential immunoreactive interest in the BEVs studied here is further discussed below.

Conversely, a comparison of predicted biological functions of identified proteins from different bifidobacterial BEVs showed species-specific variations. Although most proteins were attributed to carbohydrate metabolism and transmembrane transport, BEVs from *B. longum* subsp. *infantis* carried around 10% more proteins of these categories.[377] This variation might be due to the large portion of proteins with unknown functions in the BEV proteomes studied here. BEVs from *B. longum* AO44 carry more proteins attributed to ribosome biosynthesis and signalling, but fewer for transmembrane transport than BEVs from *B. longum* subsp. *infantis* or the *B. pseudocatenulatum* strains studied here.[308] However, given the heterogeneity of BEVs, this might be due to species and experimental condition-related differences.

### *5.1.4. Protein load in B. pseudocatenulatum BEVs is strain- and time point-dependent*

Protein levels varied between the two strains and the two time points, reflecting the stress response of the parental bacteria to changes in nutrient availability. LH660 12h BEVs showed high abundance of NTP pyrophosphohydrolase, an enzyme whose expression is upregulated in *Bifidobacterium* species in response to oxidative stress.[552,553] At 20h, LH660 BEVs contained high amounts of fructose-2,6-biphosphatase, an allosteric regulator of gluconeogenesis[554], in line with bacterial growth conditions of the strain.

Other proteins were predominant in 12h and 20h BEVs from LH663. BEVs from the earlier time point displayed high levels of proteins linked to the uptake and metabolism of starch prior to complete Glc depletion. Potentially, a metabolic shift was initiated preceding Glc unavailability, leading to lytic BEVs as a means of adaptation and survival to new growth conditions.[287] Although not significantly different between preparations, BEVs from all preparations also contained other proteins participating in

starch metabolism (e.g. amylopullulanase, alpha-amylase, and phosphorglucomutase).[555] Conversely, several of the most abundant proteins in LH663 20h BEVs are associated with glutathione metabolism. Glutathione signalling is connected with stress and starvation responses as part of bacterial survival mechanisms.[556] Nevertheless, LH663 20h BEVs also contained high amounts of proline iminopeptidase and beta-galactosidase, with the latter contributing to starch utilisation. Interestingly, it has been found that some *Bifidobacterium* species can metabolise AAs in the absence of glucose to ensure survival, highlighting further adaptation strategies reflected in the respective BEV protein load.

Increasing evidence points to phenotypical differences of LH660 and LH663 as seen in their growth behaviour (see Figure 10, Results Chapter I) and the proteomic profile of their BEVs under the same growth conditions (see Figure 23, Figure 24 and Figure 25). Indeed, LH660 20h BEVs had a higher level of transposase protein, while LH663 20h BEVs had higher abundance of proteins related to gluconeogenesis, tricarboxylic acid cycle (TCA) cycle, and AA metabolism, as well as some proteins involved in the protein translocation machinery.[557]

## 5.2. BEVs potential immune stimulatory proteins

Of the over 1000 identified proteins present in the BEVs, 20 have been reported to drive interaction with host epithelial and immune cells.[551] Seven of these proteins were found to promote and regulate bacterial adhesion to the host, namely enolase, adhesins, elongation factor Tu, ABC transporter substrate-binding protein, phosphoglycerate kinase and sortase (see Table 11). Enolase and elongation factor Tu facilitate the adhesion of *B. bifidum*, *B. longum* NCC2705, *B. breve*, *B. lactis* and *Lactobacillus* spp. to host mucus, intestinal epithelial cells and/or components of their extracellular matrix.[541,551,557–561] Additionally, enolase interacts with human plasminogen, which is associated with binding of *Bifidobacterium* strains to the human GIT.[557,559] Similar adhesion and plasminogen-binding functions have also been found for GAPDH.[536–538] Hence, BEVs containing adhesion-promoting proteins might facilitate colonisation by *Bifidobacterium* species of mucosal surfaces, thus potentially having indirect health benefits to the host.[562] Indeed, BEVs from *B. longum* NCC2705 carry numerous mucin-binding proteins that might promote adhesion of the parental bacteria.[375]

In addition to moonlighting proteins showing potential adhesion activity, others are potentially related to immune stimulation. Górska et al. (2016)[532] identified several immunoreactive proteins from *B. longum* subsp. *longum* strains CCM 7952 and CCDM372 through immunoblot analysis using different immune and non-immune sera, including enolase, aspartokinase, phosphoglycerate kinase, transaldolase, and GAPDH. In pre-clinical vaccine formulations against pathogens and parasites, GAPDH protein has been proposed as a vaccine target due to its ability to modify intracellular signalling and to contribute to immune evasion.[563] Furthermore, GAPDH activity in *L. gasseri* but not *C. difficile* was found to attenuate allergic M2 macrophages toward the M1 macrophage phenotype.[564] Interestingly, GAPDH of *B. longum* species have been found to have high homology with GAPDH proteins of *C. difficile* and *E. coli,* giving potential avenues for epitopes of cross-reactivity in vaccine formulations.[532]

Transaldolase, on the other hand, has been proposed to be involved in colonisation, favouring the establishment of *Bifidobacterium* species in the GIT.[565] Traditionally, a key enzyme of the pentose phosphate pathway, transaldolase is also a specific aggregation factor in *B. bifidum* species.[565]

Other potential immunomodulatory proteins include translocase subunit SecA and alkaline phosphatase. Translocase subunit SecA from *B. longum* DJ010A can induce strong Th17 responses in human PBMCs[566], while alkaline phosphatase can attenuate LPS-induced inflammation and intestinal immune barrier damage through inhibition of the NF-κB and ATP pathway.[567]

However, most intriguingly, Kurata et al. (2022)[377] identified a direct link between the lipoprotein ESBP loaded into *B. longum* subsp. *infantis* BEVs and its ability to stimulate macrophages via TLR2 activation to secrete IL-6. Moreover, in an *ex vivo* experiment, they were able to show that these bifidobacterial BEVs increased the production of IgA in murine PPs.

Taken together, the BEV preparations here contain several proteins that might directly or indirectly interact with host cells and stimulate favourable immune responses that could be used in therapeutic and/or vaccination strategies. Therefore, I investigated these interactions using *in vitro* and *ex vivo* assays that will be discussed in the next results chapter.

## 5.3. Further limitations and future work

To date, this is the first study to characterise BEVs deriving from *B. pseudocatenulatum* strains. Although providing initial insights, further in-depth analysis and optimisation are still needed.

Generally, optimisation and ultimately standardisation of the BEV preparation process are needed to minimise batch-to-batch variation and allow proper comparability between BEV studies. Juodeikis et al. (2024)[287] proposed the use of chemically defined media free of potential vesicle contaminants. Given growth optimisation needed to ensure sufficient bifidobacterial growth and subsequent BEV yield, I focused on the conditions and BEV preparations resulting from the vegan RCM medium as described in Results Chapter I.

Currently, size, concentration and morphology determination of nanoparticles, including BEVs, face technical limitations. For example, sample preparation steps for TEM, such as fixation and dehydration, can lead to artefacts, resulting in inaccurate size estimates, altered morphology, and falsely attributed features of the sample's nanostructure.[568] Similarly, size and concentration determination based on NTA only can lead to issues due to the indistinction between BEVs and other nano-sized particles and debris.[287] Combination of these methods, along with lipid and protein labelling and quantification, as well as support through machine learning approaches, has been proposed to improve these issues.[287,569]

Additionally, further in-depth characterisations could give a more detailed understanding of bifidobacterial BEV packaging and their respective biological functions. Therefore, a comprehensive analysis of *Bifidobacterium* strains and their BEVs using a multi-omics approach could show which cellular compounds are loaded into BEVs under which circumstances. This means under a defined condition, parental bacteria and BEVs could be characterised regarding their DNA, RNA, proteins, metabolites and lipids, allowing identification of key BEV cargo. Mandelbaum et al. (2023)[308] compared the proteomic profiles of bifidobacterial cells, culture supernatant and BEVs, revealing proteins unique to the BEV fraction. Moreover, comparision of proteomic content of BEVs from different probiotic bacteria identified conserved proteins, including enolase, phosphoglycerate kinase, and GAPDH[286], which were also present in the BEVs studied here and have potential immunomodulatory properties.

Similar results can be expected for genomic, transcriptomic and lipodomic profiles. However, more research is needed to confirm this hypothesis.

Moreover, BEV preparations at other time points could show life cycle-dependent BEV differences. Several studies of BEVs derived from Gram-negative bacteria observed that the abundance of lipoprotein and cytoplasmic proteins changes throughout bacterial growth.[287,292] Similarly, separation of BEVs in size-dependent subsets could also show important differences in vesiculogenic mechanisms. Indeed, Turner et al. (2018)[570] found BEV cargo and cell entry differences correlating to vesicular size, with smaller BEVs (20-100nm) containing less protein content, while Bitto et al. (2017)[301] found more nucleic acid associated with smaller BEVs.

The list of potential additional experiments with bifidobacterial BEVs is more extensive than what has been discussed here and will be further discussed in the next Results Chapter concerning immune stimulation and interaction with host cells and potential subsequent applications.

## 5.4. Conclusion for further study

BEVs from LH660 and LH663 harvested at 12h and 20h of growth were similar in size and morphology, with only small, non-significant differences observed in concentration, and in external levels of nucleic acids, proteins and lipids. Importantly, all preparations contained components with potential immunomodulatory properties. In-depth proteomic analysis confirmed variation in protein abundance between preparations, such as ESBP, GAPDH, enolase and alkaline phosphatase, which have been implicated in immune modulation. Other protein distribution patterns were consistent with previously reported bifidobacterial BEV profiles.

Subsequent experiments normalised BEV preparations to $1 \cdot 10^{11}$ particles/mL and assessed their effects in immune assays to explore whether these protein loads contribute to potential immunomodulatory activity.

# V. Results Chapter III – Bifidobacterial BEV-Host Interactions

## 1. Summary

Commensal members of the microbiota, especially *Bifidobacterium*, play a vital role in stimulating and developing the intestinal and systemic immune system. Similarly, BEVs from health-promoting strains were found to promote intestinal homeostasis, improve the epithelial barrier, and enhance immune cell maturation through an intricate immune stimulatory network. Here, I characterised the interactions between important host cells and BEVs from LH660 and LH663 using TEER, confocal microscopy and cell co-cultures. Results obtained revealed potential epithelial barrier and TJ modulation by and uptake of bifidobacterial BEVs with a perinuclear localisation, in the absence of significant cytokine or chemokine secretion. In human immune cells, LH660 and LH663 BEVs induced the production of TNF-α, IL-1β, IL-6, IL-8, IL-10, and TSLP in a strain- and BEV preparation-dependent manner. Primary cell co-cultures using murine splenocytes confirmed similar BEV effects, leading to higher levels of TNF-α, IL-6, and KC, and lower induction of IL-10 and IFN-γ in splenocytes. LH663 20h BEVs, but not LH663 12h and LH660 BEV preparations, also promoted IgA secretion in murine PP/GALT fragment cultures. Additionally, in an infection-simulation assay (using LPS stimulation), bifidobacterial BEVs showed protective properties in response to LPS exposure in Caco-2 cells and macrophages, inducing TJ and cytokine gene expression and altering cytokine production. These results confirm the immunomodulatory and protective properties of LH660 and LH663 BEVs in support of their future possible use in vaccination and/or disease models.

## 2. Contributions

Overall supervision and help with this chapter's writing and experimental suggestions were provided by Prof Lindsay Hall and Prof Simon Carding. Dr Emily Jones provided lab inductions and human cell culture and imaging protocols. Dr Catherine Booth provided induction and initial help with confocal imaging. Help with murine primary tissue preparation was provided by Dr Sally Dreger and Dr Christopher

Price. Initial help and induction to qRT-PCR were provided by Mar Moreno-Gonzalez. Everything else was done by me. For more detailed methodology, see the Methods chapters 4 and 5, page 57.

# 3. Background

## 3.1. Microbiota-host immune system mutualism

### *3.1.1. Interactions between GIT bacteria and key immune cells*

Early-life microbiota stimulation is essential for developing the intestinal and systemic immune system, which is crucial for efficient immune protection and vaccine responses. Studies using germ-free and antibiotic-treated neonatal mice showed impaired humoral responses, such as reduced Th1 and Th17 responses, and lower IgG and IgM production after vaccination with adjuvanted and live-attenuated vaccines.[1,571] Furthermore, the immune system of these animals was anatomically and functionally immature.[572–574] Several key immune cells depend on microbial stimulation for development, activation, maturation, polarisation, proliferation, regulation, and recruitment, such as IgA-producing B and memory plasma cells[1,3], neutrophils[575], APCs like macrophages and DCs[30], Th cells[576], as well as IECs[30,577], driving local and systemic immune responses. For instance, the microbiota enhances antigen-specific T cell response via DC-mediated production of type I interferon.[1,578] These complex interactions between the GIT microbiota, the host intestinal epithelium and associated immune cells are mediated through cell-to-cell communication, which is vital for maintaining GIT homeostasis, host health, and preventing and combating infections.[326,579] Host immune and epithelial cells express a variety of PRRs specific for distinct microbial products such as LPS (by TLR4), Flagellin (by TLR5)[580], dsRNA (by TLR3)[581], ssRNA (by TLR7), non-methylated dsDNA with CpG motifs (by TLR9)[582], and peptidoglycans and lipoproteins produced by Gram-positive bacteria (by TLR2) inducing innate immune responses via the activation of NF-κB and production of immune modulatory cytokines and chemokines.[26,27,35,583] In healthy humans, the intestinal mucus layer prevents direct contact between luminal microbes and host cells.[584] However, bacterial products, like metabolites and BEVs, can cross the mucosal and epithelial barrier, and translocate via the circulation and/or lymphatic fluid

to lymph nodes, promoting DC maturation and antigen presentation and downstream immune response modulation within and beyond the mucosal site.[43,325,326]

### *3.1.2. Commensal BEVs as key immune modulators*

BEVs contain a multitude of potential immunostimulatory ligands and antigens, including MAMPs, DNA, RNA, lipids and proteins, which can activate numerous PRRs on host cells.[43] Additionally, different adhesins enable uptake into host cells via different endocytosis pathways (micropinocytosis, dynamin-dependent, clathrin-mediated, caveolin-mediated, clathrin- and caveolin-independent endocytosis, lipid raft formation, and membrane fusion), depending on their cargo and size; often using multiple pathways simultaneously.[43,585] While BEVs from pathogens facilitate infection and invasive colonisation via the distribution of virulence factors, toxins and mediators of inflammasome activation and immune evasion[586], commensal BEVs can promote homeostatic and protective immune activation, including wound healing and anti-tumour effects.[544,587–589] For instance, BEVs derived from different *Lactobacillus* species translocate from the GIT into the lamina propria via PP, promoting IL-6 and IgA production in PP immune cells via TLR2 activation.[346,377,590–592] DNA-loaded commensal BEVs activate the cGAS-STING pathway in peripheral blood cells after entering the circulation, leading to systemic type I interferon responses and enhanced antiviral immunity.[586,593] Furthermore, BEVs can ‘prime’ neutrophils, leading to enhanced pathogen clearance due to increased production of TNF-α, IL-6, MCP-1, and ROS, and higher migration and phagocytosis.[575,594]

However, identifying specific immunomodulatory BEV cargo, underlying molecular mechanisms and pathways of biodistribution and immune stimulation after commensal BEV administration to the host remains elusive.[326,544]

## 3.2. Bifidobacterial strains and BEVs for targeted immune modulation

As a key commensal microbiota member, many studies have explored the strain-dependent immunomodulatory effects of different *Bifidobacterium* species and strains, as well as bifidobacterial molecules and products, including peptides, EPS, metabolites, DNA, and, to a lesser degree, BEVs, in promoting homeostatic immune responses.[540] For instance, intact cells of several *B. animalis* subsp. *lactis, B. longum*

subsp. *longum, B. bifidum,* and *B. breve* strains administered to PBMCs enhanced DC maturation and secretion of strain-dependent levels of IL-10, TNF-α, IFN-γ, IL-17, IL-4, IL-1β, and IL-12, driving distinct T cell polarisation towards either Th1, Th17 and/or a regulatory phenotype.[595–597] Similarly, CpG-rich DNA sequences from *B. longum* NCC2705 induced MCP-1 and TNF-α production via TLR9 activation in macrophages.[547] *B. animalis* subsp. *animalis* MB5 showed protective effects at the epithelial cell layer *in vitro* via reduction of neutrophil transmigration[598], whereas *B. animalis* subsp. *lactis* whole cells[599] and supernatant[600] improve several TJ proteins.[601] In infants, administration of *B. longum* subsp. *infantis* CECT7210 prevented sporadic diarrhoea after rotavirus infection.[602] Equally, non-vaccinated gnotobiotic piglets colonised with a combination of different *Lactobacillus* and *Bifidobacterium* strains showed less severe rotavirus infections, while vaccinated animals showed increased Th1 responses.[603] In other similar studies, administration of *Bifidobacterium* strains to neonatal piglets enriched intestinal IL-10 levels[187] and boosted B and T cell responses after rotavirus vaccination.[8,188,189]

In murine colitis models, *B. pseudocatenulatum* MY40C and CCFM680 suppressed proinflammatory cytokine levels of TNF-α and IL-6 via TLR4 inhibition of activated B cells while increasing the production of TJ proteins, mucin-2, IL-10, and PPAR-γ, alleviating intestinal barrier disruption.[604] *B. pseudocatenulatum* 7041 whole cells[605] and ultrasonically disrupted cells[606,607] induced IL-10, IL-12, IL-6, IFN-γ and IgA production in PP and mesenteric lymph node cells after oral gavage.

As discussed before, studies of bifidobacterial BEVs have been sparse. However, some specific immune stimuli of the tested bifidobacterial BEVs were identified. For instance, Morishita et al. (2023)[544] compared BEVs derived from *B. longum* subsp. *longum* and *L. plantarum* WCFS1 given intravenously or subcutaneously revealed a link between peptidoglycan and DNA load of the bifidobacterial BEVs and their elevated induction of TGF-β1 and TNF-α production and higher expression levels of immune cell maturation co-stimulatory molecules (CD40, CD80, and CD86) in a strain- and administration-dependent manner. More specifically, Kurata et al. (2022)[377] were able to demonstrate that ESBP found on BEVs derived from *B. longum* subsp. *infantis* was directly linked to TLR2 activation and IL-6 secretion in macrophages, leading to enhanced production of IgA by PP cells. Similarly, BEVs derived from *B. longum* AO44 and KACC91563 were found to be enriched in ESBPs and other proteins with

prominent anti-inflammatory functions, with the former inducing IL-10 secretion in splenocytes and DC-CD4$^+$ T cell co-cultures and the latter alleviating food allergy symptoms by inducing mast but not T cell apoptosis.[308,608] Furthermore, BEVs but not whole cells of *B. bifidum* BIA-7 were also found to activate the AhR pathway modulating the gene expression of TJ proteins, whereas BEVs from *B. bifidum* LMG13195 promoted IL-10 secretion and Treg polarisation.[373,376]

Given their multifaceted functions, advantageous properties compared to whole bacteria or traditional adjuvants, and their targeted immunomodulatory effects, in-depth characterisation of bifidobacterial BEVs from key immune-stimulating strains could give rise to a new generation of vaccine adjuvants.

# 4. Results

## 4.1. Bifidobacterial BEVs potentially maintain and strengthen the epithelial barrier

### *4.1.1. BEV modulation of epithelial TJ gene expression*

Regarding the potential adjuvant application of bifidobacterial BEVs, the possibility of BEVs altering the integrity of the IEC barrier was investigated using Caco-2 monolayers in a cell culture transwell system, measuring TEER variation over time after LH660 and LH663 20h BEV stimulation compared to PBS, as a negative control, and LPS, as a positive control. All samples showed reduced resistance within 6h of addition of BEVs, and the controls, which restored over time without fully recovering to the initial TEER values. Compared to LPS, BEVs from both LH660 and LH663 had significantly less of an effect on epithelial integrity measured by TEER ($P \leq 0.001$ for all BEV samples throughout the experiment) (Figure 26).

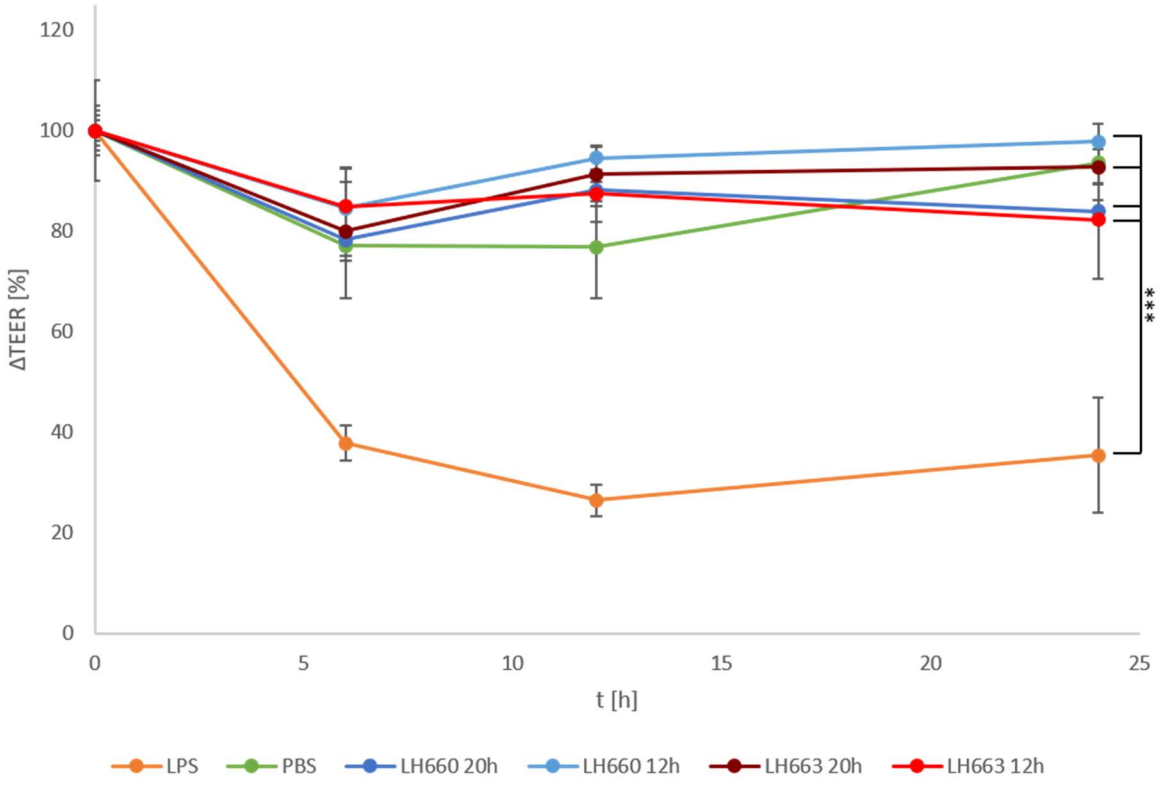


*Figure 26: TEER variation after treatment with LH660 20h BEVs (dark blue), LH660 12h BEVs (light blue), LH663 20h BEVs (dark red), LH663 12h BEVs (light red), PBS (negative control, green), and LPS (positive control, orange), respectively. Graphs depict mean TEER values, and error bars show SEM. *** P value ≤ 0.001 (two-way ANOVA followed by Dunnett's* post hoc *test). Experiment performed with 4 biological and 3 technical replicates per sample*

However, LH660 20h and LH663 12h BEVs showed diminished TEER at 12h and 24h compared to PBS, LH660 12h and LH663 20h BEVs. Surprisingly, throughout TEER differences between all BEV preparations and PBS were non-significant ($P \geq 0.05$), with the impact of all BEVs being less pronounced than PBS at 6h and 12h. Only at 24h did LH660 20h and LH663 12h BEVs result in TEER values lower than PBS. This suggests that both preparations of LH660 and LH663 BEVs transiently modulate the IEC. However, all were significantly less ($P \leq 0.001$) detrimental than LPS, which is used as an immune stimulant in some vaccine formulations.

Following this observation, RNA was extracted from Caco-2 cells at 6h and 24h after treatment with BEVs, PBS, and LPS and the expression of key TJ genes, occludin (Figure 27A and D), claudin-1 (Figure 27B and E), and ZO-1 (Figure 27C and F), was analysed via qRT-PCR.

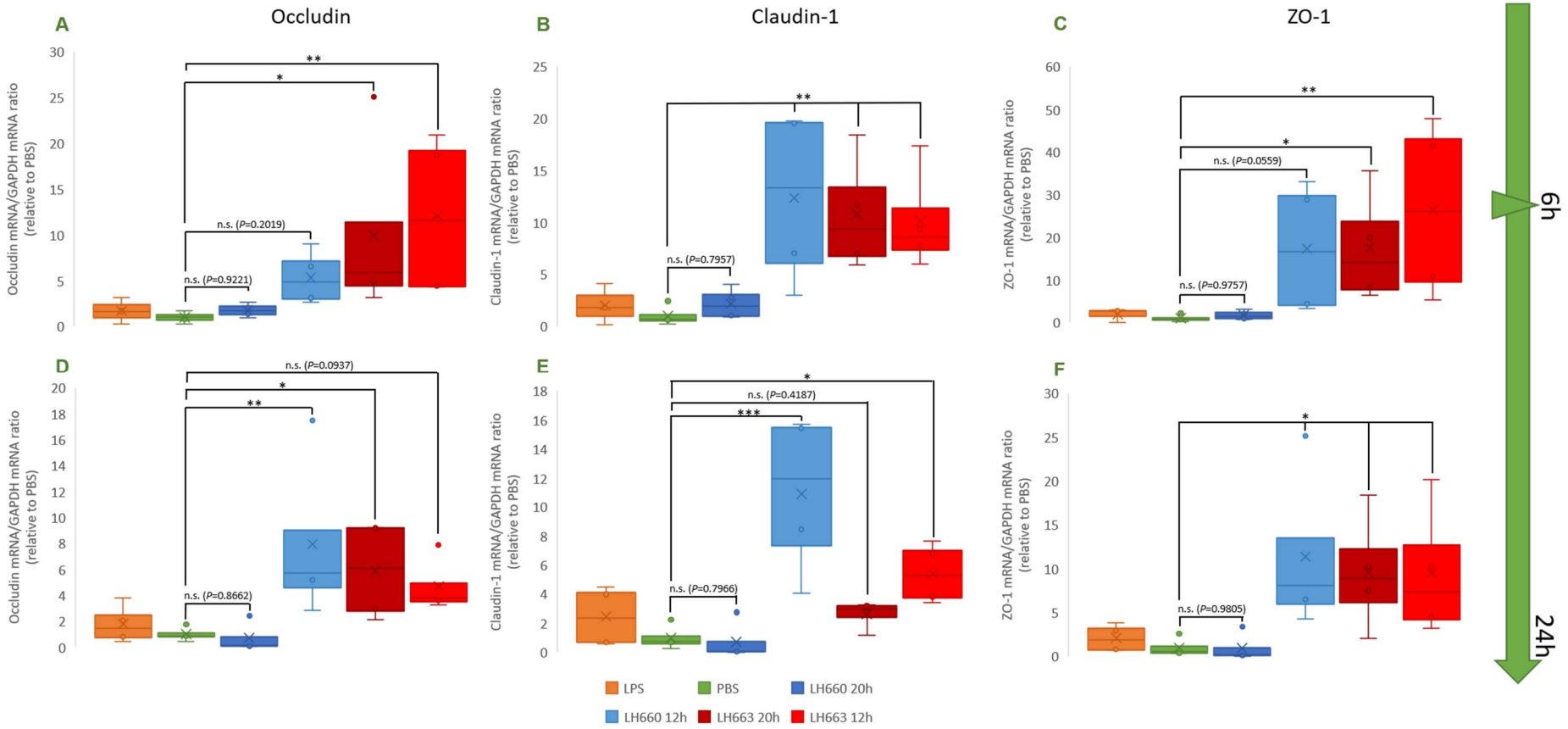


*Figure 27: Expression levels of occludin at 6h (A) and 24h (D), claudin-1 at 6h (B) and 24h (E), and ZO-1 at 6h (C) and 24h (F) in epithelial cells following respective treatment with LPS (orange) as positive control, PBS (green) as negative control, LH660 20h BEVs (dark blue), LH660 12h BEVs (light blue), LH663 20h BEVs (dark red), and LH663 12h BEVs (light red). mRNA ratios of target genes were calculated in relation to GAPDH levels in target groups compared to levels in the PBS-treated group. Boxplots show mean of each group, consisting of 4 biological and 2 technical replicates. Whiskers depict min-max values. * P ≤ 0.05, ** P ≤ 0.01, *** P ≤ 0.001 (one-way ANOVA followed by Dunnett's* post hoc *test)*

BEVs from LH663 and the 12h BEVs from LH660 induced expression of the three TJ genes at both time points, whereas LH660 20h BEVs did not modulate gene expression, with levels comparable to the PBS control ($P \geq 0.7$). Although variation between biological replicates meant that some changes were not statistically significant, trends were observed, such as higher levels of ZO-1 expression by LH660 12h BEVs at both time points. Overall, mRNA levels were higher at 6h post-BEV treatment, with ZO-1 expression approximately 2-fold greater than at 24h. Occludin was most induced by LH663 preparations, whereas LH660 12h BEVs significantly increased claudin-1 expression ($P=0.0034$ at 6h and $P=0.0003$ at 24h). At 24h, claudin-1 expression remained significantly higher in the 12h BEVs compared to LH663 20h BEVs ($P=0.0003$ for LH660 12h, and $P=0.0252$ for LH663 12h), with induction by LH663 20h BEVs being non-significant ($P=0.4187$). In contrast, only LH663 20h BEVs significantly induced occludin at both time points ($P=0.0301$ at 6h and $P=0.0441$ at 24h).

These qRT-PCR findings did not fully align with TEER measurements (Figure 26), as epithelial barrier integrity measured by electrical resistance was maintained across all BEV treatments, including LH660 20h BEVs. TEER values were lowest in LH663 12h treated cells and highest in LH660 12h treated cells, although differences between groups were not statistically significant. The key conclusion is that both strains produce BEVs containing components capable of modulating TJ gene expression without compromising epithelial barrier integrity.

### *4.1.2. Bifidobacterial BEVs protect against LPS-induced epithelial barrier disruption in a preparation-dependent manner*

These observations suggested that bifidobacterial BEVs may possess protective properties against epithelial barrier disruption. To further explore this potential protective role, TEER was measured in differentiated Caco-2 cells pre-treated with LH660 and LH663 BEVs for 24h, followed by exposure to LPS for 12h, 24h, and 48h (Figure 28) to simulate a pathogenic Gram-negative infection. LPS, a major component of Gram-negative bacterial cell walls, was used as a standard challenge to mimic pathogenic infection *in vitro*, as it is widely employed to induce epithelial barrier disruption and inflammatory stress. This approach allowed assessment of whether BEV pre-treatment could mitigate LPS-induced damage and preserve barrier integrity.

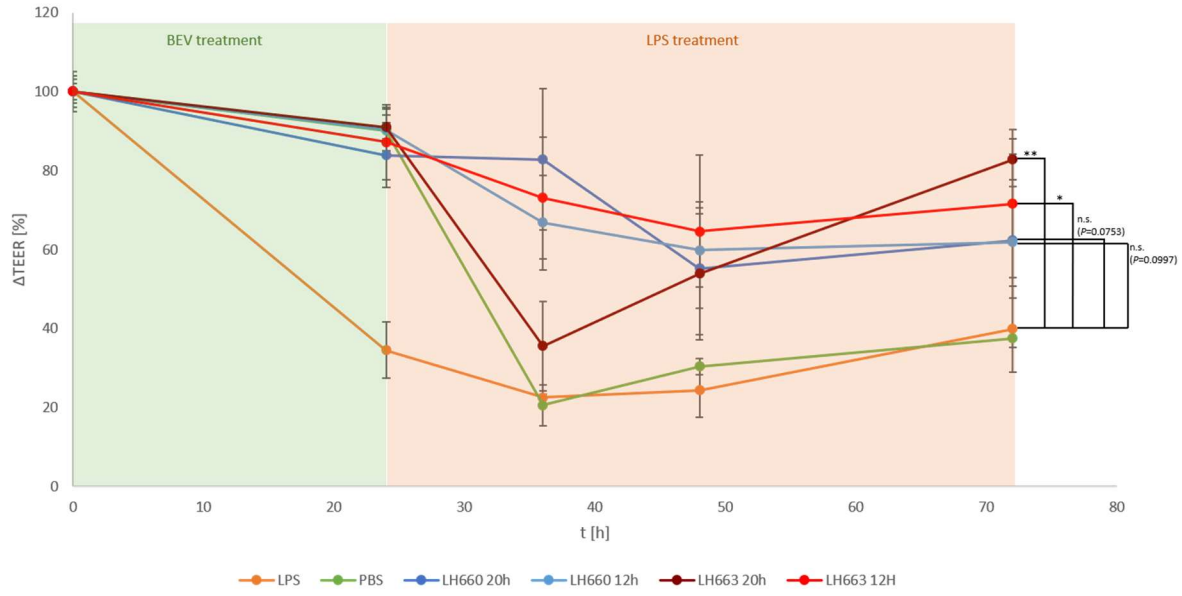


*Figure 28: TEER variation after first 24h treatment with LH660 20h BEVs (dark blue), LH660 12h BEVs (light blue), LH663 20h BEVs (dark red), LH663 12h BEVs (light red), PBS (negative control, green), and LPS (positive control, orange), respectively, followed by 12h, 24h, and 48h LPS challenge. Graphs depict mean TEER values, error bars show SEM. * P value ≤ 0.05, ** P value ≤ 0.01 (two-way ANOVA followed by Dunnett's* post hoc *test). Experiment performed with 4 biological and 3 technical replicates per sample*

As expected, PBS-treated cells exhibited a marked decline in TEER following LPS challenge, with a reduction of ~70%, while cells pre-treated with LPS maintained consistently low TEER levels (≥40%) throughout the experiment. All BEV-primed groups showed a decrease in TEER upon LPS exposure and did not fully recover to baseline levels prior to LPS introduction. However, BEV treatment conferred a measurable protective effect, as TEER values remained higher than those of PBS and LPS-only controls across all time points. Notably, both LH663 preparations ($P$=0.0489 for LH663 12h and $P$=0.0072 for LH663 20h) elicited significantly higher TEER values at 48h post-challenge.

Interestingly, BEVs harvested at 12h tended to maintain more stable TEER values during LPS exposure, whereas LH663 20h BEVs caused an initial TEER drop of over 50% at 12h before recovery, and LH660 20h BEVs showed a decline of more than 30% at 24h. Overall, endpoint TEER values were higher in LH663 BEV-treated cells compared to LH660 BEV-treated cells. Variation was greatest in the LH660 BEV groups, resulting in statistical non-significance despite TEER values being more than 25% higher than those of both controls. Consistent with the initial experiment, RNA was extracted from cells 12h, 24h and 48h post-LPS treatment to assess potential modulation of occludin, claudin-1, and ZO-1 expression (Figure 29).

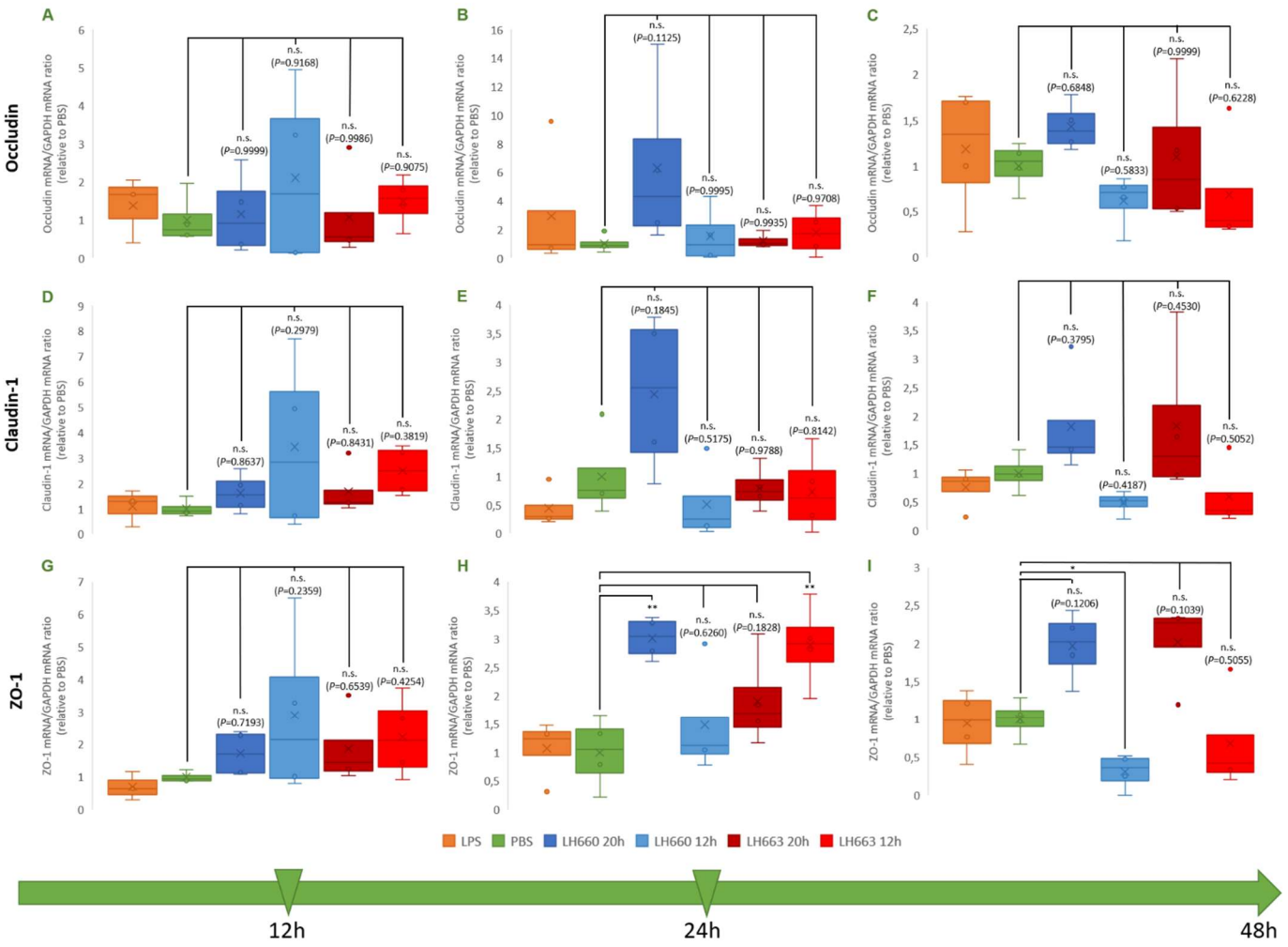


*Figure 29: Expression levels of occludin at 12h (A), 24h (B), and 48h (C), claudin-1 at 12h (D), 24h (E), and 48h (F), and ZO-1 at 12h (G), 24h (H), and 48h (I) of LPS challenge in epithelial cells first treated for 24h with LPS (orange) as positive control, PBS (green) as negative control, LH660 20h BEVs (dark blue), LH660 12h BEVs (light blue), LH663 20h BEVs (dark red), and LH663 12h BEVs (light red), respectively. mRNA ratios of target genes were calculated in relation to GAPDH levels in target groups compared to levels in the PBS-treated group. Boxplots show mean of each group, consisting of 4 biological and 2 technical replicates. Whiskers depict min-max values. * P ≤ 0.05, ** P ≤ 0.01 (one-way ANOVA followed by Dunnett's* post hoc *test)*

Unlike the initial BEV pre-treated Caco-2 cells in the absence of LPS challenge (Figure 27), the 20h BEV samples from both strains increased expression of all three tested TJ genes over time, though they were not significantly different from the PBS control throughout the experiment with the exception of claudin-1 at 24h (Figure 29H). Here, LH660 20h and LH663 12h significantly induced claudin-1 expression ($P$=0.0043 for LH660 20h and $P$=0.0068 for LH663 12h). At 48h, occludin, claudin-1, and ZO-1 showed non-significant increases with 20h BEV preparations, with high variability between replicates (Figure 29C, F, and I). Unexpectedly, the 12h BEVs reduced TJ gene expression over time, with ZO-1 levels significantly lower in the LH660 12h BEV-treated cells compared to PBS (Figure 29I; $P$=0.0377). None of the preparations mirrored the expression profiles observed in the initial BEV-only treatment (Figure 27), or TEER patterns following LPS challenge (Figure 28). These findings suggest that modulation of TJ expression may be BEV preparation-dependent and influenced by environmental conditions.

## 4.2. BEVs are taken up by intestinal epithelial cells

### *4.2.1. BEVs accumulate around the perinuclear area of Caco-2 cells*

To further investigate the uptake of BEVs by epithelial cells, DAPI-labelled Caco-2 monolayers were incubated with LH660 and LH663 20h BEVs labelled with DiO dye or PBS prior to confocal imaging. Screening (imaging n=4 per strain, n=2 per BEV batch, ≤10 images per sample) revealed distinct cell clusters with BEV uptake and accumulation in the cell cytoplasms, with adjacent cells being devoid of DiO fluorescence (Figure 30 and Figure 32C).

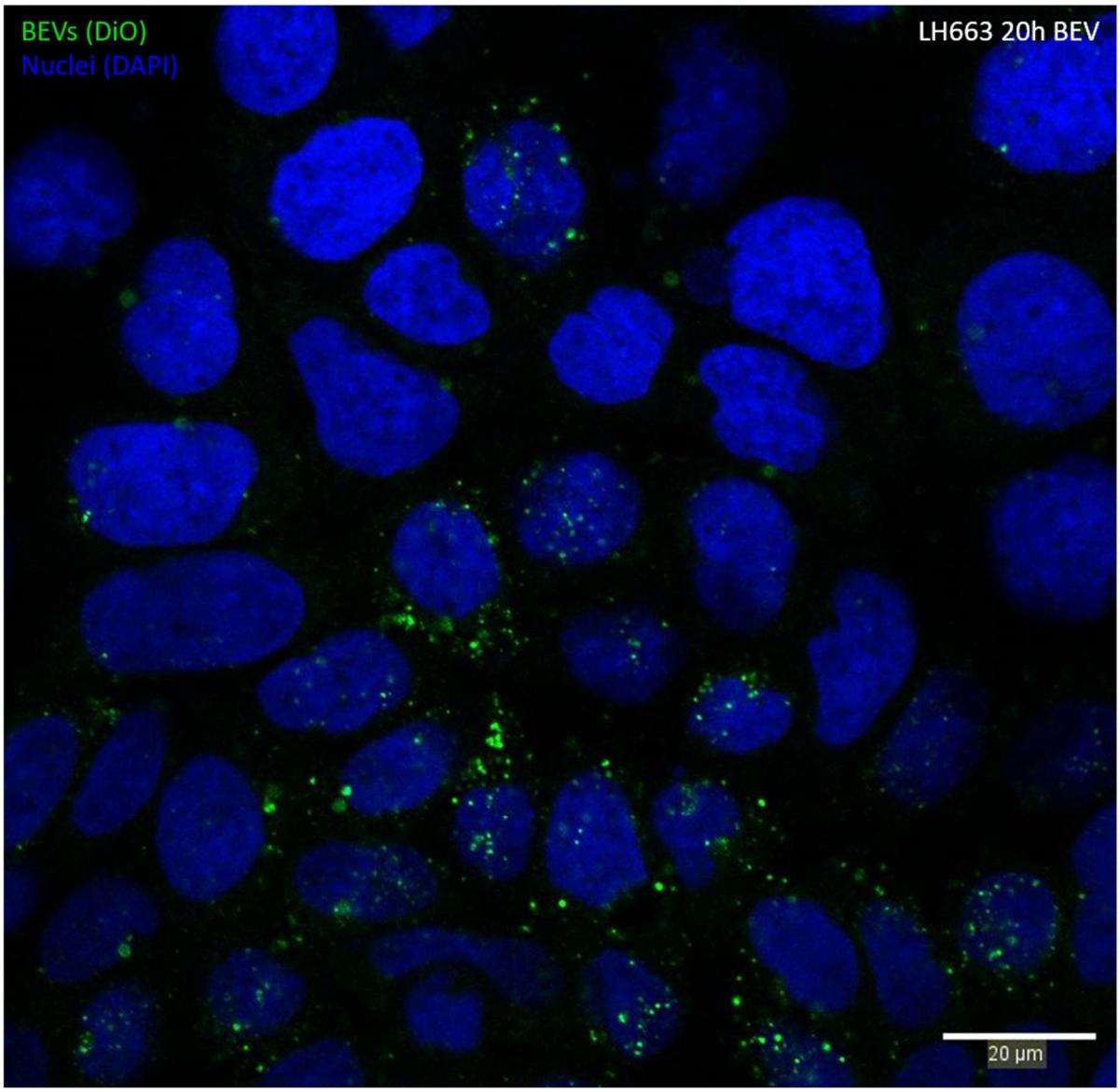


*Figure 30: Overview of Caco-2 monolayer incubated with LH663 20h BEVs. Cell nuclei stained with DAPI (blue), BEVs labelled with DiO (green)*

BEVs were found to localise around the nucleus and the perinuclear area of individual cells. Analysis of different z-levels of the selected areas suggested that BEVs were present within or in close association with nuclear pores (Figure 31).

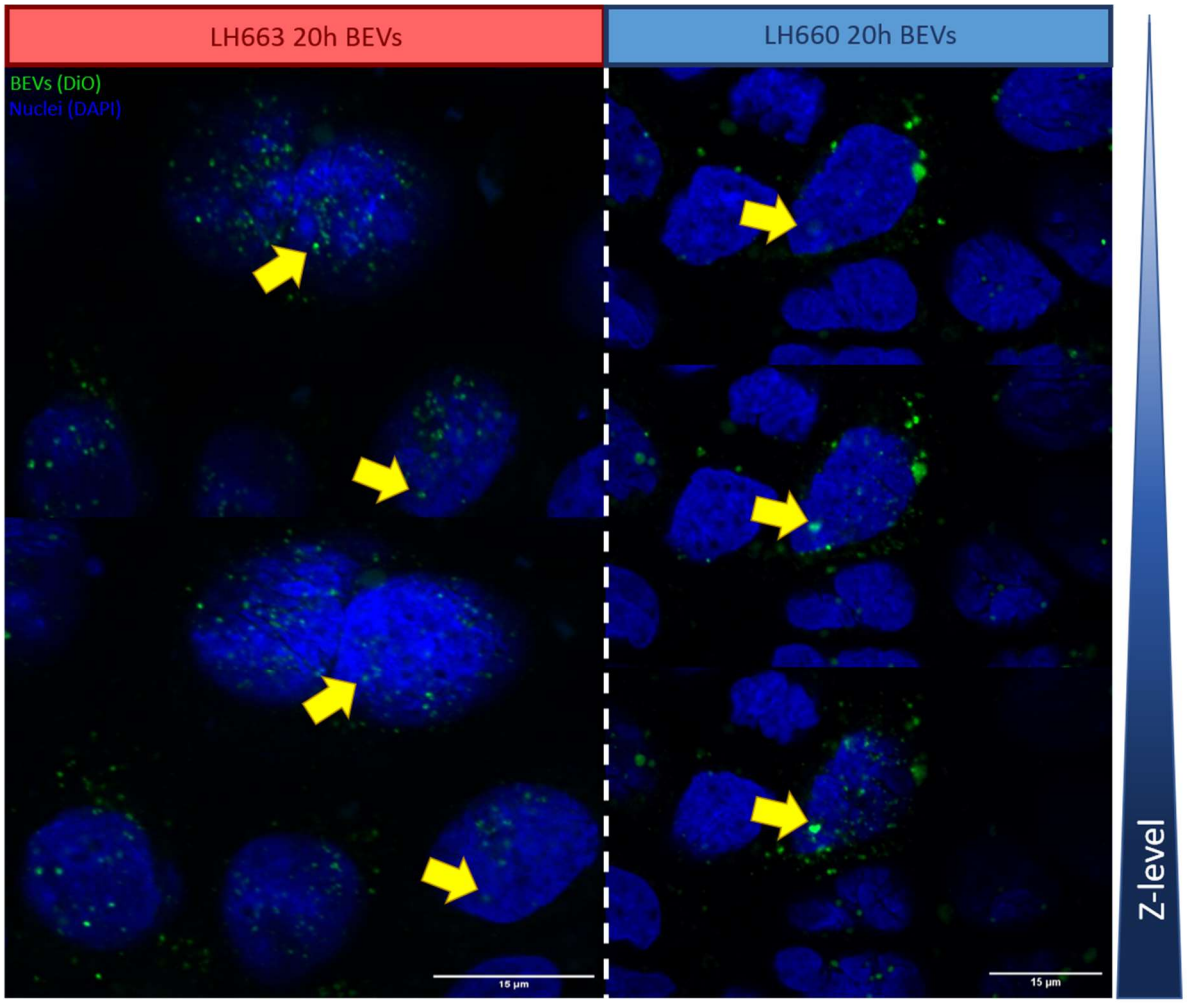


*Figure 31: Selected sections of translocated LH660 and LH663 20h BEVs (green) in the perinuclear area of Caco-2 cells (nuclei blue) with decreasing z-level. Arrows point to BEVs within nuclear pores*

### *4.2.2. BEV uptake is partly mediated via Dynamin-dependent endocytosis*

Internalisation of BEVs can follow different endocytic routes. Our lab recently showed that *B. thetaiotaomicron*-derived BEVs are primarily taken up by epithelial cells via the Dynamin-dependent endocytosis pathway.[326] Based on this, I prepared another set of Caco-2 monolayer slides treated with the Dynamin antagonist Dynasore prior to incubation with DiO-labelled LH660 and LH663 20h BEVs. Comparison of the confocal images showed an increased number of internalised BEVs in the non-treated epithelial cells (Figure 32C) and fewer BEV signal in Dynasore pre-treated cells (Figure 32B). Quantification of AU per cell using Image J/FIJI revealed that BEV signals in Dynasore-treated cells were not significantly ($P$=0.4957 for LH660 and $P$=0.1565 for LH663) different from non-treated samples (Figure 33), suggesting this is not a major route of LH660 and LH663 BEV uptake by Caco-2 cells.

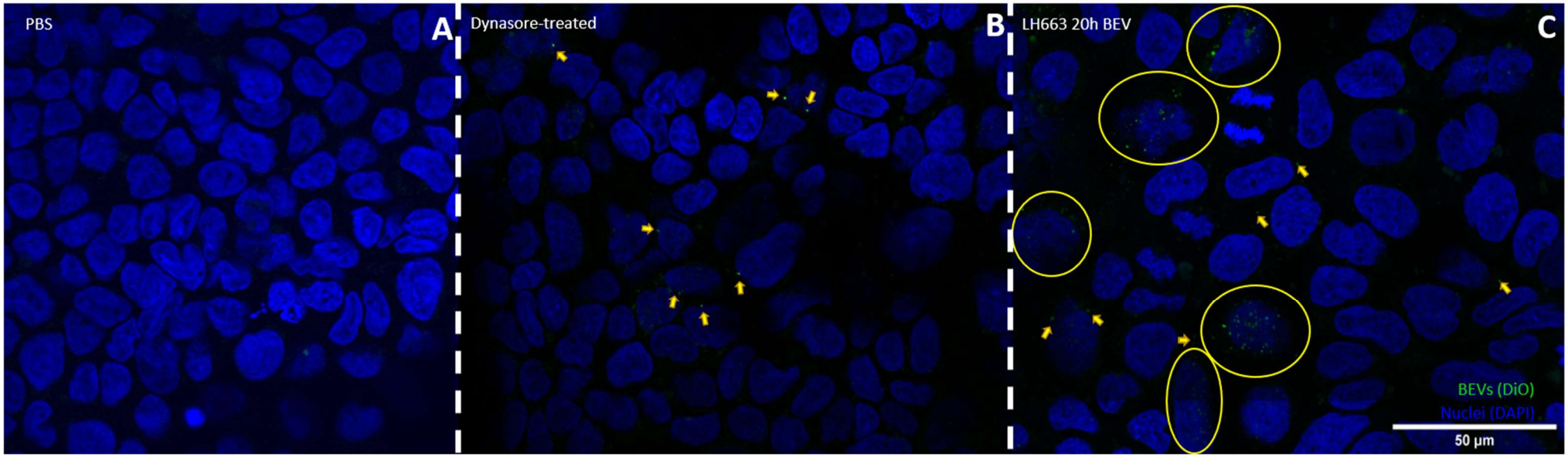


*Figure 32: Comparison of confocal images of Dynasore-treated (B) or untreated Caco-2 cells incubated with PBS (A) or LH663 20h BEVs (C). Caco-2 cell nuclei stained with DAPI (blue), BEVs labelled with DiO (green). Arrows point to single BEVs, circles show cells with BEV uptake.*

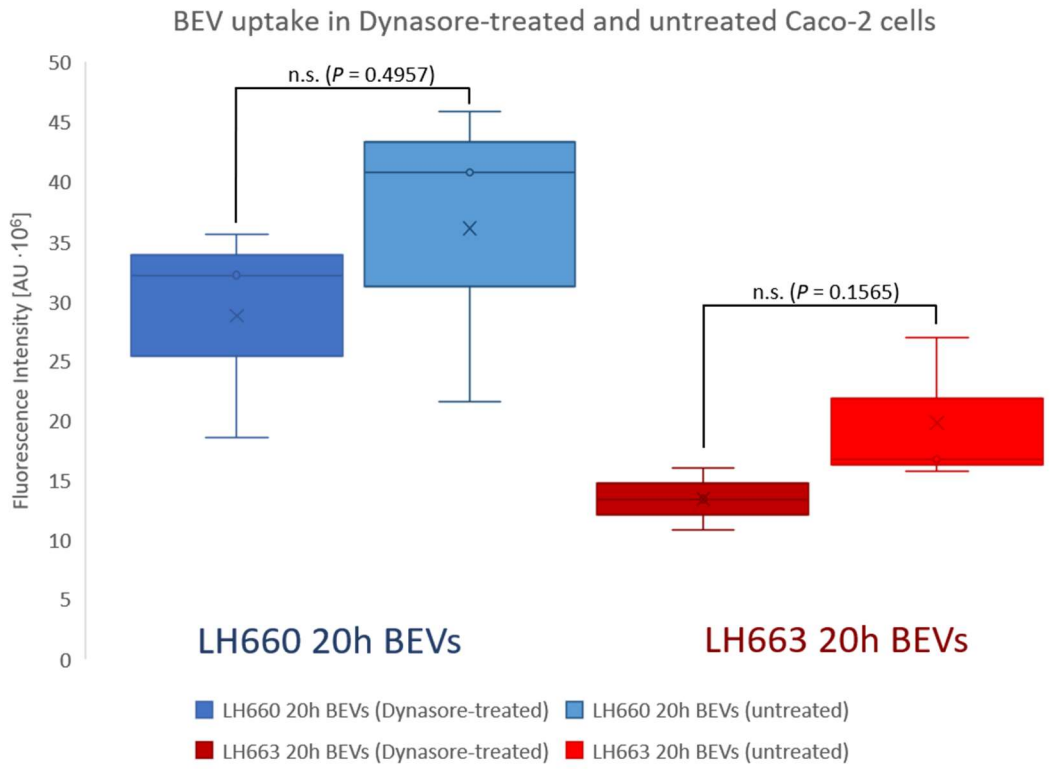


*Figure 33: Uptake of DiO-labeled 20h BEVs from LH660 and LH663 in Caco-2 monolayer with and without Dynasore treatment. Fluorescence intensity was quantified using fluorescence pixel intensity in Image J/FIJI and AU were normalised to PBS control samples. Boxplots show mean of each group of ≤10 images. Whiskers depict min-max values. Two-sample Student's t-tests were non-significant between groups. N=4 per strain, n=2 per BEV batch*

## 4.3. Bifidobacterial BEVs induce cytokine production in immune and epithelial cells in a preparation-dependent manner

### *4.3.1. All BEVs activate NF-κB pathway in a human monocyte reporter cell line*

To further investigate the potential immunomodulatory properties of BEVs derived from LH660 and LH663, I used the THP1-Blue NF-κB reporter cell line. Activation of the NF-κB pathway leads to the production of cytokines and chemokines, which are essential for mediating immune responses.[35] Stimulation of this human monocytic reporter cell line with LH660 and LH663 BEVs harvested at 12h and 20h led to activation of the NF-κB pathway ($P \leq 0.001$ for all samples compared to the PBS control) as measured by the QuantiBlue assay (Figure 34A). LH660 20h BEVs induced significant ($P=0.0077$) levels of NF-κB activation, which were lower than those seen with other BEV groups (Figure 34B). Based on this, THP-1 monocytes were differentiated into macrophages via co-culture with PMA and used in conjunction with

Caco-2 cells to investigate potential cytokine and chemokine production after co-culture with LH660 and LH663 BEVs.

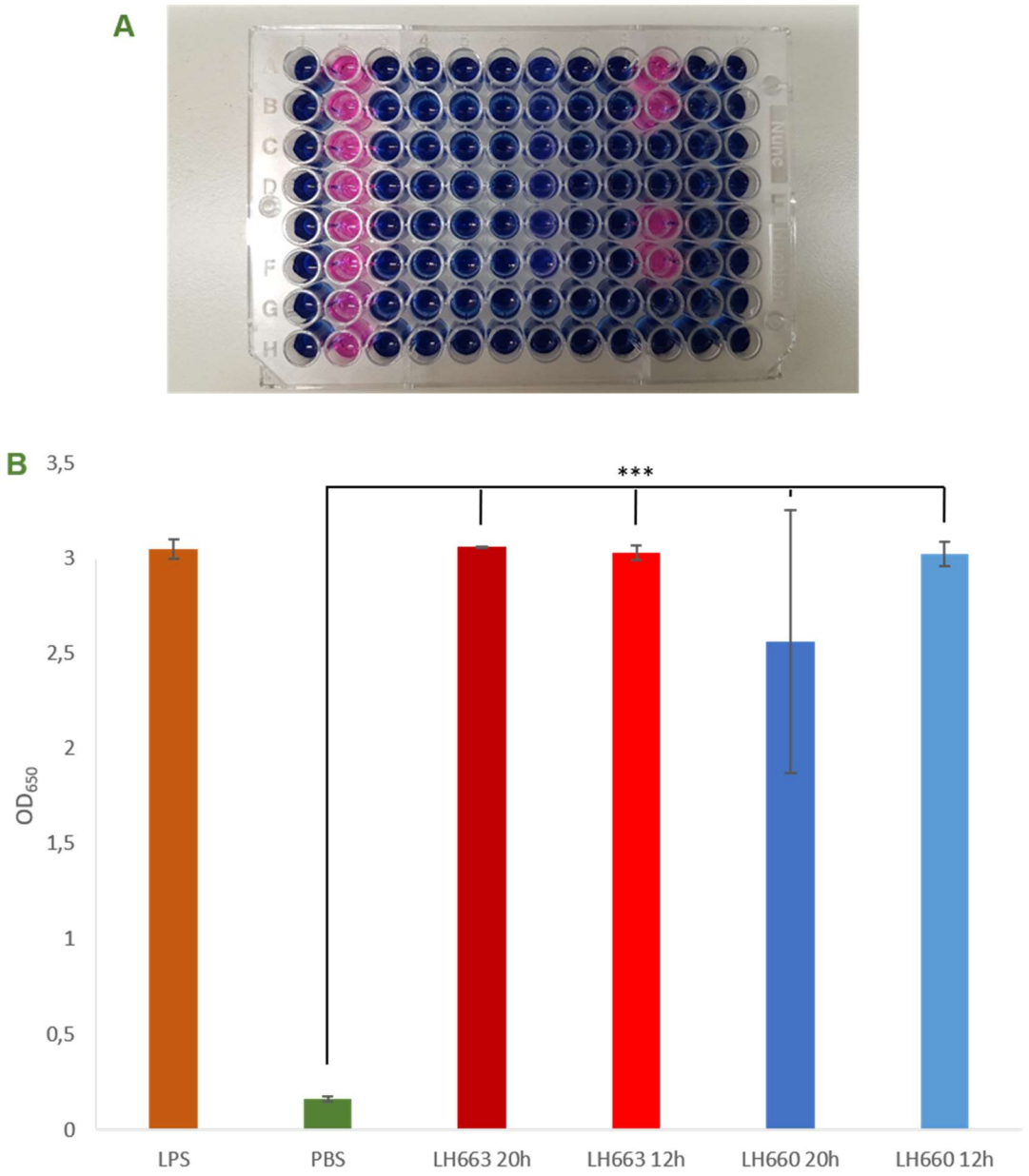


*Figure 34: Stimulation of THP1-Blue cells by LH660 and LH663 BEVs, PBS as negative control, LPS as positive control. A: QuantiBlue assay plate showing colour change, B: respective OD650 data. Data shows sample means ± SEM error bars of 3 biological and 6 technical replicates. *** P value ≤ 0.001 (one-way ANOVA followed by Dunnett's* post hoc *test). Experiments performed in biological and technical quadruplets*

### *4.3.2. BEVs stimulate cytokine production by human monocytes, macrophages, and colonic epithelial cells*

Cell cultures were treated with LH660 and LH663 BEVs for 24h, with the conditioned media and/or cells analysed for key cytokines and chemokines mRNA (TNF-α, IL-1β, IL-6, IL-10) or protein (TNF-α, IL-1β, IL-6, IL-8, IL-10, IL-12p70, IL-15, TSLP, MCP-1) levels using qRT-PCR, ELISA and MSD assays, respectively.

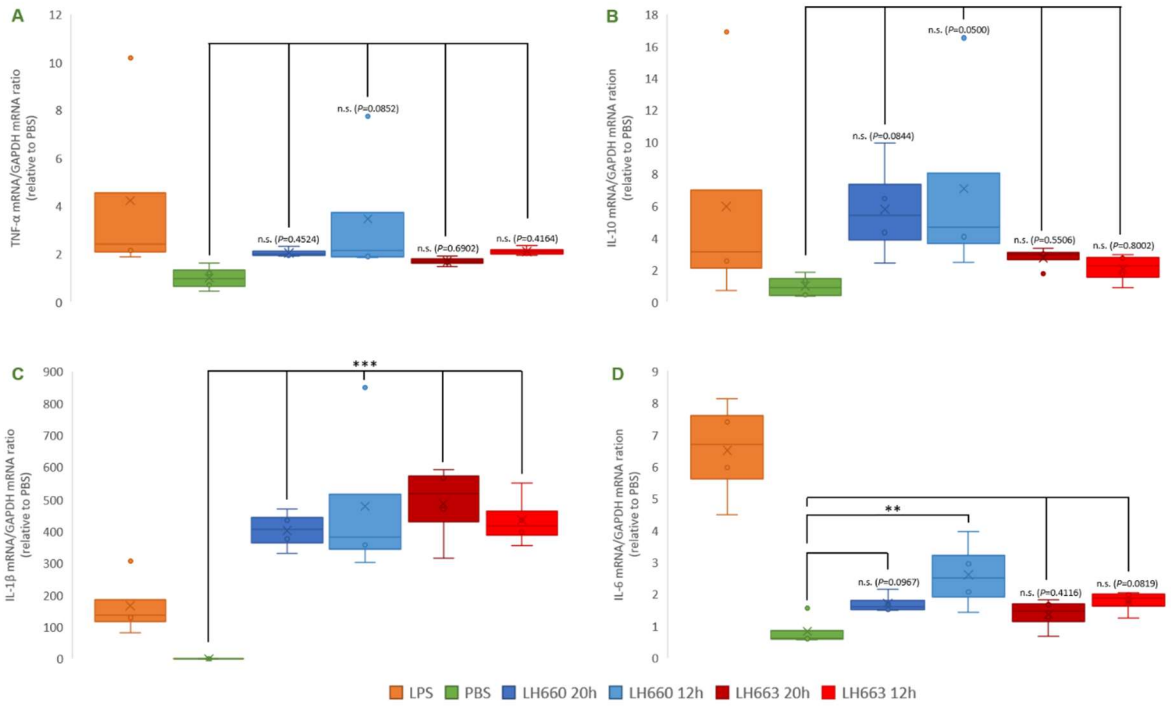


*Figure 35: Expression levels of TNF-α (A), IL-10 (B), IL-1β (C), and IL-6 (D) after 24h of treatment of differentiated THP-1 macrophages with LPS (orange) as positive control, PBS (green) as negative control, LH660 20h BEVs (dark blue), LH660 12h BEVs (light blue), LH663 20h BEVs (dark red), and LH663 12h BEVs (light red), respectively. mRNA ratios of target genes were calculated in relation to GAPDH levels in target groups compared to levels in the PBS-treated group. Boxplots show mean of each group, consisting of 4 biological and 2 technical replicates. Whiskers depict min-max values. ** P ≤ 0.01, *** P ≤ 0.001 (one-way ANOVA followed by Dunnett's* post hoc *test)*

Overall, cytokine expression was induced by BEVs in a strain- and time point-dependent manner. All BEV preparations significantly ($P \leq 0.001$) upregulated IL-1β gene expression compared to PBS controls (Figure 35C), with only LH660 12h BEVs significantly inducing higher IL-6 expression ($P=0.0034$; Figure 35D). TNF-α and IL-10 induction levels were not significantly different compared to PBS controls for all BEV samples (Figure 35A and B). LH660 12h BEVs showed high inter-sample variation. 12h BEVs generally induced higher IL-6 and TNF-α expression than 20h preparations. Similarly, LH660 BEVs elicited stronger TNF-α, IL-10, and IL-6 responses than LH663 BEVs. Interestingly, IL-1β expression reached levels 3-4-fold above LPS controls, with

LH663 20h BEVs showing the greatest stimulation. mRNA from Caco-2 layers (collected during TEER assays) showed no detectable expression of these cytokines.

To validate these findings, cytokine secretion was quantified by ELISA and MSD in supernatants from differentiated THP-1 macrophages, THP1-blue cells, and differentiated Caco-2 cells, including additional cytokines beyond those assessed at expression level (IL-8, TSLP, IL-15, IL-12p70, MCP-1), and protein-level analysis confirmed these trends.

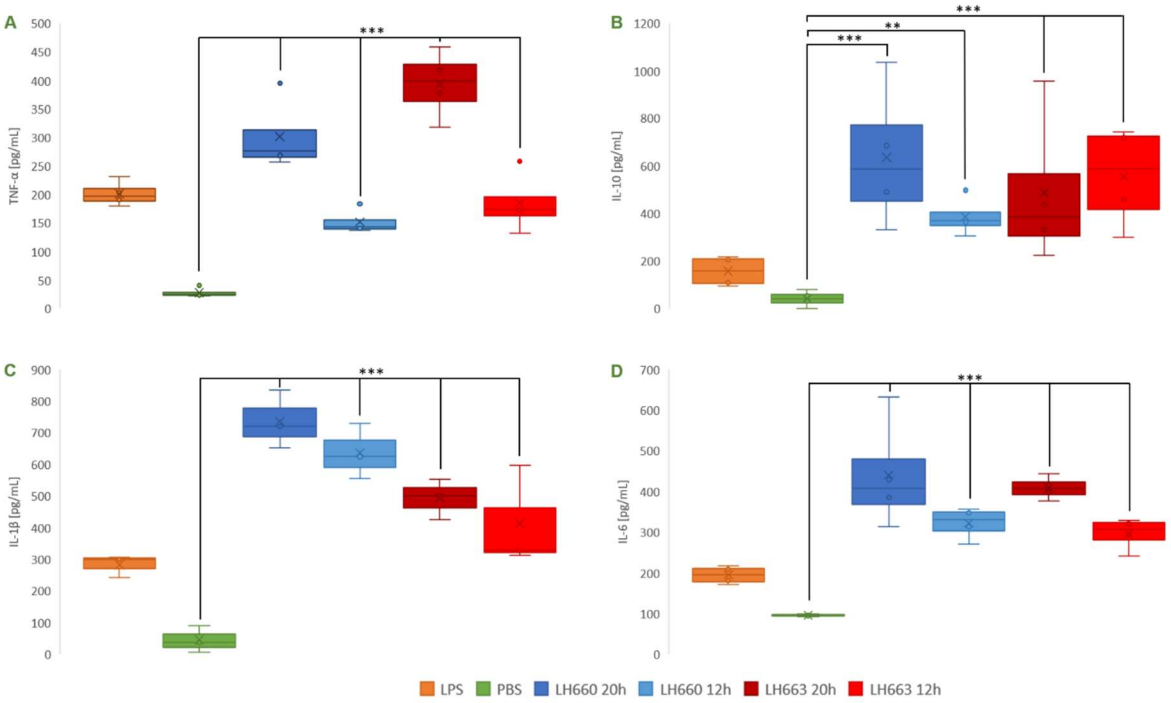


*Figure 36: Cytokine levels of TNF-α (A), IL-10 (B), IL-1β (C), and IL-6 (D) after 24h of treatment of differentiated THP-1 macrophages with LPS (orange) as positive control, PBS (green) as negative control, LH660 20h BEVs (dark blue), LH660 12h BEVs (light blue), LH663 20h BEVs (dark red), and LH663 12h BEVs (light red), respectively. Boxplots show mean of each group, consisting of 4 biological and 3 technical replicates. Whiskers depict min-max values. ** P ≤ 0.01, *** P ≤ 0.001 (one-way ANOVA followed by Dunnett's* post hoc *test)*

All BEVs significantly ($P \leq 0.01$) increased secretion of the four cytokines compared to PBS controls (Figure 36), with levels, except TNF-α, being 2-3-fold higher than LPS controls. In contrast to expression data, 20h BEVs induced greater secretion of TNF-α, IL-1β, and IL-6 than 12h BEVs. LH663 BEVs produced higher TNF-α (Figure 36A), while LH660 BEVs promoted more IL-1β (Figure 36C) and IL-6 (Figure 36D) than LH663 BEVs. IL-10 secretion peaked in LH660 20h and LH663 12h BEV-treated macrophages, with mean concentrations of 600pg/mL (Figure 36B).

Additionally, all BEV preparations significantly ($P \leq 0.001$) stimulated IL-8 secretion by macrophages (Figure 37A), but not by differentiated epithelial cells (Figure 37B).

Interestingly, all BEV preparations, except LH663 12h BEVs, significantly (P≤0.05) enhanced TSLP production by macrophages, with LH663 20h BEVs eliciting the highest TSLP levels (Figure 37C). None of the BEV preparations significantly induced IL-15 in monocyte cultures (Figure 37D), with high inter-sample variations evident. None of the BEVs induced IL-12p70 or MCP-1 in any culture.

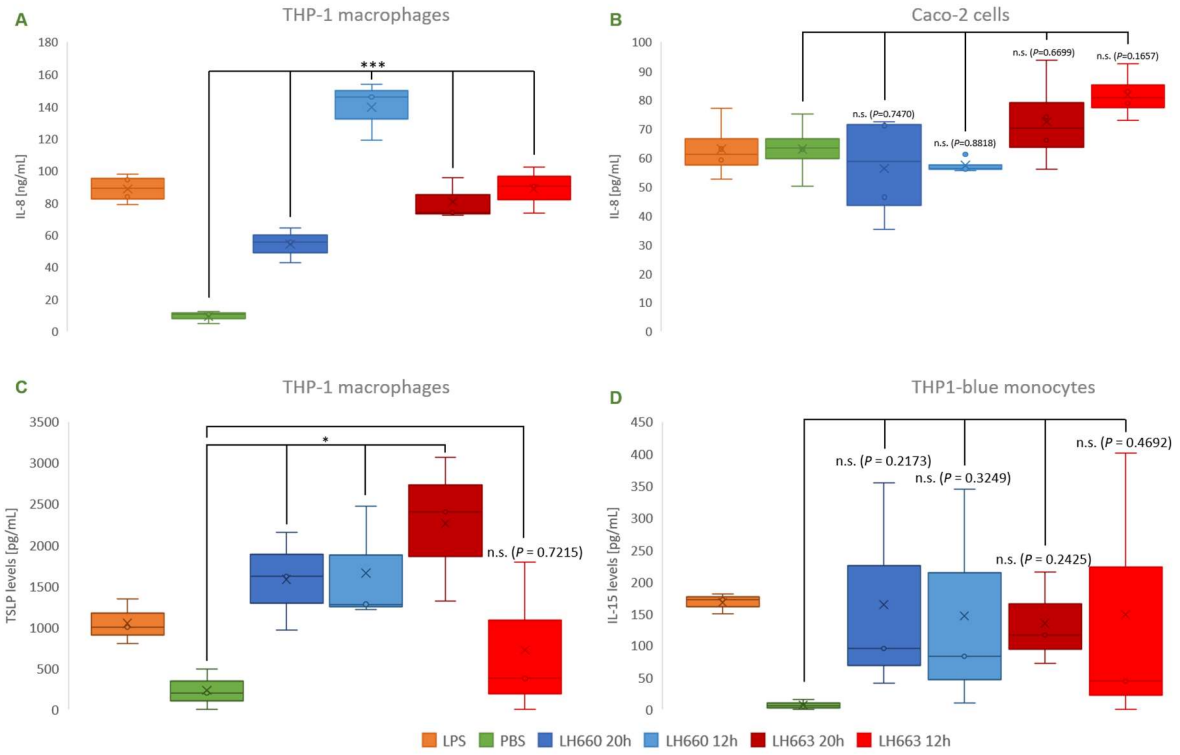


*Figure 37: Cytokine levels of IL-8 (A&B), TSLP (C), and IL-15 (D) after 24h of treatment of differentiated THP-1 macrophages (A&C), differentiated Caco-2 epithelial cells (B) and THP1-blue monocytes (D) with LPS (orange) as positive control, PBS (green) as negative control, LH660 20h BEVs (dark blue), LH660 12h BEVs (light blue), LH663 20h BEVs (dark red), and LH663 12h BEVs (light red), respectively. Boxplots show mean of each group, consisting of 4 biological and 3 technical replicates. Whiskers depict min-max values. * P ≤ 0.05, *** P ≤ 0.001 (one-way ANOVA followed by Dunnett's* post hoc *test)*

## 4.4. Interaction of bifidobacterial BEVs in complex cell samples

### *4.4.1. BEV induction of TNF-α and MCP-1 production by human PBMCs*

To verify immune stimulation in more complex multicellular samples, ELISAs were repeated using PBMCs. MCP-1 levels were significantly elevated (*P*≤0.001) by all BEV preparations but were overall very low (≥20pg/mL; Figure 38B). TNF-α levels were significantly (*P*≤0.001) increased by all BEVs, with the highest concentrations observed in cultures treated with LH663 20h and LH660 12h BEVs (Figure 38A). Compared to levels in immortalised macrophage cultures, TNF-α production was less elevated in PBMC cultures, and time point-dependent associations were not

distinguishable, suggesting potential immunostimulatory differences of BEVs in more biologically complex environments. None of the BEVs induced IL-12p70.

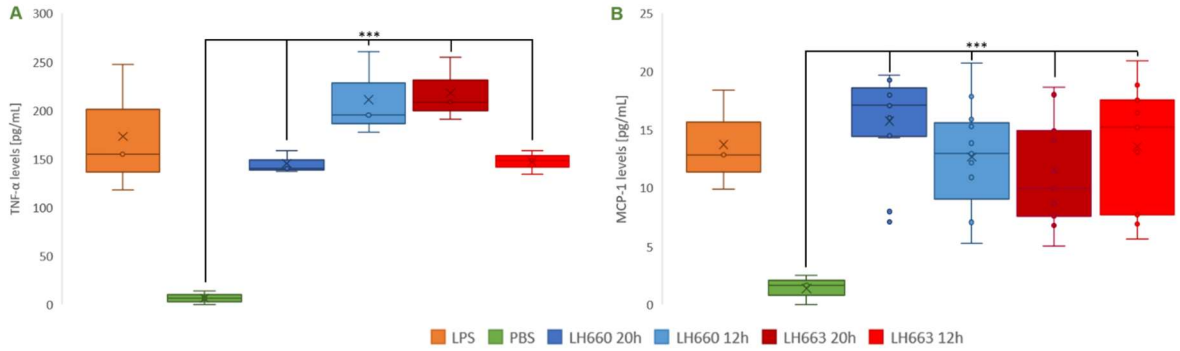


*Figure 38: Cytokine levels of TNF-α (A) and MCP-1 (B) after 24h of treatment of PBMCs with LPS (orange) as positive control, PBS (green) as negative control, LH660 20h BEVs (dark blue), LH660 12h BEVs (light blue), LH663 20h BEVs (dark red), and LH663 12h BEVs (light red), respectively. Boxplots show mean of each group, consisting of 4 biological and 3 technical replicates. Whiskers depict min-max values. *** P ≤ 0.001 (one-way ANOVA followed by Dunnett's* post hoc *test)*

### *4.4.2. BEVs elicit cytokine production by murine splenocytes but not BMDCs*

Although BM cells were enriched for $CD11c^+$ DCs using the CD11c MicroBead UltraPure system, none of the assays resulted in conclusive positive signals from the BEV samples or LPS in any of the 4 repeated experiments and were excluded from the thesis.

Interestingly, cytokine production induced by splenocyte-BEV co-cultures did not mirror cytokine profiles seen in human cell cultures. LH663 BEVs (except 12h for IL-10) significantly induced production of KC ($P \leq 0.001$), a murine analogue of IL-8 (Figure 39A), TNF-α ($P \leq 0.001$; Figure 39B), IL-6 ($P \leq 0.001$; Figure 39C), and IL-10 ($P = 0.0014$ for 20h, $P = 0.1128$ for 12h BEVs; Figure 40A), with 20h BEVs eliciting 1.5-2.5-fold higher cytokine levels than 12h BEVs. LH660 20h BEVs significantly induced levels of KC ($P = 0.0389$) that were 5-10 times lower than respective LH663 BEV-stimulated cells, and LH660 12h BEVs led to significantly increased IFN-γ levels ($P = 0.0003$). Still, 20h BEV samples of both strains induced 2-fold higher levels of all induced cytokines. An exception to this was IL-10 and IFN-γ levels, with IFN-γ being highest in LH660 and LH663 12h BEV-stimulated splenocytes (Figure 40B). However, both IFN-γ and IL-10 concentrations were low in all cultures, including those containing LPS. Additionally, no IL-1β, IL-22, IL-17A, IL-12p70, and IL-4 was detectable in the splenocyte co-cultures.

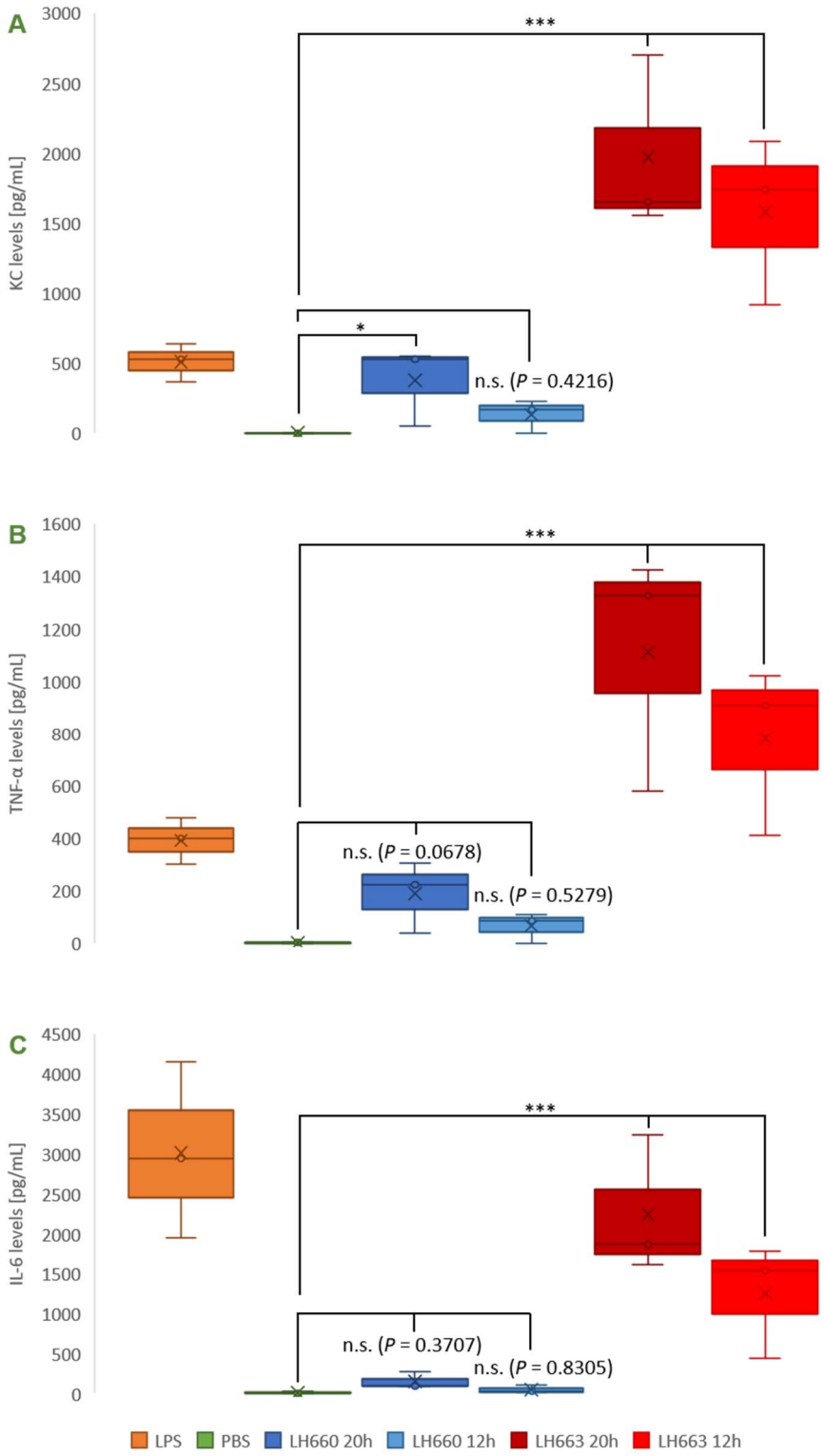


*Figure 39: Stimulation of splenocytic cells by LH660 and LH663 BEVs, PBS as negative control, LPS as positive control. MSD data for A: KC, B: TNF-α, and C: IL-6. Boxplots show mean of each group of 3 biological and 3 technical replicates. Whiskers depict min-max values. * P value ≤ 0.05, *** P value ≤ 0.001 (one-way ANOVA followed by Dunnett's* post hoc *test). Experiments performed in biological and technical triplicate*

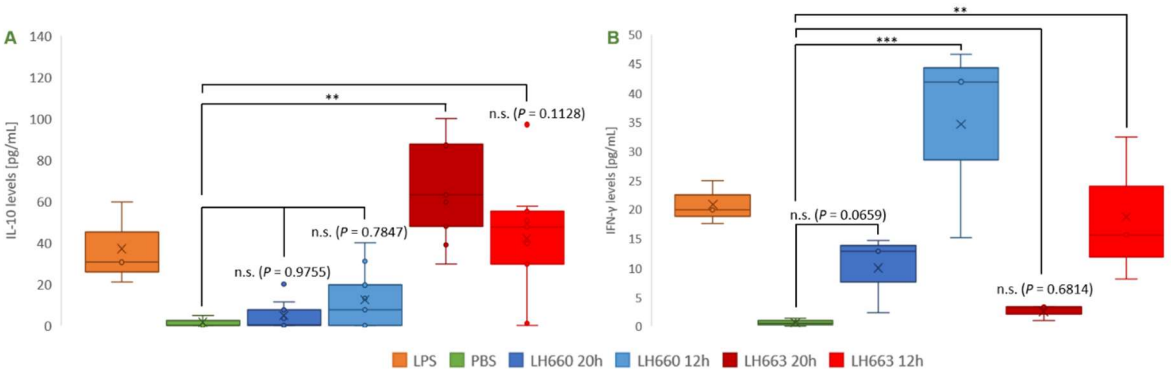


*Figure 40: Stimulation of splenocytic cells by LH660 and LH663 BEVs, PBS as negative control, LPS as positive control. ELISA data for A: IL-10 and B: IFN-γ. Boxplots show mean of each group of 3 biological and 3 technical replicates. Whiskers depict min-max values. ** P value ≤ 0.01, *** P ≤ 0.001 (one-way ANOVA followed by Dunnett's post hoc test). Experiments performed in biological and technical triplicate*

### *4.4.3. BEVs promote IgA secretion in PP/GALT fragments cultures in a strain-dependent manner*

Following the abundance of ESBP in the proteomic analysis of BEVs (see Results Chapter II, Figure 25) and its reported link to IgA secretion in PPs after stimulation with BEVs from *B. longum* subsp. *infantis*[377], I repeated the experiment of Kurata et al. (2022) using BEVs from LH660 and LH663. Surprisingly, only LH663 20h BEVs significantly induced (*P*=0.0016) higher levels of IgA in PP/GALT cell cultures. LH660 BEV-stimulated cultures showed IgA levels comparable to PBS baseline levels (*P* values close to 1; Figure 41), with LH663 12h BEVs also producing a non-significant elevation of IgA production (*P*=0.0549). Given that ESBP abundance was higher in LH660 BEVs compared to LH663 BEVs at both time points, factors other than ESBP or structural differences may influence the promotion of IgA secretion.

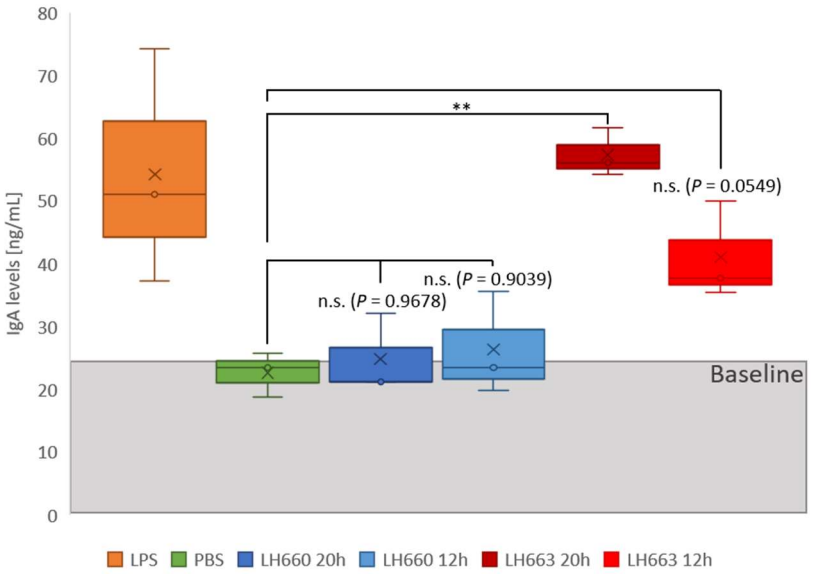


*Figure 41: Stimulation of cells derived from PP/GALT fragments by LH660 and LH663 BEVs, PBS as negative control, LPS as positive control. Baseline IgA level based on PBS data. Boxplots show mean of each group of 3 biological and 3 technical replicates. Whiskers depict min-max values. ** P value ≤ 0.01 (one-way ANOVA followed by Dunnett's post hoc test). Experiments performed in biological and technical triplicate*

## 4.5. Treatment with bifidobacterial BEVs modulates LPS-induced cytokine profiles

Similar to the protective TEER and TJ modulation assay, differentiated THP-1 macrophages and Caco-2 epithelial cells were pre-treated for 24h with bifidobacterial BEVs, LPS, or PBS before being challenged with LPS for 12h, 24h and 48h. RNA was extracted from each group, and culture supernatants were collected for downstream qRT-PCR analysis (Figure 42 and Figure 43) and ELISA quantification (Figure 44 and Figure 45) of TNF-α, IL-1β, IL-6 and IL-10, respectively, as well as IL-8.

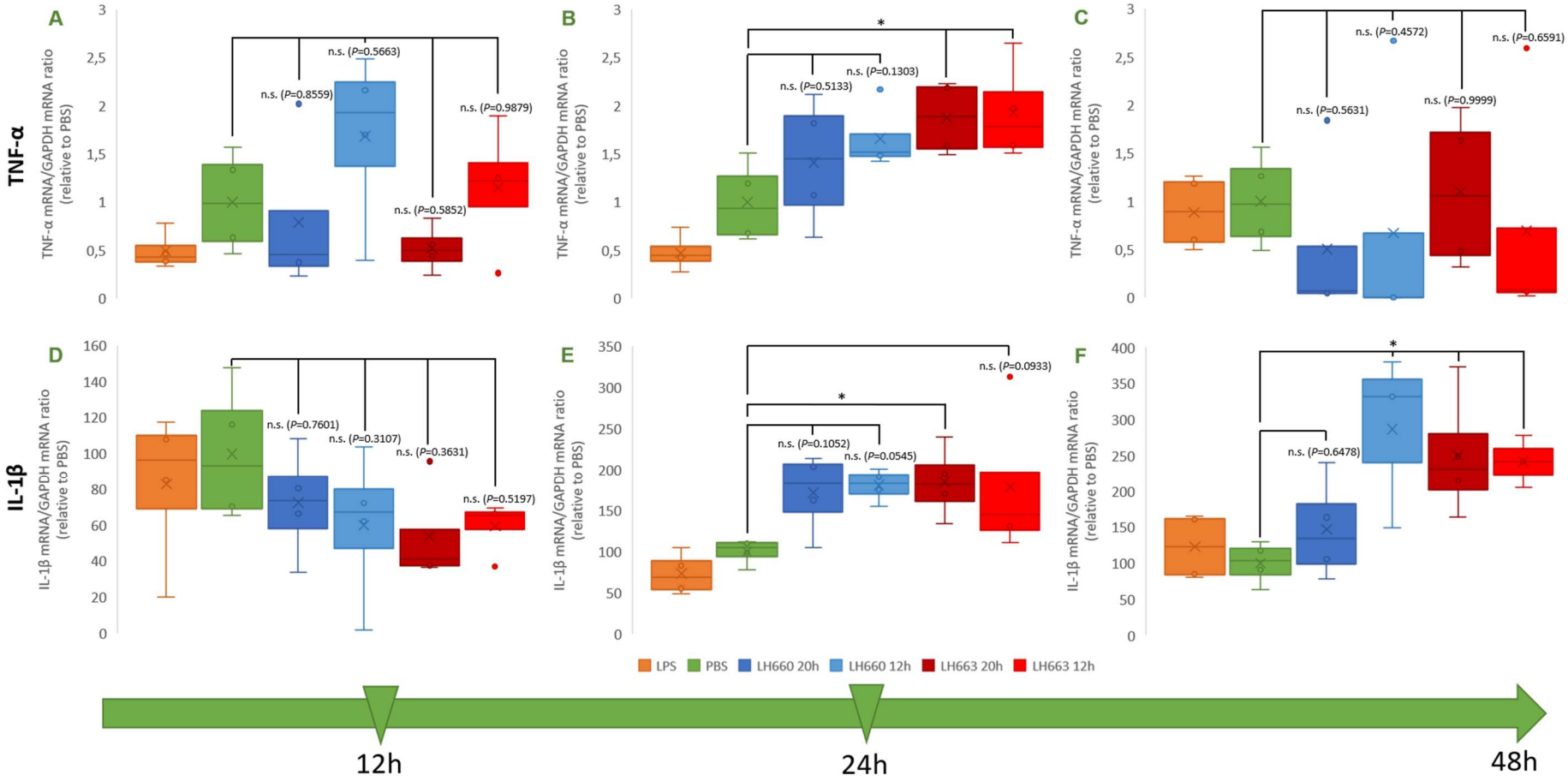


*Figure 42: Expression levels of TNF-α at 12h (A), 24h (B), and 48h (C), and IL-1β at 12h (D), 24h (E), and 48h (F) of LPS challenge in differentiated THP-1 macrophages first treated for 24h with LPS (orange) as positive control, PBS (green) as negative control, LH660 20h BEVs (dark blue), LH660 12h BEVs (light blue), LH663 20h BEVs (dark red), and LH663 12h BEVs (light red), respectively. mRNA ratios of target genes were calculated in relation to GAPDH levels in target groups compared to levels in the PBS-treated group. Boxplots show mean of each group, consisting of 4 biological and 2 technical replicates. Whiskers depict min-max values. * P ≤ 0.05 (one-way ANOVA followed by Dunnett's* post hoc *test)*

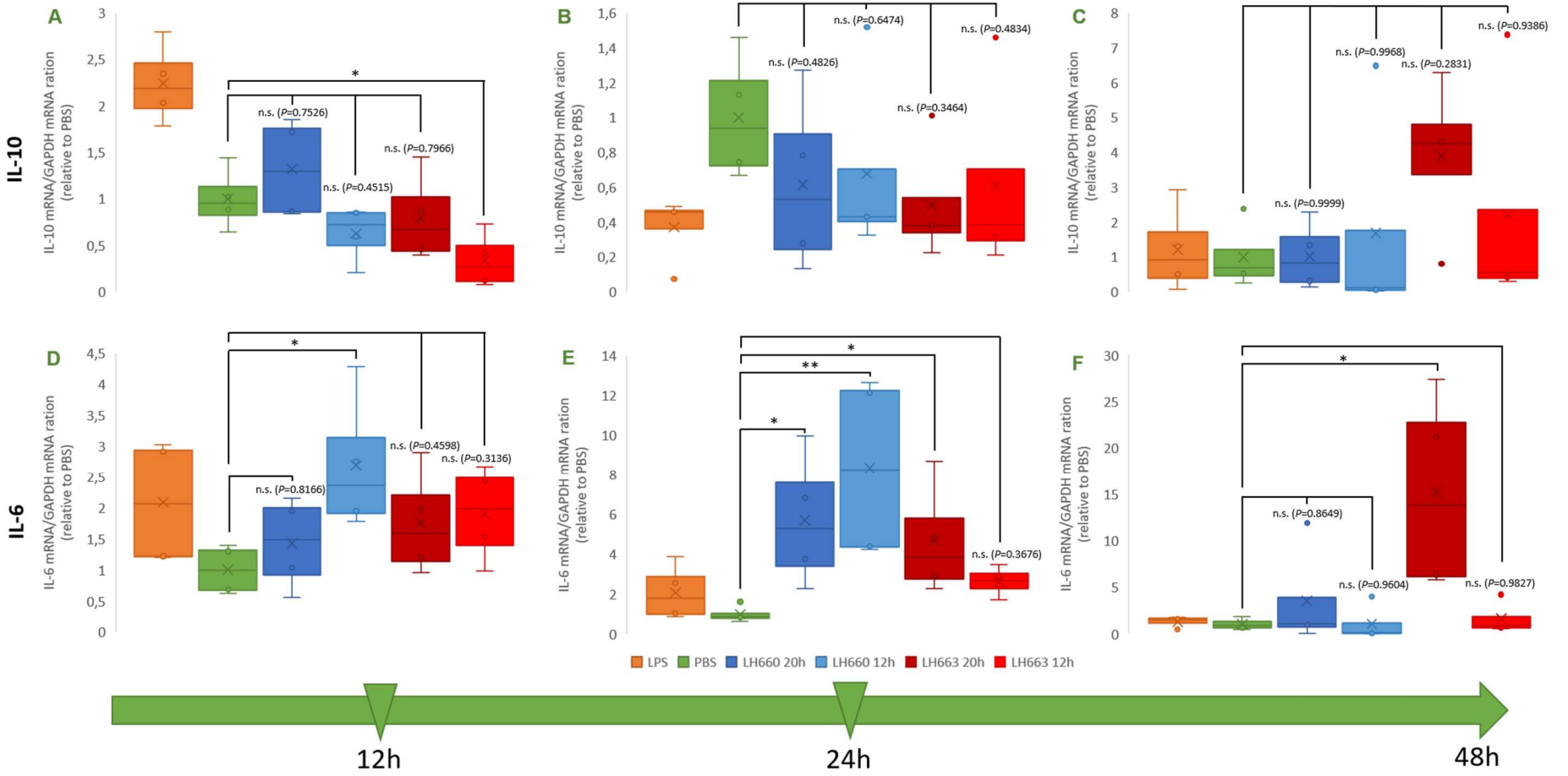


*Figure 43: Expression levels of IL-10 at 12h (A), 24h (B), and 48h (C), and IL-6 at 12h (D), 24h (E), and 48h (F) of LPS challenge in differentiated THP-1 macrophages first treated for 24h with LPS (orange) as positive control, PBS (green) as negative control, LH660 20h BEVs (dark blue), LH660 12h BEVs (light blue), LH663 20h BEVs (dark red), and LH663 12h BEVs (light red), respectively. mRNA ratios of target genes were calculated in relation to GAPDH levels in target groups compared to levels in the PBS-treated group. Boxplots show mean of each group, consisting of 4 biological and 2 technical replicates. Whiskers depict min-max values. * P ≤ 0.05, ** P ≤ 0.01 (one-way ANOVA followed by Dunnett's* post hoc *test)*

At 12h post-LPS challenge, several BEV-treated cultures showed no differences in TNF-α, IL-1β, and IL-10 expression levels compared to PBS controls. For IL-6, LH660 20h BEV-treated cells showed comparable expression to PBS ($P \geq 0.8$). Overall, at this time point, LH660 BEVs tended to produce higher mRNA levels than LH663 BEVs, although most differences were not statistically significant. Indeed, LH660 12h BEVs significantly induced IL-6 expression (Figure 43D; $P=0.0374$), while LH663 12h BEVs significantly reduced IL-10 mRNA levels (Figure 43A; $P=0.0328$). Except for IL-10 (Figure 43B), which remained lower than PBS across all BEVs, mRNA ratios generally increased after 24h of LPS challenge. At this time point, LH663 BEVs significantly ($P \leq 0.05$) stimulated TNF-α expression (Figure 42), whereas LH660 BEVs induced higher IL-6 mRNA levels( Figure 43E). IL-1β (Figure 42F) was significantly ($P=0.0475$) upregulated by LH663 20h.

By 48h post-LPS challenge, expression profiles shifted again, with most cytokine mRNA levels comparable to or lower than PBS. Interestingly, LH663 20h BEV-treated macrophages showed a tendency to synthesise more mRNA for all four cytokines than PBS, although only IL-6 (Figure 43F; $P=0.0027$) and IL-1β (Figure 42F; $P=0.0191$) reached statistical significance.

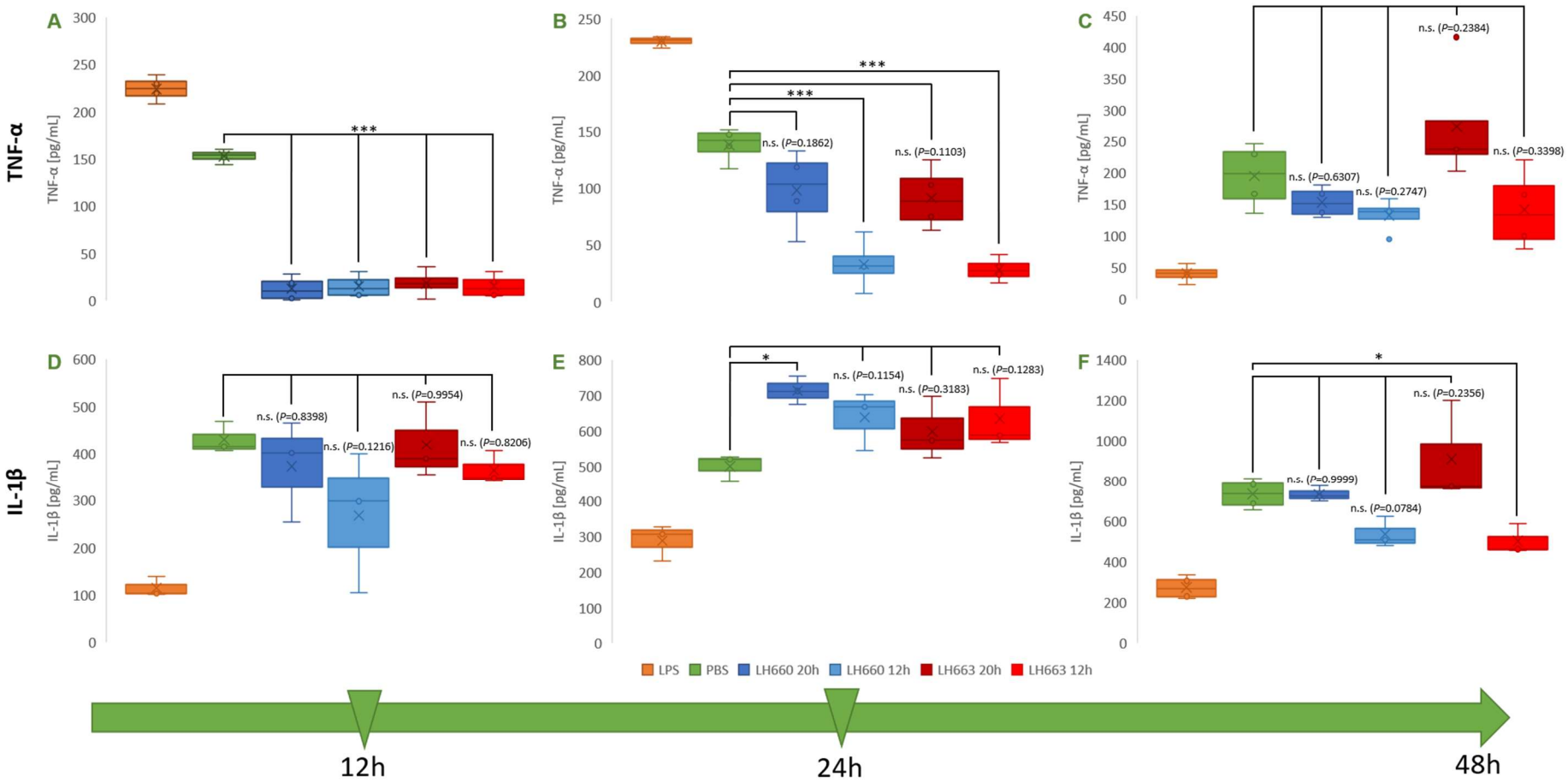


*Figure 44: Cytokine levels of TNF-α at 12h (A), 24h (B), and 48h (C), and IL-1β at 12h (D), 24h (E), and 48h (F) of LPS challenge in differentiated THP-1 macrophages first treated for 24h with LPS (orange) as positive control, PBS (green) as negative control, LH660 20h BEVs (dark blue), LH660 12h BEVs (light blue), LH663 20h BEVs (dark red), and LH663 12h BEVs (light red), respectively. Boxplots show mean of each group, consisting of 4 biological and 3 technical replicates. Whiskers depict min-max values. * P ≤ 0.05, *** P ≤ 0.001 (one-way ANOVA followed by Dunnett's* post hoc *test)*

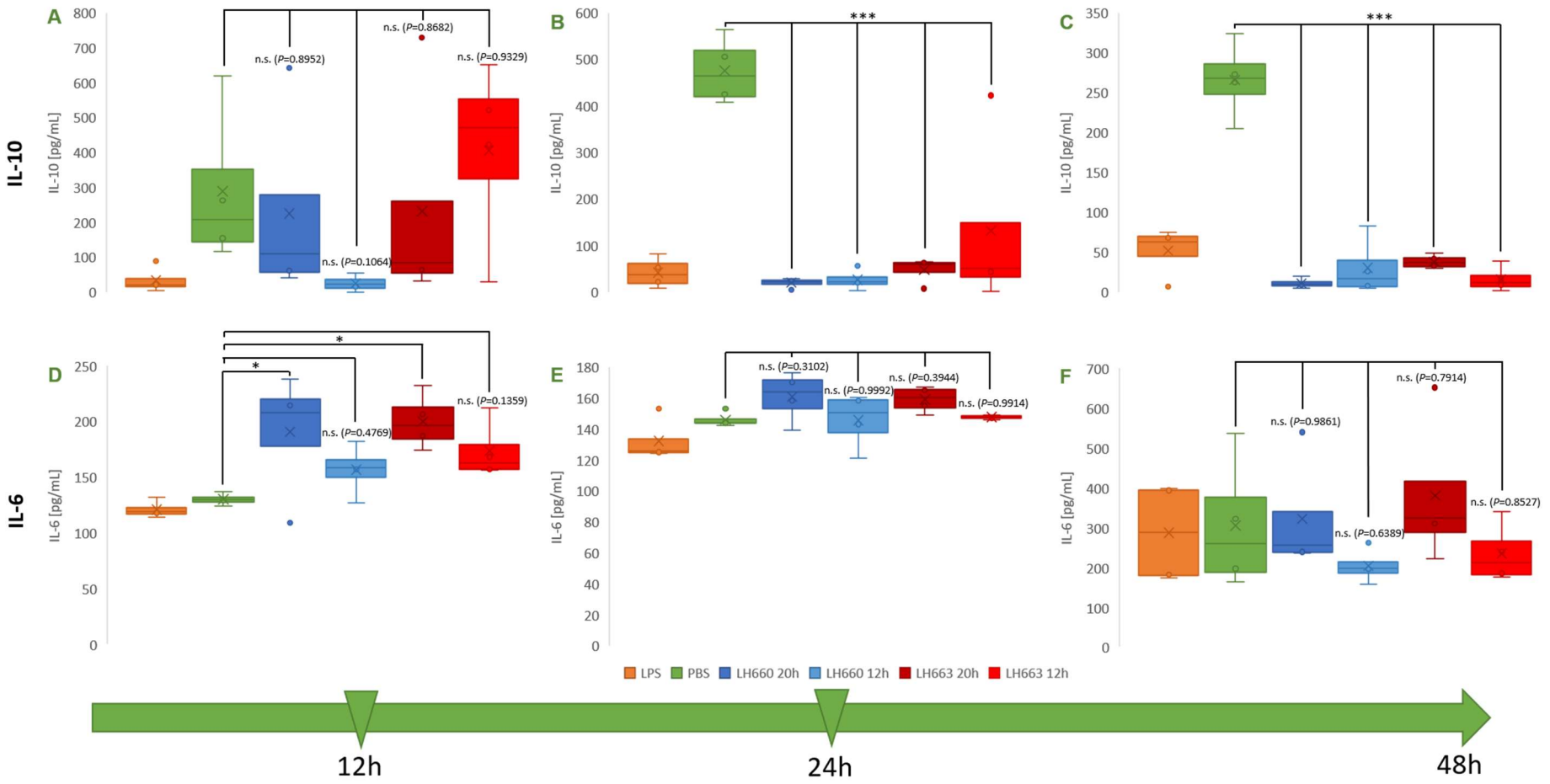


*Figure 45: Cytokine levels of IL-10 at 12h (A), 24h (B), and 48h (C), and IL-6 at 12h (D), 24h (E), and 48h (F) of LPS challenge in differentiated THP-1 macrophages first treated for 24h with LPS (orange) as positive control, PBS (green) as negative control, LH660 20h BEVs (dark blue), LH660 12h BEVs (light blue), LH663 20h BEVs (dark red), and LH663 12h BEVs (light red), respectively. Boxplots show mean of each group, consisting of 4 biological and 2 technical replicates. Whiskers depict min-max values. * P ≤ 0.05, *** P ≤ 0.001 (one-way ANOVA followed by Dunnett's* post hoc *test)*

Cytokine secretion profiles did not fully reflect expression profiles. At 12h, all tested cytokines except for IL-6 were similar to or significantly lower ($P \leq 0.001$) than PBS controls. IL-6 secretion was stimulated by all BEVs, but only 20h BEVs showed significant differences compared to PBS ($P \leq 0.05$; Figure 45D). Over time, TNF-α and IL-1β concentrations increased, yet remained comparable to PBS at 48h (Figure 44C and F). 20h BEVs generally induced higher levels than 12h preparations, while LH66312h BEVs resulted in significantly lower IL-1β than PBS ($P = 0.032$; Figure 44F). In contrast, IL-10 concentrations decreased significantly ($P \leq 0.001$) for all BEVs, starting near PBS levels at 12h and dropping below 50pg/mL by 48h (Figure 45A, B, and C). Overall, LH663 20h BEVs produced the highest cytokine concentrations at 48h, consistent with expression trends, but without statistical significance.

Interestingly, LPS controls decreased to PBS levels over time, suggesting possible immune exhaustion, affecting cytokine production but not expression levels in macrophages that had been previously challenged.

In addition to these four cytokines, IL-8 secretion was measured in differentiated THP-1 macrophages and Caco-2 cells (Figure 46). In macrophages, LH663 BEVs were more stimulatory than LH660 preparations, with LH660 BEVs eliciting significantly ($P \leq 0.05$) higher IL-8 levels than PBS at 12h post-LPS challenge, and IL-8 levels produced by LH660 12h BEV-treated cells decreased significantly ($P = 0.021$) by 48h. Conversely, IL-8 levels elicited by LH663 BEVs increased over time, reaching significantly ($P \leq 0.05$) higher concentrations at 48h, with LH663 20h BEVs inducing the highest levels (Figure 46C). In Caco-2 cells, IL-8 concentrations were generally low (≤50pg/mL) and decreased over time. LH660 and 20h BEVs were, in general, more stimulatory at 12h, but all BEV groups fell below PBS controls by 48h, with 12h preparations significantly reduced compared to PBS ($P \leq 0.05$; Figure 46F). Similar to initial BEV-treatment assays, no other cytokines were detected in Caco-2 cells.

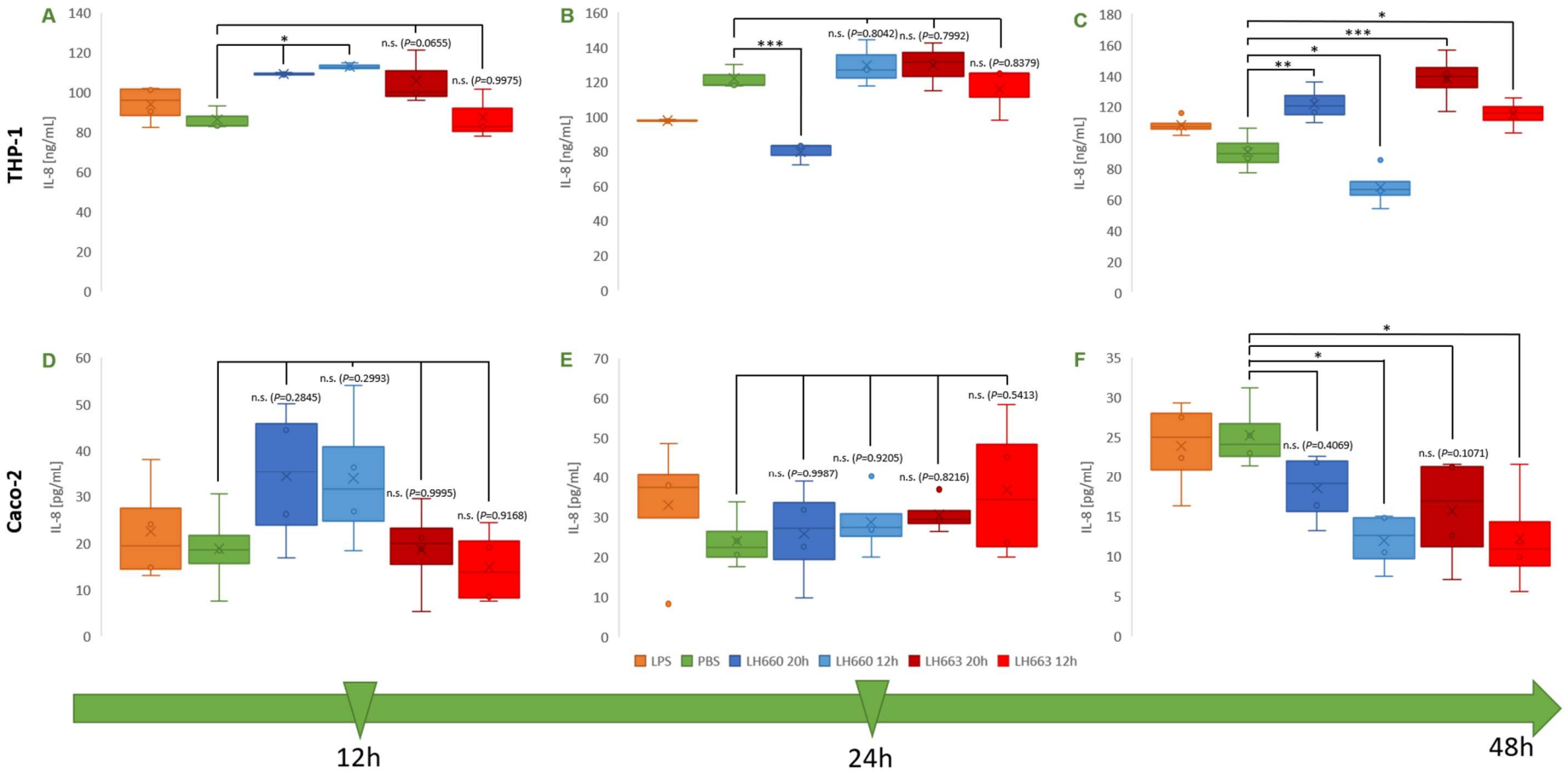


*Figure 46: Cytokine levels of IL-8 in THP-1 macrophages at 12h (A), 24h (B), and 48h (C), and in Caco-2 cells at 12h (D), 24h (E), and 48h (F) of LPS challenge first treated for 24h with LPS (orange) as positive control, PBS (green) as negative control, LH660 20h BEVs (dark blue), LH660 12h BEVs (light blue), LH663 20h BEVs (dark red), and LH663 12h BEVs (light red), respectively. Boxplots show mean of each group, consisting of 4 biological and 2 technical replicates. Whiskers depict min-max values. * P ≤ 0.05, ** P ≤ 0.01, *** P ≤ 0.001 (one-way ANOVA followed by Dunnett's* post hoc *test)*

# 5. Discussion and perspectives

## 5.1. Non-disruptive interactions of bifidobacterial BEVs with epithelial cell monolayers

### *5.1.1. Bifidobacterial BEVs modulate TJ gene expression and maintain barrier integrity*

Numerous studies have demonstrated the ability of BEVs to penetrate the mucous layer of the GIT to access and interact with underlying host cells due to their nanoscale size and unique biophysiological properties.[326–328,378] IECs form a critical physical barrier between the contents of the intestinal lumen and systemic compartments, and BEV-host interactions are increasingly recognised as key modulators that maintain GIT homeostasis.[609] However, the precise mechanisms underlying BEV biodistribution, cellular uptake, and downstream signalling remain poorly understood. Building on the hypothesis that bifidobacterial BEVs from LH660 and LH663 may exert adjuvant-like effects, I investigated their impact on epithelial barrier integrity and TJ regulation. TEER measurements, confocal imaging, qRT-PCR and immune assays were used to assess BEV uptake, intracellular localisation, TJ gene expression, and cytokine and chemokine secretion. Consistent with previous reports on commensal bacteria-derived BEVs[326,355,610–612], LH660 and LH663 BEVs did not compromise epithelial barrier integrity, in contrast to pathogen-derived bacterial products, such as LPS and BEVs.[613,614] Importantly, bifidobacterial BEVs induced expression of the key TJ genes − occludin, claudin-1, and ZO-1 − under normal conditions and appeared to support barrier integrity in an 'infection-like' (i.e. LPS-challenged) environment, in a preparation-dependent manner. This aligns with previous reports of protective effects by whole-cell *B. pseudocatenulatum* strains and their EPS against LPS-induced barrier impairment[164,604,615,616], indicating that certain bifidobacterial BEVs can maintain epithelial integrity without negatively impacting TJ structure.

While TJ expression profiles did not fully align with TEER observations, 20h BEVs stimulated TJ gene expression more strongly than 12h preparations following LPS challenge, whereas the reverse was observed under baseline conditions. This discrepancy may reflect post-translational regulation or differences in mRNA stability at the time of sampling, as TJ protein levels and subcellular localisation were not

examined in this study. Additionally, TEER phenotypes likely result from the combined action of multiple TJ and adhesion proteins, beyond the three genes assessed here.

These findings align with previous work by Hassani et al. (2021)[376], as they demonstrated that BEVs derived from B. bifidum, but not whole bacteria, activated the AhR pathway, significantly upregulating occludin and ZO-1, while failing to trigger Notch-1/Hes-1 signalling. A similar interplay between bifidobacterial strains, their BEVs, and distinct signalling pathways is also likely here. Indeed, numerous intervention studies using different Bifidobacterium species, including B. pseudocatenulatum, have reported improved epithelial barrier function under both homeostatic and inflammatory conditions through enhanced TJ expression and production.[615] Collectively, these results underscore the potential advantage of BEVs derived from probiotic strains over traditional microbial stimulants, such as LPS. Unlike pathogen-associated molecules, bifidobacterial BEVs appear to reinforce barrier integrity rather than compromise it, even under inflammatory stress. This property is particularly relevant for future *in vivo* applications, including therapeutic strategies aimed at restoring epithelial function in microbially perturbed-related disorders or leveraging BEVs as safe adjuvants to enhance mucosal vaccine responses.

### *5.1.2. Bifidobacterial BEVs access epithelial cells and accumulate in the peri-nuclear region*

Additionally, I used a lipophilic, fluorescent dye to label LH660 and LH663 BEVs to explore their epithelial uptake using confocal microscopy. Bifidobacterial BEVs accumulated in different Caco-2 cell regions across the epithelial monolayer and were found to co-localise in the cytoplasm and around the peri-nuclear membrane. Several sections also showed potential associations between BEVs and nuclear pores, although higher resolution imaging is needed to confirm this. Interestingly, similar BEV-uptake dynamics are seen in other studies. BEVs derived from *B. thetaiotaomicron* were also closely associated with the nucleus of Caco-2 cells[326], whereas *P. aeruginosa* BEVs and their DNA cargo were enriched in the nucleic fraction of epithelial cells.[617] BEVs from *Aggregatibacter actinomycetemcomitans* not only localised to the peri-nuclear space but also delivered cytolethal distending toxin into the nucleus of host cells.[617,618] Regarding whole-cell bacteria, Abdulqadir et al. (2023)[601,619] showed that administration of *B. bifidum* strains to Caco-2 cells activated PPAR-γ and led to a cyto-to-nuclear translocation in a strain-dependent manner. This gives rise to

speculation that bifidobacterial BEVs may deliver their cargo to the nucleus of epithelial cells, potentially modulating gene expression and downstream signalling, which might influence TJ gene expression.

To elicit potential uptake pathways, I treated one fraction of the epithelial cells with the endocytosis antagonist Dynasore prior to BEV administration. This antagonist blocks dynamin-dependent endocytosis. Although found to be the main driver of uptake of *B. thetaiotaomicron*-derived BEVs in IECs[326], bifidobacterial BEV endocytosis was only 1.5-fold lower than in non-treated cells. This indicates the use of different, multiple endocytosis pathways for bifidobacterial BEV uptake. Due to their size and cargo heterogeneity, selective uptake routes could mediate BEV endocytosis within the same preparation and even batch.[43,620] To date, only one study has explored endocytosis mechanisms of bifidobacterial BEVs in host cells (i.e. LL/2 lung cancer cells), identifying dynamin-mediated uptake as the main route of endocytosis.[380]

Surprisingly, administration of bifidobacterial BEVs did not lead to any increase in cytokine and chemokine secretion, except for low levels of IL-8, which contrasts with previous studies demonstrating BEV induction of IL-8, IL-6 and/or MCP-1 in epithelial cells.[575,621]

Collectively, this data suggests that BEVs derived from LH660 and LH663 can access the cytoplasm and peri-nuclear space of IECs via various endocytotic pathways. BEVs may also use passive transcellular or active, carrier-mediated paracellular or transcytosis routes to cross the epithelial barrier.[325,609,622] Furthermore, modulation of the expression of other genes (i.e. more TJ proteins and cytokines) and/or signalling molecules by IEC-incorporated bifidobacterial BEVs cannot be excluded and needs additional research.

## 5.2. Immune modulation by bifidobacterial BEVs suggests potential adjuvant-like properties

### *5.2.1. Induction of cytokine production mediating immune cell activation and polarisation*

BEVs carry a variety of microbial antigens in the form of membrane-bound MAMPs, RNA, DNA, and cytosolic proteins, lipids, and metabolites, many of which I have quantified and identified in Results Chapter II. This combination of antigen

delivery, wide biodistribution and accessibility of multifaceted stimuli can support widespread immune cell activation and specific immune responses. Established and primary cell cultures of human and murine origin were used to test the immune potentiation properties of bifidobacterial BEVs. In a monocytic reporter cell line, all tested BEVs activated the NF-κB pathway, which is essential for innate immune responses, inducing expression of distinct chemokines, cytokines, and adhesion molecules.[35] These in turn recruit and activate macrophages, granulocytes, DCs and lymphocytes, enabling pathogen containment and clearance, homeostasis, and induction of humoral immune responses.[35] The proper functioning of this complex immune network mechanism is vital for immune protection and effective vaccine responses.

Further testing for cytokine and chemokine production in different immune cells, including human monocytes, monocyte-derived macrophages, PBMCs, as well as murine splenocytes, using qRT-PCR, ELISA and MSD kits, showed expression and secretion of several pro- and anti-inflammatory cytokines for potential systemic immune activation and polarisation.

### a) TNF-α, IL-10, and IL-6 induction are dependent on environmental conditions

TNF-α, produced by splenocytes, PBMCs, monocytes, and macrophages, is a key cytokine for activation of macrophages and T cells, maturation and recruitment of DCs and leukocytes, polarisation of neutrophils towards anti-tumour N1 responses, pathogen clearance, and resistance to certain infection agents and tumours.[35,623–626] Morishita et al. (2023)[378] found that bifidobacterial BEVs, but not BEVs derived from *Lactobacillus* species, promote expression of TNF-α *in vivo*, highlighting the extensive immune-stimulatory properties of bifidobacterial BEVs compared to other commensal BEVs. However, an excess of TNF-α can have adverse effects, including induction of necrosis in healthy tissue, chronic inflammation, and autoimmune diseases.[627] Interestingly, BEVs tested here induced TNF-α production under normal growth conditions, with 20h and/or LH663 BEVs exerting stronger effects than 12h and/or LH660 preparations. In contrast, macrophages previously primed with the same BEVs displayed significantly reduced TNF-α secretion upon LPS challenge, only reaching levels comparable to untreated (PBS) controls after 48h. Again, 20h and/or LH663 BEVs tended to produce higher TNF-α concentrations than 12h and/or LH660 BEVs.

These environment-related differences in immune modulation suggest potential protective properties of bifidobacterial BEVs. A gradual increase in TNF-α rather than an abrupt surge may mitigate the risk of hyperinflammation and cytokine storm phenomenon associated with severe infections and systemic inflammatory responses.[628] Such fine-tuning of TNF-α dynamics could be particularly relevant in clinical contexts where excessive TNF-α signalling is detrimental. For instance, previous studies have shown that excessive TNF-α signalling could inhibit anti-PD-1 immunotherapy[629] in cancer models, highlighting the need for strategies that balance pro-inflammatory and regulatory responses.

Supporting this concept, a recent study demonstrated that a cocktail of BEVs derived from multiple *Bifidobacterium* strains reduced TNF-α production in a lung cancer mouse model[380], underscoring their potential as immunomodulatory agents beyond the gut. Together, these findings indicate that bifidobacterial BEVs may act as context-sensitive modulators of inflammation – stimulating immune readiness under homeostatic conditions while dampening excessive responses during infection or inflammatory stress. This dual functionality positions BEVs as promising candidates for therapeutic interventions aimed at restoring immune balance in chronic inflammatory disorders or enhancing the safety and efficacy of immunotherapies.

Other studies using other bifidobacterial BEVs or *B. pseudocatenulatum* strains found high levels of IL-6 after *in vivo* administration and/or *in vitro* treatment of macrophages under 'healthy' conditions.[377,605,607] Here, we observed that LH663 20h BEVs induced IL-6 production in splenocytes and macrophages, underlining preparation-specific differences in immune modulation. Indeed, similar to the observations for TNF-α, IL-6 secretion was strongly induced by 20h and/or LH663 BEVs than 12h and/or LH660 BEVs. IL-6 is a major pro-inflammatory cytokine responsible for differentiation of naïve $CD4^+$ T cells, Tfh cells, and $CD8^+$ T cells into Tct lymphocytes, as well as differentiation of activated B cells into antibody-producing plasma cells, making it essential for adaptive immune responses.[630] However, similar to TNF-α, excess of IL-6 can lead to the development of diseases and autoimmune conditions such as cardiac myxoma and rheumatic arthritis and needs fine-tuned regulation.[630] Moreover, IL-6 was strongly stimulated in initial BEV-treatment assays of macrophages, but, in contrast to TNF-α, decreased after exposure to LPS. IL-6 started at significantly higher levels than PBS and LPS controls at 12h post-LPS challenge and decreased progressively, reaching

comparable levels to controls by 48h, suggesting the BEV pre-conditioning may confer an early immune advantage. Future studies could investigate whether this early IL-6 surge translates into enhanced antibody production and faster pathogen clearance *in vitro* and *in vivo*.

IL-10 production followed a similar trajectory to IL-6. Under normal growth conditions, all BEVs significantly induced IL-10, but levels declined sharply in the presence of LPS. At 12h post-challenge, IL-10 concentrations were similar to PBS controls, with LH663 BEVs producing higher levels. However, at 24h and 48h, IL-10 dropped below 100pg/mL across all BEV groups, although LH663 preparations consistently maintained higher levels than LH660 BEVs. This pattern mirrors IL-10 responses observed in BEV-stimulated murine splenocytes under non-inflammatory conditions. While reduced IL-10 during infection may seem counterintuitive – given its role as a key anti-inflammatory cytokine that prevents chronic inflammation, autoimmunity, and tissue damage while supporting homeostasis[631], its suppression could reflect adjuvant-like effects of LH660 and LH663 BEVs. Excessive IL-10 can hinder pathogen clearance, particularly in intracellular infections, so limiting its production could support pathogen eradication.[632] However, IL-10 is an inflammation regulator, promoting host survival even under infectious stress, suggesting that the balance between early pro-inflammatory and later regulatory signals is crucial.[632] Studies using *in vivo* infection models preconditioned with bifidobacterial BEVs could clarify whether this modulation enhances pathogen clearance without compromising tissue protection.

Interestingly, a comparable study using BEVs from *B. thetaiotaomicron* to prime BMDCs prior to LPS challenge reported similar TNF-α and IL-6 patterns, but showed sustained IL-10 induction in both initial and pre-conditioned cultures, which was linked to a tolerance-like immune state.[353] The absence of such IL-10 persistence in this study may indicate that LH660 and LH663 BEVs favour an immunostimulatory rather than tolerance-promoting phenotype, reinforcing their potential as adjuvant candidates. This distinction highlights strain-specific differences in BEV-mediated immune modulation and underscores the need for further mechanistic studies to identify pathways driving these divergent outcomes.

### b) Stimulation of IL-1β and IL-8 is higher under normal conditions but steady following LPS challenge

LH663 BEVs and LH660 20h BEVs, but not LH660 12h BEVs, promoted the KC secretion by murine splenocytes. Initially, in human cell cultures, BEVs from both strains induced IL-8 secretion, with 12h preparations generally more stimulatory than 20h samples. However, in macrophages previously primed with BEVs and challenged with LPS, the pattern reversed: 20h preparations induced significantly higher IL-8 levels after 48h compared to 12h samples, and LH663 BEVs were consistently more potent than LH660 BEVs. Interestingly, IL-8 concentrations in LH663 BEV-treated macrophages remained steady throughout the infection-simulation assay, ranging between 100-140ng/mL, suggesting sustained chemokine signalling even under inflammatory stress. In contrast, IL-8 levels in Caco-2 cells were very low (≤50pg/mL) and either similar to or lower than PBS controls, indicating limited biological relevance in this context. This discrepancy between macrophages and epithelial cells likely reflects cell-type-specific responsiveness to BEV stimulation and the distinct roles of IL-8 in macrophages, particularly by LH663 20h BEVs, may enhance neutrophil chemotaxis and early immune activation during infection, whereas the negligible epithelial response suggests that BEVs do not promote excessive inflammatory signalling at the barrier level – a desirable feature for maintaining epithelial homeostasis. Both IL-8 and KC are major chemoattractants for neutrophils, mediating innate immune responses through antimicrobial activity and phagocytosis, elimination of cell debris, intestinal epithelial healing, anti-tumour activity and resolution of inflammation.[575] Notably, my colleague Dr Alicia Niklin from the Robinson group at QIB used LH663 20h BEVs that I prepared for her PhD project. Briefly, in a murine melanoma model, she observed decreased tumour volume due to increased cell counts and N1 anti-tumour activity of infiltrating neutrophils in LH663 20h BEV-administered mice. Fine-tuned stimulation of TNF-α and IL-8/KC production in macrophages by LH663 20h BEVs could explain these interesting observations.[633]

Under normal conditions, all BEVs also significantly induced IL-1β production by macrophages, with LH660 BEVs leading to a higher secretion than LH663 preparations. Following LPS challenge, IL-1β levels were initially comparable across all BEV groups and PBS controls at 12h, although 20h and/or LH663 BEVs tended to produce slightly higher concentrations. By 24h post-LPS challenge, IL-1β increased

more than 1.5-fold, with LH660 20h BEVs showing significant induction before PBS controls reached similar levels at 48h. Consistently, 20h and/or LH663 BEVs were more stimulatory than their counterparts. However, as PBS control levels rose between 24h and 48h, and 12h BEV-induced levels remained steady, both 12h preparations resulted in lower IL-1β than PBS at the final time point. IL-1β plays a pivotal role in DC maturation and activation, as well as facilitating CD/T cell crosstalk during immune responses. Through IL-1β signalling, pro-inflammatory cytokine release is stronger, promoting Th1 responses and cytotoxic T cell activation.[634] However, similar to TNF-α and IL-6, excessive IL-1β can lead to systemic inflammation and expansion of autoreactive $CD4^+$ T cells, contributing to tissue damage and autoimmune risk.[634] The preparation-dependent differences observed here, where 20h BEVs induced faster and stronger IL-1β responses, while 12h BEVs maintained lower levels, suggest functional divergence between BEV growth conditions. This may indicate that 20h BEVs favour rapid immune activation, whereas 12h BEVs promote a more controlled, protective response with reduced pro-inflammatory signalling. Such nuanced modulation could be advantageous for therapeutic applications: early IL-1β induction may enhance pathogen clearance and vaccine efficacy, while limiting prolonged elevation could prevent chronic inflammation. Future studies could explore whether these patterns translate into differential T cell activation and adaptive immunity *in vivo*, and whether combining BEV preparations could balance immune stimulation with regulatory control.

**c) <u>Immunomodulation varied for other tested cytokines</u>**

Similar cytokine dynamics were seen in the induction of TSLP and IL-15 production, with comparable and non-significant levels of IL-15 seen with all BEV preparations, and higher levels of TSLP in LH660 BEVs and LH663 20h BEV-treated immune cell cultures. These have direct and indirect downstream implications for T cell differentiation. TSLP acts primarily on DCs, leading to the secretion of chemokines for basophil recruitment to the lymph node and increasing expression of OX40L that drives co-stimulation in Th2 cell differentiation.[26,635,636] Additionally, TSLP suppresses the production of Th1-inducing IL-12 and CD70 in DCs mediating Th2 polarisation.[635] IL-15 supports T cell survival directly through the induction of expression of anti-apoptotic molecules.[57,58] Along with IL-7, it is also important for the survival and

homeostatic proliferation of memory CD4+ and memory CD8+ T cells and NK cells.[57,637]

Interestingly, low levels of IFN-γ and MCP-1 were induced by bifidobacterial BEVs, with no IL-1β, IL-4, IL-12p70, IL-17A or IL-22 being detected in murine splenocytes. Several studies report a significant increase in the production of IL-12p40, IL-10 and IFN-γ after administering *B. pseudocatenulatum* strains *in vivo* and/or *in vitro* to BMDCs, highlighting the strain-specific immunomodulatory properties of *Bifidobacteria* and their products.[605–607] The lack of IL-12 signal was surprising since both LH660 and LH663 were selected due to promoting IL-12 production in DCs (see Results Chapter I, page 71). However, since the BMDC experiments did not lead to any IL-12 production even in the LPS-treated groups, it is possible that these cultures lacked functional BMDCs, which are a source of IL-12p70. Additional experiments with 'working' DC cultures using a different cell isolation and preparation approach could address this issue. Also, BEVs from LH660 and LH663 may lack the microbial stimuli for IL-12 induction. Both possibilities need further investigation in more complex immune environments to be answered.

Collectively, the cytokine profile induced by bifidobacterial BEVs, especially LH663 20h BEVs, points towards an immune stimulation of innate as well as adaptive immune responses, including activation and polarisation/differentiation of key immune cells towards protective states such as anti-tumour N1 (i.e. induction of cytotoxic responses, rejection, and apoptosis to/in cancer cells, inhibition of metastasis, and promotion of further anti-tumour immune responses)[638] and Th2 responses, recruitment of specific immune cells such as neutrophils, and proliferation and survival of memory T cells and NK cells. Given the feedback loops within the complex cytokine and host cell network, it is possible that bifidobacterial BEVs could exert adjuvant-like properties in vaccination and promote protective responses in disease/cancer models (as seen in the preliminary anti-melanoma activity). Cytokine differences observed between normal and 'infection-like' (i.e., LPS-exposed) conditions highlight the dynamic, environment-dependent immunomodulatory properties of bifidobacterial BEVs. Rather than exerting uniform effects, these vesicles appear to adapt their stimulatory potential based on the surrounding immunologic context, enhancing pro-inflammatory responses under homeostatic conditions while tempering excessive activation during

LPS exposure. Such flexibility suggests that BEVs may help maintain immune balance, reducing the risk of hyperinflammation while still supporting effective pathogen clearance. Given the distinct preparation-dependent differences identified here, this opens opportunities for precision medicine, where tailored BEV formulations could be developed to meet individual therapeutic needs.

### *5.2.2. Strain-dependent stimulation of IgA production in PP/GALT cells*

IgA is a major modulator of the microbiota by coating, facilitating the clearance of microbes, and promoting the colonisation of symbionts in the intestine.[377,639–641] It is mainly secreted by PPs within the GALT of the intestinal tract after stimulation of resident immune cells with microbial antigens mediated by M cells.[377,642] These microbial antigens first trigger innate immune cells, such as macrophages, via TLR and NF-κB activation, which in turn leads to the release of IL-6 and other stimulatory activators, inducing IgA production in B cells.[377,643] During early life, IgA plays a critical role in infant health since self-production is disabled within the first month after birth and IgA is acquired maternally through breastfeeding.[85,119,644,645] Additionally, depending on exposure to health-promoting microbiota members in the maternal gut, IgA might facilitate the colonisation of microbes in the infant through the specific coating of maternal commensals, dacterial transport from the maternal intestine to the mammary gland, and finally into the child's GIT.[30,85,119,646,647] Indeed, Ding et al. (2022)[85] found that the composition of IgA-coated *Bifidobacterium* species was analogous in the faeces of tested mother-infant pairs with *B. longum* subsp. *infantis* being the most common species in infant faeces, and *B. pseudocatenulatum* being predominant in maternal breast milk and faeces.

Interestingly, oral administration of *B. longum* subsp. *infantis* strains and *B. pseudocatenulatum* JCM7041 also increases faecal IgA levels in non-breastfed infants and mice.[605,606,648,649] Moreover, Kurata et al. (2022)[377] found a direct link between the presence of lipoprotein ESBP in BEVs derived from *B. longum* subsp. *infantis* and its ability to activate PP cells in mice, leading to the production of IL-6 via TLR2 signalling in macrophages and subsequently increased release of IgA by activated B cells into the GIT.

Given the fact that the proteomic analysis of LH660 and LH663 detected ESBP in all BEVs and that they induced IL-6 production in human macrophages, I repeated the *ex*

*vivo* experiment from Kurata et al. (2022)[377] with LH660 and LH663 BEVs using murine PP/GALT fragments. Surprisingly, only LH663 20h BEVs significantly enhanced IgA secretion. This was unexpected since BEVs of LH660 had a higher abundance of ESBP than those from LH663. ESBP from LH660 may differ structurally from that in LH663 and *B. longum* subsp. *infantis.* Although LH660 BEVs significantly induced IL-6 production in human macrophages, this may be host-specific, as they did not induce biologically significant levels of IL-6 and IgA in murine cells. Indeed, in murine splenocytes, IL-6 expression was exclusively induced by LH663 BEVs, confirming that ESBP from LH660 potentially differs in structure, charge or molecular weight, and thus, lacks immunostimulatory properties. This highlights the strain-specific differences in *B. pseudocatenulatum* strains of the same origin.

Interestingly, increased secretion of IgA has recently been associated with improved outcomes in immune checkpoint blockade across several cancer models, including melanoma, where elevated IgA correlated with reduced tumour growth and enhanced infiltration of $CD8^+$ T cells.[650] In line with these findings, the significant induction of IgA observed in this study following LH663 20h BEV treatment may explain its potential anti-tumour activity. Supporting this hypothesis, my colleague Dr Alicia Niklin reported similar improvements in a melanoma mouse model upon administration of LH663 20h BEVs, including reduced tumour burden and enhanced immune infiltration. Future work could explore whether BEV-induced IgA elevation translates into improved checkpoint inhibitor efficacy and whether combining BEVs with immunotherapy could synergistically enhance tumour clearance.

## 5.3. Limitations and future work

This study provides important insights into bifidobacterial BEV-mediated modulation of epithelial barrier integrity and immune responses; however, several limitations must be addressed to fully understand their therapeutic potential.

Confocal imaging revealed BEV translocation to the peri-nuclear space of epithelial cells, suggesting active uptake and intracellular trafficking. Future work could use transcriptomic and proteomic analyses to characterise the implications of this localisation, identify specific BEV cargo, for example, nucleic acids or modulatory proteins, and determine their interactions with host receptors, as have been extensively applied to Gram-negative BEVs.[295,334,617]

Beyond epithelial monolayers, uptake dynamics could be validated in multicellular systems, such as organoids, organ-on-a-chip platforms, and in *ex vivo* or *in vivo* biodistribution assays. Biodistribution studies also need to be undertaken as a prerequisite for potential bifidobacterial BEV interventions. Previous studies have demonstrated BEV accumulation in different organs following different administration routes in healthy and disease mouse models.[326,327,651] Such experiments are not only useful for informing optimal dosing, administration routes, and intervention timing, but they may also reveal potential systemic effects. Indeed, Morishita et al. (2023) reported stronger immune stimulation in mice receiving bifidobacterial BEVs subcutaneously compared to intravenously.[378] Before progressing to *in vivo* experiments, simulating digestive conditions *in vitro* (e.g., exposure to gastric acid and bile salts) will be important to assess BEV stability and functionality.[379]

Although TJ gene expression was assessed, protein-level data may be useful to confirm underlying mechanisms. Future studies could include Western blots or ELISAs for occludin, claudin-1, and ZO-1, as well as additional TJ and adhesion proteins. Investigating bifidobacterial BEV effects on barrier recovery following chronic inflammation and/or infection is also of interest. A next step would be reversing the 'infection-mimic' challenge model: LPS challenge of differentiated Caco-2 cells and macrophages, followed by treatment with BEVs and analysing TJ and cytokine modulation, alongside TEER and viability assays.

Surprisingly, cytokine expression patterns often diverged from secretion profiles, with opposite trends observed for IL-6 between mRNA and protein levels. These differences may result from post-translational modifications, variations in mRNA and protein degradation, or secretion rates.[652] This underlines the importance of integrated transcriptomic and proteomic approaches to accurately interpret BEV-induced immune modulation.

Moreover, studies could incorporate multi-immune cell co-cultures, including T and B lymphocytes, DCs, neutrophils, and NK cells, to capture a more accurate understanding of bifidobacterial BEV-driven immunomodulation. Ultimately, *in vivo* studies would be required to determine BEV-priming effects under health, disease and vaccination contexts. These could include infection clearance assays, recovery studies, and vaccine boosting experiments, supported by multi-omics profiling,

fluorescence-activated cell sorting (FACS), and immunohistochemistry of blood, tissues, and microbiota.

Batch-dependent differences observed in this study highlight a major challenge for future BEV-based interventions. Variability in vesicle composition could lead to inconsistent immunogenicity, posing risks in therapeutic or vaccine contexts. While BEVs are generally safer than live bacteria due to their non-replicating nature, rigorous quality control and cargo characterisation are essential.

Identifying key immune stimuli (similar to the ESBP-IgA link reported by Kurata et al. (2022)[377]) and developing enrichment strategies could normalise preparations and enhance reproducibility. Comparative analysis of ESBP abundance and structural differences between LH660 and LH663 BEVs, particularly regarding TLR2 interaction, may explain the observed discrepancies in IL-6 and IgA induction. Potential association between other immunomodulatory proteins identified in the previous results chapter and the strain- and preparation-dependent differences in cytokine and TJ gene induction also need to be addressed in-depth for potential future enrichment and application assays.

BEVs from several bacterial species, including pathogens and commensals, have demonstrated strong adjuvant properties, often outperforming traditional adjuvants, such as alum or CpG DNA. For instance, Prior et al. (2021)[460] found that BEVs from *Burkholderia pseudomallei* significantly enhanced T and B cell responses and antibody titers compared to conventional adjuvants.[586] Given the immunomodulatory and barrier-protective properties of bifidobacterial BEVs, their potential as safe, microbiome-derived vaccine adjuvants is promising. Future research could focus on optimising formulations, dosing, and delivery strategies to harness these benefits in clinical settings.

## 5.4. Conclusion for further study

BEVs from *B. pseudocatenulatum* LH660 and LH663 interact with host cells and modulate protein expression and secretion in a strain-, preparation- and environment-dependent manner. Uptake studies confirmed that undifferentiated epithelial cells internalise BEVs, partly via dynamin-mediated endocytosis. In differentiated Caco-2 cells under normal conditions, all BEV preparations, except LH660 20h, stimulated

expression of occludin, claudin-1, and ZO-1, without causing barrier disruption, as indicated by TEER measurements. Under LPS-challenged conditions, TEER reduction was less pronounced in BEV-treated cells, particularly those primed with LH663 BEVs. Interestingly, both 20h preparations, but not 12h samples, induced higher TJ gene expression at 48h of LPS challenge, suggesting a growth condition-dependent effect. IL-8 secretion followed a different pattern – LH663 12h BEVs non-significantly increased IL-8 under normal conditions, whereas all BEVs led to lower IL-8 levels than PBS controls under 'infection-like' conditions, with 12h BEVs significantly reducing IL-8 at 48h, indicating context-specific chemokine modulation.

In human immune cells, bifidobacterial BEVs induced TNF-α, IL-1β, IL-6, IL-8, IL-10, IL-15, and TSLP under normal conditions, with responses varying by strain and preparation. In murine splenocytes and PPs, only LH663 BEVs stimulated KC, TNF-α, IL-6, IL-10, and IgA production. Although Kurata et al. (2022)[377] established a direct link between ESBP abundance in bifidobacterial BEVs and IL-6 and IgA induction, this correlation was not observed here, as ESBP was more abundant in LH660 BEVs, yet these did not trigger IL-6 and IgA in murine cells. Conversely, IL-6 was significantly induced by all BEVs in human macrophages, suggesting possible structural differences between ESBP and other cargo that affect receptor compatibility across species.

LPS challenge indicated marked shifts in cytokine profiles compared to normal conditions, with significantly lower IL-10 and TNF-α, but higher IL-1β and IL-8, while IL-6 remained relatively stable. Interestingly, LH663 20h BEVs generally produced the highest cytokine levels, although not always significantly. These findings demonstrate that bifidobacterial BEVs exert nuanced, environment-dependent immune modulation − enhancing barrier integrity and immune readiness under homeostasis, while tempering excessive inflammation during infection. However, these *in vitro* observations do not fully predict potential adjuvant properties in vaccination contexts or complex *in vivo* environments. Future research should focus on correlating specific BEV cargo with induced signalling pathways and validating these effects in animal models and pre-clinical settings.

# VI. CONCLUSION

The substantial health benefits associated with high levels of *Bifidobacterium* in the GIT microbiota from early life onwards are well established in the scientific literature. However, the underlying mechanisms driving these benefits are largely underexplored. This is particularly true for the role and therapeutic potential of bifidobacterial BEVs, which have only recently gained attention. This thesis investigated BEVs derived from two immunomodulatory strains of *B. pseudocatenulatum* – an understudied *Bifidobacterium* species notable for its adaptability to changing environments and broad prevalence across life stages.

To explore the potential immune responses and barrier-protective properties of BEVs from these strains, I first established optimal, standardised growth conditions and BEV-harvesting time points that coincide with the diauxic shift from Glc to starch metabolism, in order to minimise confounding factors during BEV preparation. Under identical conditions, the two strains displayed phenotypic differences in growth and vesiculogenesis. BEVs from LH663 contained higher levels of RNA and DNA, while BEVs from LH660 were enriched in protein; lipid concentrations were more uniform between BEV sets. However, batch-to-batch variations within the same condition were apparent, which also generated variation in downstream assays. This variability aligns with current challenges across the BEV field, where issues of scalability and translational readiness remain significant barriers.[273] The field would benefit from standardisation guidelines similar to those established for mammalian extracellular vesicles, as well as improved separation/purification workflows, to enhance reproducibility and inter-study comparability – even in long-term studies.[273,278,339] Furthermore, identifying subset-specific BEV biomarkers would enable flow cytometric discrimination among ambiguous BEV types within mixed preparations, improve downstream homogeneity, and ultimately define BEV type-dependent vesiculogenesis mechanisms across environmental conditions and clinical interventions.[286]

This project aimed to classify and quantify BEV cargo while assessing BEV-host cell interactions, focusing on immunomodulatory outcomes. Across morphology, concentration, particle size, and conserved proteomic features, the bifidobacterial

vesicles corresponded to key characteristics reported for BEVs.[282] Nonetheless, quantitative proteomics further underlined clear strain- and preparation-dependent differences and, while showing some similarities, diverged from previously published bifidobacterial BEV datasets in distribution of biological functions and predicted cellular location.[308,375,377] BEV cargo was predominantly cytoplasmic proteins and enriched for proteins implicated in carbohydrate metabolism and transmembrane transport. Importantly, BEVs from both strains and time points contained a large number of putative immunomodulatory proteins, such as ESBP, GAPDH, alkaline phosphatase, and glutamate synthase, with enrichment patterns varying by strain and time point. Contrary to Kurata et al. (2022)[377], however, no positive association emerged here between ESBP abundance and immune stimulation; in fact, non-stimulatory BEVs contained higher levels of ESBP than stimulatory preparations. This suggests that additional biochemical features (e.g. post-translational modifications, complexing with protein-lipid assemblies, co-packaged nucleic acids, or vesicle-surface display) may drive functional outcomes and require targeted mechanistic follow-up.

Host-interaction assays revealed that BEVs from both strains did not compromise epithelial integrity. Rather, they gained access mainly via dynamin-independent endocytic pathways to localise to the peri-nuclear space with concomitant induction of TJ gene expression of occludin, claudin-1, and ZO-1 in a strain- and preparation-dependent manner. LPS-challenged epithelial cells, pre-conditioned with bifidobacterial BEVs, yielded higher TEER measurements relative to LPS alone, consistent with a protective effect against endotoxin barrier disruption. TJ expression profiles did not fully explain these TEER dynamics; induction was BEV preparation-specific, and none of the TJ genes were significantly upregulated. Longitudinal, multi-omic profiling of BEV-primed epithelial cells under ‘healthy’ vs. ‘diseased’ conditions – integrating transcriptomics, proteomics, phosphor-signalling, and lipodomics – could clarify the temporal changes of barrier protection and support development of BEVs in personalised therapeutic scenarios.

Immunologically, BEVs exhibited stimulatory activity in a strain- and preparation-dependent manner. These BEVs activated NF-κB and induced production of TNF-α, IL-1β, IL-6, IL-8/KC, IL-10, IL-15, and TSLP, alongside low levels of IFN-γ and MCP-1, in different immune cell types under baseline conditions. Likewise, only BEVs from LH663, but not LH660, induced IgA secretion in PP/GALT cells, highlighting

phenotypic differences between strains of the same origin. Upon LPS challenge, macrophage responses shifted: TNF-α and IL-10 were generally reduced, IL-1β and IL-8 levels increased, and IL-6 was maintained. Collectively, these findings indicate that BEVs from selected *B. pseudocatenulatum* strains modulate immune cell cytokine reactions and reinforce the epithelial barrier in a condition-dependent manner, potentially protecting the host while preserving the capacity to mount appropriate antimicrobial responses.

These observations are particularly interesting in the broader context of the commensal BEV literature, which frequently emphasises anti-inflammatory skewing of various cell types, including immune cells, and its benefits. For example, BEVs from *B. thetaiotaomicron* can promote homeostasis, increasing IL-10 and reducing TNF-α in DCs via TLR2 activation.[353,472] Similarly, BEVs from *L. paracasei* and *A. muciniphila* have been reported to inhibit NF-κB, decreasing TNF-α and IL-1β, while increasing IL-10 and TGF-β.[653–655] Roughly half of the published studies on bifidobacterial BEVs report similar findings, including raised IL-10 and TGF-β production, reduced IL-1β, IL-6, TNF-α, and IL-17A, and polarisation towards regulatory phenotypes.[308,373,379–381] However, most of such studies focus on chronic inflammatory conditions, such as colitis, where reestablishing homeostasis is key. By contrast, in contexts such as vaccination and cancer therapy, controlled pro-inflammatory signalling is desirable to ensure anti-tumour and anti-pathogen efficacy while avoiding collateral damage via eliciting cytokine storms or chronic inflammation. The strain- and preparation-dependent immunomodulatory patterns identified here provide preliminary support for personalised therapy options using bifidobacterial BEVs.

Emerging evidence highlights the therapeutic potential of bifidobacterial BEVs beyond GIT homeostasis. For example, BEVs from *B. longum* subsp. *longum* have been shown to attenuate liver fibrosis, oxidative stress, suppress TGF-β1 signalling and prevent hepatocellular carcinoma development in murine models.[382] Similarly, a cocktail of bifidobacterial BEVs synergised with anti-PD-1 therapy to enhance anti-tumour efficacy via NF-κB activation, increased PD-L1, IL-2, and IFN-γ expression, and enhanced tumour-infiltrating $CD8^+$ T cells.[380] Complementing these findings, administration of LH663 20h BEVs in a mouse melanoma model demonstrated anti-tumour activity consistent with the cytokine and IgA profiles reported here.[633] This

suggests that the immunostimulatory BEV preparation characterised in this thesis retains functional activity as its parental strain and other postbiotic derivatives.[176] Moreover, these findings link to clinical and preclinical data highlighting that elevated abundance of *Bifidobacterium* species, or probiotic supplementation, slows melanoma progression.[156] BEVs offer a distinct advantage over live probiotics: they are inherently more robust, not requiring viability to confer benefits, and thus, present safer alternatives for immunocompromised populations where probiotic administration may pose risks.[656]

Coupled with recent advances in BEV modification and functionalisation, such as the versatile approach described by Morishita et al. (2024)[657] for bioengineering of bifidobacterial BEVs while preserving innate adjuvanticity, these findings position bifidobacterial BEVs as promising candidates for next-generation immunotherapies and mucosal vaccine adjuvants.[395] Their stability, cost-effectiveness and potential for needle-free delivery are practical advantages for global vaccination strategies, particularly in LMICs, where uptake and accessibility remain critical challenges. Encouragingly, commensal BEVs have already demonstrated efficacy as antigen carriers against pathogens, such as *Yersinia pestis*[337] and influenza[322], highlighting the emergence of a novel class of postbiotic adjuvants.[1]

This work provides important insights into bifidobacterial BEVs, yet several limitations and challenges remain that must be addressed before clinical translation. Batch variability in BEV yield and cargo was observed throughout this study, reflecting current technical constraints in vesicle isolation and purification and introducing variability into downstream analyses.[273] Additionally, the reliance on *in vitro* models, while valuable for mechanistic exploration, cannot fully recapitulate the complexity of host-microbiota interactions *in vivo*. A further limitation lies in the lack of causal resolution for immunomodulatory effects at the single-vesicle level, which restricts mechanistic attribution to specific cargo components and underscores the need for advanced analytical approaches.

Beyond these limitations, significant technical and biological hurdles persist. Standardisation and scalability remain critical issues, as the field currently lacks harmonised production pipelines and robust protocols for large-scale BEV generation. Long-term storage stability also poses challenges, although proteomic degradation

was mitigated here through fresh preparation and -80°C preservation, as is standard for non-bacterial EVs. Systematic optimisation of buffer composition, freeze-drying techniques, and hydrogel formulation will be essential to maintain vesicle integrity without compromising immunogenicity.

Mechanistic gaps further complicate progress, particularly concerning the regulation of bifidobacterial vesiculogenesis, discrimination of vesicle types, and identification of 'core' cargo signatures predictive of favourable immune modulation. Addressing these gaps will require integrated multi-omics strategies in different preclinical and patient contexts.

Safety and biodistribution represent additional priorities. Comprehensive mapping of BEV uptake, clearance kinetics through hepatic and renal pathways, and potential toxicity is necessary to preclude off-target effects.[339] Lessons from other probiotic BEVs highlight this need: While BEVs derived from *L. rhamnosus* GG have demonstrated benefits in colitis[658], wound healing[364], and osteoporosis[659], they have also been implicated in aggravating vascular calcification in individuals with chronic kidney disease.[660] Such findings underline the importance of systemic characterisation and downstream personalisation, even for commensal BEVs widely considered safe, to mitigate potential risks for specific populations.[339]

Building on the findings presented in this thesis, several experimental priorities have emerged to advance the mechanistic understanding and translational potential of bifidobacterial BEVs. First, functional validation of candidate immunomodulatory proteins identified in this study, such as ESBP and alkaline phosphatase, is essential to establish causal links between specific cargo components and observed immune stimulation. This could include purification of these proteins and targeted assays (e.g. more complex organoid *in vitro* assays and/or *in vivo* models of infection, vaccination and tumour growth) to confirm their role in modulating host responses. Beyond proteomics, future work could expand cargo profiling to include nucleic acids, lipids, and metabolites, as these molecules may contribute significantly to immunomodulatory activity and could reveal additional therapeutic targets. Another key aspect that was not addressed in this thesis involves assessing the influence of bifidobacterial BEVs on the GIT microbiota. Investigating their impact on microbial ecology, including SCFA production, cross-feeding networks, and pathogen suppression, would help clarify whether BEV interventions can modulate the gut-immune axis to enhance immune

responses to vaccination and/or cancer therapy. These studies should include complex faecal samples and cohorts, such as vaccine non-responders, to capture clinically relevant variability.

In summary, this thesis presents the first characterisation of BEVs derived from *B. pseudocatenulatum* strains LH660 and LH663, establishing their potential as immunomodulatory agents with relevance for vaccine development and cancer immunotherapy. The findings demonstrate that these BEVs possess key properties required for use as adjuvants and/or antigen carriers, including strain- and preparation-specific modulation of cytokine and chemokine responses, TJ regulation, and IgA induction. These insights provide a platform for future mechanistic studies and translational research, advancing the development of microbiota-derived therapeutics in precision medicine. However, challenges remain, including variability in BEV yield and cargo, reliance on simplified *in vitro* models, lack of single-vesicle mechanistic resolution, and technical hurdles in standardisation, scalability, and long-term stability. Mechanistic gaps, regarding vesiculogenesis and cargo signatures, alongside safety concerns, such as biodistribution and off-target effects, require systematic evaluation. Addressing these issues through multi-omics, advanced analytics, and validation in disease-relevant models will be critical to enable rational design of bifidobacterial BEVs as precision postbiotic adjuvants and immunotherapeutics.

# REFERENCES


1 Jordan A, Carding SR, Hall LJ. The early-life gut microbiome and vaccine efficacy. *The Lancet Microbe* 2022; **3**: e787–94.

2 Thursby E, Juge N. Introduction to the human gut microbiota. *Biochem J* 2017; **474**: 1823–36.

3 Ciabattini A, Olivieri R, Lazzeri E, Medaglini D. Role of the Microbiota in the Modulation of Vaccine Immune Responses. *Front Microbiol* 2019; **10**: 1305.

4 de Jong SE, Olin A, Pulendran B. The Impact of the Microbiome on Immunity to Vaccination in Humans. *Cell Host & Microbe* 2020; **28**: 169–79.

5 Spragge F, Bakkeren E, Jahn MT, *et al.* Microbiome diversity protects against pathogens by nutrient blocking. *Science* 2023; **382**: eadj3502.

6 Yu R, Zuo F, Ma H, Chen S. Exopolysaccharide-Producing Bifidobacterium adolescentis Strains with Similar Adhesion Property Induce Differential Regulation of Inflammatory Immune Response in Treg/Th17 Axis of DSS-Colitis Mice. *Nutrients* 2019; **11**: 782.

7 Fanning S, Hall LJ, Cronin M, *et al.* Bifidobacterial surface-exopolysaccharide facilitates commensal-host interaction through immune modulation and pathogen protection. *Proceedings of the National Academy of Sciences* 2012; **109**: 2108–13.

8 Vlasova AN, Chattha KS, Kandasamy S, *et al.* Lactobacilli and bifidobacteria promote immune homeostasis by modulating innate immune responses to human rotavirus in neonatal gnotobiotic pigs. *PLoS One* 2013; **8**: e76962.

9 Vitetta L, Saltzman E, Thomsen M, Nikov T, Hall S. Adjuvant Probiotics and the Intestinal Microbiome: Enhancing Vaccines and Immunotherapy Outcomes. *Vaccines* 2017; **5**: 50.

10 Zhao W, Ho H-E, Bunyavanich S. The gut microbiome in food allergy. *Ann Allergy Asthma Immunol* 2019; **122**: 276–82.

11 Brown EM, Kenny DJ, Xavier RJ. Gut Microbiota Regulation of T Cells During Inflammation and Autoimmunity. *Annu Rev Immunol* 2019; **37**: 599–624.

12 Nicholson JK, Holmes E, Kinross J, *et al.* Host-Gut Microbiota Metabolic Interactions. *Science* 2012; **336**: 1262–7.

13 Aron-Wisnewsky J, Warmbrunn MV, Nieuwdorp M, Clément K. Metabolism and Metabolic Disorders and the Microbiome: The Intestinal Microbiota Associated With Obesity, Lipid Metabolism, and Metabolic Health-Pathophysiology and Therapeutic Strategies. *Gastroenterology* 2021; **160**: 573–99.

14 Teng NMY, Price CA, McKee AM, Hall LJ, Robinson SD. Exploring the impact of gut microbiota and diet on breast cancer risk and progression. *Int J Cancer* 2021; published online Jan 31. DOI:10.1002/ijc.33496.

15 Routy B, Jackson T, Mählmann L, *et al.* Melanoma and microbiota: Current understanding and future directions. *Cancer Cell* 2024; **42**: 16–34.

16 Zhou C-B, Zhou Y-L, Fang J-Y. Gut Microbiota in Cancer Immune Response and Immunotherapy. *Trends Cancer* 2021; **7**: 647–60.

17 Johansson MEV, Jakobsson HE, Holmén-Larsson J, *et al.* Normalization of Host Intestinal Mucus Layers Requires Long-Term Microbial Colonization. *Cell Host Microbe* 2015; **18**: 582–92.

18 Henrick BM, Rodriguez L, Lakshmikanth T, *et al.* Bifidobacteria-mediated immune system imprinting early in life. *Cell* 2021; **184**: 3884-3898.e11.

19 Hou K, Wu Z-X, Chen X-Y, *et al.* Microbiota in health and diseases. *Signal Transduct Target Ther* 2022; **7**: 135.

20 Ostman S, Rask C, Wold AE, Hultkrantz S, Telemo E. Impaired regulatory T cell function in germ-free mice. *Eur J Immunol* 2006; **36**: 2336–46.

21 McDermott AJ, Huffnagle GB. The microbiome and regulation of mucosal immunity. *Immunology* 2014; **142**: 24–31.

22 Jamieson AM. Influence of the microbiome on response to vaccination. *Hum Vaccin Immunother* 2015; **11**: 2329–31.

23 Gay NJ, Gangloff M. Structure and function of Toll receptors and their ligands. *Annu Rev Biochem* 2007; **76**: 141–65.

24 Iwasaki A, Medzhitov R. Toll-like receptor control of the adaptive immune responses. *Nat Immunol* 2004; **5**: 987–95.

25 Geckin B, Konstantin Föhse F, Domínguez-Andrés J, Netea MG. Trained immunity: implications for vaccination. *Current Opinion in Immunology* 2022; **77**: 102190.

26 Walsh KP, Mills KHG. Dendritic cells and other innate determinants of T helper cell polarisation. *Trends in Immunology* 2013; **34**: 521–30.

27 Akira S, Uematsu S, Takeuchi O. Pathogen Recognition and Innate Immunity. *Cell* 2006; **124**: 783–801.

28 Koblansky AA, Jankovic D, Oh H, *et al.* Recognition of Profilin by Toll-like Receptor 12 Is Critical for Host Resistance to *Toxoplasma gondii*. *Immunity* 2013; **38**: 119–30.

29 Dudek AM, Martin S, Garg AD, Agostinis P. Immature, Semi-Mature, and Fully Mature Dendritic Cells: Toward a DC-Cancer Cells Interface That Augments Anticancer Immunity. *Front Immunol* 2013; **4**: 438.

30 Shvets Y, Khranovska N, Senchylo N, *et al.* Microbiota substances modulate dendritic cells activity: A critical view. *Heliyon* 2024; **0**. DOI:10.1016/j.heliyon.2024.e27125.

31 Song Y, Mehl F, Zeichner SL. Vaccine Strategies to Elicit Mucosal Immunity. *Vaccines* 2024; **12**: 191.

32 Heath WR, Kato Y, Steiner TM, Caminschi I. Antigen presentation by dendritic cells for B cell activation. *Curr Opin Immunol* 2019; **58**: 44–52.

33 Durai V, Murphy KM. Functions of Murine Dendritic Cells. *Immunity* 2016; **45**: 719–36.

34 Swiecki M, Gilfillan S, Vermi W, Wang Y, Colonna M. Plasmacytoid Dendritic Cell Ablation Impacts Early Interferon Responses and Antiviral NK and CD8+ T Cell Accrual. *Immunity* 2010; **33**: 955–66.

35 Bonizzi G, Karin M. The two NF-κB activation pathways and their role in innate and adaptive immunity. *Trends in Immunology* 2004; **25**: 280–8.

36 Chatzileontiadou DSM, Sloane H, Nguyen AT, Gras S, Grant EJ. The Many Faces of CD4+ T Cells: Immunological and Structural Characteristics. *International Journal of Molecular Sciences* 2021; **22**: 73.

37 Chen F, Liu Z, Wu W, *et al.* An essential role for TH2-type responses in limiting acute tissue damage during experimental helminth infection. *Nat Med* 2012; **18**: 260–6.

38 Rowan AG, Fletcher JM, Ryan EJ, *et al.* Hepatitis C Virus-Specific Th17 Cells Are Suppressed by Virus-Induced TGF-β1. *The Journal of Immunology* 2008; **181**: 4485–94.

39 Sonnenberg GF, Fouser LA, Artis D. Functional biology of the IL-22-IL-22R pathway in regulating immunity and inflammation at barrier surfaces. *Adv Immunol* 2010; **107**: 1–29.

40 Kumar P, Chen K, Kolls JK. Th17 cell based vaccines in mucosal immunity. *Curr Opin Immunol* 2013; **25**: 373–80.

41 Kolls JK, Khader SA. The role of Th17 cytokines in primary mucosal immunity. *Cytokine Growth Factor Rev* 2010; **21**: 443–8.

42 Mills KHG. Regulatory T cells: friend or foe in immunity to infection? *Nat Rev Immunol* 2004; **4**: 841–55.

43 Gan Y, Zhao G, Wang Z, Zhang X, Wu MX, Lu M. Bacterial Membrane Vesicles: Physiological Roles, Infection Immunology, and Applications. *Advanced Science* 2023; **10**: 2301357.

44 Coombes JL, Siddiqui KRR, Arancibia-Cárcamo CV, *et al.* A functionally specialized population of mucosal CD103+ DCs induces Foxp3+ regulatory T cells via a TGF-β– and retinoic acid–dependent mechanism. *Journal of Experimental Medicine* 2007; **204**: 1757–64.

45 Jonuleit H, Schmitt E, Schuler G, Knop J, Enk AH. Induction of interleukin 10-producing, nonproliferating CD4+ T cells with regulatory properties by repetitive stimulation with allogeneic immature human dendritic cells. *Journal of Experimental Medicine* 2000; **192**: 1213–22.

46 Luckheeram RV, Zhou R, Verma AD, Xia B. $CD4^+$T Cells: Differentiation and Functions. *Journal of Immunology Research* 2012; **2012**: e925135.

47 Milgroom MG. Vaccines, Vaccination, and Immunization. In: Milgroom MG, ed. Biology of Infectious Disease: From Molecules to Ecosystems. Cham: Springer International Publishing, 2023: 175–92.

48 Vashishtha VM, Kumar P. The durability of vaccine-induced protection: an overview. *Expert Review of Vaccines* 2024; **0**. DOI:10.1080/14760584.2024.2331065.

49 Stebegg M, Kumar SD, Silva-Cayetano A, Fonseca VR, Linterman MA, Graca L. Regulation of the Germinal Center Response. *Front Immunol* 2018; **9**: 2469.

50 Desmet CJ, Ishii KJ. Nucleic acid sensing at the interface between innate and adaptive immunity in vaccination. *Nat Rev Immunol* 2012; **12**: 479–91.

51 Pulendran B, Ahmed R. Immunological mechanisms of vaccination. *Nat Immunol* 2011; **12**: 509–17.

52 Chen Z, Gao X, Yu D. Longevity of vaccine protection: Immunological mechanism, assessment methods, and improving strategy. *VIEW* 2022; **3**: 20200103.

53 Hill A, Beitelshees M, Pfeifer BA. Vaccine Delivery and Immune Response Basics. In: Pfeifer BA, Hill A, eds. Vaccine Delivery Technology. New York, NY: Springer US, 2021: 1–8.

54 Chaplin DD. Overview of the immune response. *J Allergy Clin Immunol* 2010; **125**: S3-23.

55 Wu X, Wu P, Shen Y, Jiang X, Xu F. CD8+ Resident Memory T Cells and Viral Infection. *Front Immunol* 2018; **9**: 2093.

56 Purton JF, Tan JT, Rubinstein MP, Kim DM, Sprent J, Surh CD. Antiviral CD4+ memory T cells are IL-15 dependent. *J Exp Med* 2007; **204**: 951–61.

57 van Leeuwen EMM, Sprent J, Surh CD. Generation and maintenance of memory CD4(+) T Cells. *Curr Opin Immunol* 2009; **21**: 167–72.

58 Khaled AR, Durum SK. Lymphocide: cytokines and the control of lymphoid homeostasis. *Nat Rev Immunol* 2002; **2**: 817–30.

59 Obst R, van Santen H-M, Mathis D, Benoist C. Antigen persistence is required throughout the expansion phase of a CD4+ T cell response. *J Exp Med* 2005; **201**: 1555–65.

60 Kaech SM, Ahmed R. Memory CD8+ T cell differentiation: initial antigen encounter triggers a developmental program in naïve cells. *Nat Immunol* 2001; **2**: 415–22.

61 Messi M, Giacchetto I, Nagata K, Lanzavecchia A, Natoli G, Sallusto F. Memory and flexibility of cytokine gene expression as separable properties of human T(H)1 and T(H)2 lymphocytes. *Nat Immunol* 2003; **4**: 78–86.

62 Kartjito MS, Yosia M, Wasito E, Soloan G, Agussalim AF, Basrowi RW. Defining the Relationship of Gut Microbiota, Immunity, and Cognition in Early Life—A Narrative Review. *Nutrients* 2023; **15**: 2642.

63 Shao L, Fischer DD, Kandasamy S, Saif LJ, Vlasova AN. Tissue-specific mRNA expression profiles of porcine Toll-like receptors at different ages in germ-free and conventional pigs. *Vet Immunol Immunopathol* 2016; **171**: 7–16.

64 Salazar N, González S, Nogacka AM, *et al.* Microbiome: Effects of Ageing and Diet. *Curr Issues Mol Biol* 2020; **36**: 33–62.

65 Yatsunenko T, Rey FE, Manary MJ, *et al.* Human gut microbiome viewed across age and geography. *Nature* 2012; **486**: 222–7.

66 Rizzetto L, Fava F, Tuohy KM, Selmi C. Connecting the immune system, systemic chronic inflammation and the gut microbiome: The role of sex. *J Autoimmun* 2018; **92**: 12–34.

67 Vemuri R, Sylvia KE, Klein SL, *et al.* The microgenderome revealed: sex differences in bidirectional interactions between the microbiota, hormones, immunity and disease susceptibility. *Semin Immunopathol* 2019; **41**: 265–75.

68 Munyaka PM, Khafipour E, Ghia J-E. External influence of early childhood establishment of gut microbiota and subsequent health implications. *Front Pediatr* 2014; **2**: 109.

69 Sbihi H, Boutin RC, Cutler C, Suen M, Finlay BB, Turvey SE. Thinking bigger: How early-life environmental exposures shape the gut microbiome and influence the development of asthma and allergic disease. *Allergy* 2019; **74**: 2103–15.

70 Gaulke CA, Sharpton TJ. The influence of ethnicity and geography on human gut microbiome composition. *Nat Med* 2018; **24**: 1495–6.

71 Humberg A, Fortmann I, Siller B, *et al.* Preterm birth and sustained inflammation: consequences for the neonate. *Semin Immunopathol* 2020; **42**: 451–68.

72 Mueller NT, Bakacs E, Combellick J, Grigoryan Z, Dominguez-Bello MG. The infant microbiome development: mom matters. *Trends Mol Med* 2015; **21**: 109–17.

73 Rutayisire E, Huang K, Liu Y, Tao F. The mode of delivery affects the diversity and colonization pattern of the gut microbiota during the first year of infants' life: a systematic review. *BMC Gastroenterol* 2016; **16**: 86.

74 Guaraldi F, Salvatori G. Effect of breast and formula feeding on gut microbiota shaping in newborns. *Front Cell Infect Microbiol* 2012; **2**: 94.

75 Conlon MA, Bird AR. The impact of diet and lifestyle on gut microbiota and human health. *Nutrients* 2014; **7**: 17–44.

76 Lange K, Buerger M, Stallmach A, Bruns T. Effects of Antibiotics on Gut Microbiota. *Dig Dis* 2016; **34**: 260–8.

77 Mercer EM, Arrieta M-C. Probiotics to improve the gut microbiome in premature infants: are we there yet? *Gut Microbes* 2023; **15**: 2201160.

78 Wang X, Zhang P, Zhang X. Probiotics Regulate Gut Microbiota: An Effective Method to Improve Immunity. *Molecules* 2021; **26**: 6076.

79 Becattini S, Taur Y, Pamer EG. Antibiotic-Induced Changes in the Intestinal Microbiota and Disease. *Trends Mol Med* 2016; **22**: 458–78.

80 Walker WA, Iyengar RS. Breast milk, microbiota, and intestinal immune homeostasis. *Pediatr Res* 2015; **77**: 220–8.

81 Yakabe K, Uchiyama J, Akiyama M, Kim Y-G. Understanding Host Immunity and the Gut Microbiota Inspires the New Development of Vaccines and Adjuvants. *Pharmaceutics* 2021; **13**: 163.

82 Bäckhed F, Roswall J, Peng Y, *et al.* Dynamics and Stabilization of the Human Gut Microbiome during the First Year of Life. *Cell Host Microbe* 2015; **17**: 690–703.

83 Matamoros S, Gras-Leguen C, Le Vacon F, Potel G, de La Cochetiere M-F. Development of intestinal microbiota in infants and its impact on health. *Trends Microbiol* 2013; **21**: 167–73.

84 Weng M, Walker WA. The role of gut microbiota in programming the immune phenotype. *J Dev Orig Health Dis* 2013; **4**: 203–14.

85 Ding M, Chen H, Yu R, *et al.* Shared and Non-Shared sIgA-Coated and -Uncoated Bacteria in Intestine of Mother-Infant Pairs. *Int J Mol Sci* 2022; **23**: 9873.

86 Kordy K, Gaufin T, Mwangi M, *et al.* Contributions to human breast milk microbiome and enteromammary transfer of Bifidobacterium breve. *PLoS One* 2020; **15**: e0219633.

87 Arboleya S, Watkins C, Stanton C, Ross RP. Gut Bifidobacteria Populations in Human Health and Aging. *Front Microbiol* 2016; **7**: 1204.

88 Lawson MAE, O'Neill IJ, Kujawska M, *et al.* Breast milk-derived human milk oligosaccharides promote Bifidobacterium interactions within a single ecosystem. *ISME J* 2020; **14**: 635–48.

89 Derrien M, Alvarez A-S, de Vos WM. The Gut Microbiota in the First Decade of Life. *Trends Microbiol* 2019; **27**: 997–1010.

90 Huda MN, Ahmad SM, Alam MJ, *et al.* Bifidobacterium Abundance in Early Infancy and Vaccine Response at 2 Years of Age. *Pediatrics* 2019; **143**: e20181489.

91 Lewis ZT, Mills DA. Differential Establishment of Bifidobacteria in the Breastfed Infant Gut. *Nestle Nutr Inst Workshop Ser* 2017; **88**: 149–59.

92 Hill DL, Carr EJ, Rutishauser T, *et al.* Immune system development varies according to age, location, and anemia in African children. *Sci Transl Med* 2020; **12**: eaaw9522.

93 Miyazaki A, Kandasamy S, Michael H, *et al.* Protein deficiency reduces efficacy of oral attenuated human rotavirus vaccine in a human infant fecal microbiota transplanted gnotobiotic pig model. *Vaccine* 2018; **36**: 6270–81.

94 Korpe PS, Petri WA. Environmental enteropathy: critical implications of a poorly understood condition. *Trends Mol Med* 2012; **18**: 328–36.

95 Reyman M, van Houten MA, Watson RL, *et al.* Effects of early-life antibiotics on the developing infant gut microbiome and resistome: a randomized trial. *Nat Commun* 2022; **13**: 893.

96 Pichichero ME. Variability of vaccine responsiveness in early life. *Cellular Immunology* 2023; **393–394**: 104777.

97 Hicks LA, Taylor TH, Hunkler RJ. U.S. outpatient antibiotic prescribing, 2010. *N Engl J Med* 2013; **368**: 1461–2.

98 Madan JC, Salari RC, Saxena D, *et al.* Gut microbial colonisation in premature neonates predicts neonatal sepsis. *Arch Dis Child Fetal Neonatal Ed* 2012; **97**: F456-462.

99 Sim K, Shaw AG, Randell P, *et al.* Dysbiosis Anticipating Necrotizing Enterocolitis in Very Premature Infants. *Clinical Infectious Diseases* 2015; **60**: 389–97.

100 Manichanh C, Rigottier-Gois L, Bonnaud E, *et al.* Reduced diversity of faecal microbiota in Crohn's disease revealed by a metagenomic approach. *Gut* 2006; **55**: 205–11.

101 Zimmermann P, Messina N, Mohn WW, Finlay BB, Curtis N. Association between the intestinal microbiota and allergic sensitization, eczema, and asthma: A systematic review. *J Allergy Clin Immunol* 2019; **143**: 467–85.

102 Hufnagl K, Pali-Schöll I, Roth-Walter F, Jensen-Jarolim E. Dysbiosis of the gut and lung microbiome has a role in asthma. *Semin Immunopathol* 2020; **42**: 75–93.

103 Kim H, Sitarik AR, Woodcroft K, Johnson CC, Zoratti E. Birth Mode, Breastfeeding, Pet Exposure, and Antibiotic Use: Associations With the Gut Microbiome and Sensitization in Children. *Curr Allergy Asthma Rep* 2019; **19**: 22.

104 Faith JJ, Guruge JL, Charbonneau M, *et al.* The Long-Term Stability of the Human Gut Microbiota. *Science* 2013; **341**: 1237439.

105 Wang S, Mu L, Yu C, *et al.* Microbial collaborations and conflicts: unraveling interactions in the gut ecosystem. *Gut Microbes* 2024; **16**: 2296603.

106 Fan L, Xia Y, Wang Y, *et al.* Gut microbiota bridges dietary nutrients and host immunity. *Sci China Life Sci* 2023; **66**: 2466–514.

107 J Salvatella-Flores M, Bermúdez-Humarán LG. Malnutrition and Fragility: From Children to Elderly with Probiotics. *Arch Clin Biomed Res* 2020; **04**. DOI:10.26502/acbr.50170136.

108 Parker EPK, Bronowski C, Sindhu KNC, *et al.* Impact of maternal antibodies and microbiota development on the immunogenicity of oral rotavirus vaccine in African, Indian, and European infants. *Nat Commun* 2021; **12**: 7288.

109 Parker EP, Ramani S, Lopman BA, *et al.* Causes of impaired oral vaccine efficacy in developing countries. *Future Microbiol* 2018; **13**: 97–118.

110 Iwase SC, Osawe S, Happel A-U, *et al.* Longitudinal gut microbiota composition of South African and Nigerian infants in relation to tetanus vaccine responses. *Microbiology Spectrum* 2024; **12**: e03190-23.

111 Pan Z, Wu N, Jin C. Intestinal Microbiota Dysbiosis Promotes Mucosal Barrier Damage and Immune Injury in HIV-Infected Patients. *Canadian Journal of Infectious Diseases and Medical Microbiology* 2023; **2023**: e3080969.

112 Church JA, Rukobo S, Govha M, *et al.* The Impact of Improved Water, Sanitation, and Hygiene on Oral Rotavirus Vaccine Immunogenicity in Zimbabwean Infants: Substudy of a Cluster-randomized Trial. *Clinical Infectious Diseases* 2019; **69**: 2074–81.

113 Van Pee T, Nawrot TS, van Leeuwen R, Hogervorst J. Ambient particulate air pollution and the intestinal microbiome; a systematic review of epidemiological, *in vivo* and, *in vitro* studies. *Science of The Total Environment* 2023; **878**: 162769.

114 Collins JM, Cryan JF, OMahony SM. Chapter 2 - Importance of the Microbiota in Early Life and Influence on Future Health. In: Hyland N, Stanton C, eds. The Gut-Brain Axis (Second Edition). Academic Press, 2024: 37–76.

115 Vlasova AN, Paim FC, Kandasamy S, *et al.* Protein Malnutrition Modifies Innate Immunity and Gene Expression by Intestinal Epithelial Cells and Human Rotavirus Infection in Neonatal Gnotobiotic Pigs. *mSphere* 2017; **2**: e00046-17.

116 Zhang M, Differding MK, Benjamin-Neelon SE, Østbye T, Hoyo C, Mueller NT. Association of prenatal antibiotics with measures of infant adiposity and the gut microbiome. *Ann Clin Microbiol Antimicrob* 2019; **18**: 18.

117 Dierikx T, Berkhout D, Eck A, *et al.* Influence of timing of maternal antibiotic administration during caesarean section on infant microbial colonisation: a randomised controlled trial. *Gut* 2021; : gutjnl-2021-324767.

118 Dierikx TH, Visser DH, Benninga MA, *et al.* The influence of prenatal and intrapartum antibiotics on intestinal microbiota colonisation in infants: A systematic review. *J Infect* 2020; **81**: 190–204.

119 Rogier EW, Frantz AL, Bruno MEC, *et al.* Secretory antibodies in breast milk promote long-term intestinal homeostasis by regulating the gut microbiota and host gene expression. *Proc Natl Acad Sci U S A* 2014; **111**: 3074–9.

120 Macpherson AJ, Geuking MB, Slack E, Hapfelmeier S, McCoy KD. The habitat, double life, citizenship, and forgetfulness of IgA. *Immunol Rev* 2012; **245**: 132–46.

121 Fackelmann G, Sommer S. Microplastics and the gut microbiome: How chronically exposed species may suffer from gut dysbiosis. *Mar Pollut Bull* 2019; **143**: 193–203.

122 Naqvi A, Qadir A, Mahmood A, *et al.* Screening of human health risk to infants associated with the polychlorinated biphenyl (PCB) levels in human milk from Punjab Province, Pakistan. *Environ Sci Pollut Res* 2020; **27**: 6837–50.

123 Shin M-Y, Lee S, Kim H-J, *et al.* Polybrominated Diphenyl Ethers in Maternal Serum, Breast Milk, Umbilical Cord Serum, and House Dust in a South Korean Birth Panel of Mother-Neonate Pairs. *International Journal of Environmental Research and Public Health* 2016; **13**: 767.

124 Revich BA, Sotskov IP, Kliuev NA, *et al.* [Dioxins in the environment and in the blood and breast milk of residents of the town of Chapayevsk]. *Gig Sanit* 2001; : 6–11.

125 Song S, Ma X, Tong L, *et al.* Residue levels of hexachlorocyclohexane and dichlorodiphenyltrichloroethane in human milk collected from Beijing. *Environ Monit Assess* 2013; **185**: 7225–9.

126 Brahmand MB, Yunesian M, Nabizadeh R, Nasseri S, Alimohammadi M, Rastkari N. Evaluation of chlorpyrifos residue in breast milk and its metabolite in urine of mothers and their infants feeding exclusively by breast milk in north of Iran. *J Environ Health Sci Engineer* 2019; **17**: 817–25.

127 Srivastava S, Narvi S, Prasad S. Levels of select organophosphates in human colostrum and mature milk samples in rural region of Faizabad district, Uttar Pradesh, India. *Hum Exp Toxicol* 2011; **30**: 1458–63.

128 Tao L, Ma J, Kunisue T, Libelo EL, Tanabe S, Kannan K. Perfluorinated Compounds in Human Breast Milk from Several Asian Countries, and in Infant Formula and Dairy Milk from the United States. *Environ Sci Technol* 2008; **42**: 8597–602.

129 Lindell AE, Zimmermann-Kogadeeva M, Patil KR. Multimodal interactions of drugs, natural compounds and pollutants with the gut microbiota. *Nat Rev Microbiol* 2022; **20**: 431–43.

130 Polanco Rodríguez ÁG, Inmaculada Riba López M, Angel DelValls Casillas T, León JAA, Anjan Kumar Prusty B, Álvarez Cervera FJ. Levels of persistent organic pollutants in breast milk of Maya women in Yucatan, Mexico. *Environ Monit Assess* 2017; **189**: 59.

131 Panigrahi P. The neonatal gut microbiome and global health. *Gut Microbes* 2024; **16**: 2352175.

132 Naik NC, Holzhausen EA, Chalifour BN, *et al.* Air pollution exposure may impact the composition of human milk oligosaccharides. *Sci Rep* 2024; **14**: 6730.

133 Cabrera-Rubio R, Collado MC, Laitinen K, Salminen S, Isolauri E, Mira A. The human milk microbiome changes over lactation and is shaped by maternal weight and mode of delivery. *Am J Clin Nutr* 2012; **96**: 544–51.

134 Kuss SK, Best GT, Etheredge CA, *et al.* Intestinal Microbiota Promote Enteric Virus Replication and Systemic Pathogenesis. *Science* 2011; **334**: 249–52.

135 Kim AH, Hogarty MP, Harris VC, Baldridge MT. The Complex Interactions Between Rotavirus and the Gut Microbiota. *Front Cell Infect Microbiol* 2021; **10**. DOI:10.3389/fcimb.2020.586751.

136 Manouana GP, Kuk S, Linh LTK, *et al.* Gut microbiota in vaccine naïve Gabonese children with rotavirus A gastroenteritis. *Heliyon* 2024; **10**. DOI:10.1016/j.heliyon.2024.e28727.

137 Amaruddin AI, Hamid F, Koopman JPR, *et al.* The Bacterial Gut Microbiota of Schoolchildren from High and Low Socioeconomic Status: A Study in an Urban Area of Makassar, Indonesia. *Microorganisms* 2020; **8**: 961.

138 Ma C, Wu X, Nawaz M, *et al.* Molecular Characterization of Fecal Microbiota in Patients with Viral Diarrhea. *Curr Microbiol* 2011; **63**: 259–66.

139 Sadeghpour Heravi F, Hu H. Bifidobacterium: Host-Microbiome Interaction and Mechanism of Action in Preventing Common Gut-Microbiota-Associated Complications in Preterm Infants: A Narrative Review. *Nutrients* 2023; **15**: 709.

140 Kan Z, Luo B, Cai J, Zhang Y, Tian F, Ni Y. Genotyping and plant-derived glycan utilization analysis of Bifidobacterium strains from mother-infant pairs. *BMC Microbiol* 2020; **20**: 277.

141 Duranti S, Lugli GA, Mancabelli L, *et al.* Maternal inheritance of bifidobacterial communities and bifidophages in infants through vertical transmission. *Microbiome* 2017; **5**: 66.

142 Lanigan N, Kelly E, Arzamasov AA, Stanton C, Rodionov DA, van Sinderen D. Transcriptional control of central carbon metabolic flux in Bifidobacteria by two functionally similar, yet distinct LacI-type regulators. *Sci Rep* 2019; **9**: 17851.

143 Salazar N, Gueimonde M, Hernández-Barranco AM, Ruas-Madiedo P, de los Reyes-Gavilán CG. Exopolysaccharides Produced by Intestinal Bifidobacterium Strains Act as Fermentable Substrates for Human Intestinal Bacteria. *AEM* 2008; **74**: 4737–45.

144 Abdelhamid AG, Esaam A, Hazaa MM. Cell free preparations of probiotics exerted antibacterial and antibiofilm activities against multidrug resistant E. coli. *Saudi Pharm J* 2018; **26**: 603–7.

145 Hidalgo-Cantabrana C, López P, Gueimonde M, *et al.* Immune Modulation Capability of Exopolysaccharides Synthesised by Lactic Acid Bacteria and Bifidobacteria. *Probiotics & Antimicro Prot* 2012; **4**: 227–37.

146 Cheng CC, Duar RM, Lin X, *et al.* Ecological Importance of Cross-Feeding of the Intermediate Metabolite 1,2-Propanediol between Bacterial Gut Symbionts. *Applied and Environmental Microbiology* 2020; **86**: e00190-20.

147 Kondepudi KK, Ambalam P, Nilsson I, Wadström T, Ljungh A. Prebiotic-non-digestible oligosaccharides preference of probiotic bifidobacteria and antimicrobial activity against Clostridium difficile. *Anaerobe* 2012; **18**: 489–97.

148 Lin C, Lin Y, Wang S, *et al.* Bifidobacterium animalis subsp. lactis boosts neonatal immunity: unravelling systemic defences against Salmonella. *Food Funct* 2024; **15**: 236–54.

149 Vlasova AN, Takanashi S, Miyazaki A, Rajashekara G, Saif LJ. How the gut microbiome regulates host immune responses to viral vaccines. *Current Opinion in Virology* 2019; **37**: 16–25.

150 Rabe H, Lundell A-C, Sjöberg F, *et al.* Neonatal gut colonization by Bifidobacterium is associated with higher childhood cytokine responses. *Gut Microbes* 2020; **12**: 1–14.

151 Wu B-B, Yang Y, Xu X, Wang W-P. Effects of Bifidobacterium supplementation on intestinal microbiota composition and the immune response in healthy infants. *World J Pediatr* 2016; **12**: 177–82.

152 Ma L, Zheng A, Ni L, *et al.* Bifidobacterium animalis subsp. lactis lkm512 Attenuates Obesity-Associated Inflammation and Insulin Resistance Through the Modification of Gut Microbiota in High-Fat Diet-Induced Obese Mice. *Mol Nutr Food Res* 2022; **66**: e2100639.

153 Wang M, Li M, Wu S, *et al.* Fecal Microbiota Composition of Breast-Fed Infants Is Correlated With Human Milk Oligosaccharides Consumed. *Journal of Pediatric Gastroenterology and Nutrition* 2015; **60**: 825–33.

154 Pareek S, Kurakawa T, Das B, *et al.* Comparison of Japanese and Indian intestinal microbiota shows diet-dependent interaction between bacteria and fungi. *npj Biofilms and Microbiomes* 2019; **5**: 1–13.

155 Zhou L, Yin X, Fang B, *et al.* Effects of Bifidobacterium animalis subsp. lactis IU100 on Immunomodulation and Gut Microbiota in Immunosuppressed Mice. *Microorganisms* 2024; **12**: 493.

156 Sivan A, Corrales L, Hubert N, *et al.* Commensal Bifidobacterium promotes antitumor immunity and facilitates anti–PD-L1 efficacy. *Science* 2015; **350**: 1084–9.

157 Shinha H a. N, Kyunghae CHO, Chong-Kil LEE, *et al.* Enhancement of Antigen Presentation Capability of Dendritic Cells and Activation of Macrophages by the Components of Bifidobacterium pseudocatenulatum SPM 1204. *Biomolecules & Therapeutics* 2005; **13**: 174–80.

158 Young SL, Simon MA, Baird MA, *et al.* Bifidobacterial species differentially affect expression of cell surface markers and cytokines of dendritic cells harvested from cord blood. *Clin Diagn Lab Immunol* 2004; **11**: 686–90.

159 Wu Q, Li W, Kwok L-Y, Lv H, Sun J, Sun Z. Regional variation and adaptive evolution in Bifidobacterium pseudocatenulatum: Insights into genomic and functional diversity in human gut. *Food Res Int* 2024; **192**: 114840.

160 Sanchez-Gallardo R, Bottacini F, Friess L, *et al.* Unveiling metabolic pathways of selected plant-derived glycans by Bifidobacterium pseudocatenulatum. *Front Microbiol* 2024; **15**. DOI:10.3389/fmicb.2024.1414471.

161 Sanchez-Gallardo R, Bottacini F, O'Neill IJ, *et al.* Selective human milk oligosaccharide utilization by members of the Bifidobacterium pseudocatenulatum taxon. *Applied and Environmental Microbiology* 2024; **90**: e00648-24.

162 Zeng Q, Qi Z, He X, *et al.* Bifidobacterium pseudocatenulatum NCU-08 ameliorated senescence via modulation of the AMPK/Sirt1 signaling pathway and gut microbiota in mice. *Food Funct* 2024; **15**: 4095–108.

163 Chung The H, Nguyen Ngoc Minh C, Tran Thi Hong C, *et al.* Exploring the Genomic Diversity and Antimicrobial Susceptibility of Bifidobacterium pseudocatenulatum in a Vietnamese Population. *Microbiol Spectr* 2021; **9**: e0052621.

164 Sun Y, Zhou J, Du H, *et al.* The Anti-inflammatory Potential of a Strain of Probiotic Bifidobacterium pseudocatenulatum G7: In Vitro and In Vivo Evidence. *J Agric Food Chem* 2024; **72**: 10355–65.

165 Wang H, Lu F, Feng X, *et al.* Characterization of a novel antioxidant exopolysaccharide from an intestinal-originated bacteria *Bifidobacterium pseudocatenulatum* Bi-OTA128. *Microbiological Research* 2024; **289**: 127914.

166 Fang D, Shi D, Lv L, *et al.* Bifidobacterium pseudocatenulatum LI09 and Bifidobacterium catenulatum LI10 attenuate D-galactosamine-induced liver injury by modifying the gut microbiota. *Sci Rep* 2017; **7**: 8770.

167 Moya-Pérez A, Perez-Villalba A, Benítez-Páez A, Campillo I, Sanz Y. Bifidobacterium CECT 7765 modulates early stress-induced immune, neuroendocrine and behavioral alterations in mice. *Brain Behav Immun* 2017; **65**: 43–56.

168 Wu G, Zhang C, Wu H, *et al.* Genomic Microdiversity of Bifidobacterium pseudocatenulatum Underlying Differential Strain-Level Responses to Dietary Carbohydrate Intervention. *mBio* 2017; **8**: e02348-16.

169 Wu H, Li Y, Jiang Y, *et al.* Machine learning prediction of obesity-associated gut microbiota: identifying Bifidobacterium pseudocatenulatum as a potential therapeutic target. *Front Microbiol* 2025; **15**. DOI:10.3389/fmicb.2024.1488656.

170 Lin G, Zhang B, Qu Z, *et al.* Galactooligosaccharide-Metabolism-Related Genes of Bifidobacterium pseudocatenulatum Contribute to the Regulation of Glucose and Lipid Metabolism in Type 2 Diabetic Mice. *J Agric Food Chem* 2025; **73**: 1855–73.

171 Zha A, Qi M, Deng Y, *et al.* Gut Bifidobacterium pseudocatenulatum protects against fat deposition by enhancing secondary bile acid biosynthesis. *iMeta* 2024; **3**: e261.

172 Zhao L, Zhang F, Ding X, *et al.* Gut bacteria selectively promoted by dietary fibers alleviate type 2 diabetes. *Science* 2018; **359**: 1151–6.

173 Cano PG, Santacruz A, Trejo FM, Sanz Y. Bifidobacterium CECT 7765 improves metabolic and immunological alterations associated with obesity in high-fat diet-fed mice. *Obesity (Silver Spring)* 2013; **21**: 2310–21.

174 Lin G, Liu Q, Wang L, *et al.* The Comparative Analysis of Genomic Diversity and Genes Involved in Carbohydrate Metabolism of Eighty-Eight Bifidobacterium pseudocatenulatum Isolates from Different Niches of China. *Nutrients* 2022; **14**: 2347.

175 Shani G, Hoeflinger JL, Heiss BE, *et al.* Fucosylated Human Milk Oligosaccharide Foraging within the Species Bifidobacterium pseudocatenulatum Is Driven by Glycosyl Hydrolase Content and Specificity. *Appl Environ Microbiol* 2022; **88**: e0170721.

176 Price CA, Nicklin A, Kujawska M, *et al.* Bifidobacterium pseudocatenulatum capsular exopolysaccharide enhances systemic anti-tumour immunity in pre-clinical breast cancer. 2024; : 2024.09.23.614466.

177 Foligne B, Zoumpopoulou G, Dewulf J, *et al.* A Key Role of Dendritic Cells in Probiotic Functionality. *PLoS One* 2007; **2**: e313.

178 Gibson GR, Hutkins R, Sanders ME, *et al.* Expert consensus document: The International Scientific Association for Probiotics and Prebiotics (ISAPP) consensus statement on the definition and scope of prebiotics. *Nat Rev Gastroenterol Hepatol* 2017; **14**: 491–502.

179 Bouhnik Y, Raskine L, Simoneau G, *et al.* The capacity of nondigestible carbohydrates to stimulate fecal bifidobacteria in healthy humans: a double-blind, randomized, placebo-controlled, parallel-group, dose-response relation study2. *The American Journal of Clinical Nutrition* 2004; **80**: 1658–64.

180 Yen C-H, Tseng Y-H, Kuo Y-W, Lee M-C, Chen H-L. Long-term supplementation of isomalto-oligosaccharides improved colonic microflora profile, bowel function, and blood cholesterol levels in constipated elderly people—A placebo-controlled, diet-controlled trial. *Nutrition* 2011; **27**: 445–50.

181 Matsuzaki C, Takagi H, Saiga S, *et al.* Prebiotic effect of galacto- *N* -biose on the intestinal lactic acid bacteria as enhancer of acetate production and hypothetical colonization. *Appl Environ Microbiol* 2024; : e01445-23.

182 Fu X, Liu Z, Zhu C, Mou H, Kong Q. Nondigestible carbohydrates, butyrate, and butyrate-producing bacteria. *Crit Rev Food Sci Nutr* 2019; **59**: S130–52.

183 Zhang H, Qin S, Zhang X, *et al.* Dietary resistant starch alleviates Escherichia coli-induced bone loss in meat ducks by promoting short-chain fatty acid production and inhibiting Malt1/NF-κB inflammasome activation. *J Animal Sci Biotechnol* 2022; **13**: 92.

184 Miles M, Grantham M, Walton KLW. Effects of Prebiotic Fructooligosaccharides on Cytokine and Tight Junction Protein Expression in Cultured Intestinal Epithelial Cells. *The FASEB Journal* 2022; **36**: fasebj.2022.36.S1.R5484.

185 FAO/WHO. Evaluation of health and nutritional properties of powder milk and live lactic acid bacteria. *Report from FAO/WHO Expert Consultation* 2001; : 1–4.

186 Paineau D, Carcano D, Leyer G, *et al.* Effects of seven potential probiotic strains on specific immune responses in healthy adults: a double-blind, randomized, controlled trial. *FEMS Immunology & Medical Microbiology* 2008; **53**: 107–13.

187 Herfel TM, Jacobi SK, Lin X, *et al.* Dietary supplementation of Bifidobacterium longum strain AH1206 increases its cecal abundance and elevates intestinal interleukin-10 expression in the neonatal piglet. *Food Chem Toxicol* 2013; **60**: 116–22.

188 Kandasamy S, Chattha KS, Vlasova AN, Rajashekara G, Saif LJ. Lactobacilli and Bifidobacteria enhance mucosal B cell responses and differentially modulate systemic antibody responses to an oral human rotavirus vaccine in a neonatal gnotobiotic pig disease model. *Gut Microbes* 2014; **5**: 639–51.

189 Ishizuka T, Kanmani P, Kobayashi H, *et al.* Immunobiotic Bifidobacteria Strains Modulate Rotavirus Immune Response in Porcine Intestinal Epitheliocytes via Pattern Recognition Receptor Signaling. *PLoS One* 2016; **11**: e0152416.

190 Mandal S, Mondal C, Lyndem LM. Probiotics: an alternative anti-parasite therapy. *J Parasit Dis* 2024; published online May 13. DOI:10.1007/s12639-024-01680-4.

191 Fawzy IM, ElGindy EM, Abdel-Samie O, Aly H. Probiotic therapy in patients with irritable bowel syndrome: does it have a real role? *The Egyptian Journal of Internal Medicine* 2021; **33**: 20.

192 Mao N, Cubillos-Ruiz A, Cameron DE, Collins JJ. Probiotic strains detect and suppress cholera in mice. *Sci Transl Med* 2018; **10**: eaao2586.

193 Wastnedge E, Waters D, Murray SR, *et al.* Interventions to reduce preterm birth and stillbirth, and improve outcomes for babies born preterm in low- and middle-income countries: A systematic review. *J Glob Health* 2021; **11**: 04050.

194 Šmid A, Strniša L, Bajc K, Vujić-Podlipec D, Bogovič Matijašić B, Rogelj I. Randomized clinical trial: The effect of fermented milk with the probiotic cultures *Lactobacillus acidophilus La-5*® and *Bifidobacterium BB-12*® and Beneo dietary fibres on health-related quality of life and the symptoms of irritable bowel syndrome in adults. *Journal of Functional Foods* 2016; **24**: 549–57.

195 Larke JA, Heiss BE, Ehrlich AM, *et al.* Milk oligosaccharide-driven persistence of Bifidobacterium pseudocatenulatum modulates local and systemic microbial metabolites upon synbiotic treatment in conventionally colonized mice. *Microbiome* 2023; **11**: 194.

196 Salminen S, Collado MC, Endo A, *et al.* The International Scientific Association of Probiotics and Prebiotics (ISAPP) consensus statement on the definition and scope of postbiotics. *Nat Rev Gastroenterol Hepatol* 2021; **18**: 649–67.

197 Ayechu-Muruzabal V, Xiao L, Wehkamp T, *et al.* A Fermented Milk Matrix Containing Postbiotics Supports Th1- and Th17-Type Immunity In Vitro and Modulates the Influenza-Specific Vaccination Response In Vivo in Association with Altered Serum Galectin Ratios. *Vaccines (Basel)* 2021; **9**: 254.

198 Ozma MA, Moaddab SR, Hosseini H, *et al.* A critical review of novel antibiotic resistance prevention approaches with a focus on postbiotics. *Crit Rev Food Sci Nutr* 2023; : 1–19.

199 Morales-Ferré C, Azagra-Boronat I, Massot-Cladera M, *et al.* Effects of a Postbiotic and Prebiotic Mixture on Suckling Rats' Microbiota and Immunity. *Nutrients* 2021; **13**: 2975.

200 Morales-Ferré C, Azagra-Boronat I, Massot-Cladera M, *et al.* Preventive Effect of a Postbiotic and Prebiotic Mixture in a Rat Model of Early Life Rotavirus Induced-Diarrhea. *Nutrients* 2022; **14**: 1163.

201 Chénard T, Prévost K, Dubé J, Massé E. Immune System Modulations by Products of the Gut Microbiota. *Vaccines (Basel)* 2020; **8**. DOI:10.3390/vaccines8030461.

202 Fushinobu S. Unique sugar metabolic pathways of bifidobacteria. *Biosci Biotechnol Biochem* 2010; **74**: 2374–84.

203 Smith PM, Howitt MR, Panikov N, *et al.* The microbial metabolites, short-chain fatty acids, regulate colonic Treg cell homeostasis. *Science* 2013; **341**: 569–73.

204 Fukuda S, Toh H, Hase K, *et al.* Bifidobacteria can protect from enteropathogenic infection through production of acetate. *Nature* 2011; **469**: 543–7.

205 Stewart CJ. Breastfeeding promotes bifidobacterial immunomodulatory metabolites. *Nat Microbiol* 2021; **6**: 1335–6.

206 Macia L, Tan J, Vieira AT, *et al.* Metabolite-sensing receptors GPR43 and GPR109A facilitate dietary fibre-induced gut homeostasis through regulation of the inflammasome. *Nat Commun* 2015; **6**: 6734.

207 Wu W, Sun M, Chen F, *et al.* Microbiota metabolite short-chain fatty acid acetate promotes intestinal IgA response to microbiota which is mediated by GPR43. *Mucosal Immunol* 2017; **10**: 946–56.

208 Kim CH, Park J, Kim M. Gut Microbiota-Derived Short-Chain Fatty Acids, T Cells, and Inflammation. *Immune Netw* 2014; **14**: 277.

209 Vinolo MAR, Ferguson GJ, Kulkarni S, *et al.* SCFAs induce mouse neutrophil chemotaxis through the GPR43 receptor. *PLoS One* 2011; **6**: e21205.

210 Carretta MD, Conejeros I, Hidalgo MA, Burgos RA. Propionate induces the release of granules from bovine neutrophils. *J Dairy Sci* 2013; **96**: 2507–20.

211 Kim MH, Kang SG, Park JH, Yanagisawa M, Kim CH. Short-chain fatty acids activate GPR41 and GPR43 on intestinal epithelial cells to promote inflammatory responses in mice. *Gastroenterology* 2013; **145**: 396-406.e1-10.

212 Mosca F, Gianni ML, Rescigno M. Can Postbiotics Represent a New Strategy for NEC? 2019; **1125**: 37–45.

213 Morniroli D, Vizzari G, Consales A, Mosca F, Giannì ML. Postbiotic Supplementation for Children and Newborn's Health. *Nutrients* 2021; **13**: 781.

214 Tsilingiri K, Rescigno M. Postbiotics: what else? *Beneficial Microbes* 2013; **4**: 101–7.

215 Sánchez B, Urdaci MC, Margolles A. Extracellular proteins secreted by probiotic bacteria as mediators of effects that promote mucosa-bacteria interactions. *Microbiology (Reading)* 2010; **156**: 3232–42.

216 Heiss BE, Ehrlich AM, Maldonado-Gomez MX, *et al.* Bifidobacterium catabolism of human milk oligosaccharides overrides endogenous competitive exclusion driving colonization and protection. *Gut Microbes* 2021; **13**: 1986666.

217 Krishnan S, Ding Y, Saedi N, *et al.* Gut Microbiota-Derived Tryptophan Metabolites Modulate Inflammatory Response in Hepatocytes and Macrophages. *Cell Rep* 2018; **23**: 1099–111.

218 Zimmermann P, Curtis N. The influence of probiotics on vaccine responses – A systematic review. *Vaccine* 2018; **36**: 207–13.

219 Akatsu H. Exploring the Effect of Probiotics, Prebiotics, and Postbiotics in Strengthening Immune Activity in the Elderly. *Vaccines* 2021; **9**: 136.

220 Yeh T-L, Shih P-C, Liu S-J, *et al.* The influence of prebiotic or probiotic supplementation on antibody titers after influenza vaccination: a systematic review and meta-analysis of randomized controlled trials. *DDDT* 2018; **Volume 12**: 217–30.

221 Kazemifard N, Dehkohneh A, Baradaran Ghavami S. Probiotics and probiotic-based vaccines: A novel approach for improving vaccine efficacy. *Front Med (Lausanne)* 2022; **9**: 940454.

222 Soh SE, Ong DQR, Gerez I, *et al.* Effect of probiotic supplementation in the first 6 months of life on specific antibody responses to infant Hepatitis B vaccination. *Vaccine* 2010; **28**: 2577–9.

223 Kukkonen K, Nieminen T, Poussa T, Savilahti E, Kuitunen M. Effect of probiotics on vaccine antibody responses in infancy--a randomized placebo-controlled double-blind trial. *Pediatr Allergy Immunol* 2006; **17**: 416–21.

224 Mullié C, Yazourh A, Thibault H, *et al.* Increased poliovirus-specific intestinal antibody response coincides with promotion of Bifidobacterium longum-infantis and Bifidobacterium breve in infants: a randomized, double-blind, placebo-controlled trial. *Pediatr Res* 2004; **56**: 791–5.

225 Youngster I, Kozer E, Lazarovitch Z, Broide E, Goldman M. Probiotics and the immunological response to infant vaccinations: a prospective, placebo controlled pilot study. *Arch Dis Child* 2011; **96**: 345–9.

226 West CE, Gothefors L, Granström M, Käyhty H, Hammarström M-LKC, Hernell O. Effects of feeding probiotics during weaning on infections and antibody responses to diphtheria, tetanus and Hib vaccines. *Pediatr Allergy Immunol* 2008; **19**: 53–60.

227 Isolauri E, Joensuu J, Suomalainen H, Luomala M, Vesikari T. Improved immunogenicity of oral D x RRV reassortant rotavirus vaccine by Lactobacillus casei GG. *Vaccine* 1995; **13**: 310–2.

228 Holscher HD, Czerkies LA, Cekola P, *et al.* Bifidobacterium lactis Bb12 enhances intestinal antibody response in formula-fed infants: a randomized, double-blind, controlled trial. *JPEN J Parenter Enteral Nutr* 2012; **36**: 106S-17S.

229 Matsuda F, Chowdhury MI, Saha A, *et al.* Evaluation of a probiotics, Bifidobacterium breve BBG-01, for enhancement of immunogenicity of an oral inactivated cholera vaccine and safety: a randomized, double-blind, placebo-controlled trial in Bangladeshi children under 5 years of age. *Vaccine* 2011; **29**: 1855–8.

230 Pérez N, Iannicelli JC, Girard-Bosch C, *et al.* Effect of probiotic supplementation on immunoglobulins, isoagglutinins and antibody response in children of low socio-economic status. *Eur J Nutr* 2010; **49**: 173–9.

231 Licciardi PV, Ismail IH, Balloch A, *et al.* Maternal Supplementation with LGG Reduces Vaccine-Specific Immune Responses in Infants at High-Risk of Developing Allergic Disease. *Front Immunol* 2013; **4**. DOI:10.3389/fimmu.2013.00381.

232 Redondo N, Nova E, Gheorghe A, Díaz LE, Hernández A, Marcos A. Evaluation of Lactobacillus coryniformis CECT5711 strain as a coadjuvant in a vaccination process: a randomised clinical trial in healthy adults. *Nutr Metab (Lond)* 2017; **14**: 2.

233 Fernández-Ferreiro A, Formigo-Couceiro FJ, Veiga-Gutierrez R, *et al.* Effects of Loigolactobacillus coryniformis K8 CECT 5711 on the Immune Response of Elderly Subjects to COVID-19 Vaccination: A Randomized Controlled Trial. *Nutrients* 2022; **14**: 228.

234 Maruyama M, Abe R, Shimono T, Iwabuchi N, Abe F, Xiao J-Z. The effects of non-viable Lactobacillus on immune function in the elderly: a randomised, double-blind, placebo-controlled study. *International Journal of Food Sciences and Nutrition* 2016; **67**: 67–73.

235 Jespersen L, Tarnow I, Eskesen D, *et al.* Effect of Lactobacillus paracasei subsp. paracasei, L. casei 431 on immune response to influenza vaccination and upper respiratory tract infections in healthy adult volunteers: a randomized, double-blind, placebo-controlled, parallel-group study. *Am J Clin Nutr* 2015; **101**: 1188–96.

236 Akatsu H, Arakawa K, Yamamoto T, *et al.* Lactobacillus in Jelly Enhances the Effect of Influenza Vaccination in Elderly Individuals. *Journal of the American Geriatrics Society* 2013; **61**: 1828–30.

237 Van Puyenbroeck K, Hens N, Coenen S, *et al.* Efficacy of daily intake of Lactobacillus casei Shirota on respiratory symptoms and influenza vaccination immune response: a randomized, double-blind, placebo-controlled trial in healthy elderly nursing home residents. *Am J Clin Nutr* 2012; **95**: 1165–71.

238 Bosch M. LACTOBACILLUS PLANTARUM CECT315 Y CECT7316 ESTIMULA LA PRODUCCIÓN DE INMUNOGLOBULINAS TRAS LA VACUNACIÓN CONTRA LA INFLUENZA EN ANCIANOS. *NUTRICION HOSPITALARIA* 2012; : 504–9.

239 Rizzardini G, Eskesen D, Calder P, Capetti A, Jespersen L, Clerici M. Evaluation of the immune benefits of two probiotic strains Bifidobacterium animalis ssp lactis, BB-12 (R) and Lactobacillus paracasei ssp paracasei, L. casei 431 (R) in an influenza vaccination model: a randomised, double-blind, placebo-controlled study. *The British journal of nutrition* 2011; **107**: 876–84.

240 Davidson LE, Fiorino A-M, Snydman DR, Hibberd PL. Lactobacillus GG as an Immune Adjuvant for Live Attenuated Influenza Vaccine in Healthy Adults: A Randomized Double Blind Placebo Controlled Trial. *Eur J Clin Nutr* 2011; **65**: 501–7.

241 Namba K, Hatano M, Yaeshima T, Takase M, Suzuki K. Effects of Bifidobacterium longum BB536 administration on influenza infection, influenza vaccine antibody titer, and cell-mediated immunity in the elderly. *Biosci Biotechnol Biochem* 2010; **74**: 939–45.

242 Boge T, Rémigy M, Vaudaine S, Tanguy J, Bourdet-Sicard R, van der Werf S. A probiotic fermented dairy drink improves antibody response to influenza vaccination in the elderly in two randomised controlled trials. *Vaccine* 2009; **27**: 5677–84.

243 Olivares M, Díaz-Ropero MP, Sierra S, *et al.* Oral intake of Lactobacillus fermentum CECT5716 enhances the effects of influenza vaccination. *Nutrition* 2007; **23**: 254–60.

244 de Vrese M, Rautenberg P, Laue C, Koopmans M, Herremans T, Schrezenmeir J. Probiotic bacteria stimulate virus-specific neutralizing antibodies following a booster polio vaccination. *Eur J Nutr* 2005; **44**: 406–13.

245 Fang H, Elina T, Heikki A, Seppo S. Modulation of humoral immune response through probiotic intake. *FEMS Immunol Med Microbiol* 2000; **29**: 47–52.

246 Akatsu H, Nagafuchi S, Kurihara R, *et al.* Enhanced vaccination effect against influenza by prebiotics in elderly patients receiving enteral nutrition. *Geriatrics & Gerontology International* 2016; **16**: 205–13.

247 Nagafuchi S, Yamaji T, Kawashima A, *et al.* Effects of a Formula Containing Two Types of Prebiotics, Bifidogenic Growth Stimulator and Galacto-oligosaccharide, and Fermented Milk Products on Intestinal Microbiota and Antibody Response to Influenza Vaccine in Elderly Patients: A Randomized Controlled Trial. *Pharmaceuticals (Basel)* 2015; **8**: 351–65.

248 Arimori Y, Nakamura R, Hirose Y, *et al.* Daily intake of heat-killed Lactobacillus plantarum L-137 enhances type I interferon production in healthy humans and pigs. *Immunopharmacol Immunotoxicol* 2012; **34**: 937–43.

249 Bunout D, Hirsch S, de la Maza M, *et al.* Effects of prebiotics on the immune response to vaccination in the elderly. *Journal of Parenteral and Enteral Nutrition* 2002; **26**: 372–6.

250 Langkamp-Henken B, Wood SM, Herlinger-Garcia KA, *et al.* Nutritional formula improved immune profiles of seniors living in nursing homes. *J Am Geriatr Soc* 2006; **54**: 1861–70.

251 Langkamp-Henken B, Bender BS, Gardner EM, *et al.* Nutritional formula enhanced immune function and reduced days of symptoms of upper respiratory tract infection in seniors. *J Am Geriatr Soc* 2004; **52**: 3–12.

252 Lomax AR, Cheung LVY, Noakes PS, Miles EA, Calder PC. Inulin-Type β2-1 Fructans have Some Effect on the Antibody Response to Seasonal Influenza Vaccination in Healthy Middle-Aged Humans. *Front Immunol* 2015; **6**: 490.

253 Enani S, Przemska-Kosicka A, Childs CE, *et al.* Impact of ageing and a synbiotic on the immune response to seasonal influenza vaccination; a randomised controlled trial. *Clin Nutr* 2018; **37**: 443–51.

254 Przemska-Kosicka A, Childs CE, Enani S, *et al.* Effect of a synbiotic on the response to seasonal influenza vaccination is strongly influenced by degree of immunosenescence. *Immunity & Ageing* 2016; **13**: 6.

255 Püngel D, Treveil A, Dalby MJ, *et al.* Bifidobacterium breve UCC2003 Exopolysaccharide Modulates the Early Life Microbiota by Acting as a Potential Dietary Substrate. *Nutrients* 2020; **12**: 948.

256 Ferrario C, Milani C, Mancabelli L, *et al.* Modulation of the eps -ome transcription of bifidobacteria through simulation of human intestinal environment. *FEMS Microbiology Ecology* 2016; **92**: fiw056.

257 Bales PM, Renke EM, May SL, Shen Y, Nelson DC. Purification and Characterization of Biofilm-Associated EPS Exopolysaccharides from ESKAPE Organisms and Other Pathogens. *PLOS ONE* 2013; **8**: 8.

258 Lv H, Teng Q, Chen J, *et al.* Probiotic potential of a novel exopolysaccharide produced by *Bifidobacterium animalis* subsp. *Lactis* SF. *LWT* 2024; **193**: 115764.

259 Li S, Chen T, Xu F, *et al.* The beneficial effect of exopolysaccharides from *Bifidobacterium bifidum* WBIN03 on microbial diversity in mouse intestine: Exopolysaccharides from *Bifidobacterium bifidum* and microbial diversity in mouse intestine. *J Sci Food Agric* 2014; **94**: 256–64.

260 Li S, Huang R, Shah NP, Tao X, Xiong Y, Wei H. Antioxidant and antibacterial activities of exopolysaccharides from Bifidobacterium bifidum WBIN03 and Lactobacillus plantarum R315. *Journal of Dairy Science* 2014; **97**: 7334–43.

261 Round JL, Mazmanian SK. Inducible Foxp3+ regulatory T-cell development by a commensal bacterium of the intestinal microbiota. *Proceedings of the National Academy of Sciences* 2010; **107**: 12204–9.

262 Wu M-H, Pan T-M, Wu Y-J, Chang S-J, Chang M-S, Hu C-Y. Exopolysaccharide activities from probiotic bifidobacterium: Immunomodulatory effects (on J774A.1 macrophages) and antimicrobial properties. *International Journal of Food Microbiology* 2010; **144**: 104–10.

263 Schiavi E, Gleinser M, Molloy E, *et al.* The Surface-Associated Exopolysaccharide of Bifidobacterium longum 35624 Plays an Essential Role in Dampening Host Proinflammatory Responses and Repressing Local T $_{H}$ 17 Responses. *Appl Environ Microbiol* 2016; **82**: 7185–96.

264 Fanning S, Hall LJ, van Sinderen D. Bifidobacterium breve UCC2003 surface exopolysaccharide production is a beneficial trait mediating commensal-host interaction through immune modulation and pathogen protection. *Gut Microbes* 2012; **3**: 420–5.

265 Hickey A, Stamou P, Udayan S, *et al.* Bifidobacterium breve Exopolysaccharide Blocks Dendritic Cell Maturation and Activation of CD4+ T Cells. *Front Microbiol* 2021; **12**: 653587.

266 Zhang X, Gong J, Huang W, *et al.* Structural Analysis and Antioxidant and Immunoregulatory Activities of an Exopolysaccharide Isolated from Bifidobacterium longum subsp. longum XZ01. *Molecules* 2023; **28**: 7448.

267 Niu M-M, Guo H-X, Shang J-C, Meng X-C. Structural Characterization and Immunomodulatory Activity of a Mannose-Rich Polysaccharide Isolated from Bifidobacterium breve H4-2. *J Agric Food Chem* 2023; **71**: 19791–803.

268 Niu M-M, Guo H-X, Cai J-W, Meng X-C. Bifidobacterium breve Alleviates DSS-Induced Colitis in Mice by Maintaining the Mucosal and Epithelial Barriers and Modulating Gut Microbes. *Nutrients* 2022; **14**: 3671.

269 Inturri R, Mangano K, Santagati M, Intrieri M, Di Marco R, Blandino G. Immunomodulatory Effects of Bifidobacterium longum W11 Produced Exopolysaccharide on Cytokine Production. *Curr Pharm Biotechnol* 2017; **18**: 883–9.

270 Yue Y, Wang Y, Yang R, *et al.* Exopolysaccharides of *Bifidobacterium longum* subsp. *infantis* E4 on the immune and anti-inflammatory effects in *vitro*. *Journal of Functional Foods* 2023; **107**: 105699.

271 Xiu L, Zhang H, Hu Z, *et al.* Immunostimulatory activity of exopolysaccharides from probiotic Lactobacillus casei WXD030 strain as a novel adjuvant in vitro and in vivo. *Food and Agricultural Immunology* 2018; **29**: 1086–105.

272 Deatherage BL, Cookson BT. Membrane vesicle release in bacteria, eukaryotes, and archaea: a conserved yet underappreciated aspect of microbial life. *Infect Immun* 2012; **80**: 1948–57.

273 Sangiorgio G, Nicitra E, Bivona D, *et al.* Interactions of Gram-Positive Bacterial Membrane Vesicles and Hosts: Updates and Future Directions. *International Journal of Molecular Sciences* 2024; **25**: 2904.

274 Kulp A, Kuehn MJ. Biological functions and biogenesis of secreted bacterial outer membrane vesicles. *Annu Rev Microbiol* 2010; **64**: 163–84.

275 Nagakubo T, Nomura N, Toyofuku M. Cracking Open Bacterial Membrane Vesicles. *Frontiers in Microbiology* 2020; **10**. https://www.frontiersin.org/journals/microbiology/articles/10.3389/fmicb.2019.03026 (accessed Feb 5, 2024).

276 Knox KW, Vesk M, Work E. Relation Between Excreted Lipopolysaccharide Complexes and Surface Structures of a Lysine-Limited Culture of Escherichia coli. *Journal of Bacteriology* 1966; **92**: 1206–17.

277 Dorward DW, Garon CF. DNA Is Packaged within Membrane-Derived Vesicles of Gram-Negative but Not Gram-Positive Bacteria. *Applied and Environmental Microbiology* 1990; **56**: 1960–2.

278 De Langhe N, Van Dorpe S, Guilbert N, *et al.* Mapping bacterial extracellular vesicle research: insights, best practices and knowledge gaps. *Nat Commun* 2024; **15**: 9410.

279 Toyofuku M, Nomura N, Eberl L. Types and origins of bacterial membrane vesicles. *Nat Rev Microbiol* 2019; **17**: 13–24.

280 Briaud P, Carroll RK. Extracellular Vesicle Biogenesis and Functions in Gram-Positive Bacteria. *Infect Immun* 2020; **88**: e00433-20.

281 Brown L, Wolf JM, Prados-Rosales R, Casadevall A. Through the wall: extracellular vesicles in Gram-positive bacteria, mycobacteria and fungi. *Nat Rev Microbiol* 2015; **13**: 620–30.

282 Marquez-Paradas E, Torrecillas-Lopez M, Barrera-Chamorro L, del Rio-Vazquez JL, Gonzalez-de la Rosa T, Montserrat-de la Paz S. Microbiota-derived extracellular vesicles: current knowledge, gaps, and challenges in precision nutrition. *Front Immunol* 2025; **16**: 1514726.

283 Toyofuku M, Schild S, Kaparakis-Liaskos M, Eberl L. Composition and functions of bacterial membrane vesicles. *Nat Rev Microbiol* 2023; **21**: 415–30.

284 Yu Y, Wang X, Fan G-C. Versatile effects of bacterium-released membrane vesicles on mammalian cells and infectious/inflammatory diseases. *Acta Pharmacol Sin* 2018; **39**: 514–33.

285 Mozaheb N, Mingeot-Leclercq M-P. Membrane Vesicle Production as a Bacterial Defense Against Stress. *Front Microbiol* 2020; **11**: 600221.

286 Sanwlani R, Bramich K, Mathivanan S. Role of probiotic extracellular vesicles in inter-kingdom communication and current technical limitations in advancing their therapeutic utility. *Extracell Vesicles Circ Nucl Acids* 2024; **5**: 509–26.

287 Juodeikis R, Martins C, Saalbach G, *et al.* Differential temporal release and lipoprotein loading in B. thetaiotaomicron bacterial extracellular vesicles. *Journal of Extracellular Vesicles* 2024; **13**: 12406.

288 Lee JH, Choi C-W, Lee T, Kim SI, Lee J-C, Shin J-H. Transcription Factor σB Plays an Important Role in the Production of Extracellular Membrane-Derived Vesicles in Listeria monocytogenes. *PLOS ONE* 2013; **8**: e73196.

289 Wang X, Thompson CD, Weidenmaier C, Lee JC. Release of Staphylococcus aureus extracellular vesicles and their application as a vaccine platform. *Nat Commun* 2018; **9**: 1379.

290 Resch U, Tsatsaronis JA, Le Rhun A, *et al.* A Two-Component Regulatory System Impacts Extracellular Membrane-Derived Vesicle Production in Group A Streptococcus. *mBio* 2016; **7**: e00207-16.

291 Cao Y, Lin H. Characterization and function of membrane vesicles in Gram-positive bacteria. *Appl Microbiol Biotechnol* 2021; **105**: 1795–801.

292 Bitto NJ, Zavan L, Johnston EL, Stinear TP, Hill AF, Kaparakis-Liaskos M. Considerations for the Analysis of Bacterial Membrane Vesicles: Methods of Vesicle Production and Quantification Can Influence Biological and Experimental Outcomes. *Microbiology Spectrum* 2021; **9**: e01273-21.

293 Lee E, Choi D, Kim D, *et al.* Gram-positive bacteria produce membrane vesicles: Proteomics-based characterization of *Staphylococcus aureus* -derived membrane vesicles. *Proteomics* 2009; **9**: 5425–36.

294 Zavan L, Bitto NJ, Johnston EL, Greening DW, Kaparakis-Liaskos M. Back Cover: Helicobacter pylori Growth Stage Determines the Size, Protein Composition, and Preferential Cargo Packaging of Outer Membrane Vesicles. *PROTEOMICS* 2019; **19**: 1970004.

295 Bitto NJ, Cheng L, Johnston EL, *et al.* Staphylococcus aureus membrane vesicles contain immunostimulatory DNA, RNA and peptidoglycan that activate innate immune receptors and induce autophagy. *Journal of Extracellular Vesicles* 2021; **10**: e12080.

296 Irving AT, Mimuro H, Kufer TA, *et al.* The Immune Receptor NOD1 and Kinase RIP2 Interact with Bacterial Peptidoglycan on Early Endosomes to Promote Autophagy and Inflammatory Signaling. *Cell Host & Microbe* 2014; **15**: 623–35.

297 Kaparakis M, Turnbull L, Carneiro L, *et al.* Bacterial membrane vesicles deliver peptidoglycan to NOD1 in epithelial cells. *Cellular Microbiology* 2010; **12**: 372–85.

298 Koeppen K, Hampton TH, Jarek M, *et al.* A Novel Mechanism of Host-Pathogen Interaction through sRNA in Bacterial Outer Membrane Vesicles. *PLoS Pathog* 2016; **12**: e1005672.

299 Choi J-W, Kim S-C, Hong S-H, Lee H-J. Secretable Small RNAs via Outer Membrane Vesicles in Periodontal Pathogens. *J Dent Res* 2017; **96**: 458–66.

300 Blenkiron C, Simonov D, Muthukaruppan A, *et al.* Uropathogenic Escherichia coli Releases Extracellular Vesicles That Are Associated with RNA. *PLOS ONE* 2016; **11**: e0160440.

301 Bitto NJ, Chapman R, Pidot S, *et al.* Bacterial membrane vesicles transport their DNA cargo into host cells. *Sci Rep* 2017; **7**: 7072.

302 Liao S, Klein MI, Heim KP, *et al.* Streptococcus mutans Extracellular DNA Is Upregulated during Growth in Biofilms, Actively Released via Membrane Vesicles, and Influenced by Components of the Protein Secretion Machinery. *Journal of Bacteriology* 2014; **196**: 2355–66.

303 Wang X, Eagen WJ, Lee JC. Orchestration of human macrophage NLRP3 inflammasome activation by Staphylococcus aureus extracellular vesicles. *Proceedings of the National Academy of Sciences* 2020; **117**: 3174–84.

304 Ellis TN, Kuehn MJ. Virulence and Immunomodulatory Roles of Bacterial Outer Membrane Vesicles. *Microbiol Mol Biol Rev* 2010; **74**: 81–94.

305 Zhang Y, Liang F, Zhang D, Qi S, Liu Y. Metabolites as extracellular vesicle cargo in health, cancer, pleural effusion, and cardiovascular diseases: An emerging field of study to diagnostic and therapeutic purposes. *Biomedicine & Pharmacotherapy* 2023; **157**: 114046.

306 Yoshimura A, Saeki R, Nakada R, *et al.* Membrane-Vesicle-Mediated Interbacterial Communication Activates Silent Secondary Metabolite Production. *Angewandte Chemie International Edition* 2023; **62**: e202307304.

307 Tartaglia NR, Nicolas A, Rodovalho V de R, *et al.* Extracellular vesicles produced by human and animal Staphylococcus aureus strains share a highly conserved core proteome. *Sci Rep* 2020; **10**: 8467.

308 Mandelbaum N, Zhang L, Carasso S, *et al.* Extracellular vesicles of the Gram-positive gut symbiont Bifidobacterium longum induce immune-modulatory, anti-inflammatory effects. *npj Biofilms Microbiomes* 2023; **9**: 30.

309 Toyofuku M, Morinaga K, Hashimoto Y, *et al.* Membrane vesicle-mediated bacterial communication. *ISME J* 2017; **11**: 1504–9.

310 Stentz R, Horn N, Cross K, *et al.* Cephalosporinases associated with outer membrane vesicles released by Bacteroides spp. protect gut pathogens and commensals against β-lactam antibiotics. *Journal of Antimicrobial Chemotherapy* 2015; **70**: 701–9.

311 Dell'Annunziata F, Folliero V, Giugliano R, *et al.* Gene Transfer Potential of Outer Membrane Vesicles of Gram-Negative Bacteria. *Int J Mol Sci* 2021; **22**: 5985.

312 Lee J, Lee E-Y, Kim S-H, *et al.* Staphylococcus aureus Extracellular Vesicles Carry Biologically Active β-Lactamase. *Antimicrob Agents Chemother* 2013; **57**: 2589–95.

313 Arntzen MØ, Várnai A, Mackie RI, Eijsink VGH, Pope PB. Outer membrane vesicles from Fibrobacter succinogenes S85 contain an array of carbohydrate-active enzymes with versatile polysaccharide-degrading capacity. *Environ Microbiol* 2017; **19**: 2701–14.

314 Li J, Azam F, Zhang S. Outer membrane vesicles containing signalling molecules and active hydrolytic enzymes released by a coral pathogen Vibrio shilonii AK1. *Environ Microbiol* 2016; **18**: 3850–66.

315 Mashburn LM, Whiteley M. Membrane vesicles traffic signals and facilitate group activities in a prokaryote. *Nature* 2005; **437**: 422–5.

316 Lehmkuhl J, Schneider JS, Werth KL vom, Scherff N, Mellmann A, Kampmeier S. Role of membrane vesicles in the transmission of vancomycin resistance in Enterococcus faecium. *Sci Rep* 2024; **14**: 1895.

317 Schwechheimer C, Kuehn MJ. Outer-membrane vesicles from Gram-negative bacteria: biogenesis and functions. *Nat Rev Microbiol* 2015; **13**: 605–19.

318 Jhelum H, Sori H, Sehgal D. A novel extracellular vesicle-associated endodeoxyribonuclease helps Streptococcus pneumoniae evade neutrophil extracellular traps and is required for full virulence. *Sci Rep* 2018; **8**: 7985.

319 Kengmo Tchoupa A, Peschel A. Staphylococcus aureus Releases Proinflammatory Membrane Vesicles To Resist Antimicrobial Fatty Acids. *mSphere* 2020; **5**: 10.1128/msphere.00804-20.

320 Codemo M, Muschiol S, Iovino F, *et al.* Immunomodulatory Effects of Pneumococcal Extracellular Vesicles on Cellular and Humoral Host Defenses. *mBio* 2018; **9**: 10.1128/mbio.00559-18.

321 Augustyniak D, Olszak T, Drulis-Kawa Z. Outer Membrane Vesicles (OMVs) of Pseudomonas aeruginosa Provide Passive Resistance but Not Sensitization to LPS-Specific Phages. *Viruses* 2022; **14**: 121.

322 Carvalho AL, Miquel-Clopés A, Wegmann U, *et al.* Use of bioengineered human commensal gut bacteria-derived microvesicles for mucosal plague vaccine delivery and immunization. *Clin Exp Immunol* 2019; **196**: 287–304.

323 Juodeikis R, Jones E, Deery E, *et al.* Nutrient smuggling: Commensal gut bacteria-derived extracellular vesicles scavenge vitamin B12 and related cobamides for microbe and host acquisition. *Journal of Extracellular Biology* 2022; **1**: e61.

324 Liu Y, Defourny KAY, Smid EJ, Abee T. Gram-Positive Bacterial Extracellular Vesicles and Their Impact on Health and Disease. *Front Microbiol* 2018; **9**: 1502.

325 Stentz R, Carvalho AL, Jones EJ, Carding SR. Fantastic voyage: the journey of intestinal microbiota-derived microvesicles through the body. *Biochem Soc Trans* 2018; **46**: 1021–7.

326 Jones EJ, Booth C, Fonseca S, *et al.* The Uptake, Trafficking, and Biodistribution of Bacteroides thetaiotaomicron Generated Outer Membrane Vesicles. *Front Microbiol* 2020; **11**: 57.

327 Schaack B, Mercier C, Katby M, *et al.* Rapid Biodistribution of Fluorescent Outer-Membrane Vesicles from the Intestine to Distant Organs via the Blood in Mice. *International Journal of Molecular Sciences* 2024; **25**: 1821.

328 Kaisanlahti A, Turunen J, Byts N, *et al.* Maternal microbiota communicates with the fetus through microbiota-derived extracellular vesicles. *Microbiome* 2023; **11**: 249.

329 Dean SN, Rimmer MA, Turner KB, *et al.* Lactobacillus acidophilus Membrane Vesicles as a Vehicle of Bacteriocin Delivery. *Front Microbiol* 2020; **11**. DOI:10.3389/fmicb.2020.00710.

330 Juodeikis R, Ulrich R, Clarke C, *et al.* Extracellular Vesicle-Linked Vitamin B12 Acquisition via Novel Binding Proteins in Bacteroides thetaiotaomicron. *Biochem J* 2025; : BCJ20253340.

331 Gurung M, Moon DC, Choi CW, *et al.* Staphylococcus aureus produces membrane-derived vesicles that induce host cell death. *PLoS One* 2011; **6**: e27958.

332 Choi E-J, Lee HG, Bae I-H, *et al.* Propionibacterium acnes-Derived Extracellular Vesicles Promote Acne-Like Phenotypes in Human Epidermis. *J Invest Dermatol* 2018; **138**: 1371–9.

333 Thay B, Wai SN, Oscarsson J. Staphylococcus aureus α-toxin-dependent induction of host cell death by membrane-derived vesicles. *PLoS One* 2013; **8**: e54661.

334 Mancini F, Rossi O, Necchi F, Micoli F. OMV Vaccines and the Role of TLR Agonists in Immune Response. *Int J Mol Sci* 2020; **21**: 4416.

335 Cai W, Kesavan DK, Wan J, Abdelaziz MH, Su Z, Xu H. Bacterial outer membrane vesicles, a potential vaccine candidate in interactions with host cells based. *Diagn Pathol* 2018; **13**: 95.

336 Adriani R, Mousavi Gargari SL, Nazarian S, Sarvary S, Noroozi N. Immunogenicity of Vibrio cholerae outer membrane vesicles secreted at various environmental conditions. *Vaccine* 2018; **36**: 322–30.

337 Carvalho AL, Fonseca S, Miquel-Clopés A, *et al.* Bioengineering commensal bacteria-derived outer membrane vesicles for delivery of biologics to the gastrointestinal and respiratory tract. *Journal of Extracellular Vesicles* 2019; **8**: 1632100.

338 Li M, Zhou H, Yang C, *et al.* Bacterial outer membrane vesicles as a platform for biomedical applications: An update. *J Control Release* 2020; **323**: 253–68.

339 Zhang X, Wang Y, E Q, *et al.* The biological activity and potential of probiotics-derived extracellular vesicles as postbiotics in modulating microbiota-host communication. *J Nanobiotechnol* 2025; **23**: 349.

340 Naskar A, Cho H, Kim K-S. A Nanocomposite with Extracellular Vesicles from Lactobacillus paracasei as a Bioinspired Nanoantibiotic Targeting Staphylococcus aureus. *Pharmaceutics* 2022; **14**: 2273.

341 Li M, Lee K, Hsu M, Nau G, Mylonakis E, Ramratnam B. Lactobacillus-derived extracellular vesicles enhance host immune responses against vancomycin-resistant enterococci. *BMC Microbiol* 2017; **17**: 66.

342 Kadurugamuwa JL, Beveridge TJ. Bacteriolytic effect of membrane vesicles from Pseudomonas aeruginosa on other bacteria including pathogens: conceptually new antibiotics. *J Bacteriol* 1996; **178**: 2767–74.

343 Tzipilevich E, Habusha M, Ben-Yehuda S. Acquisition of Phage Sensitivity by Bacteria through Exchange of Phage Receptors. *Cell* 2017; **168**: 186-199.e12.

344 Martínez-Ruiz S, Olivo-Martínez Y, Cordero C, *et al.* Microbiota-Derived Extracellular Vesicles as a Postbiotic Strategy to Alleviate Diarrhea and Enhance Immunity in Rotavirus-Infected Neonatal Rats. *International Journal of Molecular Sciences* 2024; **25**: 1184.

345 Yamasaki-Yashiki S, Miyoshi Y, Nakayama T, Kunisawa J, Katakura Y. IgA-enhancing effects of membrane vesicles derived from Lactobacillus sakei subsp. sakei NBRC15893. *Biosci Microbiota Food Health* 2019; **38**: 23–9.

346 Miyoshi Y, Saika A, Nagatake T, *et al.* Mechanisms underlying enhanced IgA production in Peyer's patch cells by membrane vesicles derived from Lactobacillus sakei. *Biosci Biotechnol Biochem* 2021; **85**: 1536–45.

347 Diaz-Garrido N, Badia J, Baldomà L. Modulation of Dendritic Cells by Microbiota Extracellular Vesicles Influences the Cytokine Profile and Exosome Cargo. *Nutrients* 2022; **14**: 344.

348 Jiang B, Huang J. Influences of bacterial extracellular vesicles on macrophage immune functions. *Front Cell Infect Microbiol* 2024; **14**: 1411196.

349 Müller L, Kuhn T, Koch M, Fuhrmann G. Stimulation of Probiotic Bacteria Induces Release of Membrane Vesicles with Augmented Anti-inflammatory Activity. *ACS Appl Bio Mater* 2021; **4**: 3739–48.

350 Kim W, Lee EJ, Bae I-H, *et al.* Lactobacillus plantarum-derived extracellular vesicles induce anti-inflammatory M2 macrophage polarization in vitro. *Journal of Extracellular Vesicles* 2020; **9**: 1793514.

351 Liang L, Yang C, Liu L, *et al.* Commensal bacteria-derived extracellular vesicles suppress ulcerative colitis through regulating the macrophages polarization and remodeling the gut microbiota. *Microbial Cell Factories* 2022; **21**: 88.

352 Hu R, Lin H, Li J, *et al.* Probiotic Escherichia coli Nissle 1917-derived outer membrane vesicles enhance immunomodulation and antimicrobial activity in RAW264.7 macrophages. *BMC Microbiol* 2020; **20**: 268.

353 Fonseca S, Carvalho AL, Miquel-Clopés A, *et al.* Extracellular vesicles produced by the human gut commensal bacterium Bacteroides thetaiotaomicron elicit anti-inflammatory responses from innate immune cells. *Front Microbiol* 2022; **13**: 1050271.

354 Shen Y, Giardino Torchia ML, Lawson GW, Karp CL, Ashwell JD, Mazmanian SK. Outer membrane vesicles of a human commensal mediate immune regulation and disease protection. *Cell Host Microbe* 2012; **12**: 509–20.

355 Alvarez C-S, Giménez R, Cañas M-A, *et al.* Extracellular vesicles and soluble factors secreted by Escherichia coli Nissle 1917 and ECOR63 protect against enteropathogenic E. coli-induced intestinal epithelial barrier dysfunction. *BMC Microbiology* 2019; **19**: 166.

356 Xu J, Wang L, Wang D, *et al.* Extracellular Vesicles for Therapeutic Applications. IntechOpen, 2024 DOI:10.5772/intechopen.113969.

357 Rabiei N, Ahmadi Badi S, Ettehad Marvasti F, Nejad Sattari T, Vaziri F, Siadat SD. Induction effects of Faecalibacterium prausnitzii and its extracellular vesicles on toll-like receptor signaling pathway gene expression and cytokine level in human intestinal epithelial cells. *Cytokine* 2019; **121**: 154718.

358 Lajqi T, Köstlin-Gille N, Hillmer S, *et al.* Gut Microbiota-Derived Small Extracellular Vesicles Endorse Memory-like Inflammatory Responses in Murine Neutrophils. *Biomedicines* 2022; **10**: 442.

359 Lee KH, Kronbichler A, Park DDY, *et al.* Neutrophil extracellular traps (NETs) in autoimmune diseases: A comprehensive review. *Autoimmunity Reviews* 2017; **16**: 1160–73.

360 Yang Z, Gao Z, Yang Z, *et al. Lactobacillus plantarum*-derived extracellular vesicles protect against ischemic brain injury via the microRNA-101a-3p/c-Fos/TGF-β axis. *Pharmacological Research* 2022; **182**: 106332.

361 Kim MH, Choi SJ, Choi HI, *et al.* Lactobacillus plantarum-derived Extracellular Vesicles Protect Atopic Dermatitis Induced by Staphylococcus aureus-derived Extracellular Vesicles. *Allergy Asthma Immunol Res* 2018; **10**: 516–32.

362 Han F, Wang K, Shen K, *et al.* Extracellular vesicles from Lactobacillus druckerii inhibit hypertrophic scar fibrosis. *Journal of Nanobiotechnology* 2023; **21**: 113.

363 Chen Y, Huang X, Liu A, *et al.* Lactobacillus Reuteri Vesicles Regulate Mitochondrial Function of Macrophages to Promote Mucosal and Cutaneous Wound Healing. *Adv Sci (Weinh)* 2024; **11**: e2309725.

364 Wang J, Li X, Zhao X, *et al.* Lactobacillus rhamnosus GG-derived extracellular vesicles promote wound healing via miR-21-5p-mediated re-epithelization and angiogenesis. *Journal of Nanobiotechnology* 2024; **22**: 644.

365 Ñahui Palomino RA, Vanpouille C, Laghi L, *et al.* Extracellular vesicles from symbiotic vaginal lactobacilli inhibit HIV-1 infection of human tissues. *Nat Commun* 2019; **10**: 5656.

366 Zhang W, Xie J, Wang Z, *et al.* Androgen deficiency-induced loss of Lactobacillus salivarius extracellular vesicles is associated with the pathogenesis of osteoporosis. *Microbiol Res* 2025; **293**: 128047.

367 Nabavi-Rad A, Jamshidizadeh S, Azizi M, *et al.* The synergistic effect of Levilactobacillus brevis IBRC-M10790 and vitamin D3 on Helicobacter pylori-induced inflammation. *Front Cell Infect Microbiol* 2023; **13**. DOI:10.3389/fcimb.2023.1171469.

368 Kim OY, Park HT, Dinh NTH, *et al.* Bacterial outer membrane vesicles suppress tumor by interferon-γ-mediated antitumor response. *Nat Commun* 2017; **8**: 626.

369 Gujrati V, Kim S, Kim S-H, *et al.* Bioengineered bacterial outer membrane vesicles as cell-specific drug-delivery vehicles for cancer therapy. *ACS Nano* 2014; **8**: 1525–37.

370 Kim Y-M, Bae J. Extracellular vesicles derived from a specific strain of commensal bacteria promote anticancer immune responses and synergize with anticancer therapies. *The Journal of Immunology* 2023; **210**: 172.11.

371 Behzadi E, Mahmoodzadeh Hosseini H, Imani Fooladi AA. The inhibitory impacts of *Lactobacillus rhamnosus* GG-derived extracellular vesicles on the growth of hepatic cancer cells. *Microbial Pathogenesis* 2017; **110**: 1–6.

372 Shi Y, Meng L, Zhang C, Zhang F, Fang Y. Extracellular vesicles of Lacticaseibacillus paracasei PC-H1 induce colorectal cancer cells apoptosis via PDK1/AKT/Bcl-2 signaling pathway. *Microbiol Res* 2022; **255**: 126921.

373 López P, González-Rodríguez I, Sánchez B, Gueimonde M, Margolles A, Suárez A. Treg-inducing membrane vesicles from Bifidobacterium bifidum LMG13195 as potential adjuvants in immunotherapy. *Vaccine* 2012; **30**: 825–9.

374 Kim J-H, Jeun E-J, Hong C-P, *et al.* Extracellular vesicle–derived protein from Bifidobacterium longum alleviates food allergy through mast cell suppression. *Journal of Allergy and Clinical Immunology* 2016; **137**: 507-516.e8.

375 Nishiyama K, Takaki T, Sugiyama M, *et al.* Extracellular Vesicles Produced by Bifidobacterium longum Export Mucin-Binding Proteins. *Appl Environ Microbiol* 2020; **86**. DOI:10.1128/AEM.01464-20.

376 Hassani S, Sotoodehnejadnematalahi F, Fateh A, Siadat SD. Evaluation of Association between Bifidobacterium bifidum Derived Extracellular Vesicles and Intestinal Epithelium Tight Junction Proteins through Notch-1 and AhR Activation in Caco-2 Cell Line. *Mol Genet Microbiol Virol* 2021; **36**: S1–6.

377 Kurata A, Yamasaki-Yashiki S, Imai T, Miyazaki A, Watanabe K, Uegaki K. Enhancement of IgA production by membrane vesicles derived from *Bifidobacterium longum* subsp. *infantis*. *Bioscience, Biotechnology, and Biochemistry* 2022; **87**: 119–28.

378 Morishita M, Kida M, Motomura T, *et al.* Elucidation of the Tissue Distribution and Host Immunostimulatory Activity of Exogenously Administered Probiotic-Derived Extracellular Vesicles for Immunoadjuvant. *Mol Pharmaceutics* 2023; **20**: 6104–13.

379 Nie X, Li Q, Ji H, *et al.* Bifidobacterium longum NSP001-derived extracellular vesicles ameliorate ulcerative colitis by modulating T cell responses in gut microbiota-(in)dependent manners. *npj Biofilms Microbiomes* 2025; **11**: 1–15.

380 Preet R, Islam MA, Shim J, *et al.* Gut commensal Bifidobacterium-derived extracellular vesicles modulate the therapeutic effects of anti-PD-1 in lung cancer. *Nat Commun* 2025; **16**: 3500.

381 Jeon HJ, Seo S, Lee HS, *et al.* DOP032 Extracellular vesicles from Bifidobacterium longum Subspecies infantis attenuate intestinal inflammation via macrophage polarization. *Journal of Crohn's and Colitis* 2025; **19**: i144–5.

382 Li B, Chi X, Huang Y, Wang W, Liu Z. Bifidobacterium longum-Derived Extracellular Vesicles Prevent Hepatocellular Carcinoma by Modulating the TGF-β1/Smad Signaling in Mice. *FBL* 2024; **29**: 241.

383 Huda MN, Lewis Z, Kalanetra KM, *et al.* Stool microbiota and vaccine responses of infants. *Pediatrics* 2014; **134**: e362-372.

384 Harris VC, Armah G, Fuentes S, *et al.* Significant Correlation Between the Infant Gut Microbiome and Rotavirus Vaccine Response in Rural Ghana. *The Journal of Infectious Diseases* 2017; **215**: 34–41.

385 Harris V, Ali A, Fuentes S, *et al.* Rotavirus vaccine response correlates with the infant gut microbiota composition in Pakistan. *Gut Microbes* 2018; **9**: 93–101.

386 Fix J, Chandrashekhar K, Perez J, *et al.* Association between Gut Microbiome Composition and Rotavirus Vaccine Response among Nicaraguan Infants. *The American Journal of Tropical Medicine and Hygiene* 2020; **102**: 213–9.

387 Parker EPK, Praharaj I, Zekavati A, *et al.* Influence of the intestinal microbiota on the immunogenicity of oral rotavirus vaccine given to infants in south India. *Vaccine* 2018; **36**: 264–72.

388 Sindhu KNC, Cunliffe N, Peak M, *et al.* Impact of maternal antibodies and infant gut microbiota on the immunogenicity of rotavirus vaccines in African, Indian and European infants: protocol for a prospective cohort study. *BMJ Open* 2017; **7**: e016577.

389 Robertson RC, Church JA, Edens TJ, *et al.* The fecal microbiome and rotavirus vaccine immunogenicity in rural Zimbabwean infants. *Vaccine* 2021; **39**: 5391–400.

390 Cunningham-Oakes E, Bronowski C, Chinyama E, *et al.* Increased bacterial taxonomic and functional diversity is associated with impaired rotavirus vaccine immunogenicity in infants from India and Malawi. *BMC Microbiology* 2023; **23**: 354.

391 Zhao T, Li J, Fu Y, *et al.* Influence of gut microbiota on mucosal IgA antibody response to the polio vaccine. *npj Vaccines* 2020; **5**: 47.

392 Ng SC, Peng Y, Zhang L, *et al.* Gut microbiota composition is associated with SARS-CoV-2 vaccine immunogenicity and adverse events. *Gut* 2022; **71**: 1106–16.

393 Nyangahu DD, Happel A-U, Wendoh J, *et al.* Bifidobacterium infantis associates with T cell immunity in human infants and is sufficient to enhance antigen-specific T cells in mice. *Science Advances* 2023; **9**: eade1370.

394 Hosomi K, Kunisawa J. Impact of the intestinal environment on the immune responses to vaccination. *Vaccine* 2020; **38**: 6959–65.

395 Wang G, Wang Y, Ma F. Exploiting bacterial-origin immunostimulants for improved vaccination and immunotherapy: current insights and future directions. *Cell & Bioscience* 2024; **14**: 24.

396 Cui Y, Ho M, Hu Y, Shi Y. Vaccine adjuvants: current status, research and development, licensing, and future opportunities. *J Mater Chem B* 2024; : 10.1039.D3TB02861E.

397 Verma SK, Mahajan P, Singh NK, *et al.* New-age vaccine adjuvants, their development, and future perspective. *Front Immunol* 2023; **14**. DOI:10.3389/fimmu.2023.1043109.

398 Riese P, Schulze K, Ebensen T, Prochnow B, Guzmán CA. Vaccine Adjuvants: Key Tools for Innovative Vaccine Design. *Current Topics in Medicinal Chemistry*; **13**: 2562–80.

399 Oleszycka E, Lavelle EC. Immunomodulatory properties of the vaccine adjuvant alum. *Curr Opin Immunol* 2014; **28**: 1–5.

400 Lu F, HogenEsch H. Kinetics of the inflammatory response following intramuscular injection of aluminum adjuvant. *Vaccine* 2013; **31**: 3979–86.

401 Counoupas C, Pino P, Stella AO, *et al.* High-Titer Neutralizing Antibodies against the SARS-CoV-2 Delta Variant Induced by Alhydroxyquim-II-Adjuvanted Trimeric Spike Antigens. *Microbiol Spectr* 2022; **10**: e0169521.

402 Lv X, Song H, Yang J, Li T, Xi T, Xing Y. A multi-epitope vaccine CTB-UE relieves Helicobacter pylori-induced gastric inflammatory reaction via up-regulating microRNA-155 to inhibit Th17 response in C57/BL6 mice model. *Hum Vaccin Immunother* 2014; **10**: 3561–9.

403 Maeto C, Rodríguez AM, Holgado MP, Falivene J, Gherardi MM. Novel Mucosal DNA-MVA HIV Vaccination in Which DNA-IL-12 Plus Cholera Toxin B Subunit (CTB) Cooperates to Enhance Cellular Systemic and Mucosal Genital Tract Immunity. *PLOS ONE* 2014; **9**: e107524.

404 Miyata T, Harakuni T, Taira T, Matsuzaki G, Arakawa T. Merozoite surface protein-1 of Plasmodium yoelii fused via an oligosaccharide moiety of cholera toxin B subunit glycoprotein expressed in yeast induced protective immunity against lethal malaria infection in mice. *Vaccine* 2012; **30**: 948–58.

405 Guo L, Liu K, Xu G, *et al.* Prophylactic and therapeutic efficacy of the epitope vaccine CTB-UA against Helicobacter pylori infection in a BALB/c mice model. *Appl Microbiol Biotechnol* 2012; **95**: 1437–44.

406 Sun J-B, Czerkinsky C, Holmgren J. Mucosally induced immunological tolerance, regulatory T cells and the adjuvant effect by cholera toxin B subunit. *Scand J Immunol* 2010; **71**: 1–11.

407 Baldauf KJ, Royal JM, Hamorsky KT, Matoba N. Cholera toxin B: one subunit with many pharmaceutical applications. *Toxins (Basel)* 2015; **7**: 974–96.

408 Holmgren J, Adamsson J, Anjuere F, *et al.* Mucosal adjuvants and anti-infection and anti-immunopathology vaccines based on cholera toxin, cholera toxin B subunit and CpG DNA. *Immunology Letters* 2005; **97**: 181–8.

409 Cooper CL, Davis HL, Morris ML, *et al.* CPG 7909, an immunostimulatory TLR9 agonist oligodeoxynucleotide, as adjuvant to Engerix-B HBV vaccine in healthy adults: a double-blind phase I/II study. *J Clin Immunol* 2004; **24**: 693–701.

410 Sa H, G VN, B S, S A, H W, Jj E. A phase I study of the safety and immunogenicity of recombinant hepatitis B surface antigen co-administered with an immunostimulatory phosphorothioate oligonucleotide adjuvant. *Vaccine* 2003; **21**. DOI:10.1016/s0264-410x(03)00045-8.

411 Bode C, Zhao G, Steinhagen F, Kinjo T, Klinman DM. CpG DNA as a vaccine adjuvant. *Expert Rev Vaccines* 2011; **10**: 499–511.

412 Kheirvari M, Liu H, Tumban E. Virus-like Particle Vaccines and Platforms for Vaccine Development. *Viruses* 2023; **15**: 1109.

413 Moser C, Müller M, Kaeser MD, Weydemann U, Amacker M. Influenza virosomes as vaccine adjuvant and carrier system. *Expert Review of Vaccines* 2013; **12**: 779–91.

414 Buonaguro FM, Tornesello ML, Buonaguro L. Virus-like particle vaccines and adjuvants: the HPV paradigm. *Expert Review of Vaccines* 2009; **8**: 1379–98.

415 Cimica V, Galarza JM. Adjuvant formulations for virus-like particle (VLP) based vaccines. *Clinical Immunology* 2017; **183**: 99–108.

416 Corthésy B, Bioley G. Lipid-Based Particles: Versatile Delivery Systems for Mucosal Vaccination against Infection. *Front Immunol* 2018; **9**. DOI:10.3389/fimmu.2018.00431.

417 Lartey S, Pathirana RD, Zhou F, *et al.* Single dose vaccination of the ASO3-adjuvanted A(H1N1)pdm09 monovalent vaccine in health care workers elicits homologous and cross-reactive cellular and humoral responses to H1N1 strains. *Human Vaccines & Immunotherapeutics* 2015; **11**: 1654–62.

418 O'Hagan DT, Ott GS, De Gregorio E, Seubert A. The mechanism of action of MF59 – An innately attractive adjuvant formulation. *Vaccine* 2012; **30**: 4341–8.

419 Lin Y-J, Wen C-N, Lin Y-Y, *et al.* Oil-in-water emulsion adjuvants for pediatric influenza vaccines: a systematic review and meta-analysis. *Nat Commun* 2020; **11**: 315.

420 Pleguezuelos O, Dille J, de Groen S, *et al.* Immunogenicity, Safety, and Efficacy of a Standalone Universal Influenza Vaccine, FLU-v, in Healthy Adults: A Randomized Clinical Trial. *Ann Intern Med* 2020; **172**: 453–62.

421 Aucouturier J, Dupuis L, Deville S, Ascarateil S, Ganne V. Montanide ISA 720 and 51: a new generation of water in oil emulsions as adjuvants for human vaccines. *Expert Review of Vaccines* 2002; **1**: 111–8.

422 Mata-Haro V, Cekic C, Martin M, Chilton PM, Casella CR, Mitchell TC. The vaccine adjuvant monophosphoryl lipid A as a TRIF-biased agonist of TLR4. *Science* 2007; **316**: 1628–32.

423 Giannini SL, Hanon E, Moris P, *et al.* Enhanced humoral and memory B cellular immunity using HPV16/18 L1 VLP vaccine formulated with the MPL/aluminium salt combination (AS04) compared to aluminium salt only. *Vaccine* 2006; **24**: 5937–49.

424 Didierlaurent AM, Morel S, Lockman L, *et al.* AS04, an aluminum salt- and TLR4 agonist-based adjuvant system, induces a transient localized innate immune response leading to enhanced adaptive immunity. *J Immunol* 2009; **183**: 6186–97.

425 Wang P. Natural and Synthetic Saponins as Vaccine Adjuvants. *Vaccines* 2021; **9**: 222.

426 Martin LBB, Kikuchi S, Rejzek M, *et al.* Complete biosynthesis of the potent vaccine adjuvant QS-21. *Nat Chem Biol* 2024; **20**: 493–502.

427 Mallory RM, Formica N, Pfeiffer S, *et al.* Safety and immunogenicity following a homologous booster dose of a SARS-CoV-2 recombinant spike protein vaccine (NVX-CoV2373): a secondary analysis of a randomised, placebo-controlled, phase 2 trial. *The Lancet Infectious Diseases* 2022; **22**: 1565–76.

428 Stertman L, Palm A-KE, Zarnegar B, *et al.* The Matrix-M™ adjuvant: A critical component of vaccines for the 21st century. *Hum Vaccin Immunother* 2023; **19**: 2189885.

429 Hayashi F, Smith KD, Ozinsky A, *et al.* The innate immune response to bacterial flagellin is mediated by Toll-like receptor 5. *Nature* 2001; **410**: 1099–103.

430 Mizel SB, Bates JT. Flagellin as an Adjuvant: Cellular Mechanisms and Potential. *J Immunol* 2010; **185**: 5677–82.

431 Cui B, Liu X, Fang Y, Zhou P, Zhang Y, Wang Y. Flagellin as a vaccine adjuvant. *Expert Rev Vaccines* 2018; **17**: 335–49.

432 Tussey L, Strout C, Davis M, *et al.* Phase 1 Safety and Immunogenicity Study of a Quadrivalent Seasonal Flu Vaccine Comprising Recombinant Hemagglutinin-Flagellin Fusion Proteins. *Open Forum Infect Dis* 2016; **3**: ofw015.

433 Dn T, Jj T, C S, *et al.* Induction of a potent immune response in the elderly using the TLR-5 agonist, flagellin, with a recombinant hemagglutinin influenza-flagellin fusion vaccine (VAX125, STF2.HA1 SI). *Vaccine* 2011; **29**. DOI:10.1016/j.vaccine.2011.05.001.

434 Turley CB, Rupp RE, Johnson C, *et al.* Safety and immunogenicity of a recombinant M2e-flagellin influenza vaccine (STF2.4xM2e) in healthy adults. *Vaccine* 2011; **29**: 5145–52.

435 Frey SE, Lottenbach K, Graham I, *et al.* A phase I safety and immunogenicity dose escalation trial of plague vaccine, Flagellin/F1/V, in healthy adult volunteers (DMID 08-0066). *Vaccine* 2017; **35**: 6759–65.

436 Saxena M, Sabado RL, La Mar M, *et al.* Poly-ICLC, a TLR3 Agonist, Induces Transient Innate Immune Responses in Patients With Treated HIV-Infection: A Randomized Double-Blinded Placebo Controlled Trial. *Front Immunol* 2019; **10**. DOI:10.3389/fimmu.2019.00725.

437 Overton ET, Goepfert PA, Cunningham P, *et al.* Intranasal seasonal influenza vaccine and a TLR-3 agonist, rintatolimod, induced cross-reactive IgA antibody formation against avian H5N1 and H7N9 influenza HA in humans. *Vaccine* 2014; **32**: 5490–5.

438 Kalimuddin S, Wijaya L, Chan YFZ, *et al.* A phase II randomized study to determine the safety and immunogenicity of the novel PIKA rabies vaccine containing the PIKA adjuvant using an accelerated regimen. *Vaccine* 2017; **35**: 7127–32.

439 Shen E, Li L, Li L, *et al.* PIKA as an adjuvant enhances specific humoral and cellular immune responses following the vaccination of mice with HBsAg plus PIKA. *Cell Mol Immunol* 2007; **4**: 113–20.

440 Brekke K, Sommerfelt M, Ökvist M, Dyrhol-Riise AM, Kvale D. The therapeutic HIV Env C5/gp41 vaccine candidate Vacc-C5 induces specific T cell regulation in a phase I/II clinical study. *BMC Infectious Diseases* 2017; **17**: 228.

441 Petrina M, Martin J, Basta S. Granulocyte macrophage colony-stimulating factor has come of age: From a vaccine adjuvant to antiviral immunotherapy. *Cytokine & Growth Factor Reviews* 2021; **59**: 101–10.

442 Tovey MG, Lallemand C. Adjuvant activity of cytokines. *Methods Mol Biol* 2010; **626**: 287–309.

443 Zhang C, Wang B, Wang M. GM-CSF and IL-2 as adjuvant enhance the immune effect of protein vaccine against foot-and-mouth disease. *Virology Journal* 2011; **8**: 7.

444 Heath AW, Playfair JHL. Cytokines as immunological adjuvants. *Vaccine* 1992; **10**: 427–34.

445 Launay O, Grabar S, Bloch F, *et al.* Effect of sublingual administration of interferon-α on the immune response to influenza vaccination in institutionalized elderly individuals. *Vaccine* 2008; **26**: 4073–9.

446 Schaller TH, Batich KA, Suryadevara CM, Desai R, Sampson JH. Chemokines as adjuvants for immunotherapy: implications for immune activation with CCL3. *Expert Rev Clin Immunol* 2017; **13**: 1049–60.

447 Woltman AM, ter Borg MJ, Binda RS, *et al.* α-Galactosylceramide in Chronic Hepatitis B Infection: Results from a Randomized Placebo-Controlled Phase I/ II Trial. *Antiviral Therapy* 2009; **14**: 809–18.

448 Feng H, Sun R, Song G, *et al.* A Glycolipid α-GalCer Derivative, 7DW8-5 as a Novel Mucosal Adjuvant for the Split Inactivated Influenza Vaccine. *Viruses* 2022; **14**: 1174.

449 Meijlink MA, Chua YC, Chan STS, *et al.* 6″-Modifed α-GalCer-peptide conjugate vaccine candidates protect against liver-stage malaria. *RSC Chem Biol* 2022; **3**: 551–60.

450 Khan MA, Malik A, Alruwetei AM, *et al.* Delivery of MERS antigen encapsulated in α-GalCer-bearing liposomes elicits stronger antigen-specific immune responses. *J Drug Target* 2022; **30**: 884–93.

451 Atmar Robert L., Bernstein David I., Harro Clayton D., *et al.* Norovirus Vaccine against Experimental Human Norwalk Virus Illness. *New England Journal of Medicine* 2011; **365**: 2178–87.

452 Narayanan RR, Maanvizhi S. Applications of Chitosan Derivatives as Adjuvant for Nanoparticles Based Vaccines. *Infect Disord Drug Targets* 2023; **23**: e220922209066.

453 Gong Y, Tao L, Wang F, *et al.* Chitosan as an adjuvant for a Helicobacter pylori therapeutic vaccine. *Mol Med Rep* 2015; **12**: 4123–32.

454 Zhu Z, Antenucci F, Villumsen KR, Bojesen AM. Bacterial Outer Membrane Vesicles as a Versatile Tool in Vaccine Research and the Fight against Antimicrobial Resistance. *mBio*; **12**: e01707-21.

455 Holst J, Martin D, Arnold R, *et al.* Properties and clinical performance of vaccines containing outer membrane vesicles from Neisseria meningitidis. *Vaccine* 2009; **27**: B3–12.

456 Holst J, Oster P, Arnold R, *et al.* Vaccines against meningococcal serogroup B disease containing outer membrane vesicles (OMV): lessons from past programs and implications for the future. *Hum Vaccin Immunother* 2013; **9**: 1241–53.

457 Jounai N, Kobiyama K, Takeshita F, Ishii KJ. Recognition of damage-associated molecular patterns related to nucleic acids during inflammation and vaccination. *Front Cell Infect Microbiol* 2012; **2**: 168.

458 Cohen Tervaert JW, Martinez-Lavin M, Jara LJ, *et al.* Autoimmune/inflammatory syndrome induced by adjuvants (ASIA) in 2023. *Autoimmun Rev* 2023; **22**: 103287.

459 Huang B, Wang J, Li L. Recent five-year progress in the impact of gut microbiota on vaccination and possible mechanisms. *Gut Pathog* 2023; **15**: 27.

460 Prior JT, Davitt C, Kurtz J, Gellings P, McLachlan JB, Morici LA. Bacterial-Derived Outer Membrane Vesicles are Potent Adjuvants that Drive Humoral and Cellular Immune Responses. *Pharmaceutics* 2021; **13**: 131.

461 Prados-Rosales R, Carreño LJ, Batista-Gonzalez A, *et al.* Mycobacterial Membrane Vesicles Administered Systemically in Mice Induce a Protective Immune Response to Surface Compartments of Mycobacterium tuberculosis. *mBio* 2014; **5**: 10.1128/mbio.01921-14.

462 Choi C-W, Park EC, Yun SH, Lee S-Y, Kim SI, Kim G-H. Potential Usefulness of *Streptococcus pneumoniae* Extracellular Membrane Vesicles as Antibacterial Vaccines. *Journal of Immunology Research* 2017; **2017**: 1–8.

463 van der Ley P, Steeghs L, Hamstra HJ, ten Hove J, Zomer B, van Alphen L. Modification of lipid A biosynthesis in Neisseria meningitidis lpxL mutants: influence on lipopolysaccharide structure, toxicity, and adjuvant activity. *Infect Immun* 2001; **69**: 5981–90.

464 Davenport V, Groves E, Horton RE, *et al.* Mucosal immunity in healthy adults after parenteral vaccination with outer-membrane vesicles from Neisseria meningitidis serogroup B. *J Infect Dis* 2008; **198**: 731–40.

465 Stentz R, Jones E, Juodeikis R, *et al.* The Proteome of Extracellular Vesicles Produced by the Human Gut Bacteria Bacteroides thetaiotaomicron *In Vivo* Is Influenced by Environmental and Host-Derived Factors. *Appl Environ Microbiol* 2022; **88**: e00533-22.

466 Sartorio MG, Pardue EJ, Scott NE, Feldman MF. Human gut bacteria tailor extracellular vesicle cargo for the breakdown of diet- and host-derived glycans. *Proc Natl Acad Sci USA* 2023; **120**: e2306314120.

467 Cho B, Moore G, Pham L-D, Patel C, Kostic A. DNA characterization reveals potential operon-unit packaging of extracellular vesicle cargo from a gut bacterial symbiont. 2023; published online Dec 4. DOI:10.21203/rs.3.rs-3689023/v1.

468 Lynn DJ, Benson SC, Lynn MA, Pulendran B. Modulation of immune responses to vaccination by the microbiota: implications and potential mechanisms. *Nat Rev Immunol* 2022; **22**: 33–46.

469 Alcon-Giner C, Dalby MJ, Caim S, *et al.* Microbiota Supplementation with Bifidobacterium and Lactobacillus Modifies the Preterm Infant Gut Microbiota and Metabolome: An Observational Study. *Cell Reports Medicine* 2020; **1**: 100077.

470 The Wellcome Trust Sanger Institute. High-Throughput DNA Sequencing. Wellcome Sanger Institute. 2019. https://www.sanger.ac.uk/group/high-throughput-dna-sequencing/ (accessed Jan 24, 2024).

471 Gibson GR, Wang X. Enrichment of bifidobacteria from human gut contents by oligofructose using continuous culture. *FEMS Microbiol Lett* 1994; **118**: 121–7.

472 Durant L, Stentz R, Noble A, *et al.* Bacteroides thetaiotaomicron-derived outer membrane vesicles promote regulatory dendritic cell responses in health but not in inflammatory bowel disease. *Microbiome* 2020; **8**: 88.

473 Nickerson JL, Doucette AA. Rapid and Quantitative Protein Precipitation for Proteome Analysis by Mass Spectrometry. *J Proteome Res* 2020; **19**: 2035–42.

474 Sayers EW, Beck J, Bolton EE, *et al.* Database resources of the National Center for Biotechnology Information in 2025. *Nucleic Acids Res* 2024; **53**: D20–9.

475 The UniProt Consortium, Bateman A, Martin M-J, *et al.* UniProt: the Universal Protein Knowledgebase in 2023. *Nucleic Acids Research* 2023; **51**: D523–31.

476 Kanehisa M, Goto S. KEGG: kyoto encyclopedia of genes and genomes. *Nucleic Acids Res* 2000; **28**: 27–30.

477 Schindelin J, Arganda-Carreras I, Frise E, *et al.* Fiji: an open-source platform for biological-image analysis. *Nat Methods* 2012; **9**: 676–82.

478 Javvadi SG, Kujawska M, Papp D, *et al.* A novel bacteriocin produced by Bifidobacterium longum subsp. infantis has dual antimicrobial and immunomodulatory activity. 2022; : 2022.01.27.477972.

479 Pastori C, Lopalco L. Isolation and in vitro Activation of Mouse Peyer's Patch Cells from Small Intestine Tissue. *BIO-PROTOCOL* 2014; **4**. DOI:10.21769/BioProtoc.1282.

480 Andre FE, Booy R, Bock HL, *et al.* Vaccination greatly reduces disease, disability, death and inequity worldwide. *Bull World Health Organ* 2008; **86**: 140–6.

481 Patel M, Glass RI, Jiang B, Santosham M, Lopman B, Parashar U. A systematic review of anti-rotavirus serum IgA antibody titer as a potential correlate of rotavirus vaccine efficacy. *J Infect Dis* 2013; **208**: 284–94.

482 Clark A, van Zandvoort K, Flasche S, *et al.* Efficacy of live oral rotavirus vaccines by duration of follow-up: a meta-regression of randomised controlled trials. *Lancet Infect Dis* 2019; **19**: 717–27.

483 Patriarca PA, Wright PF, John TJ. Factors affecting the immunogenicity of oral poliovirus vaccine in developing countries: review. *Rev Infect Dis* 1991; **13**: 926–39.

484 Lalor MK, Ben-Smith A, Gorak-Stolinska P, *et al.* Population differences in immune responses to BCG in infancy. *J Infect Dis* 2009; **199**: 795–800.

485 Nascimento Silva JR, Camacho LAB, Siqueira MM, *et al.* Mutual interference on the immune response to yellow fever vaccine and a combined vaccine against measles, mumps and rubella. *Vaccine* 2011; **29**: 6327–34.

486 Tan P-L, Jacobson RM, Poland GA, Jacobsen SJ, Pankratz VS. Twin studies of immunogenicity — determining the genetic contribution to vaccine failure. *Vaccine* 2001; **19**: 2434–9.

487 Newport MJ, Goetghebuer T, Weiss HA, Whittle H, Siegrist C-A, Marchant A. Genetic regulation of immune responses to vaccines in early life. *Genes Immun* 2004; **5**: 122–9.

488 Klein SL, Flanagan KL. Sex differences in immune responses. *Nat Rev Immunol* 2016; **16**: 626–38.

489 Grassly NC, Jafari H, Bahl S, *et al.* Waning intestinal immunity after vaccination with oral poliovirus vaccines in India. *J Infect Dis* 2012; **205**: 1554–61.

490 Zimmermann P, Curtis N. Factors That Influence the Immune Response to Vaccination. *Clin Microbiol Reviews* 2019; **32**: e00084-18, /cmr/32/2/CMR.00084-18.atom.

491 Henneke P, Kierdorf K, Hall LJ, Sperandio M, Hornef M. Perinatal development of innate immune topology. *Elife* 2021; **10**: e67793.

492 Rakoff-Nahoum S, Medzhitov R. Innate immune recognition of the indigenous microbial flora. *Mucosal Immunology* 2008; **1**: S10–4.

493 Geuking MB, Cahenzli J, Lawson MAE, *et al.* Intestinal Bacterial Colonization Induces Mutualistic Regulatory T Cell Responses. *Immunity* 2011; **34**: 794–806.

494 Chapman TJ, Pham M, Bajorski P, Pichichero ME. Antibiotic Use and Vaccine Antibody Levels. *Pediatrics* 2022; **149**: e2021052061.

495 Nadeem S, Maurya SK, Das DK, Khan N, Agrewala JN. Gut Dysbiosis Thwarts the Efficacy of Vaccine Against Mycobacterium tuberculosis. *Front Immunol* 2020; **11**. DOI:10.3389/fimmu.2020.00726.

496 Olin A, Henckel E, Chen Y, *et al.* Stereotypic Immune System Development in Newborn Children. *Cell* 2018; **174**: 1277-1292.e14.

497 Derrien M, Turroni F, Ventura M, van Sinderen D. Insights into endogenous Bifidobacterium species in the human gut microbiota during adulthood. *Trends Microbiol* 2022; **30**: 940–7.

498 Bajic D, Wiens F, Wintergerst E, Deyaert S, Baudot A, Van den Abbeele P. HMOs Exert Marked Bifidogenic Effects on Children's Gut Microbiota Ex Vivo, Due to Age-Related Bifidobacterium Species Composition. *Nutrients* 2023; **15**: 1701.

499 Taft DH, Lewis ZT, Nguyen N, *et al.* Bifidobacterium Species Colonization in Infancy: A Global Cross-Sectional Comparison by Population History of Breastfeeding. *Nutrients* 2022; **14**: 1423.

500 Henrick BM, Chew S, Casaburi G, *et al.* Colonization by B. infantis EVC001 modulates enteric inflammation in exclusively breastfed infants. *Pediatr Res* 2019; **86**: 749–57.

501 Karav S, Casaburi G, Frese SA. Reduced colonic mucin degradation in breastfed infants colonized by Bifidobacterium longum subsp. infantis EVC001. *FEBS Open Bio* 2018; **8**: 1649–57.

502 Casaburi G, Duar RM, Vance DP, *et al.* Early-life gut microbiome modulation reduces the abundance of antibiotic-resistant bacteria. *Antimicrobial Resistance & Infection Control* 2019; **8**: 131.

503 Grönlund MM, Arvilommi H, Kero P, Lehtonen OP, Isolauri E. Importance of intestinal colonisation in the maturation of humoral immunity in early infancy: a prospective follow up study of healthy infants aged 0-6 months. *Arch Dis Child Fetal Neonatal Ed* 2000; **83**: F186-192.

504 Lundell A-C, Björnsson V, Ljung A, *et al.* Infant B cell memory differentiation and early gut bacterial colonization. *J Immunol* 2012; **188**: 4315–22.

505 Millar ME. Starch Utilisation by the Beneficial Microbiota Genus Bifidobacterium for Improved Health Outcomes. 2023; published online Sept 5. https://ueaeprints.uea.ac.uk/id/eprint/92991/.

506 Belenguer A, Duncan SH, Calder AG, *et al.* Two routes of metabolic cross-feeding between Bifidobacterium adolescentis and butyrate-producing anaerobes from the human gut. *Appl Environ Microbiol* 2006; **72**: 3593–9.

507 Taghinezhad-S S, Keyvani H, Bermúdez-Humarán LG, Donders GGG, Fu X, Mohseni AH. Twenty years of research on HPV vaccines based on genetically modified lactic acid bacteria: an overview on the gut-vagina axis. *Cell Mol Life Sci* 2021; **78**: 1191–206.

508 Matsuki T, Yahagi K, Mori H, *et al.* A key genetic factor for fucosyllactose utilization affects infant gut microbiota development. *Nat Commun* 2016; **7**: 11939.

509 Bode L. Human milk oligosaccharides: Every baby needs a sugar mama. *Glycobiology* 2012; **22**: 1147–62.

510 Sakanaka M, Gotoh A, Yoshida K, *et al.* Varied Pathways of Infant Gut-Associated Bifidobacterium to Assimilate Human Milk Oligosaccharides: Prevalence of the Gene Set and Its Correlation with Bifidobacteria-Rich Microbiota Formation. *Nutrients* 2020; **12**: 71.

511 Kujawska M, Raulo A, Millar M, *et al.* Bifidobacterium castoris strains isolated from wild mice show evidence of frequent host switching and diverse carbohydrate metabolism potential. *ISME Communications* 2022; **2**. DOI:10.1038/s43705-022-00102-x.

512 Kujawska M, La Rosa SL, Pope PB, Hoyles L, McCartney AL, Hall LJ. Succession of Bifidobacterium longum strains in response to the changing early-life nutritional environment reveals specific adaptations to distinct dietary substrates. Microbiology, 2020 DOI:10.1101/2020.02.20.957555.

513 Bottacini F, Morrissey R, Esteban-Torres M, *et al.* Comparative genomics and genotype-phenotype associations in Bifidobacterium breve. *Sci Rep* 2018; **8**: 10633.

514 Solopova A, van Gestel J, Weissing FJ, *et al.* Bet-hedging during bacterial diauxic shift. *Proc Natl Acad Sci U S A* 2014; **111**: 7427–32.

515 Wang Z, Lazinski DW, Camilli A. Immunity Provided by an Outer Membrane Vesicle Cholera Vaccine Is Due to O-Antigen-Specific Antibodies Inhibiting Bacterial Motility. *Infect Immun* 2017; **85**. DOI:10.1128/IAI.00626-16.

516 Leduc I, Connolly KL, Begum A, *et al.* The serogroup B meningococcal outer membrane vesicle-based vaccine 4CMenB induces cross-species protection against Neisseria gonorrhoeae. *PLoS Pathog* 2020; **16**: e1008602.

517 Jiang L, Schinkel M, van Essen M, Schiffelers RM. Bacterial membrane vesicles as promising vaccine candidates. *Eur J Pharm Biopharm* 2019; **145**: 1–6.

518 Byvalov AA, Konyshev IV, Uversky VN, Dentovskaya SV, Anisimov AP. Yersinia Outer Membrane Vesicles as Potential Vaccine Candidates in Protecting against Plague. *Biomolecules* 2020; **10**. DOI:10.3390/biom10121694.

519 Behrens F, Funk-Hilsdorf TC, Kuebler WM, Simmons S. Bacterial Membrane Vesicles in Pneumonia: From Mediators of Virulence to Innovative Vaccine Candidates. *Int J Mol Sci* 2021; **22**. DOI:10.3390/ijms22083858.

520 Solanki KS, Varshney R, Qureshi S, *et al.* Non-infectious outer membrane vesicles derived from Brucella abortus S19Δper as an alternative acellular vaccine protects mice against virulent challenge. *Int Immunopharmacol* 2021; **90**: 107148.

521 Keiser PB, Biggs-Cicatelli S, Moran EE, *et al.* A phase 1 study of a meningococcal native outer membrane vesicle vaccine made from a group B strain with deleted lpxL1 and synX, over-expressed factor H binding protein, two PorAs and stabilized OpcA expression. *Vaccine* 2011; **29**: 1413–20.

522 Basto AP, Piedade J, Ramalho R, *et al.* A new cloning system based on the OprI lipoprotein for the production of recombinant bacterial cell wall-derived immunogenic formulations. *Journal of Biotechnology* 2012; **157**: 50–63.

523 Huang W, Wang S, Yao Y, *et al.* Employing Escherichia coli-derived outer membrane vesicles as an antigen delivery platform elicits protective immunity against Acinetobacter baumannii infection. *Sci Rep* 2016; **6**: 37242.

524 Irene C, Fantappiè L, Caproni E, *et al.* Bacterial outer membrane vesicles engineered with lipidated antigens as a platform for *Staphylococcus aureus* vaccine. *Proc Natl Acad Sci U S A* 2019; **116**: 21780–8.

525 Price NL, Goyette-Desjardins G, Nothaft H, *et al.* Glycoengineered Outer Membrane Vesicles: A Novel Platform for Bacterial Vaccines. *Sci Rep* 2016; **6**: 24931.

526 Kuipers K, Daleke-Schermerhorn MH, Jong WSP, *et al.* Salmonella outer membrane vesicles displaying high densities of pneumococcal antigen at the surface offer protection against colonization. *Vaccine* 2015; **33**: 2022–9.

527 Jiang L, Driedonks TAP, Jong WSP, *et al.* A bacterial extracellular vesicle-based intranasal vaccine against SARS-CoV-2 protects against disease and elicits neutralizing antibodies to wild-type and Delta variants. *Journal of Extracellular Vesicles* 2022; **11**: e12192.

528 Gilad O, Svensson B, Viborg AH, Stuer-Lauridsen B, Jacobsen S. The extracellular proteome of Bifidobacterium animalis subsp. lactis BB-12 reveals proteins with putative roles in probiotic effects. *PROTEOMICS* 2011; **11**: 2503–14.

529 Ruiz L, Delgado S, Ruas-Madiedo P, Margolles A, Sánchez B. Proteinaceous Molecules Mediating Bifidobacterium-Host Interactions. *Front Microbiol* 2016; **7**: 1193.

530 Lee Y-S, Kim T-Y, Kim Y, *et al.* Microbiota-Derived Lactate Accelerates Intestinal Stem-Cell-Mediated Epithelial Development. *Cell Host & Microbe* 2018; **24**: 833-846.e6.

531 Whitfield GB, Marmont LS, Bundalovic-Torma C, *et al.* Discovery and characterization of a Gram-positive Pel polysaccharide biosynthetic gene cluster. *PLOS Pathogens* 2020; **16**: e1008281.

532 Górska S, Dylus E, Rudawska A, *et al.* Immunoreactive Proteins of Bifidobacterium longum ssp. longum CCM 7952 and Bifidobacterium longum ssp. longum CCDM 372 Identified by Gnotobiotic Mono-Colonized Mice Sera, Immune Rabbit Sera and Non-immune Human Sera. *Front Microbiol* 2016; **7**. DOI:10.3389/fmicb.2016.01537.

533 Rader BA. Alkaline Phosphatase, an Unconventional Immune Protein. *Front Immunol* 2017; **8**: 897.

534 Morais J, Marques C, Faria A, *et al.* Influence of Human Milk on Very Preterms' Gut Microbiota and Alkaline Phosphatase Activity. *Nutrients* 2021; **13**: 1564.

535 Audrito V, Messana VG, Deaglio S. NAMPT and NAPRT: Two Metabolic Enzymes With Key Roles in Inflammation. *Frontiers in Oncology* 2020; **10**. https://www.frontiersin.org/journals/oncology/articles/10.3389/fonc.2020.00358 (accessed Feb 9, 2024).

536 Jin H, Song YP, Boel G, Kochar J, Pancholi V. Group A streptococcal surface GAPDH, SDH, recognizes uPAR/CD87 as its receptor on the human pharyngeal cell and mediates bacterial adherence to host cells. *J Mol Biol* 2005; **350**: 27–41.

537 Terrasse R, Tacnet-Delorme P, Moriscot C, *et al.* Human and pneumococcal cell surface glyceraldehyde-3-phosphate dehydrogenase (GAPDH) proteins are both ligands of human C1q protein. *J Biol Chem* 2012; **287**: 42620–33.

538 Giménez R, Aguilera L, Ferreira E, Aguilar J, Baldomà L, Badia J. 11. Glyceraldehyde-3-phosphate dehydrogenase as a moonlighting protein in bacteria. 2014.

539 Xu R, Wu B, Liang J, *et al.* Altered gut microbiota and mucosal immunity in patients with schizophrenia. *Brain, Behavior, and Immunity* 2020; **85**: 120–7.

540 Ruiz L, Delgado S, Ruas-Madiedo P, Sánchez B, Margolles A. Bifidobacteria and Their Molecular Communication with the Immune System. *Front Microbiol* 2017; **8**: 2345.

541 Wei X, Yan X, Chen X, *et al.* Proteomic analysis of the interaction of Bifidobacterium longum NCC2705 with the intestine cells Caco-2 and identification of plasminogen receptors. *J Proteomics* 2014; **108**: 89–98.

542 Ishikawa E, Yamada T, Yamaji K, *et al.* Critical roles of a housekeeping sortase of probiotic *Bifidobacterium bifidum* in bacterium–host cell crosstalk. *iScience* 2021; **24**: 103363.

543 Milani C, Mangifesta M, Mancabelli L, *et al.* The Sortase-Dependent Fimbriome of the Genus Bifidobacterium: Extracellular Structures with Potential To Modulate Microbe-Host Dialogue. *Appl Environ Microbiol* 2017; **83**: e01295-17.

544 Morishita M, Horita M, Higuchi A, Marui M, Katsumi H, Yamamoto A. Characterizing Different Probiotic-Derived Extracellular Vesicles as a Novel Adjuvant for Immunotherapy. *Mol Pharm* 2021; **18**: 1080–92.

545 Alves NJ, Turner KB, Medintz IL, Walper SA. Emerging therapeutic delivery capabilities and challenges utilizing enzyme/protein packaged bacterial vesicles. *Therapeutic Delivery* 2015; **6**: 873–87.

546 Pathirana RD, Kaparakis-Liaskos M. Bacterial membrane vesicles: Biogenesis, immune regulation and pathogenesis. *Cellular Microbiology* 2016; **18**: 1518–24.

547 Ménard O, Gafa V, Kapel N, Rodriguez B, Butel M-J, Waligora-Dupriet A-J. Characterization of Immunostimulatory CpG-Rich Sequences from Different Bifidobacterium Species. *Applied and Environmental Microbiology* 2010; **76**: 2846–55.

548 Pérez-Cruz C, Delgado L, López-Iglesias C, Mercade E. Outer-Inner Membrane Vesicles Naturally Secreted by Gram-Negative Pathogenic Bacteria. *PLOS ONE* 2015; **10**: e0116896.

549 Biller SJ, Schubotz F, Roggensack SE, Thompson AW, Summons RE, Chisholm SW. Bacterial Vesicles in Marine Ecosystems. *Science* 2014; **343**: 183–6.

550 Pérez-Cruz C, Carrión O, Delgado L, Martinez G, López-Iglesias C, Mercade E. New type of outer membrane vesicle produced by the Gram-negative bacterium Shewanella vesiculosa M7T: implications for DNA content. *Appl Environ Microbiol* 2013; **79**: 1874–81.

551 Wei X, Wang S, Zhao X, *et al.* Proteomic Profiling of Bifidobacterium bifidum S17 Cultivated Under In Vitro Conditions. *Front Microbiol* 2016; **7**: 97.

552 Gagnon M, Savard P, Rivière A, LaPointe G, Roy D. Bioaccessible Antioxidants in Milk Fermented by Bifidobacterium longum subsp. longum Strains. *Biomed Res Int* 2015; **2015**: 169381.

553 Xiao M, Xu P, Zhao J, *et al.* Oxidative stress-related responses of Bifidobacterium longum subsp. longum BBMN68 at the proteomic level after exposure to oxygen. *Microbiology* 2011; **157**: 1573–88.

554 Hines JK, Kruesel CE, Fromm HJ, Honzatko RB. Structure of inhibited fructose-1,6-bisphosphatase from Escherichia coli: distinct allosteric inhibition sites for AMP and glucose 6-phosphate and the characterization of a gluconeogenic switch. *J Biol Chem* 2007; **282**: 24697–706.

555 Jung D-H, Park C-S. Resistant starch utilization by Bifidobacterium, the beneficial human gut bacteria. *Food Sci Biotechnol* 2023; **32**: 441–52.

556 Asteri I-A, Boutou E, Anastasiou R, *et al.* In silico evidence for the horizontal transfer of gsiB, a σ(B)-regulated gene in gram-positive bacteria, to lactic acid bacteria. *Appl Environ Microbiol* 2011; **77**: 3526–31.

557 Gilad O, Hjernø K, Østerlund EC, *et al.* Insights into physiological traits of Bifidobacterium animalis subsp. lactis BB-12 through membrane proteome analysis. *Journal of Proteomics* 2012; **75**: 1190–200.

558 Granato D, Bergonzelli GE, Pridmore RD, Marvin L, Rouvet M, Corthésy-Theulaz IE. Cell surface-associated elongation factor Tu mediates the attachment of Lactobacillus johnsonii NCC533 (La1) to human intestinal cells and mucins. *Infect Immun* 2004; **72**: 2160–9.

559 Candela M, Biagi E, Centanni M, *et al.* Bifidobacterial enolase, a cell surface receptor for human plasminogen involved in the interaction with the host. *Microbiology (Reading)* 2009; **155**: 3294–303.

560 Ramiah K, van Reenen CA, Dicks LMT. Surface-bound proteins of Lactobacillus plantarum 423 that contribute to adhesion of Caco-2 cells and their role in competitive exclusion and displacement of Clostridium sporogenes and Enterococcus faecalis. *Res Microbiol* 2008; **159**: 470–5.

561 Dhanani AS, Bagchi T. The expression of adhesin EF-Tu in response to mucin and its role in Lactobacillus adhesion and competitive inhibition of enteropathogens to mucin. *J Appl Microbiol* 2013; **115**: 546–54.

562 Sun Y, Zhu D-Q, Zhang Q-X, *et al.* The Expression of GroEL Protein Amplified from *Bifidobacterium animalis* subsp. *lactis* KLDS 2.0603 and its Role in Competitive Adhesion to Caco-2. *Food Biotechnology* 2016; **30**: 292–305.

563 Perez-Casal J, Potter AA. Glyceradehyde-3-phosphate dehydrogenase as a suitable vaccine candidate for protection against bacterial and parasitic diseases. *Vaccine* 2016; **34**: 1012–7.

564 Chen P-C, Hsieh M-H, Kuo W-S, *et al.* Moonlighting glyceraldehyde-3-phosphate dehydrogenase (GAPDH) protein of Lactobacillus gasseri attenuates allergic asthma via immunometabolic change in macrophages. *J Biomed Sci* 2022; **29**: 75.

565 González-Rodríguez I, Sánchez B, Ruiz L, *et al.* Role of Extracellular Transaldolase from Bifidobacterium bifidum in Mucin Adhesion and Aggregation. *Appl Environ Microbiol* 2012; **78**: 3992–8.

566 Hidalgo-Cantabrana C, Moro-García MA, Blanco-Míguez A, *et al.* In Silico Screening of the Human Gut Metaproteome Identifies Th17-Promoting Peptides Encrypted in Proteins of Commensal Bacteria. *Frontiers in Microbiology* 2017; **8**. https://www.frontiersin.org/journals/microbiology/articles/10.3389/fmicb.2017.01726 (accessed Feb 10, 2024).

567 Gao C, Koko MY, Hong W, *et al.* Protective Properties of Intestinal Alkaline Phosphatase Supplementation on the Intestinal Barrier: Interactions and Effects. *J Agric Food Chem* 2024; **72**: 27–45.

568 Ayache J, Beaunier L, Boumendil J, Ehret G, Laub D. Artifacts in Transmission Electron Microscopy. In: Ayache J, Beaunier L, Boumendil J, Ehret G, Laub D, eds. Sample Preparation Handbook for Transmission Electron Microscopy: Methodology. New York, NY: Springer, 2010: 125–70.

569 Aviles KM, Lear BJ. Practical Guide to Automated TEM Image Analysis for Increased Accuracy and Precision in the Measurement of Particle Size and Morphology. *ACS Nanosci Au* 2025; **5**: 117–27.

570 Turner L, Bitto NJ, Steer DL, *et al.* Helicobacter pylori Outer Membrane Vesicle Size Determines Their Mechanisms of Host Cell Entry and Protein Content. *Frontiers in Immunology* 2018; **9**. https://www.frontiersin.org/journals/immunology/articles/10.3389/fimmu.2018.01466 (accessed Feb 17, 2024).

571 Kim D, Kim Y-G, Seo S-U, *et al.* Nod2-mediated recognition of the microbiota is critical for mucosal adjuvant activity of cholera toxin. *Nat Med* 2016; **22**: 524–30.

572 Xue J, Ajuwon KM, Fang R. Mechanistic insight into the gut microbiome and its interaction with host immunity and inflammation. *Animal Nutrition* 2020; **6**: 421–8.

573 Al-Asmakh M, Zadjali F. Use of Germ-Free Animal Models in Microbiota-Related Research. 2015; **25**: 1583–8.

574 Kennedy EA, King KY, Baldridge MT. Mouse Microbiota Models: Comparing Germ-Free Mice and Antibiotics Treatment as Tools for Modifying Gut Bacteria. *Front Physiol* 2018; **9**. DOI:10.3389/fphys.2018.01534.

575 Danne C, Skerniskyte J, Marteyn B, Sokol H. Neutrophils: from IBD to the gut microbiota. *Nat Rev Gastroenterol Hepatol* 2023; : 1–14.

576 Ivanov II, Atarashi K, Manel N, *et al.* Induction of Intestinal Th17 Cells by Segmented Filamentous Bacteria. *Cell* 2009; **139**: 485–98.

577 Zargar A, Quan DN, Carter KK, *et al.* Bacterial Secretions of Nonpathogenic Escherichia coli Elicit Inflammatory Pathways: a Closer Investigation of Interkingdom Signaling. *mBio* 2015; **6**: e00025-15.

578 Schaupp L, Muth S, Rogell L, *et al.* Microbiota-Induced Type I Interferons Instruct a Poised Basal State of Dendritic Cells. *Cell* 2020; **181**: 1080-1096.e19.

579 Sommer F, Bäckhed F. The gut microbiota — masters of host development and physiology. *Nat Rev Microbiol* 2013; **11**: 227–38.

580 Gewirtz AT, Navas TA, Lyons S, Godowski PJ, Madara JL. Cutting edge: bacterial flagellin activates basolaterally expressed TLR5 to induce epithelial proinflammatory gene expression. *J Immunol* 2001; **167**: 1882–5.

581 Alexopoulou L, Holt AC, Medzhitov R, Flavell RA. Recognition of double-stranded RNA and activation of NF-κB by Toll-like receptor 3. *Nature* 2001; **413**: 732–8.

582 Hemmi H, Takeuchi O, Kawai T, *et al.* A Toll-like receptor recognizes bacterial DNA. *Nature* 2000; **408**: 740–5.

583 Fukata M, Arditi M. The role of pattern recognition receptors in intestinal inflammation. *Mucosal Immunology* 2013; **6**: 451–63.

584 Cornick S, Tawiah A, Chadee K. Roles and regulation of the mucus barrier in the gut. *Tissue Barriers* 2015; **3**: e982426.

585 O'Donoghue EJ, Sirisaengtaksin N, Browning DF, *et al.* Lipopolysaccharide structure impacts the entry kinetics of bacterial outer membrane vesicles into host cells. *PLOS Pathogens* 2017; **13**: e1006760.

586 Kumari P, Wright SS, Rathinam VA. Role of Extracellular Vesicles in Immunity and Host Defense. *Immunological Investigations* 2024; **0**: 1–16.

587 Rawal S, Ali SA. Probiotics and postbiotics play a role in maintaining dermal health. *Food Funct* 2023; **14**: 3966–81.

588 Kaur H, Ali SA. Probiotics and gut microbiota: mechanistic insights into gut immune homeostasis through TLR pathway regulation. *Food Funct* 2022; **13**: 7423–47.

589 Aintablian A, Jaber DF, Jallad MA, Abdelnoor AM. The Effect of Lactobacillus Plantarum and Bacterial Peptidoglycan on the Growth of Mouse Tumors in vivo and in vitro. *AJI* 2017; **13**: 201–8.

590 Champagne-Jorgensen K, Mian MF, McVey Neufeld K-A, Stanisz AM, Bienenstock J. Membrane vesicles of Lacticaseibacillus rhamnosus JB-1 contain immunomodulatory lipoteichoic acid and are endocytosed by intestinal epithelial cells. *Sci Rep* 2021; **11**: 13756.

591 Yamasaki-Yashiki S, Miyoshi Y, Nakayama T, Kunisawa J, Katakura Y. IgA-enhancing effects of membrane vesicles derived from *Lactobacillus sakei* subsp. *sakei* NBRC15893. *Bioscience of Microbiota, Food and Health* 2019; **38**: 23–9.

592 Kurata A, Kiyohara S, Imai T, *et al.* Characterization of extracellular vesicles from Lactiplantibacillus plantarum. *Sci Rep* 2022; **12**: 13330.

593 Erttmann SF, Swacha P, Aung KM, *et al.* The gut microbiota prime systemic antiviral immunity via the cGAS-STING-IFN-I axis. *Immunity* 2022; **55**: 847-861.e10.

594 Lajqi T, Köstlin-Gille N, Gille C. Trained Innate Immunity in Pediatric Infectious Diseases. *The Pediatric Infectious Disease Journal* 2023; : 10.1097/INF.0000000000004157.

595 Medina M, Izquierdo E, Ennahar S, Sanz Y. Differential immunomodulatory properties of Bifidobacterium logum strains: relevance to probiotic selection and clinical applications. *Clinical and Experimental Immunology* 2007; **150**: 531–8.

596 López P, Gueimonde M, Margolles A, Suárez A. Distinct *Bifidobacterium* strains drive different immune responses *in vitro*. *International Journal of Food Microbiology* 2010; **138**: 157–65.

597 Nicola S, Amoruso A, Deidda F, *et al.* Searching for the Perfect Homeostasis: Five Strains of Bifidobacterium longum From Centenarians Have a Similar Behavior in the Production of Cytokines. *Journal of Clinical Gastroenterology* 2016; **50**: S126.

598 Roselli M, Finamore A, Britti MS, Mengheri E. Probiotic bacteria Bifidobacterium animalis MB5 and Lactobacillus rhamnosus GG protect intestinal Caco-2 cells from the inflammation-associated response induced by enterotoxigenic Escherichia coli K88. *Br J Nutr* 2006; **95**: 1177–84.

599 Martín R, Laval L, Chain F, *et al.* Bifidobacterium animalis ssp. lactis CNCM-I2494 Restores Gut Barrier Permeability in Chronically Low-Grade Inflamed Mice. *Front Microbiol* 2016; **7**. DOI:10.3389/fmicb.2016.00608.

600 Mokkala K, Laitinen K, Röytiö H. *Bifidobacterium lactis* 420 and fish oil enhance intestinal epithelial integrity in Caco-2 cells. *Nutrition Research* 2016; **36**: 246–52.

601 Abdulqadir R, Engers J, Al-Sadi R. Role of Bifidobacterium in Modulating the Intestinal Epithelial Tight Junction Barrier: Current Knowledge and Perspectives. *Current Developments in Nutrition* 2023; **7**: 102026.

602 Muñoz JAM, Chenoll E, Casinos B, *et al.* Novel probiotic Bifidobacterium longum subsp. infantis CECT 7210 strain active against rotavirus infections. *Appl Environ Microbiol* 2011; **77**: 8775–83.

603 Chattha KS, Vlasova AN, Kandasamy S, Rajashekara G, Saif LJ. Divergent Immunomodulating Effects of Probiotics on T Cell Responses to Oral Attenuated Human Rotavirus Vaccine and Virulent Human Rotavirus Infection in a Neonatal Gnotobiotic Piglet Disease Model. *The Journal of Immunology* 2013; **191**: 2446–56.

604 Chen Y, Yang B, Stanton C, *et al.* Bifidobacterium pseudocatenulatum Ameliorates DSS-Induced Colitis by Maintaining Intestinal Mechanical Barrier, Blocking Proinflammatory Cytokines, Inhibiting TLR4/NF-κB Signaling, and Altering Gut Microbiota. *J Agric Food Chem* 2021; **69**: 1496–512.

605 Hiramatsu Y, Hosono A, Konno T, *et al.* Orally administered Bifidobacterium triggers immune responses following capture by CD11c(+) cells in Peyer's patches and cecal patches. *Cytotechnology* 2011; **63**: 307–17.

606 Nakanishi Y, Hosono A, Hiramatsu Y, Kimura T, Nakamura R, Kaminogawa S. Characteristic Immune Response in Peyer's Patch Cells Induced by Oral Administration of Bifidobacterium Components. *Cytotechnology* 2005; **47**: 69–77.

607 Hiramatsu Y, Hosono A, Takahashi K, Kaminogawa S. Bifidobacterium components have immunomodulatory characteristics dependent on the method of preparation. *Cytotechnology* 2007; **55**: 79–87.

608 Kim J-H, Jeun E-J, Hong C-P, *et al.* Extracellular vesicle–derived protein from Bifidobacterium longum alleviates food allergy through mast cell suppression. *Journal of Allergy and Clinical Immunology* 2016; **137**: 507-516.e8.

609 Srinivasan B, Kolli AR, Esch MB, Abaci HE, Shuler ML, Hickman JJ. TEER Measurement Techniques for In Vitro Barrier Model Systems. *SLAS Technology* 2015; **20**: 107–26.

610 Alvarez C-S, Badia J, Bosch M, Giménez R, Baldomà L. Outer Membrane Vesicles and Soluble Factors Released by Probiotic Escherichia coli Nissle 1917 and Commensal ECOR63 Enhance Barrier Function by Regulating Expression of Tight Junction Proteins in Intestinal Epithelial Cells. *Front Microbiol* 2016; **7**. DOI:10.3389/fmicb.2016.01981.

611 Cañas M-A, Giménez R, Fábrega M-J, Toloza L, Baldomà L, Badia J. Outer Membrane Vesicles from the Probiotic Escherichia coli Nissle 1917 and the Commensal ECOR12 Enter Intestinal Epithelial Cells via Clathrin-Dependent Endocytosis and Elicit Differential Effects on DNA Damage. *PLOS ONE* 2016; **11**: e0160374.

612 Fábrega MJ, Aguilera L, Giménez R, *et al.* Activation of Immune and Defense Responses in the Intestinal Mucosa by Outer Membrane Vesicles of Commensal and Probiotic Escherichia coli Strains. *Front Microbiol* 2016; **7**. DOI:10.3389/fmicb.2016.00705.

613 Furuta N, Takeuchi H, Amano A. Entry of Porphyromonas gingivalis Outer Membrane Vesicles into Epithelial Cells Causes Cellular Functional Impairment. *Infection and Immunity* 2009; **77**: 4761–70.

614 Tulkens J, Vergauwen G, Deun JV, *et al.* Increased levels of systemic LPS-positive bacterial extracellular vesicles in patients with intestinal barrier dysfunction. *Gut* 2020; **69**: 191–3.

615 Wang H, Zhang X, Kou X, Zhai Z, Hao Y. A Ropy Exopolysaccharide-Producing Strain Bifidobacterium pseudocatenulatum Bi-OTA128 Alleviates Dextran Sulfate Sodium-Induced Colitis in Mice. *Nutrients* 2023; **15**: 4993.

616 Yang Z, Wang X, Wu S, *et al.* Safety evaluation of *Bifidobacterium pseudocatenulatum* E−0810 and its synbiotic formulation with xylooligosaccharides in alleviating LPS-induced inflammation in intestinal epithelial cells. *Food Bioscience* 2025; **71**: 107069.

617 Bitto NJ, Chapman R, Pidot S, *et al.* Bacterial membrane vesicles transport their DNA cargo into host cells. *Sci Rep* 2017; **7**: 7072.

618 Rompikuntal PK, Thay B, Khan MK, *et al.* Perinuclear localization of internalized outer membrane vesicles carrying active cytolethal distending toxin from Aggregatibacter actinomycetemcomitans. *Infect Immun* 2012; **80**: 31–42.

619 Abdulqadir RF, Al-Sadi R, Ma TY. Tu1113: BIFIDOBACTERIUM BIFIDUM CAUSES AN ENHANCEMENT OF INTESTINAL EPITHELIAL TIGHT JUNCTION BARRIER BY A NOVEL MECHANISM INVOLVING PEROXISOME PROLIFERATION-ACTIVATED RECEPTOR GAMMA (PPAR-γ). *Gastroenterology* 2022; **162**: S-887-S-888.

620 O'Donoghue EJ, Krachler AM. Mechanisms of outer membrane vesicle entry into host cells. *Cellular Microbiology* 2016; **18**: 1508–17.

621 Kang L, Fang X, Song Y-H, *et al.* Neutrophil-Epithelial Crosstalk During Intestinal Inflammation. *Cell Mol Gastroenterol Hepatol* 2022; **14**: 1257–67.

622 Artursson P, Palm K, Luthman K. Caco-2 monolayers in experimental and theoretical predictions of drug transport. *Adv Drug Deliv Rev* 2001; **46**: 27–43.

623 Calzascia T, Pellegrini M, Hall H, *et al.* TNF-alpha is critical for antitumor but not antiviral T cell immunity in mice. *J Clin Invest* 2007; **117**: 3833–45.

624 Kayamuro H, Abe Y, Yoshioka Y, *et al.* The use of a mutant TNF-α as a vaccine adjuvant for the induction of mucosal immune responses. *Biomaterials* 2009; **30**: 5869–76.

625 Idriss HT, Naismith JH. TNF alpha and the TNF receptor superfamily: structure-function relationship(s). *Microsc Res Tech* 2000; **50**: 184–95.

626 Raftopoulou S, Valadez-Cosmes P, Mihalic ZN, Schicho R, Kargl J. Tumor-Mediated Neutrophil Polarization and Therapeutic Implications. *International Journal of Molecular Sciences* 2022; **23**. DOI:10.3390/ijms23063218.

627 Bradley JR. TNF-mediated inflammatory disease. *J Pathol* 2008; **214**: 149–60.

628 Nie J, Zhou L, Tian W, *et al.* Deep insight into cytokine storm: from pathogenesis to treatment. *Signal Transduct Target Ther* 2025; **10**: 112.

629 Bertrand F, Montfort A, Marcheteau E, *et al.* TNFα blockade overcomes resistance to anti-PD-1 in experimental melanoma. *Nat Commun* 2017; **8**: 2256.

630 Tanaka T, Narazaki M, Kishimoto T. IL-6 in inflammation, immunity, and disease. *Cold Spring Harb Perspect Biol* 2014; **6**: a016295.

631 Saraiva M, O'Garra A. The regulation of IL-10 production by immune cells. *Nat Rev Immunol* 2010; **10**: 170–81.

632 Peñaloza HF, Schultz BM, Nieto PA, *et al.* Opposing roles of IL-10 in acute bacterial infection. *Cytokine & Growth Factor Reviews* 2016; **32**: 17–30.

633 Nicklin AD. Developing Bifidobacterium-based therapeutics to improve cancer outcome and prevent occurrence. 2025; published online Jan 9. https://ueaeprints.uea.ac.uk/id/eprint/98129/ (accessed Jan 15, 2026).

634 Van Den Eeckhout B, Tavernier J, Gerlo S. Interleukin-1 as Innate Mediator of T Cell Immunity. *Front Immunol* 2021; **11**: 621931.

635 Tang H, Cao W, Kasturi SP, *et al.* The T helper type 2 response to cysteine proteases requires dendritic cell–basophil cooperation via ROS-mediated signaling. *Nat Immunol* 2010; **11**: 608–17.

636 Ito T, Wang Y-H, Duramad O, *et al.* TSLP-activated dendritic cells induce an inflammatory T helper type 2 cell response through OX40 ligand. *Journal of Experimental Medicine* 2005; **202**: 1213–23.

637 Surh CD, Sprent J. Homeostasis of naive and memory T cells. *Immunity* 2008; **29**: 848–62.

638 Antuamwine BB, Bosnjakovic R, Hofmann-Vega F, *et al.* N1 versus N2 and PMN-MDSC: A critical appraisal of current concepts on tumor-associated neutrophils and new directions for human oncology. *Immunological Reviews* 2023; **314**: 250–79.

639 Okai S, Usui F, Yokota S, *et al.* High-affinity monoclonal IgA regulates gut microbiota and prevents colitis in mice. *Nat Microbiol* 2016; **1**: 16103.

640 Donaldson GP, Ladinsky MS, Yu KB, *et al.* Gut microbiota utilize immunoglobulin A for mucosal colonization. *Science* 2018; **360**: 795–800.

641 Nakajima A, Vogelzang A, Maruya M, *et al.* IgA regulates the composition and metabolic function of gut microbiota by promoting symbiosis between bacteria. *Journal of Experimental Medicine* 2018; **215**: 2019–34.

642 Dillon A, Lo DD. M Cells: Intelligent Engineering of Mucosal Immune Surveillance. *Front Immunol* 2019; **10**. DOI:10.3389/fimmu.2019.01499.

643 Takeuchi T, Ohno H. Reciprocal regulation of IgA and the gut microbiota: a key mutualism in the intestine. *International Immunology* 2021; **33**: 781–6.

644 Rognum TO, Thrane PS, Stoltenberg L, Vege Å, Brandtzaeg P. Development of Intestinal Mucosal Immunity in Fetal Life and the First Postnatal Months. *Pediatr Res* 1992; **32**: 145–8.

645 Donald K, Petersen C, Turvey SE, Finlay BB, Azad MB. Secretory IgA: Linking microbes, maternal health, and infant health through human milk. *Cell Host & Microbe* 2022; **30**: 650–9.

646 Bunker JJ, Erickson SA, Flynn TM, *et al.* Natural polyreactive IgA antibodies coat the intestinal microbiota. *Science* 2017; **358**: eaan6619.

647 Rodríguez JM. The Origin of Human Milk Bacteria: Is There a Bacterial Entero-Mammary Pathway during Late Pregnancy and Lactation? *Advances in Nutrition* 2014; **5**: 779–84.

648 Rozé J-C, Barbarot S, Butel M-J, *et al.* An α-lactalbumin-enriched and symbiotic-supplemented v. a standard infant formula: a multicentre, double-blind, randomised trial. *Br J Nutr* 2012; **107**: 1616–22.

649 Escribano J, Ferré N, Gispert-Llaurado M, *et al.* Bifidobacterium longum subsp infantis CECT7210-supplemented formula reduces diarrhea in healthy infants: a randomized controlled trial. *Pediatr Res* 2018; **83**: 1120–8.

650 De Ponte Conti B, Marino R, Rezzonico-Jost T, *et al.* Secretory IgA amplification during immune checkpoint blockade enhances the control of tumor growth by enterotropic T cells. *Science Advances* 2025; **11**: eaeb5308.

651 Wiklander OPB, Nordin JZ, O'Loughlin A, *et al.* Extracellular vesicle in vivo biodistribution is determined by cell source, route of administration and targeting. *Journal of Extracellular Vesicles* 2015; **4**: 26316.

652 Jovanovic M, Rooney MS, Mertins P, *et al.* Dynamic profiling of the protein life cycle in response to pathogens. *Science* 2015; **347**: 1259038.

653 Choi JH, Moon CM, Shin T-S, *et al.* Lactobacillus paracasei-derived extracellular vesicles attenuate the intestinal inflammatory response by augmenting the endoplasmic reticulum stress pathway. *Exp Mol Med* 2020; **52**: 423–37.

654 Mofrad LZ, Fateh A, Sotoodehnejadnematalahi F, Asbi DNS, Davar Siadat S. The Effect of Akkermansia muciniphila and Its Outer Membrane Vesicles on MicroRNAs Expression of Inflammatory and Anti-inflammatory Pathways in Human Dendritic Cells. *Probiotics Antimicrob Proteins* 2024; **16**: 367–82.

655 Zheng T, Hao H, Liu Q, *et al.* Effect of Extracelluar Vesicles Derived from Akkermansia muciniphila on Intestinal Barrier in Colitis Mice. *Nutrients* 2023; **15**: 4722.

656 Mojgani N, Ashique S, Moradi M, *et al.* Gut Microbiota and Postbiotic Metabolites: Biotic Intervention for Enhancing Vaccine Responses and Personalized Medicine for Disease Prevention. *Probiotics & Antimicro Prot* 2025; published online Feb 18. DOI:10.1007/s12602-025-10477-7.

657 Morishita M, Makabe M, Shinohara C, *et al.* Versatile functionalization of *Bifidobacteria*-derived extracellular vesicles using amino acid metabolic labeling and click chemistry for immunotherapy. *International Journal of Pharmaceutics* 2024; **661**: 124410.

658 Tong L, Zhang X, Hao H, *et al.* Lactobacillus rhamnosus GG Derived Extracellular Vesicles Modulate Gut Microbiota and Attenuate Inflammatory in DSS-Induced Colitis Mice. *Nutrients* 2021; **13**: 3319.

659 Mehvish HB, Zhang S, Liang Y, *et al.* Enhanced Osteoporosis Treatment via Nano Drug Coating Encapsulating Lactobacillus rhamnosus GG. *ACS Appl Mater Interfaces* 2025; **17**: 5326–39.

660 Wei J, Li Z, Fan Y, *et al. Lactobacillus rhamnosus* GG aggravates vascular calcification in chronic kidney disease: A potential role for extracellular vesicles. *Life Sciences* 2023; **331**: 122001.

# LIST OF ABBREVIATIONS

| | |
|---|---|
| 2'FL | 2'-Fucosyllactose |
| 3'SL | 3′-Sialyllactose |
| 6'SL | 6'-Sialyllactose |
| AA | Amino acids |
| Acetyl-CoA | Acetyl-coenzyme A |
| AhR | Aryl hydrocarbon receptor |
| AMP | Anti-microbial peptide |
| AMR | Anti-microbial resistance |
| ANOVA | Analysis of variance |
| APC | Antigen-presenting cell |
| AU | Average fluorescence intensity units |
| BAMBI | Baby-Associated MicroBiota of the Intestine |
| BCG | Bacillus Calmette-Guérin |
| BCL-2 | B cell lymphoma-2 |
| BEV | Bacterial extracellular vesicle |
| BGS | Bifidogenic growth stimulator |
| BHI | Brain heart infusion |
| BM | Bone marrow |
| BMDC | Bone marrow-derived dendritic cell |
| BMI | Body-mass index |
| BR | Broad range |
| CAZymes | Carbohydrate-active enzymes |
| CBM | Carbohydrate-Binding Module Family |
| CCL | Chemokine c-c motif ligand |
| CD | Cluster of differentiation |
| CD40L | CD40 ligand |
| cDC | Conventional dendritic cell |
| CFU | Colony forming unit |
| CMV | Cytoplasmic membrane vesicles |
| CpG ODN | Cytosine-phosphate-guanine oligodeoxynucleotides |
| CXCL | C-X-C motif chemokine ligand |
| CYP1A1 | Cytochrome P450 family 1 subfamily A member 1 |

| | |
|---|---|
| DAMP | Danger-associated molecular pattern |
| DC | Dendritic cell |
| DMEM | Dulbecco's Modified Eagle Medium |
| dNTP | deoxynucleotide triphosphates |
| ds | Double-stranded |
| DTaP | Diphtheria-Tetanus-acellular Pertussis |
| DTT | Dithiothreitol |
| EB | Elution buffer |
| ECMV | Explosive cytoplasmic membrane vesicles |
| eDNA | Extracellular DNA |
| ELISA | Enzyme-linked immunosorbent assay |
| EPS | Exopolysaccharide |
| ESBP | Extracellular solute-binding protein |
| EV | Extracellular membrane vesicle |
| FACS | Fluorescence-activated cell sorting |
| FBS | Foetal bovine serum |
| fDC | Follicular dendritic cell |
| FMT | Faecal microbiota transplantation |
| FOS | Fructooligosaccharides |
| GALT | Gut-associated lymphoid tissue |
| GAPDH | Glyceraldehyde-3-phosphate dehydrogenase |
| GC | Germinal centre |
| gDNA | Genomic DNA |
| GF | Germ-free |
| GH | Glycosyl hydrolase |
| GIT | Gastrointestinal tract |
| Glc | Glucose |
| Gl-OS | Glucose-derived oligosaccharides |
| GM-CSF | Granulocyte-macrophage colony-stimulating factor |
| GO | Gene ontology |
| GOS | Galactooligosaccharides |
| GPR | G-protein coupled receptor |
| GRAS | Generally regarded as safe |
| HEPES | 4-(2-hydroxyethyl)-1-piperazine-ethanesulfonic acid |
| Hib | Haemophilus influenzae type b |

| | |
|---|---|
| HIV | Human immunodeficiency virus |
| HMO | Human milk oligosaccharides |
| HPV | Human papillomavirus |
| HS | High sensitivity |
| IBD | Inflammatory bowel disease |
| IBS | Irritable bowel syndrome |
| IEC | Intestinal epithelial cell |
| IFN | Interferon |
| Ig | Immunoglobulin |
| IL | Interleukin |
| ILC | Innate lymphoid cell |
| IMO | Isomaltooligosaccharides |
| KC | Keratinocyte-derived cytokine |
| KEGG | Kyoto Encyclopedia of Genes and Genomes |
| LMIC | Low- and middle-income country |
| LNnT | Lacto-N-neotetraose |
| LPS | Lipopolysaccharide |
| LTA | lipoteichoic acid |
| MAMP | Microbe-associated molecular patterns |
| MCL-1 | Myeloid cell leukemia-1 |
| MCP-1 | Monocyte chemoattractant protein 1 |
| MD2 | Myeloid differentiation protein 2 |
| MenB | Meningitis B |
| MERS | Middle East Respiratory Syndrome |
| MHC | Major histocompatibility complex |
| MLV | Murine leukaemia virus |
| MMR | Measles, mumps and rubella |
| MPL | Monophosphoryl lipid A |
| mRNA | Messenger RNA |
| MRS | De Man, Rogosa and Sharpe medium |
| MSD | Meso Scale Discovery |
| NEC | Necrotising enterocolitis |
| NET | Neutrophil extracellular trap |
| NF-κB | Nuclear factor ‘κ-light chain enhancer’ of activated B cells |
| NK | Natural killer |

| | |
|---|---|
| NO | Nitric oxide |
| NTA | Nanoparticle tracking analysis |
| OD | Optical density |
| OPV | Oral Polio vaccine |
| ORV | Oral rotavirus vaccine |
| PBMC | Peripheral blood mononuclear cell |
| PBS | Phosphate-buffered saline |
| PCB | Polycarbonated biphenyl |
| PCV | Pneumococcal conjugate vaccine |
| PD-1 | Programmed cell death |
| pDC | Plasmacytoid DC |
| PD-L1 | Programmed cell death 1 ligand 1 |
| PEG | Polyethylene glycol |
| Pen/Strep | Penicillin/Streptomycin mix |
| PET | Polyethylene terephthalate |
| PMA | Phorbol 12-myristate 13-acetate |
| PP | Peyer’s patch |
| PRR | Pattern recognition receptor |
| QIBAM | QIB - Advanced Microscopy Facility |
| qRT-PCR | Quantitative Reverse Transcriptase-Polymerase Chain Reaction |
| RA | Retinoic acid |
| RANTES | Regulated on activation, normal T cell expressed and secreted |
| RBC | Red blood cell |
| RCM | Reinforced clostridial medium |
| RCMveg | Vegan RCM |
| ROS | Reactive oxygen species |
| RPMI | Roswell Park Memorial Institute |
| rRNA | ribosomal RNA |
| RSV | Respiratory syncytial virus |
| RT | Room temperature |
| RV | Rotavirus |
| SARS-CoV-2 | Severe Acute Respiratory Syndrome Coronavirus-2 |
| SCFA | Short-chain fatty acid |
| SDC | Sodium deoxycholate |

| | |
|---|---|
| SDS | Sodium dodecyl sulphate |
| SEC | Size exclusion chromatography |
| SEM | Standard error of mean |
| siRNA | Small interfering RNA |
| SOP | Standard operation procedure |
| sRNA | Small RNA |
| ss | Single-stranded |
| TCA | Tricarboxylic acid cycle |
| Tcm | Central memory T cell |
| Tct | Cytotoxic T cell |
| TEER | Transepithelial Electrical Resistance |
| Tem | Effector memory T cell |
| TEM | Transmission electron microscope/microscopy |
| TFA | Trifluoroacetic acid |
| Tfh | T follicular helper cell |
| TGF-β | Transforming growth factor-beta |
| Th | T helper cell |
| TJ | Tight junction |
| TLR | Toll-like receptor |
| TNF-α | Tumour necrosis factor-alpha |
| Treg | Regulatory T cell |
| tRNA | transfer RNA |
| TSLP | Thymic stromal lymphopoietin |
| UA | Uranyl acetate |
| VLP | Virus-like particle |
| WGS | Whole Genome Sequencing |
| WHO | World Health Organisation |
| WS | Working stock |
| wt | Wild type |
| ZO-1 | Zonula Occludens-1 |

# APPENDIX

## 1. Supplementary Data

### 1.1. Kraken reports

```
 4.66  293547  293547  U       0       unclassified
95.34  6001406 18      R       1       root
95.34  6001379 417     R1      131567    cellular organisms
95.33  6000925 4617    D       2           Bacteria
95.17  5990942 273     D1      1783272       Terrabacteria group
95.15  5989374 55      P       201174          Actinobacteria
95.14  5988883 8986    C       1760              Actinobacteria
94.91  5974809 0       O       85004               Bifidobacteriales
94.91  5974809 198     F       31953                 Bifidobacteriaceae
94.91  5974583 413775  G       1678                    Bifidobacterium
49.35  3106536 0       S       28026                     Bifidobacterium pseudocatenulatum
49.35  3106536 3106536 S1      547043                      Bifidobacterium pseudocatenulatum DSM 20438 = JCM 1200 = LMG 10505
26.54  1670778 1670778 S       35760                     Bifidobacterium choerinum
 5.92  372509  31912   S       630129                    Bifidobacterium kashiwanohense
 3.12  196304  196304  S1      1447716                     Bifidobacterium kashiwanohense PV20-2
 2.29  144293  144293  S1      1150460                     Bifidobacterium kashiwanohense JCM 15439 = DSM 21854
 2.15  135060  0       S       1686                      Bifidobacterium catenulatum
 2.15  135060  135060  S1      566552                      Bifidobacterium catenulatum DSM 16992 = JCM 1194 = LMG 11043
 1.63  102745  95471   S       1680                      Bifidobacterium adolescentis
 0.12  7274    7274    S1      367928                      Bifidobacterium adolescentis ATCC 15703
 1.08  68243   38915   S       216816                    Bifidobacterium longum
 0.25  15509   10758   S1      1682                        Bifidobacterium longum subsp. infantis
 0.05  3101    3101    S2      391904                        Bifidobacterium longum subsp. infantis ATCC 15697 = JCM 1222 = DSM 20088
 0.03  1650    1650    S2      565040                        Bifidobacterium longum subsp. infantis 157F
 0.21  13257   4588    S1      1679                        Bifidobacterium longum subsp. longum
 0.13  8235    8235    S2      890402                        Bifidobacterium longum subsp. longum BBMN68
 0.01  414     414     S2      1300227                       Bifidobacterium longum subsp. longum GT15
 0.00  11      11      S2      565042                        Bifidobacterium longum subsp. longum JCM 1217
 0.00  5       5       S2      722911                        Bifidobacterium longum subsp. longum F8
 0.00  4       4       S2      1035817                       Bifidobacterium longum subsp. longum KACC 91563
 0.01  552     552     S1      206672                      Bifidobacterium longum NCC2705
 0.00  10      10      S1      205913                      Bifidobacterium longum DJO10A
 0.46  28794   22352   S       1681                      Bifidobacterium bifidum
 0.05  2999    2999    S1      484020                      Bifidobacterium bifidum BGN4
 0.03  1885    1885    S1      702459                      Bifidobacterium bifidum PRL2010
 0.02  1543    1543    S1      500634                      Bifidobacterium bifidum ATCC 29521 = JCM 1255 = DSM 20456
 0.00  15      15      S1      883062                      Bifidobacterium bifidum S17
```

*Supplementary Figure 1: Extract of the Kraken report of LH660 stocks revealing contamination with two other Bifidobacterium species*

```
 3.93  249991  249991  U       0       unclassified
96.07  6109741 23      R       1       root
96.07  6109715 212     R1      131567    cellular organisms
96.06  6109473 5888    D       2           Bacteria
95.91  6099830 107     D1      1783272       Terrabacteria group
95.91  6099321 29      P       201174          Actinobacteria
95.90  6099285 10741   C       1760              Actinobacteria
95.67  6084330 0       O       85004               Bifidobacteriales
95.67  6084330 232     F       31953                 Bifidobacteriaceae
95.67  6084078 579008  G       1678                    Bifidobacterium
70.12  4459284 0       S       28026                     Bifidobacterium pseudocatenulatum
70.12  4459284 4459284 S1      547043                      Bifidobacterium pseudocatenulatum DSM 20438 = JCM 1200 = LMG 10505
 8.33  529636  45409   S       630129                    Bifidobacterium kashiwanohense
 4.37  277703  277703  S1      1447716                     Bifidobacterium kashiwanohense PV20-2
 3.25  206524  206524  S1      1150460                     Bifidobacterium kashiwanohense JCM 15439 = DSM 21854
 3.02  192227  0       S       1686                      Bifidobacterium catenulatum
 3.02  192227  192227  S1      566552                      Bifidobacterium catenulatum DSM 16992 = JCM 1194 = LMG 11043
 1.85  117512  109399  S       1680                      Bifidobacterium adolescentis
 0.13  8113    8113    S1      367928                      Bifidobacterium adolescentis ATCC 15703
 1.49  94684   53958   S       216816                    Bifidobacterium longum
 0.33  21072   14341   S1      1682                        Bifidobacterium longum subsp. infantis
 0.07  4320    4320    S2      391904                        Bifidobacterium longum subsp. infantis ATCC 15697 = JCM 1222 = DSM 20088
 0.04  2411    2411    S2      565040                        Bifidobacterium longum subsp. infantis 157F
 0.30  18793   6463    S1      1679                        Bifidobacterium longum subsp. longum
 0.18  11722   11722   S2      890402                        Bifidobacterium longum subsp. longum BBMN68
 0.01  595     595     S2      1300227                       Bifidobacterium longum subsp. longum GT15
 0.00  5       5       S2      1035817                       Bifidobacterium longum subsp. longum KACC 91563
 0.00  4       4       S2      565042                        Bifidobacterium longum subsp. longum JCM 1217
 0.00  4       4       S2      722911                        Bifidobacterium longum subsp. longum F8
 0.01  846     846     S1      206672                      Bifidobacterium longum NCC2705
 0.00  11      11      S1      205913                      Bifidobacterium longum DJO10A
 0.00  4       4       S1      1322347                     Bifidobacterium longum E18
 0.64  40819   31470   S       1681                      Bifidobacterium bifidum
 0.07  4236    4236    S1      484020                      Bifidobacterium bifidum BGN4
 0.04  2859    2859    S1      702459                      Bifidobacterium bifidum PRL2010
```

*Supplementary Figure 2: Extract of the Kraken report of LH663 stocks confirming lack of contamination*

## 1.2. Initial growth assays

This data was acquired prior to confirmed contamination of LH660 stocks.

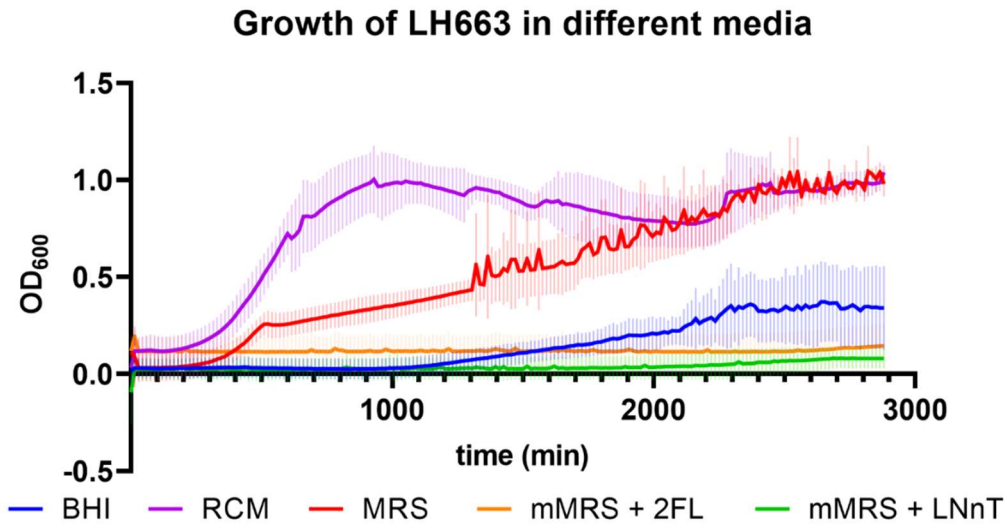


*Supplementary Figure 3: Growth of LH663 in BHI (blue), RCM (purple), MRS (red) and minimal MRS supplemented with 2'FL (orange) or LNnT (green). $OD_{600}$ taken every 15min for 48h. Mean growth displayed in bold lines, error bars in respectively coloured lines above and below mean growth at each time point*

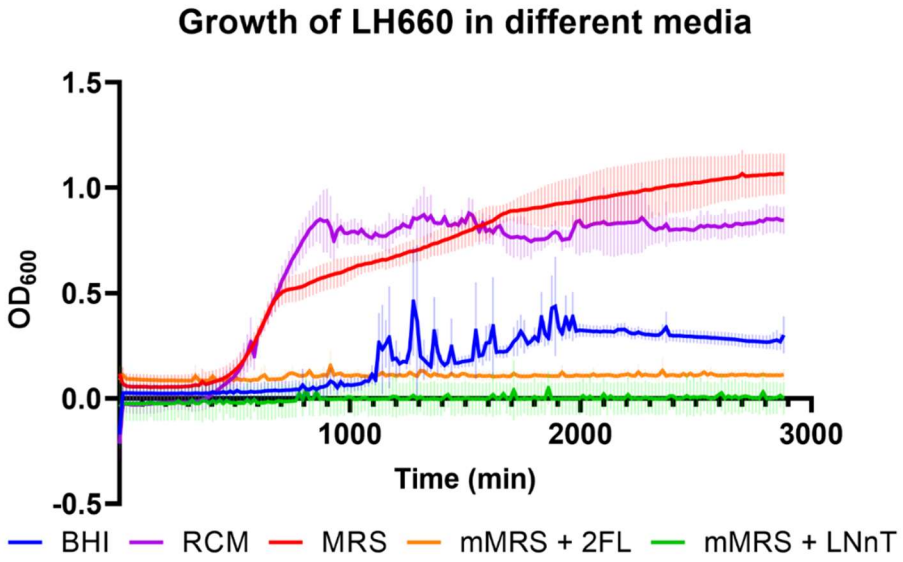


*Supplementary Figure 4: Growth of contaminated LH660 in BHI (blue), RCM (purple), MRS (red) and minimal MRS supplemented with 2'FL (orange) or LNnT (green). $OD_{600}$ taken every 15min for 48h. Mean growth displayed in bold lines, error bars in respectively coloured lines above and below mean growth at each time point*

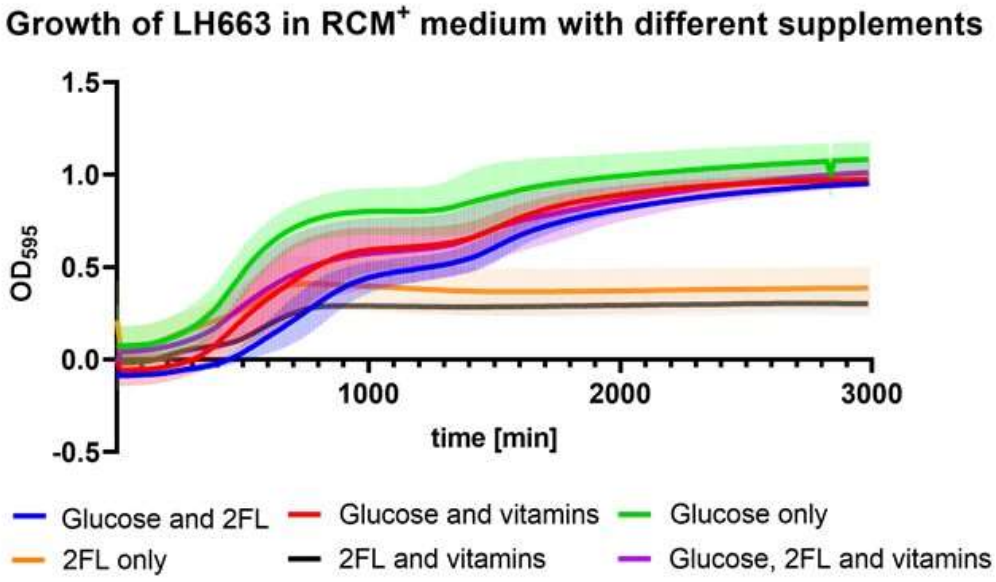


*Supplementary Figure 5: Growth of LH663 in RCMveg supplemented with Glc and 2'FL (blue), Glc and vitamins (red), Glc only (green), 2'FL only (orange), 2'FL and vitamins (black) or Glc, 2'FL and vitamins (purple). $OD_{600}$ taken every 15min for 48h. Mean growth displayed in bold lines, error bars in respectively coloured lines above and below mean growth at each time point*